[redacted]

TM 23-200/OPNAV INSTRUCTION 03400.1C/AFM 136-1/FMFM 11-2

THIS PUBLICATION SUPERSEDES TM 23-200, OPNAV INSTRUCTION 03400.1B, AFM 136-1/NAVMC 1104 REV, NOVEMBER 1957, INCLUDING CHANGE 1, 24 JUNE 1960 AND CHANGE 2, 3 OCTOBER 1960 THERETO.

105483

R

CAPABILITIES OF NUCLEAR WEAPONS [U]

United States Govemment Printing Office
Washington: 1964

[redacted]

[redacted]

DISTRIBUTION:

Active Army:

CofSA (2)
VCofSA (2)
DCSPER (5)
ACSI (5)
DCSLOG (5)
DCSOPS (10)
ACSFOR (10)
SGS (5)
COA (2)
OCAR (2)
CINFO (1)
CNGB (2)
CRD (2)
CLL (1)
TIG (1)
TAG (2)
TJAG (1)
CMH (2)
CofCh (2)
USASA (5)
CofSptS (5)
USACDC (10)
USACDC Nuc Gp (10)
USACDC Agcy (2) except
  USACDCCBRA (5)
USAMC (10)
USAMC Comds (2)
USAMC Bds (2)
USA Nuc Effects Lab (10)
ARADCOM (5)
ARADCOM Rgn (5)
OS Maj Comd (5)
OS Base Comd (5)
LOGCOMD (5)
MDW (2)
Armies (10)
Corps (10)
USA Corps (3)
Div (10)
Div Arty (5)
Bde (5)
USMA (2)
USAWC (5)
Joint Sch (2)
Br Svc Sch (2)
USAINTC (5)
Army Hosp (1)
POE (5)
Dist Engr (5)
Army Dep (1)
PG (2)
Arsenals (1) except
  Picatinny Arsenal (2)
Field Comd, DASA (5)
MAAG (2)
Mil Msn (2)
Units org under fol TOE:
17-22 (5)

NG: State AG (3); Div (1)

USAR: Div (2), Bde (2)

For explanation of abbreviations used, see AR 320-50.

Air Force: X (Special distribution controlled by HQ USAF (AFNINDE)).

[redacted]

[redacted]

TM 23-200
OPNAVINST 03400.1C
AFM 136-1
FMFM 11-2

Departments of The Army, The Navy,
and The Air Force
Washington, D. C., 30 November 1964

TM 23-200/OPNAVINST 03400.1C/AFM 136-1/FMFM 11-2., Capabilities of Nuclear Weapons (U), is published for the use of all concerned.

BY ORDER OF THE SECRETARIES OF THE ARMY, THE NAVY, AND THE AIR FORCE:

HAROLD K. JOHNSON,
General, United States Army,
Chief of Staff

OFFICIAL:
J. C. LAMBERT,
Major General, United States Army,
The Adjutant General.

ROY S. BENSON,
Rear Admiral, United States Navy,
Assistant Vice Chief of Naval Operations/Director of Naval Administration.

CURTIS E. LeMAY,
Chief of Staff, United States Air Force

OFFICIAL:
R. J. PUGH,
Colonel, United States Air Force,
Director of Administrative Services.

H. W. BUSE, Jr.,
Major General, U. S. Marine Corps,
Deputy Chief of Staff
(Plans and Programs).

[redacted]

[redacted]

FOREWORD

This edition of the *Capabilities of Nuclear Weapons* represents the continuing effort by the Defense Atomic Support Agency to correlate and make available nuclear weapons effects information obtained from recent full-scale testing, small-scale experiments, laboratory effort and theoretical analysis. This document presents the phenomena and effects of a nuclear detonation and relates weapons effects manifestations in terms of damage to targets of military interest. It provides the source material and references needed for the preparation of operational and employment manuals by the Military Services.

The *Capabilities of Nuclear Weapons* is not intended to be used as an employment or design manual by itself, since more complete descriptions of phenomenological details should be obtained from the noted references. Every effort has been made to include in this edition the most current reliable data available at the time of publication in order to assist the armed forces in meeting their particular requirements for operational and target analysis purposes.

H. C. DONNELLY
Lt General, USAF
Director, Defense Atomic
Support Agency

[redacted]

[redacted]

TABLE OF CONTENTS

PART I PHYSICAL PHENOMENA

[redacted]

5

[redacted]

TABLE OF CONTENTS (cont)

[redacted]

[redacted]

TABLE OF CONTENTS (cont)

CHAPTER 3 THERMAL RADIATION PHENOMENA

[redacted]

7

[redacted]

TABLE OF CONTENTS (cont)

[redacted]

8

[redacted]

TABLE OF CONTENTS (cont)

[redacted]

[redacted]

TABLE OF CONTENTS (cont)

CHAPTER 8 DAMAGE TO STRUCTURES

[redacted]

[redacted]

TABLE OF CONTENTS (cont)

CHAPTER 10 DAMAGE TO AIRCRAFT

[redacted]

[redacted]

TABLE OF CONTENTS (cont)

[redacted]

[redacted]

TABLE OF CONTENTS (cont)

[redacted]

[redacted]

TABLE OF CONTENTS (cont)

[redacted]

PROBLEMS

PART I

[redacted]

PROBLEMS (cont)

PART II

[redacted]

[redacted]

PROBLEMS (cont)

[redacted]

762-909 O - 65 - 2

[redacted]

LIST OF ILLUSTRATIONS

PART I

[redacted]

[redacted]

LIST OF ILLUSTRATIONS (cont)

[redacted]

[redacted]

LIST OF ILLUSTRATIONS (cont)

[redacted]

LIST OF ILLUSTRATIONS (cont)

[redacted]

LIST OF ILLUSTRATIONS (cont)

[redacted]

[redacted]

LIST OF ILLUSTRATIONS (cont)

[redacted]

[redacted]

LIST OF ILLUSTRATIONS (cont)

[redacted]

PART II

[redacted]

LIST OF ILLUSTRATIONS (cont)

[redacted]

[redacted]

LIST OF ILLUSTRATIONS (cont)

[redacted]

[redacted]

LIST OF ILLUSTRATIONS (cont)

[redacted]

[redacted]

LIST OF ILLUSTRATIONS (cont)

[redacted]

[redacted]

LIST OF ILLUSTRATIONS (cont)

[redacted]

[redacted]

LIST OF ILLUSTRATIONS (cont)

[redacted]

LIST OF ILLUSTRATIONS (cont)

LIST OF TABLES

PART I

PART II

762-909 O - 65 - 3

[redacted]

LIST OF TABLES (cont)

[redacted]

[redacted]

PART I

PHYSICAL PHENOMENA

Chapter 1
INTRODUCTION

METHOD OF PRESENTATION

This manual presents the capabilities of nuclear weapons, graphically for the most part, in two ways: by giving the effects of these weapons, and by giving the response of personnel and military targets to these effects. Part I, Physical Phenomena, treats the basic phenomena of blast and shock, thermal radiation, nuclear radiation, and electromagnetic phenomena resulting from a nuclear explosion in various media and under various conditions. Part II, Damage Criteria, discusses the mechanisms of casualty production and damage to military targets, and describes the response of these targets by correlating the basic physical phenomena with various defined degrees of damage.*

The data presented here are interpretations of complex results of the nuclear weapons effects research and test programs of the Department of Defense. A constant effort is made to deduce theoretical models and scaling laws for the various weapons effects that permit a quantitative prediction of the extent of a given effect from a weapon of one yield related to weapons of other yields. For simplicity and convenience, most physical phenomena data and much of the damage data are presented as a function of the range from a 1-kt burst, from which the phenomena or damage for other yields may be readily obtained, by the appropriate scaling procedures given wherever their use is required.

*Effects of Nuclear Weapons (DA PAM 39-3 and AFP 136-1-3) which contains a more detailed qualitative discussion of these basic phenomena, other than the electromagnetic phenomena, supplements this manual.

1-1 RELIABILITY. An estimate of the degree of reliability accompanies most of the physical phenomena data. With the exception of high altitude nuclear bursts, this estimated reliability indicates a range of values above and below the curve such that, for a large number of events, 90 per cent of the data will fall within this range. Statements of reliability of damage data, however, which describe the source and relative quantity of the data, pertain only to the basic effects data and hence for the target analyst, the "radius of effect." They should not be confused with the terms variability and probability of damage, which pertain to target response; nor do these estimates include operational considerations such as linear, circular, or spherical aiming and fuzing errors, yield variations, and target intelligence.

The experimental data from high-altitude bursts are still too meager to present reliability of physical phenomena statistically, or damage data directly from test results. Estimates of upper and lower limits are given to indicate the uncertainty believed to be associated with the phenomena and damage data presented.

1-2 WEAPON RATINGS. To provide a yardstick for rating the total energy release of a nuclear detonation, one usually expresses the total yield of a nuclear device in terms of a TNT energy equivalent. For example, if the total energy of the blast, thermal radiation, and nuclear radiation released by a nuclear weapon is the same as the energy released by the detonation of 1000 tons of TNT, the nuclear weapon is rated as a 1000-ton, or 1-kt (kiloton) weapon. When 1 kg (kilogram) of U-235 or plutonium undergoes fission, nearly 1 g (1/450 lb) of matter is converted into energy. This energy expressed in terms of TNT energy equivalence

[redacted]

would be the same as for the detonation of 20,000 tons of TNT. Similarly the fusion of 1 kg of deuterium results in the transformation of 2.65 g of matter into energy, with an energy release equivalent to that resulting from the detonation of 57,000 tons of TNT.

Another method used, and one that is often confused with the rating of energy in terms of TNT energy equivalence, is the rating of effects in terms of TNT effects equivalence, i.e., the effect of a particular phenomenon of a nuclear detonation expressed in terms of the amount of TNT that would produce the same effect. An example of TNT effect equivalence would be the expression of the crater radius of a nuclear surface burst in terms of the amount of TNT that would be required to produce the same radius.

For convenience, TNT equivalences are expressed in 1000 ton or 1,000,000 ton units, kt (kiloton) or mt (megaton), where 1 ton equals 2000 lb and the energy content of TNT is defined as 1100 calories per gram.

A "nominal" weapon is one whose yield is 20 kt. The use of this term arose from the approximately 20-kt yields at Hiroshima, Nagasaki, and the Bikini (Crossroads) tests. In some reports nuclear weapons effects data are based on the nominal weapon.

EXPLOSION OF A NUCLEAR WEAPON

1-3 GENERAL. An explosion is defined as the sudden release of a large amount of energy in a small space. For high explosives, this explosion is a chemical reaction, and the energy manifests itself primarily as blast energy, regardless of environmental conditions. In a nuclear explosion or detonation, however, the energy manifests itself in the form of blast, thermal, and nuclear radiation, and other electromagnetic phenomena. The energy released from a nuclear detonation is essentially from a point source, whereas a comparable amount of energy released from a high explosive detonation would require an enormous volume of explosive. Further, the energy released in a nuclear detonation results from a fission process, a fusion process, or a combination of the two, whereas the energy released in a high explosive detonation results from a chemical process that does not affect the nuclei of the atoms involved. In the fission process, the nuclei of heavy atoms are split into pairs of lighter radioactive atoms, whereas in the fusion process two light atoms are combined to form a heavier atom. In both processes there is a net loss of mass that appears as energy, and there is also an emission of nuclear radiation. Because of these fundamental differences between a nuclear and a conventional explosion, including the greater destructive capacity of the former, the effects and capabilities of nuclear weapons require special consideration and understanding.

1-4 EFFECT OF ENVIRONMENT AND TIME. The effects of nuclear weapons of particular design and yield are determined by the environment in which the weapon is burst, and the time frame under consideration. The initial physical phenomena from nuclear detonations are grossly the same during the first microsecond after initiation. Several minutes after detonation, the remaining effects will be only those of residual radiation, e.g., fallout, or perhaps atmospheric ionization and associated phenomena. Because the density, composition, physical state, and pressure of the medium surrounding the detonation primarily determine the resulting effects after the first microsecond, a time history of a nuclear detonation is given. This description is carried to the point when the energy released in the explosion begins to interact with its environment.

1-5 EARLY TIME HISTORY. When a nuclear weapon or device is detonated, the actual duration of the process, which depends on the design of the weapon, varies considerably. It is sufficient, however, to assume that the energy is released during the first microsecond. In this period, all the prompt nuclear radiation (neutrons, gammas, and neutrinos) has been emitted and has departed from the immediate environment of the weapon disintegration, leaving behind the energetic reaction products. These products rapidly approach an equilibrium state where the total mass of the weapon attains a high temperature and behaves as a Planckian radiator. (Although the fraction of reaction products that come from fission will continue to decay radioactively and emit additional gamma radiation and beta particles, they should be considered as secondary effects in this time frame.)

[redacted]

The high energy content of the residual weapon debris manifests itself by raising the debris temperature, and simultaneously creating tremendous internal pressures. Under the influence of these pressures, the hot debris immediately starts expanding at a very high velocity. Because it is radiating energy rapidly, and, because it is being cooled by its own adiabatic expansion, the residual weapon debris loses its high temperature rapidly. In times of the order of a microsecond, more than half of the debris energy has been radiated as X-rays and the debris effectively ceases to radiate. At the end of the period, the kinetic energy of the nuclear reaction products has either radiated away or has been converted into the kinetic energy of the directed motion outward of the debris. At this time, when all the important detonation processes have taken place, the weapon is ready to, or has begun to, react with its environment.

THE AIR BURST

1-6 DESCRIPTION. An air burst is defined as the explosion of a nuclear weapon at such a height that the weapon phenomenon of interest is not significantly modified by the earth's surface. (Also see description of high altitude burst in paragraph 1-26 to 1-29.) For example, when considering blast this height is such that the reflected wave passing through the fireball does not overtake the incident wave above the fireball (heights greater than about 160 $W^{0.4}$ ft $\pm$ 15 percent, where W is the weapon yield in kilotons). For thermal radiation, an air burst occurs at such heights above the surface that the apparent thermal yield viewed from the ground is not affected by surface phenomena, such as heat transfer to the surface, distortion of the fireball by the reflected shock wave, thermal reflection from the surface (heights above the surface greater than about 180 $W^{0.4}$ ft $\pm$ 20 percent for yields of 10 kt to 100 kt, and $\pm$ 30 percent for other yields). When considering fallout, an air burst occurs at such heights that militarily significant local fallout does not result (for yields less than 100 kt, a minimum height of burst of 100 $W^{0.4}$ ft; for yields greater than 100 kt, in the absence of data, the minimum height of burst may be taken conservatively to equal 180 $W^{0.4}$ ft). For certain other phenomena of interest, e.g., neutron-induced activity, initial gamma or neutron flux, the height of burst at which the earth's surface fails to produce an effect is difficult or impossible to distinguish.

1-7 DEVELOPMENT. (See figure 1-1.) The first interaction between weapon output and the surrounding atmosphere comes from the initial gamma rays emitted during the weapon detonation. These initial gammas arise both from the fission gammas and from gammas produced by inelastic neutron scattering in the weapon mass. The average energy of this complex spectrum is approximately 3 mev. These initial gamma rays, the mean free path (m.f.p.) of which is about 600 m in air at sea level, interact mainly by Compton collisions with the electrons of the air molecules. In this interaction, the gamma-ray (primary) photon collides with an electron and some of the energy of the photon is transferred to the electron, which is stopped after a very short distance. Another (secondary) photon, with less energy, then moves off in a new direction at an angle to the direction of motion of the primary photon. Consequently, Compton interaction results in a change of direction (or scattering) of the gamma-ray photon and a degradation in its energy.

In a typical case 40 percent of the gamma energy is given to the recoil electron, which is then stopped in a distance of about 5 m. Because the scattered gamma still has around 2 mev energy it will travel another mean free path of roughly the same length before it experiences a second collision, and in 3 or 4 m.f.p.'s, 90 percent or more of the gamma energy will have been deposited in the air. Of course, because of the exponential character of gamma absorption, the deposition will occur mainly in the first 1 or 2 m.f.p.'s.

The next important interaction between the weapon and the surrounding atmosphere occurs when the weapon mass begins to radiate. The radiating temperature depends on the weapon design and the total yield of the weapon. Typically, Planckian temperatures of [redacted] are reached. The major portion of the radiated energy then consists of soft X-ray photons of [redacted] energy. Because these X-rays have m.f.p.'s of less than

[redacted]

20 cm in normal density air, the radiated energy is absorbed by the air in a sphere that initially may be only a few meters larger than the weapon. But because this sphere itself is at a high temperature and again radiates X-rays (although at a lower temperature) the process of re-radiation and absorption (called radiation diffusion) continues until the energy radiated by the weapon may occupy a sphere of air of approximately 50 m diameter (for a 20-kt weapon). The emission of this additional electromagnetic radiation covers a wide range of frequencies from about 1 cycle per second through radio, infrared, and visible to the soft X-rays.

Until the temperature falls to about 300,000°K (540,000°F), this additional electromagnetic radiation is the most rapid means of energy transfer, and hence is the means by which the surrounding air is heated to incandescence. When the temperature drops below about 300,000°K, the transport of energy by hydrodynamic motion becomes faster than by radiation diffusion and a shock wave becomes the primary mechanism for making the surrounding air incandescent. At this point the expansion of the hot sphere of gas, the fireball phase, begins. As long as the shock wave is strong enough to cause the shock-heated air to be luminescent, the boundary of the observable luminous sphere (the fireball) is the shock front. Actually this observable sphere consists of two concentric regions; the inner (hotter) region is a sphere of uniform temperature, surrounded by a layer of shock-heated air at a somewhat lower but still very high temperature.

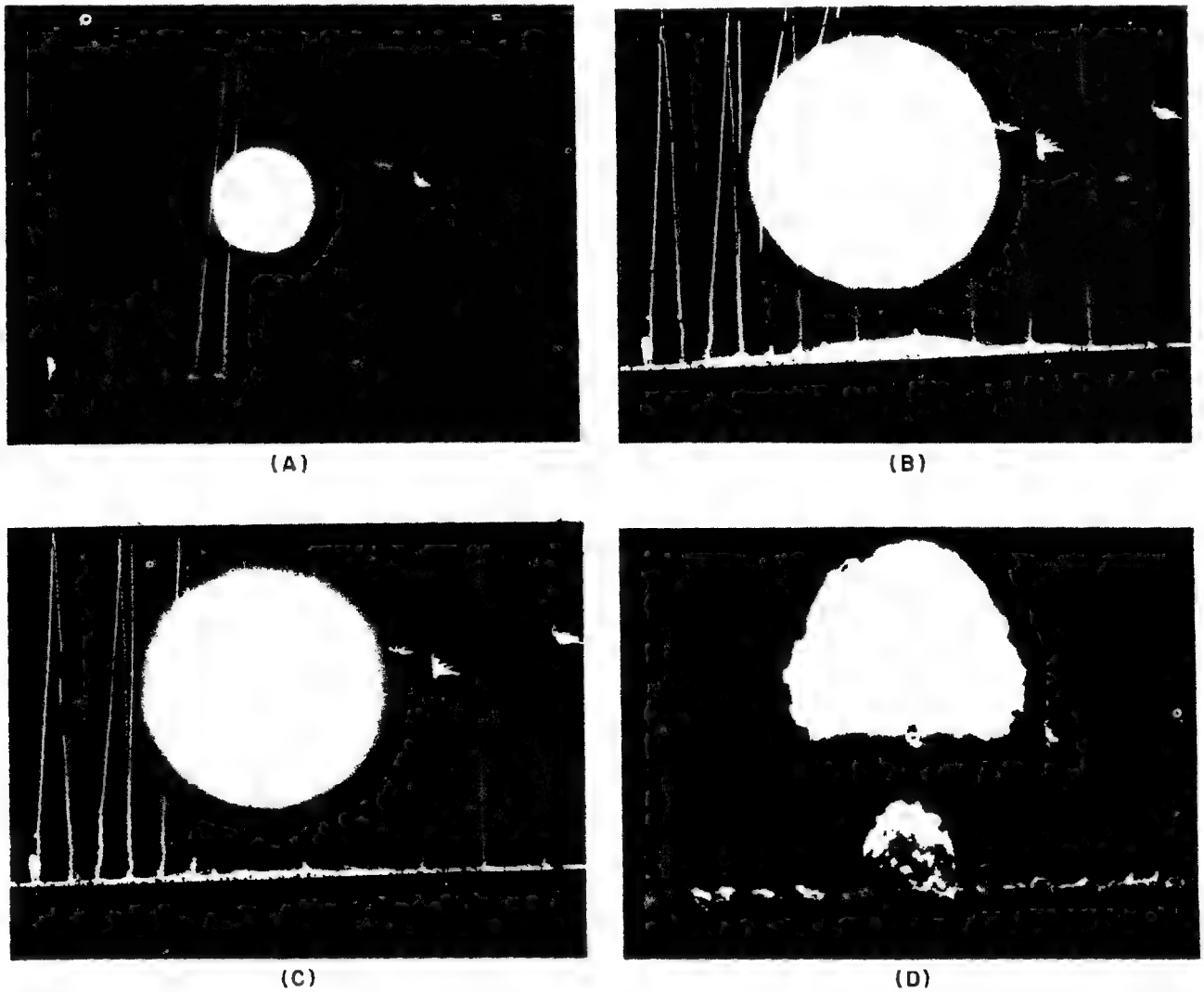

Figure 1-1. Development of an Air Burst

During the early stages of expansion of the incandescent shock front, the emitted radiant power increases as the luminous sphere increases in size, even though expansion causes a temperature decrease, until a maximum (the first maximum) is reached. At this point, the effect of the rapid rate of decrease in temperature overrides the enhancement of radiant power resulting from the increasing area of the luminous sphere.

Subsequently, further expansion causes a reduction in the radiant power. Eventually the shock front temperature is reduced to a point where the shock front is no longer incandescent, at which time the rate of emission of radiation from the shock front will be negligible. In effect, the shock front has become transparent, and the hotter incandescent inner core would be expected to be observable. Initially, however, the radiation emitted from the inner core is absorbed by compounds formed in the shock-heated air, and the radiant power reaches a minimum. As these compounds break down, the radiant power emitted from the inner core begins to pass through, and the inner core becomes the visible source of radiation. Thus, the radiant power increases again. This change in boundary of the observable luminous sphere from the shock front to the incandescent inner core gives rise to the term "breakaway."

As the opacity of the shock-heated air decreases, the apparent temperature as measured from a distance approaches that of the hot gases of the inner core, and the emitted radiant power approaches a second maximum. Further expansion and radiative cooling of the hot gases, however, give rise to a slow decrease in the radiant power. This decrease is so slow, relative to the previous rises and decline, that a large percentage of the total radiant energy emitted is delivered during this period. Finally, the rate of delivery of radiant energy drops to a low value.

The subsequent characteristics of the shock, or blast, wave are discussed in paragraph 1-8 below and Chapter 2. The effects of the thermal pulse are discussed in Chapter 3.

1-8 Blast Wave. A blast wave is characterized by a sharp rise in pressure, temperature, and density at its shock front. Thus, upon the arrival of a blast wave at a given location from the burst point, the sequence of events is a sudden increase in pressure, temperature, and density, followed by a subsequent decrease in pressure, temperature, and density to values below ambient, and a more gradual return to ambient conditions with the temperature going slightly above ambient. The overall characteristics of the blast wave are preserved over long distances from the burst point, but vary in magnitude with distance. With increase in distance, for example, the maximum pressure in the shock wave decreases, and the length of time over which the blast pressure is above ambient, the "positive phase," increases. Also, under conditions of high relative humidity (50 percent or higher), the drop in air pressure below ambient lowers the temperature sufficiently to cause condensation of atmospheric moisture to form a large cloud called the Wilson Cloud. When the air pressure again becomes normal, in a matter of seconds, the cloud disappears. Although the Wilson Cloud is spectacular, because it always occurs too far behind the shock front to modify the blast effects, and too late to reduce the thermal effects appreciably, it has no military significance.

The motion of the air away from the burst point during the positive phase and toward the burst point during the negative phase, is also characteristic of a blast wave. The pattern of the air motion or air velocity is the same as for the other characteristics, with maximum velocity occurring just behind the shock front and decreasing with distance from the burst point. At 300 yd from the burst point of a 1-kt weapon, the peak wind velocity is about 240 miles per hour.

1-9 Thermal Radiation. The relatively large amount of thermal radiation emitted in a nuclear detonation is one of its most striking characteristics. This radiant energy amounts to approximately one-third of the total energy of an air burst weapon. For a 50-kt weapon, for example, most of this radiation is emitted in about 2 sec, and is sufficient to cause serious burns to exposed personnel and to ignite some combustible materials out to distances of about 5000 yd.

[redacted]

1-10 Nuclear Radiation. A unique feature of a nuclear explosion is the nuclear radiation released. This consists of, but is not limited to, gamma rays, neutrons, alpha particles, and beta particles. About a third of this energy is emitted within the first second after detonation, the remainder being released from radioactive fission products and unfissioned bomb materials over long periods of time after the burst. Nuclear radiation is primarily an anti-personnel effect, with the penetrating radiations (gamma rays and neutrons) being the most dangerous. Lethal doses of initial gamma radiation from a 1-kt burst are received by exposed personnel out to about 700 yd. Residual nuclear radiation, due either to fallout or to neutron-induced gamma activity, can under certain conditions deny entry in a bombed area for some period of time after a detonation. Nuclear radiation effects on materials and equipment are of less significance, except for sensitive photographic materials and certain electronic components.

1-11 Electromagnetic Pulse Radiation. The pulse of electromagnetic energy in the frequency range from 1 cps to approximately 100 mc can cause disturbance or permanent damage to inadequately shielded or exposed electrical and electronic equipment at distances up to several thousand yards slant range. The energy of this pulse can also be directly transferred to electrically conducting media, such as wire transmission lines and cables, or to antenna devices, and transferred over longer distances to equipment where such damage may occur.

1-12 Cloud. Because of its relatively low density compared to ambient conditions, the mass of hot gases making up the fireball rises. The rate of rise may reach several hundred feet per second, after which it decreases rapidly. As the gases rise, they expand, cool, and condense, forming a radioactive cloud that consists largely of water vapor and metallic oxides from the weapon. As the fireball cools, the color changes gradually from red to a reddish brown, and ultimately water vapor from the air condenses sufficiently to produce a white color. As the heated mass of air in the fireball rises, cool air is pulled in from the sides and below, which may cause a doughnut-shaped ring to form around the column of hot air. This part of the cloud rolls violently as it rises. The cloud from a 1-kt detonation may reach a height of 5000 to 10,000 ft above the burst point, after which it is gradually dispersed by the winds.

THE SURFACE BURST

A surface burst is defined as the explosion of a nuclear weapon at the earth's surface. (Figure 1-2 shows the development of a surface burst.) When a nuclear weapon is burst at the surface of the earth the sequence of events in the development of the fireball and the formation of the blast wave is the same as that for an air burst, except that the fireball boundary and the shock front are roughly hemispherical. Because the earth's surface is an almost perfect reflector for the blast wave, the resulting blast effects are about the same as for a burst of twice the yield in free air.

1-13 GROUND SHOCK. When a burst takes place on the ground surface, part of the energy is directly transmitted to the earth in the form of ground shock. Also, the air blast wave induces a ground shock wave that, at shallow depths, has essentially the same magnitude as the air blast wave at the same distance from the burst. The directly transmitted ground shock, although of higher magnitude initially, attenuates radially faster than the air blast induced shock.

1-14 CRATER. For a burst on land, pressures of hundreds of thousands of pounds per square inch are exerted at the earth's surface, displacing material to form a crater and causing a downward compression of the soil. In addition to the material thrown out and compressed, a considerable quantity of earth is vaporized by the intense heat. A crater approximately 140 ft in diameter and 28 ft in depth is formed by a 1-kt weapon burst on a dry soil surface.

1-15 THERMAL RADIATION. Because of the heat transfer to the surface, the hemispherical shape of the fireball and the partial obscuration of the fireball by earth or water, the radiant exposure received by surface targets from a nuclear weapon burst on the surface is somewhat less than would be delivered by an air burst nuclear weapon of the same yield.

[redacted]

1-16 NUCLEAR RADIATION.

1-17 Initial. For a small yield weapon, owing largely to absorption by the surface, the initial gamma radiation from a surface burst is somewhat less at the same distance from the burst point than that from a burst of the same yield in free air. For high-yield weapons, where hydrodynamic effects (see paragraph 4-5) become important, a surface burst can be expected to produce as much or more initial gamma radiation as a burst of the same yield in free air, at the same distance from the burst point.

1-18 Residual. The contamination effects of residual nuclear radiation from a surface burst are greater than for an air burst, and hazardous radiological effects are produced over greater areas than those seriously affected by blast or by thermal radiation. Roughly half the available radioactivity resulting from a nuclear explosion on land, for example, can be expected to fall out in the general vicinity of the burst point. Dose rate contours near the burst point as great as 10,000 r/hr at $H + 1$ hr have been observed at tests, regardless of yield.

1-19 ELECTROMAGNETIC PULSE RADIATION. The statement of paragraph 1-18 applies.

1-20 CLOUD. For a burst on the surface, a great quantity of material is thrown out from the point of detonation. As the fireball rises, some material is drawn up under the fireball,

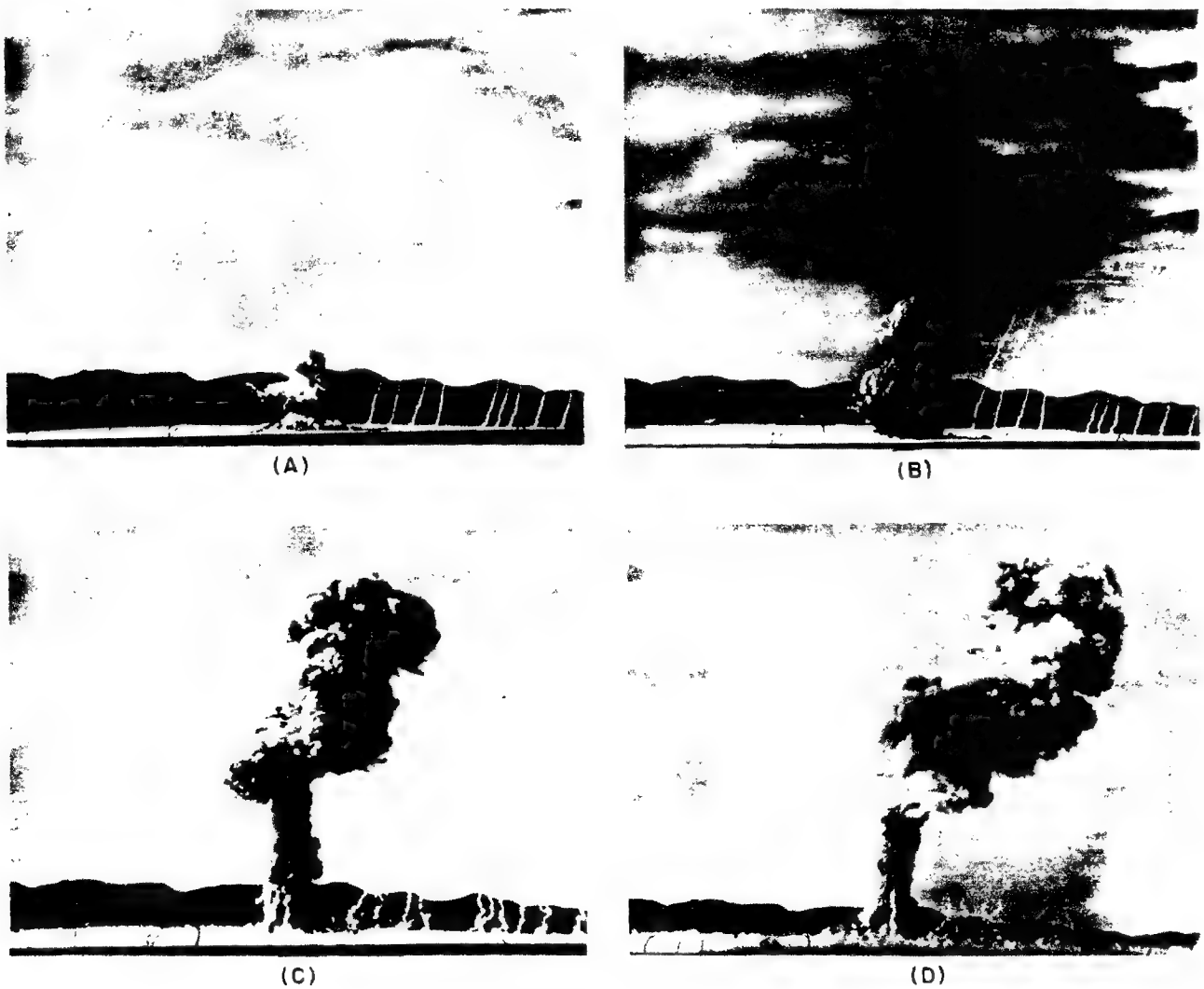

Figure 1-2. Development of a Surface Burst

forming a stem and sometimes forming a second cloud below the one that develops from the fireball. The stem and cloud(s) continue to rise and follow the course described for air burst.

1-21 SURFACE BURSTS ON WATER. In general, the phenomena as outlined in paragraphs 1-6 to 1-20 will occur for a surface burst on water. Also, the expanding sphere of hot gases depresses the water, causing the formation of a surface wave train and the transmission of a directly coupled shock wave into the water. The expanding air blast wave induces a shock wave in the water, which at shallow depths has essentially the same magnitude as the air blast wave at the same distance from the burst. Although the directly coupled water shock is of higher magnitude initially, it attenuates faster than the air blast induced water shock. As the height of burst increases from zero, depression, surface waves, and directly coupled water shock become smaller in magnitude. The formation of a crater on the bottom as the result of a surface burst in shallow water will depend on the depth of the water, yield of the weapon, and other factors. A 1-kt weapon, for example, detonated on the surface of water 50 ft deep with a soft rock bottom, will form a crater 130 ft in diameter and 4 ft deep.

THE TRANSITION ZONE BETWEEN AN AIR BURST AND A SURFACE BURST

1-22 DESCRIPTION. There is a sizable zone above the earth's surface where, for weapons detonated in the zone, the presence of the earth's surface significantly modifies one or more of the basic weapon phenomena. As the height of burst is successively lowered in this transition zone, the earth's surface plays an increasingly important role in modifying weapon phenomena; there is a gradual transition from the characteristics of an air burst to those of a surface burst. The upper boundary of the transition zone varies depending upon the phenomenon being considered, because the effect of the earth's surface ceases to be of importance at different scaled heights of burst for different phenomena, as mentioned in paragraph 1-4 above and covered in more detail in the discussion of specific weapon phenomena.

1-23 DEVELOPMENT. The development of a burst in the transition zone generally follows the sequence of events described in paragraph 1-7 above for an air burst.

1-24 Blast Wave, Thermal, and Nuclear Radiation. From the standpoint of blast, as the height of burst decreases from that of an air burst, peak air overpressures are more and more affected by the blast wave deflected from the surface, until total coalescence of the incident wave and the reflected wave occurs for a surface burst. From the standpoint of thermal radiation, the apparent thermal yield viewed from the ground decreases with increasing distortion of the fireball by the reflected blast wave, until the thermal yield and the fireball shape approach those characteristic of a surface burst. For nuclear radiation, local fallout becomes increasingly significant with decreasing height of burst, and, especially for large-yield weapons burst close to the surface, the hydrodynamic enhancement (see paragraph 4-5) of the initial gamma radiation becomes of considerable importance.

1-25 Ground Shock and Crater Formation. As the height of burst is lowered, directly induced ground shock increases in magnitude. Crater formation commences at a height of burst in the region of 60 $W^{1/3}$ ft by the mechanism of compression and scouring of the soil. At a height of burst less than about 10 $W^{1/3}$ ft, the expanding gases from a nuclear detonation form a crater by vaporization, throwing and compressing the soil in an outward direction from the detonation. Below this height of burst, crater radius and depth approach those of a surface burst.

THE HIGH ALTITUDE BURST

1-26 DESCRIPTION. A high altitude burst is here defined as the explosion of a nuclear weapon at such a height that the air density is so low that the interaction of the weapon energy with the surroundings is markedly different than at lower altitudes. At altitudes above 100,000 ft, the proportion of energy appearing as blast decreases markedly whereas the proportion of thermal energy increases. One phenomenological effect of primary interest is persistent ionization in the atmosphere. In contrast

to explosions below about 50,000 ft, high altitude bursts are unmuffled; the primary products of the weapon can escape to great distances, and the attendant ionization (in the atmosphere) can persist from minutes to hours. Although large yield air bursts at low altitude may also cause significant atmospheric ionization, the major phenomena are usually considered to be blast and thermal effects. It is known that large electromagnetic pulses are generated by high altitude bursts, but the mechanism is not yet understood.

The important consequences of high altitude bursts probably will be damage to weapon systems operating in the upper atmosphere or in space, or effects on electronic systems relying on electromagnetic waves propagating through or near the region of the burst. For weapons less than a megaton, blast and thermal effects produced at the earth's surface are likely to be incidental, although they must still be considered.

1-27 DEVELOPMENT. As the detonation altitude is raised, the energy carried away from the weapon mass by radiation transport penetrates to greater distances before being stopped by interaction with the air. About 70 percent of the weapon energy is quickly transferred to the surrounding air by radiation in the form of X-rays. Some 25 percent of the weapon energy remains contained as kinetic energy of the debris particles. The X-rays are absorbed by the surrounding air, heating it to incandescence. The incandescent air further radiates softer X-rays and ultraviolet radiation, which are absorbed by a larger surrounding shell of air, and so forth. By such radiation the inner part of the heated region is cooled and the outer part is heated. Within a millisecond a region at a temperature [redacted] is formed that now radiates less rapidly and principally in the visible and infrared part of the spectrum. The increase in pressure above that of surrounding air starts the region expanding. The strong vertical pressure gradient causes an upward force on all parts of the region that gives it a boost or ballistic impulse upward.

From the diffuse boundary of this heated region, the expansion starts an outward moving shock wave, and also an inward moving wave that relieves the large pressure gradients within the region. The inward moving wave moves at the speed of sound in that medium, so that the strong pressure gradients, and the upward acceleration resulting from them, last longer for particles nearer the center of the region than for those near the periphery. This gives the center a higher upward velocity than the outer part of the heated region. Also, expansion of the heated region reduces its density, and a region of reduced density tends to rise until it is in equilibrium with the surrounding atmosphere. The short ballistic impulse and the continuing buoyancy caused by the expansion determine the upward rise of the heated region and the central core of debris particles that it contains. One or the other of these forces may dominate, depending on the altitude of burst.

The debris, which contains about 25 percent of the weapon's yield as kinetic energy, expands rapidly. Most of this kinetic energy is seen in the form of radial velocity from the burst point. It generates a strong shock wave in the X-ray heated air surrounding the burst point, so this air is also given a large radial velocity. The net result of this debris-initiated shock wave, and the buoyancy and upward ballistic impulse forces, is that the central part of the X-ray heated region moves upward far above the burst point and there continues to expand.

A chronological development of the early time history following a high altitude burst, shown in figure 1-3, is discussed below.

1-28 Debris Expansion. The innermost region shown in figure 1-3 is the debris composing principally the material of the weapon and its casing. It is characterized by continuing radioactive emissions from the fission products. Depending on the detonation altitude and weapon yield, the initial ballistic impulse may be much greater than necessary to carry the debris to the altitude for buoyant equilibrium. As a result, under the force of gravity, the debris will rise ballistically high into the atmosphere, lose its vertical velocity and begin to fall again. Most of the debris will fall until it encounters denser air that decelerates it rapidly and produces a fairly thin layer that continues to expand.

1-29 Dissociated Region Expansion. Surrounding the debris and also rising and expanding is a considerably larger region of many

times the debris mass, which was originally wholly dissociated into atomic oxygen and nitrogen and almost completely ionized into electrons and positive ions by X-rays. This is called the "dissociated region" after its initial state, although partial reassociation may occur rapidly for some altitudes of burst. The ballistic impulse and buoyancy forces carry the debris and surrounding dissociated region far above the burst point where they expand in rarified air to radii of hundreds to thousands of kilometers. The radial velocities are reduced by half when the regions encounter a mass of air equal to their own mass.

The debris-initiated shock wave, which in expanding imparts large radial velocities to the heated, dissociated, and ionized air surrounding the burst point, continues to expand and bound the "dissociated region." This outer boundary is termed the "ionospheric wave." The material between the ionospheric wave and the dissociated region is composed principally of ambient air molecules entrained by the outward moving ionospheric wave.

Figure 1-4 is a photograph taken from Mt. Haleakala on Maui, Hawaii 100 sec after the high altitude TEAK burst. Figure 1-5 is an artist's sketch from the photograph illustrating the regions discussed and indicating the major effects on various electronic systems.

THE UNDERGROUND BURST

1-30 DESCRIPTION. An underground burst is defined as the explosion of a nuclear weapon in which the center of the detonation lies at any point beneath the surface of the ground.

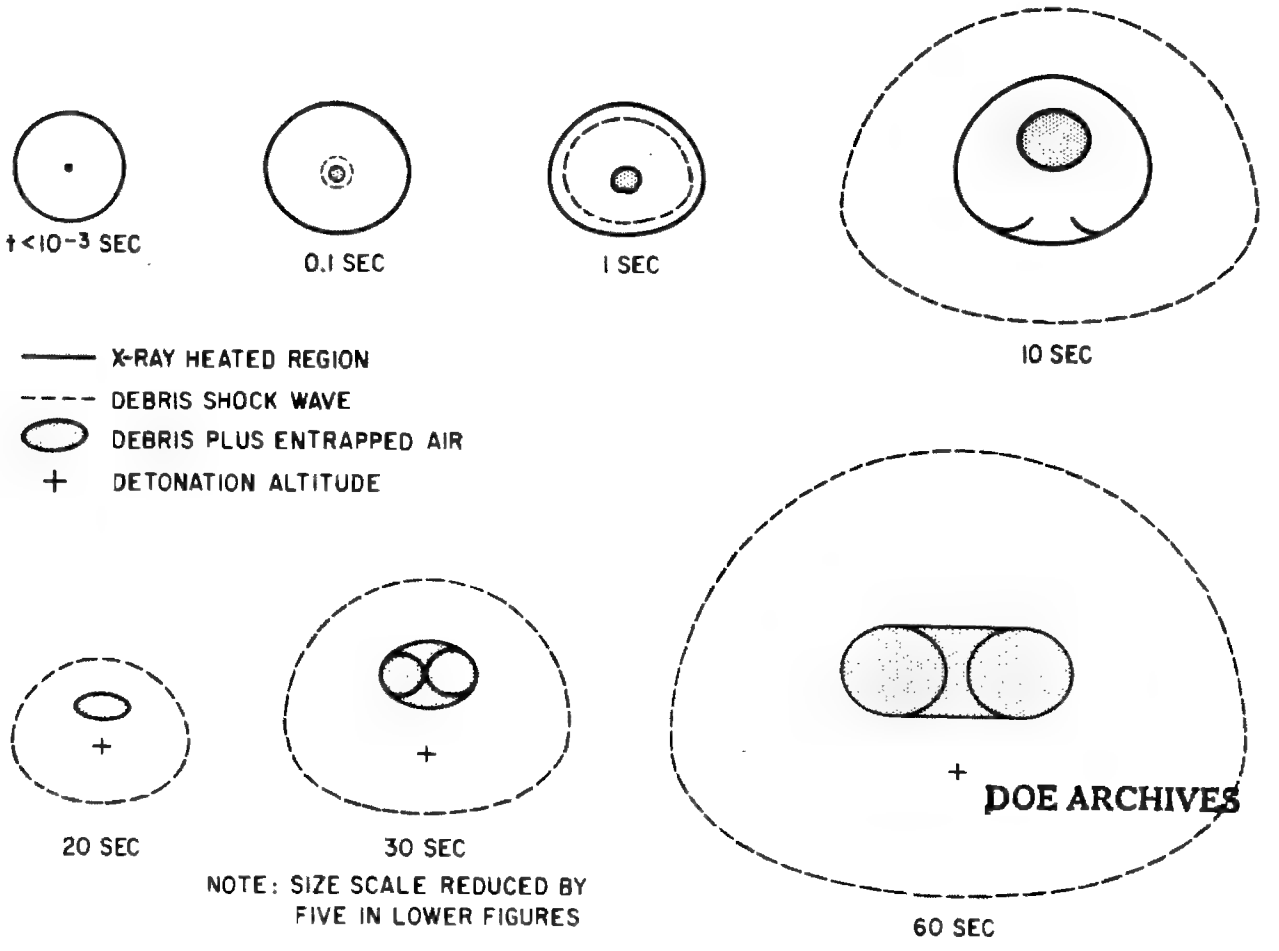

Figure 1-3. Chronological Development of High Altitude Nuclear Burst 80-km Megaton Burst

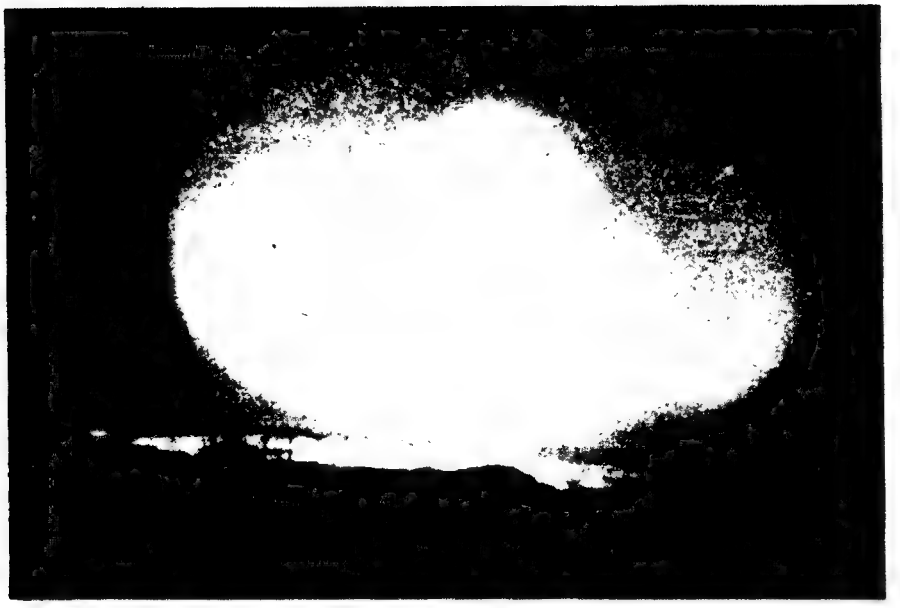

Figure 1-4. Photograph of TEAK from Maui (1300 km Away) After 100 Sec

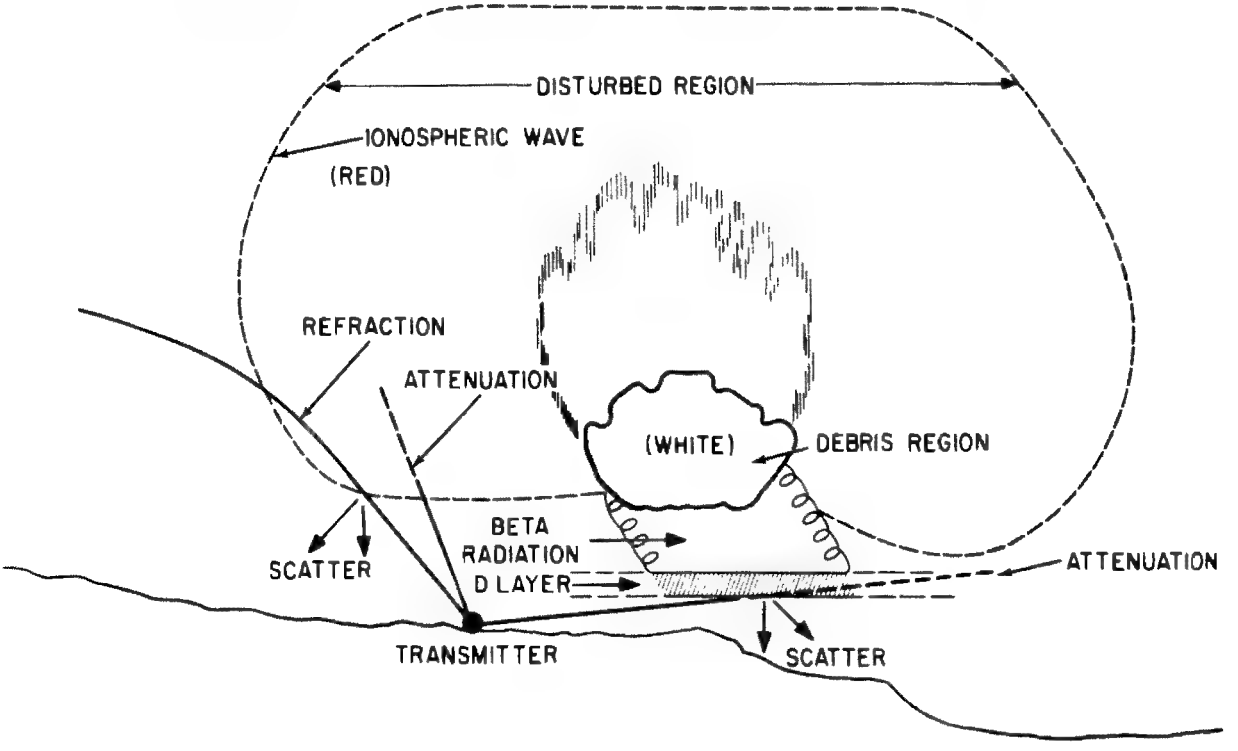

Figure 1-5. Sketch of Photograph in figure 1-4 to Identify Regions and Phenomena

[redacted]

1-31 DEVELOPMENT. Figure 1-6 shows the development of a shallow underground burst, figure 1-7 shows a deep underground burst. When a nuclear weapon is detonated at a sufficient depth underground, the ball of fire formed is composed primarily of vaporized materials from the bomb and vaporized earth. At shallow depths, light from the fireball generally may be seen from the time it breaks through the surface until it is obscured by dust and vapor clouds, a matter of a few milliseconds. The characteristics of the explosion and their related effects depend upon the depth, yield, and soil type. As the depth below the surface is increased, the characteristics depart gradually from those of a surface burst and finally, at depths of the order of 20 ft for a 1-kt detonation, the explosion exhibits the phenomena commonly associated with underground explosions. It is emphasized that the transition from the observed characteristics of a surface burst to those of an underground burst is not sudden, but that the characteristics change gradually.

1-32 Air Blast. Bursts at depths shallow enough to permit significant venting will produce air blast waves similar to those of air or surface bursts. As the depth of burst increases, the magnitude of the air blast will decrease.

1-33 Column, Cloud, and Base Surge. The first physical manifestation of an underground explosion at shallow depths is an incandescence

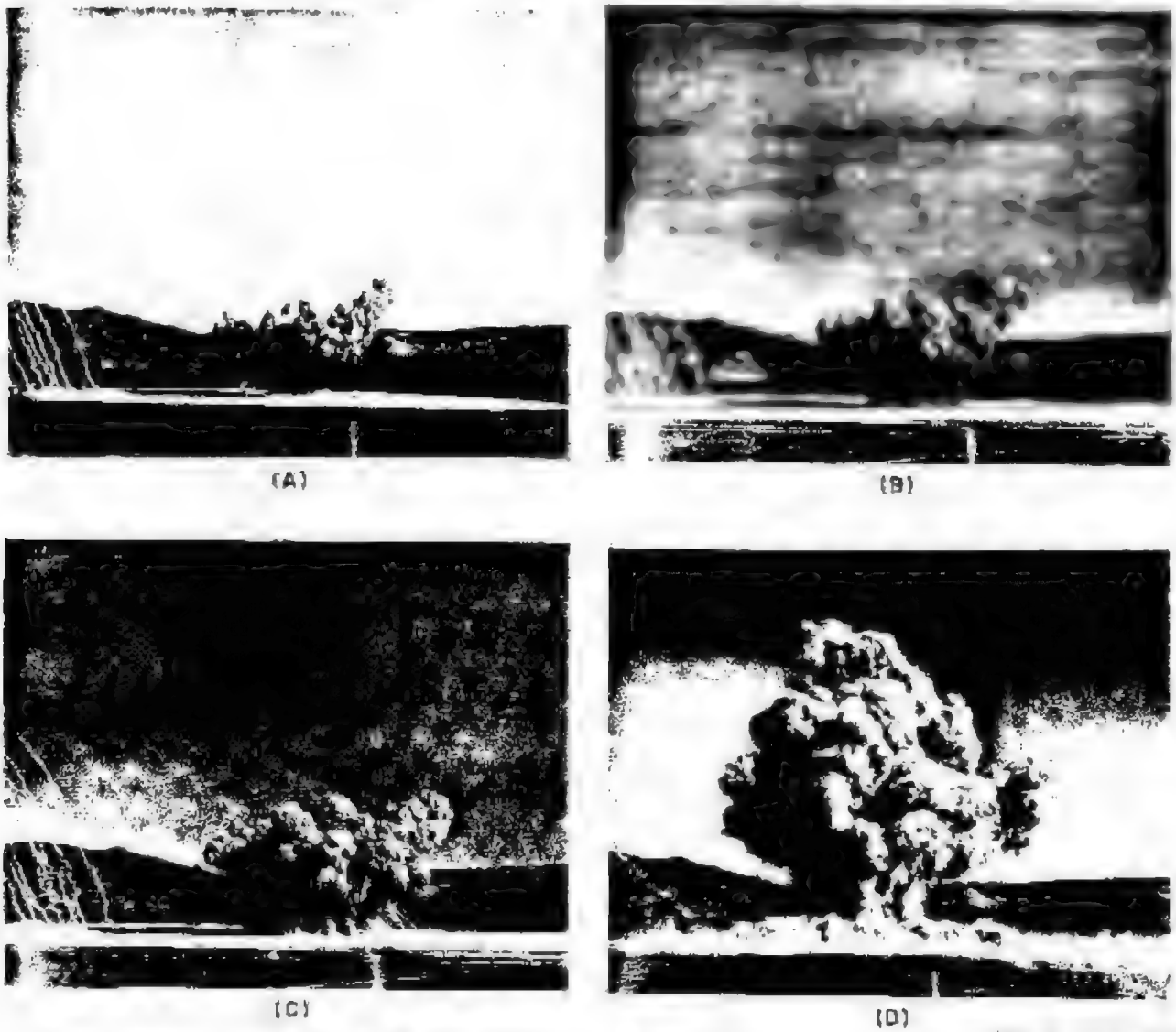

Figure 1-6. Development of a Shallow Underground Burst

[redacted]

at the ground surface directly above the point of detonation. This is almost immediately followed by large quantities of material being thrown vertically as a consequence of the direct ground shock reflection along the ground surface. Concurrently, large quantities of gas are released. These gases entrain additional quantities of material and carry them high into the air in the form of a cylindrical column. As the column rises it fans out and forms a dense cloud. Some of the particles thrown vertically, together with the entrained particles, behave like an aerosol with a density considerably greater than the surrounding air. This aerosol subsequently falls in the immediate vicinity of ground zero, and the finer soil particles spread out radially along the ground to form a low dust cloud called the base surge. For a 1-kt weapon burst at a depth of 20 ft, it is estimated that the column will reach a height of approximately 420 ft and a diameter of 660 ft, the base surge will be 4400 ft in diameter and the upper cloud will be 5000 ft in height. Dimensions of the base surge are discussed in paragraph 2-51. For shallower depths of burst, the column tends to assume the shape of an inverted cone rather than a cylindrical column and has a more pronounced radial throwout. Shallower depths of burst also become less favorable for the formation of a base surge, approaching the conditions of a surface burst where no base surge is expected.

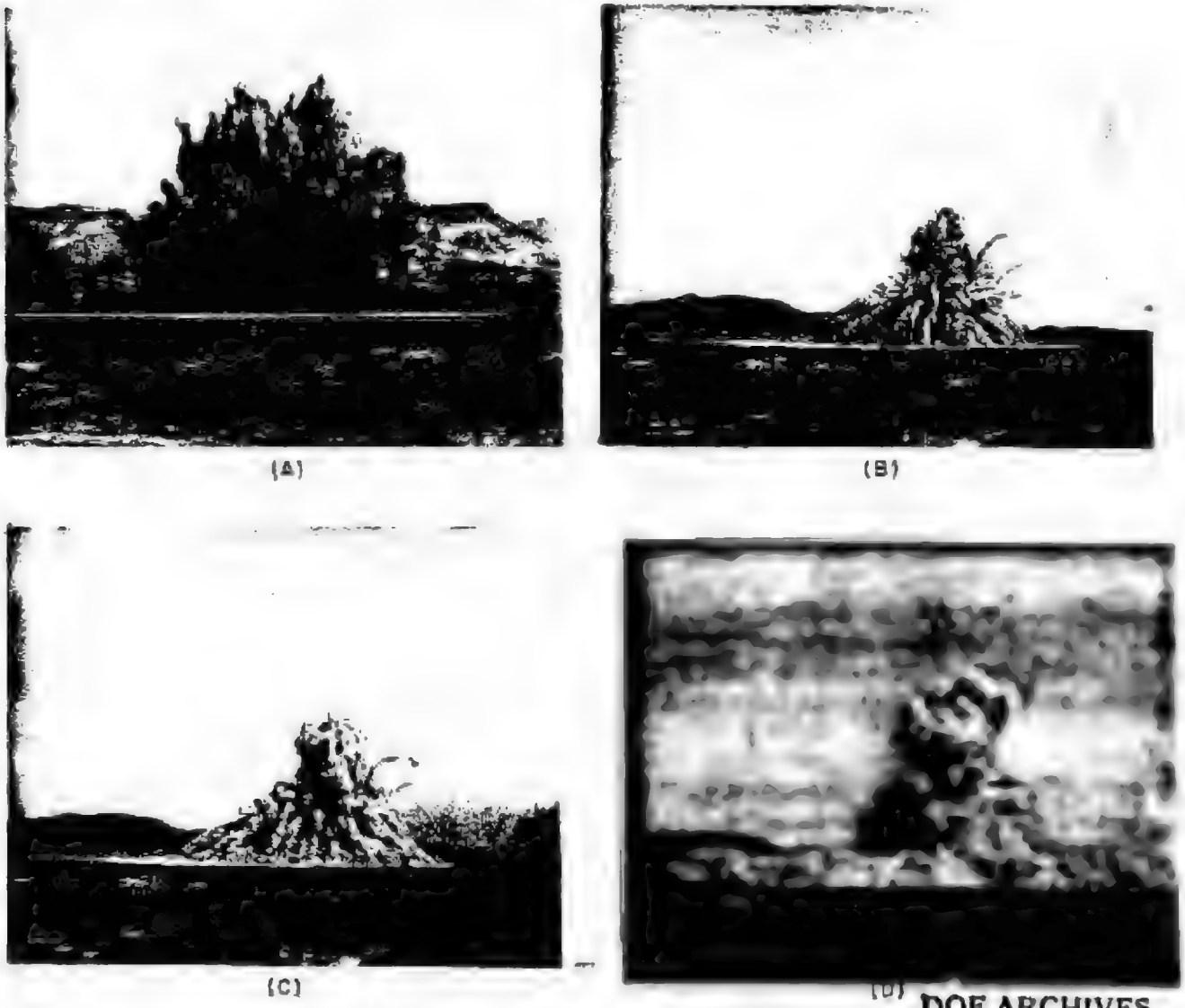

Figure 1-7. Development of a Deep Underground Burst

[redacted]

1-34 Ground Shock. As a burst is moved deeper and deeper into the ground, the directly transmitted ground shock increases in importance and the air induced ground shock becomes less important.

1-35 Crater. Formation of the crater from an underground burst is essentially the same as for the surface burst, except that more material is thrown vertically. At sufficiently deep depths the explosion will not vent to the surface and a cavity (camouflet) will be formed. There may or may not be disturbances at the surface, depending on the depth of the detonation and the material comprising the ground.

1-36 Thermal Radiation. If the underground burst is sufficiently deep, the fireball is obscured by the earth column; therefore, thermal radiation effects are negligible.

1-37 Nuclear Radiation. The *initial* gamma radiation becomes less than that described for a surface burst as the depth of burst increases, until it becomes insignificant for depths where a camouflet is formed. For shallow depths of burst, the *residual* radiation effects are similar to those of a surface burst; a large amount of residual radiation is deposited by the column, the cloud, and the base surge. As the depth of burst increases however, more and more of the contaminant is deposited in the immediate vicinity of the detonation, until for the case of no surface venting, all of the contaminant is contained in the volume of the ruptured earth surrounding the point of detonation.

1-38 Electromagnetic Pulse. For shallow depth of burst, the electromagnetic pulse should be similar to, but of lesser magnitude than, that for a surface burst of the same size. As depth of burst increases, the extent and magnitude of the pulse will diminish. In general, the electromagnetic pulse from such bursts should be a much less significant damage mechanism than ground shock. Adequate test data for prediction are, however lacking.

THE UNDERWATER BURST

1-39 DESCRIPTION. An underwater burst is defined as the explosion of a nuclear weapon in which the center of the detonation lies at any point beneath the surface of the water.

1-40 DEVELOPMENT AND BUBBLE. (Figure 1-8 shows development of a shallow underwater burst; figure 1-9 shows development of a deep underwater burst.) An underwater nuclear explosion releases large amounts of thermal and nuclear radiation, essentially all of which is absorbed by the surrounding water within several feet of the explosion. (Some radiation within the visible spectrum can be radiated to greater distances depending on the transparency of the water.)

During the early stages of the explosion, the bomb materials attain a very high temperature (on the order of millions of degrees) and a very high pressure (on the order of millions of atmospheres). Energy acquired by these materials is transferred to the layer of water closest to the bomb, which is heated and compressed and which, then, heats and compresses the next outward layer. By this mechanism, a wave of compression (the hydrodynamic or shock front) is formed and moves outward from the bomb. This front moves faster than the material it engulfs, which also moves outward but at a slower rate.

As the shock front moves away from the point of explosion, energy is dissipated in the form of heat, which raises the temperature of the water passed over by the front. The largest temperature increase occurs near the center of the explosion, where it is great enough that the water is not only vaporized, but dissociated as well. At somewhat greater distances, the water is vaporized and turned to steam; at still greater distances, the water is heated, but not to its boiling point.

Thus, shortly after an underwater burst, there exists an expanding bubble, composed largely of vaporized water with radioactive debris at its center, surrounded by heated water. Continued expansion of this bubble results in a pressure reduction within it. As the bubble pressure falls below the vapor pressure of the heated water, vaporization of additional water occurs at the interface of the bubble and the water.

In a deep underwater explosion, the bubble continues to expand at a decreasing rate until a maximum size is reached. If not too near the surface or the bottom, the bubble remains roughly spherical to this point. Because of the

[redacted]

inertia of the water set in motion by the "bubbles" early expansion, the bubble actually overexpands, i.e., when it does attain its maximum size, its contents are at a pressure well below the ambient water pressure.

The higher pressure around the bubble causes it to contract, with a resultant increase in internal bubble pressure, and condensation of some of the bubble contents. Because the hydrostatic pressure at the bubble bottom is larger than at the top, the bubble does not remain spherical during the contracting phase. Its bottom moves inward faster than its top (which may remain stationary or even rise slightly), contacts the top (forming a doughnut-shaped bubble viewed from above), and causes turbulence and mixing of the bubble contents with the surrounding water.

The inertia of the water set in motion by the bubble contraction causes it to overcontract, i.e., to contract to a point at which its internal pressure is very much higher than ambient water pressure. A second compression wave (the first bubble pulse) is emitted at this point, with a lower peak pressure but a longer duration than the initial shock, and a second cycle of bubble expansion and contraction begins.

During the initial expansion cycle, the bubble is relatively stationary, but upon contracting begins to migrate upward under the action of buoyant forces. The rate of upward migration is greatest at times of bubble minimum size, and

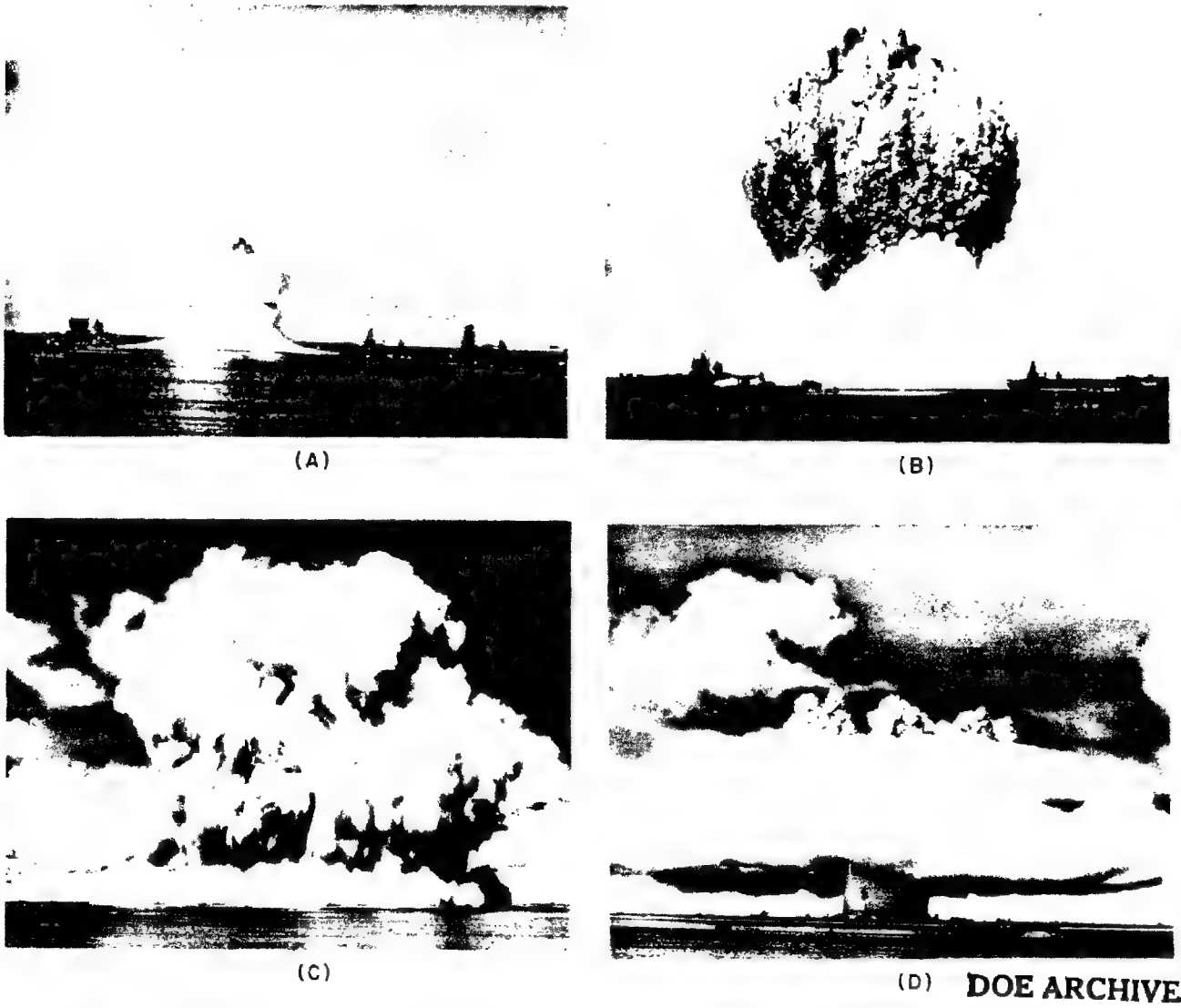

Figure 1-8. Development of a Shallow Underwater Burst

762-909 O - 65 - 4

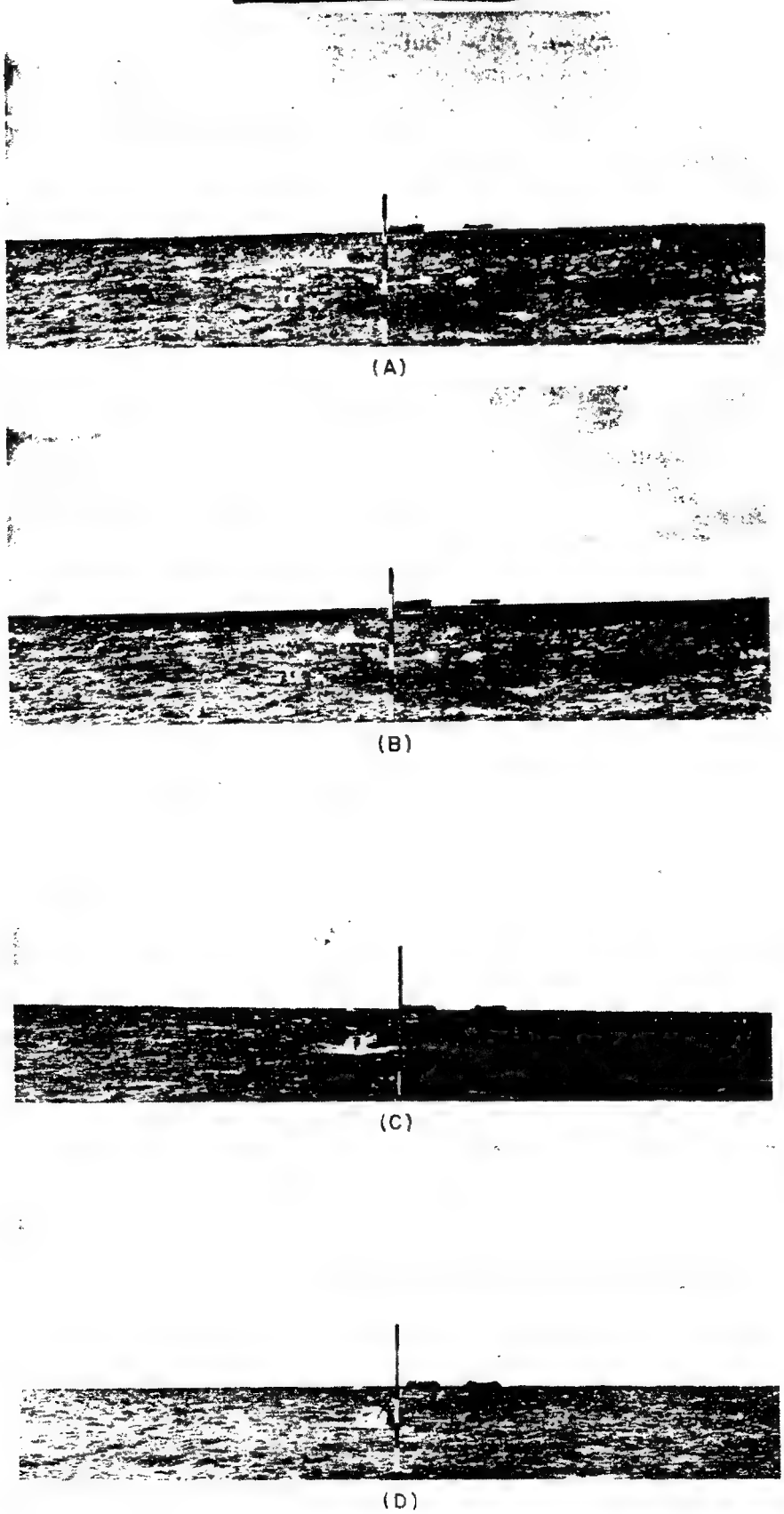

Figure 1-9. Development of a Deep Underwater Burst

is almost zero at times of maximum size, when the bubble is again almost spherical.

If far enough from the surface, the bubble continues to pulsate and rise, though after three complete cycles enough condensation of steam has taken place to make it unlikely that additional pulsations will occur. During pulsation and upward migration, however, the water in the vicinity of the bubble acquires considerable upward momentum, and eventually breaks through the surface with some violence.

For shallower bursts, the bubble may break through the surface during one of the early pulsations or even before completion of a single pulsation cycle. If such a breakthrough occurs during the portion of the cycle at which bubble pressure is higher than ambient pressure (as with a very shallow explosion), a phenomenon known as a blowout occurs. If breakthrough occurs when bubble pressure is below ambient pressure, the reverse phenomenon, blow-in, occurs. The character of the surface effects differs for the two phenomena. (See paragraph 1-43.)

If a burst occurs near the sea (or harbor) bottom, the general bubble behavior is as described above. A pulsating bubble, however, is drawn toward the bottom and, therefore, bubble migration toward the surface is slowed.

1-41 Water Shock Waves and Other Pressure Pulses. The primary shock wave that moves out from the explosion center is characterized by an extremely rapid increase in pressure (virtually instantaneous) to a very high initial or peak pressure, and then an almost exponential decrease to a value less than the hydrostatic pressure at the explosion point. Though a water shock wave superficially resembles an air blast wave, its peak pressures are generally much higher, and durations much shorter. In the absence of nearby boundaries, the shock wave proceeds outward radially at a very high initial velocity, which soon decreases to nearly the velocity of sound in water (about 5000 ft/sec). Shock wave velocity depends on water temperature, density, and salinity; and therefore, a shock wave may be bent (refracted) as it moves through regions of differing characteristics.

Shock wave reflections from the surface and bottom effect the shock and pressure field at a point distant from the explosion. Since reflection from the surface is in the form of a negative, or tension wave, it can cause a shortening of the pressure pulse (cutoff), and, when the shock wave encounters the surface at a small enough angle, can even reduce the magnitude of the primary pressure pulse. Reflection from the bottom generates a second compression wave in the water that can be effective in damaging ships.

Additional shock and pressure waves, generally of lesser importance than the primary shock wave or the bottom reflected shock waves, can be generated by shock wave energy that has been transmitted to bottom material or to the air and retransmitted to the water, by the collapse of a cavitation region near the surface, and by re-reflections of any of these.

Shock or compression waves from subsequent bubble pulses generally behave in the same manner as the initial shock wave and undergo reflection and refraction of the same character.

1-42 Air Blast. As in the underground burst, air blast waves are formed whose propagation depends upon the depth of burst. The first air blast wave from an underwater burst is that formed by the transfer of the shock front across the water-air interface. This front appears as a flat dome. The second air blast wave is transmitted by the venting bubble. This front will propagate essentially hemispherically. For shallow burst depths, the air blast wave resulting from venting is more intense than the shock wave transmitted across the water-air interface. For deep bursts, on the other hand, the shock wave transmitted across the water-air interface yields the higher pressures.

1-43 Surface Effects. The first surface effect of an underwater burst is caused by the intersection of the primary shock wave and the surface. Viewed from above, the effect appears to be a rapidly expanding ring of darkened water (often called the "slick"). Following closely behind the darkened region is a white circular patch (the "crack") probably caused by underwater cavitation produced by the reflected rarefaction wave. Shortly after appearance of the crack, the water above the explosion

rises vertically and forms a white mound of spray (the "spray dome"). This dome is caused by the velocity imparted to the water near the surface by the reflection of the shock wave and to the subsequent breakup of the surface layer into drops of spray. Additional slick, crack, and spray dome phenomena may result if the bottom-reflected shock waves and bubble pulse compression waves reach the surface with sufficient intensity.

For shallow bursts, the spray dome appears to be rapidly converted to a column formed by the upward and outward acceleration of the water surrounding the explosion. If blowout occurs, the upper part of the column is likely to be marked by a crown of explosion products. If blow-in occurs, the crown is likely to be absent. In its later stages the column may break up into plumes (relatively broad jets or spouts of water that disintegrate into spray as they travel through the air).

For bursts deep enough that blowout does not occur, but not so deep that bubble pulsation has ceased, plumes form.

If an explosion takes place deep enough for bubble pulsations to have ceased before the bubble reaches the surface, plumes caused by the upwelling of the water (and any uncondensed vapor or gas) may occur.

Upon subsidence of the column and plumes from an underwater explosion, a misty, generally highly radioactive, "doughnut-shaped ring" or series of rings, (the base surge) is formed. This ring spreads out radially in the absence of wind, but elongates and moves in the direction of wind, and eventually dissipates. A train of surface waves is also formed that moves radially outward from the explosion point.

After dissipation of the base surge, the water surface around the explosion is seen to be white. This area (the "foam patch") results from the upward motion of the water and uncondensed explosion products in the vicinity of the bubble; their spreading over the surface of the patch; and their downward motion at the edge of the patch. In its later stages, this area is marked mainly by a ring of foam and debris that shows where downward circulation has taken place.

1-44 Thermal and Nuclear Radiation. Thermal and nuclear effects, except in residual radiation effects, are considered insignificant for underwater bursts, except in shallow water where the effects will approximate those of a ground surface burst.

1-45 Electromagnetic Pulse Radiation. The degree to which an electromagnetic pulse is generated by an underwater burst is not known, but it is expected to be insignificant except for very shallow bursts. In such cases, it is believed that a diminishing effect above the surface, approximating that described for a shallow underground burst, will result.

2/21/85

PARTIAL DOCUMENT RECORD SHEET

Parts of this document were judged irrelevant to the CIC collection effort and were not copied:

Pages _____

Enclosures _____

Attachments _____

Other CHAPTERS 2 AND 3

Title page and table of contents have been copied for reference.

Dick Koogle
signature

9-15-87
date

DOE ARCHIVES

[redacted]

Chapter 4
NUCLEAR RADIATION PHENOMENA

GENERAL

4-1 RADIATIONS PRODUCED. When a nuclear weapon explodes, part of the energy appears as nuclear radiation made up of electromagnetic waves (including gamma rays), neutrons, alpha particles, and beta particles. One may distinguish two types of nuclear radiation when discussing effects on military personnel: initial radiation, which is delivered during approximately the first minute after detonation; and residual radiation, which is delivered thereafter, and which includes radiation from weapon debris and from neutron-induced activity in material outside the weapon case. Gamma rays are produced by the initial fission and fusion reactions, the fission-product decay, and the capture and inelastic scattering of neutrons in weapon materials, atmospheric nitrogen, soil, and other materials. They result from a rearrangement of protons and neutrons within the nucleus and, in this sense, differ from the X-rays generated by nuclear detonations, which result from a rearrangement of electrons outside the nucleus. (See Chapter 3 for a discussion of X-ray phenomena.) Also, because of the greater energy of the released gamma rays generated by the weapon, the effects differ appreciably from those of X-rays. Most of the neutrons are released in the initial fission and fusion reactions. Alpha particles originate either in the fusion reaction or in the decay of fissionable material, and beta particles are emitted by radioactive fission products. These general considerations apply to fission devices as well as to weapons combining fusion and fission reactions.

4-2 RELATIVE IMPORTANCE. The intensity and composition of nuclear radiation vary with weapon construction, and the environment in which the weapon is detonated. But, in general, weapons of large physical size, which usually contain relatively large amounts of material that attenuates (or absorbs) neutrons, deliver relatively low doses of neutron radiation as compared to initial gamma radiation. For weapons of small physical size, however, neutrons and initial gamma radiation will contribute approximately equally to the total initial radiation dose. Shielding can change the relative abundance of gamma rays and neutrons received at a target.

Most neutrons are produced within the first second after detonation, whereas gamma rays continue to be produced over a much longer period of time. Both neutrons and gamma rays result from the initial fission and fusion reactions, but gamma rays also continue to be emitted by the fireball, radioactive cloud, fission products deposited in the surface, and from elements in which radioactivity has been induced by neutron irradiation. Thus, both neutrons and gamma rays are significant in initial radiation but only gamma rays are significant in residual radiation.

Because the ranges of alpha and beta particles are very limited in air, and the particles are readily absorbed in most materials, they are of little military importance. But beta radiation may become a hazard where significant amounts of weapon debris are concentrated in proximity to the human skin.

4-3 ATMOSPHERIC EFFECTS. In a vacuum, gamma rays travel in straight lines with the speed of light and neutrons travel in straight lines with velocities determined by their energies. When passing through the atmosphere, however, both gamma rays and neutrons are scattered and absorbed by atmospheric constituents, particularly oxygen and nitrogen, so that they may arrive at a given point from many directions other than the line of sight path to the radiation source. This fact is important when providing shielding from nuclear radiations. The scattering also reduces gamma ray and neutron energies.

Air density is the controlling factor in attenuating radiation in the atmosphere. As air

[redacted]

density increases so, too, does the concentration of atmospheric constituents that absorb or scatter gamma rays and neutrons, and thus decrease the radiation dose delivered at a given range from a given source. Air density depends mainly on temperature and pressure changes—relative humidity has a negligible effect.

Relative air density is the ratio of the density of the atmosphere under a given condition to its density at 0°C and standard pressure. (Standard pressure = 1 atm = 1013 mb = 14.7 psi = 29.9 in. of mercury.) Average relative air density is the ratio of the average air density between two points (target and detonation) to density at 0°C and standard pressure. The curves of initial gamma radiation versus slant range (figures 4-9 to 4-16) and neutron dose versus slant range (figures 4-17 to 4-20) reflect the variation of initial gamma radiation and neutron dose with air density in terms of average relative air density. Appendix B gives typical relative air densities at various altitudes, and formulas and a chart for obtaining average relative air densities in various situations.

4-4 UNITS. Three common units of measuring nuclear radiation are the roentgen, the rad, and the rem. The roentgen is a unit of exposure dose, the rad is a unit of absorbed dose, and the rem (as discussed in Chapter 7) is a unit of biological dose. (See Appendix B for a discussion of other units.)

a. Gamma Radiation. Because gamma rays interact with matter in a number of ways, different materials may show different effects when exposed to gamma rays at a specified energy and intensity. One of the oldest units used to measure gamma rays (or X-rays) is the roentgen, which is defined in terms of the effect of radiation on dry air under conditions of standard temperature and pressure. The roentgen is not a measure of the effect of gamma radiation on any other materials. Human tissue exposed to a gamma radiation field, of say 1000 roentgens, may absorb more or less energy than a similar amount of some other substance exposed to the same field. Also, different gamma radiation fields, of again say 1000 roentgens, may deposit different amounts of energy in the same material. The roentgen does not describe effects on personnel.

A radiation-absorbed dose describes the amount of energy actually deposited in any given material exposed to a radiation environment. A commonly used unit of absorbed dose is the rad, which is defined as the absorption of 100 ergs of energy per gram of material exposed to radiation. With the development of "tissue equivalent" instrumentation for gamma radiation, one can describe gamma radiation in terms of its effect on soft tissue rather than air. Gamma radiation fields described in this manner are given in units of rads (tissue). A gamma radiation field described in terms of a given number of rads (tissue) means that soft tissue placed in the field will absorb an equivalent number of rads of radiation dose. Although the figures in this chapter use the term rad, for brevity, all the curves are for tissue. Thus, one rad of gamma radiation obtained from figures in this chapter means the dose of gamma radiation that will deposit 100 ergs of energy per gram of soft tissue.

b. Neutron Radiation. Neutron radiation dose may also be given in rads where one rad is defined as the absorption of 100 ergs of energy per gram of specified material. Again, because the curves given in this chapter are for tissue, a rad of neutrons obtained from the figures means the dose of neutron radiation that will deposit 100 ergs of energy per gram of soft tissue.

INITIAL RADIATION

4-5 GAMMA RADIATION. The initial gamma radiation delivered as a result of a nuclear detonation varies with weapon yield and design; relative positions of target, detonation, and earth surface, hydrodynamic enhancement resulting from the effect of the blast wave on the atmosphere; and average ambient air density. Table 4-4 and figures 4-8 through 4-16 allow computation of initial gamma radiation doses delivered to a target while taking into consideration the interaction of all these factors. Table 4-4 lists factors required to correct the data from figures 4-9 to 4-16 for various target and burst positions relative to the earth, figure 4-8 is a plot of hydrodynamic scaling factor times yield versus yield to account for hydrodynamic enhancement effects, and figures 4-9 through 4-16 represent the initial gamma

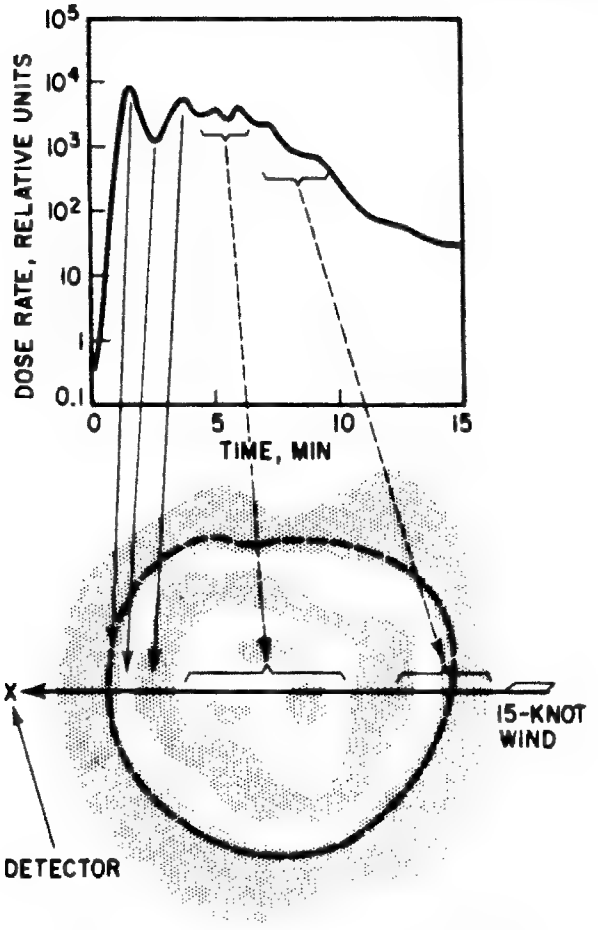

Figure 4-7. Dose Rate vs. Time for a Deep Underwater Burst

4-54 shows the cloud diameter-versus-time relationships. Figure 4-55 gives the dose received by personnel in aircraft flying through an atomic cloud at various times after the detonation.

RESIDUAL BETA RADIATION

In general, the hazard due to residual gamma radiation exceeds the beta hazard for all cases except those in which intimate contact with beta-active materials occurs, as when an individual lies prone in a contaminated area, or when particles fall out directly upon the skin or scalp. For such cases, superficial burns may result, as discussed in paragraph 7-21.

SHIELDING

The dose rates obtained from the contours described, and the total doses derived therefrom, are free-field values that must be reduced if the individual concerned is protected by some shelter. Shielding factors can be estimated from the considerations stated in paragraphs 7-26 through 7-28. For example, personnel in the open in a built-up city area would receive 0.7 of the free-field dose, whereas personnel in shelter such as the basement of a dwelling would receive about 0.1 of the free-field dose.

[redacted]

Problem 4-1 Initial Gamma Radiation Dose Curves For Yields Less Than 400 kt

The curves of figure 4-9 present the initial gamma-radiation dose in rads delivered to a surface target by a 1-kt air burst (height of burst greater than 1500 $W^{1/3}$ ft) as a function of slant range for several average relative air densities. These curves may be regarded as representative for weapons having yields less than 400 kt. The information from the curves in figure 4-9 may be extrapolated to other conditions (except subsurface bursts) and yields when multiplied by appropriate factors from table 4-4 and figure 4-8 using the following equation:

$$D_x = (f_{tb})(h_c \times W)D_1$$

where

D_x = initial gamma radiation delivered for a given average relative air density and slant range by detonation of a weapon of interest

f_{tb} = target-burst factor obtained from table 4-4 to account for the target and burst positions relative to the surface

$(h_c \times W)$ = hydrodynamic enhancement factor times yield obtained from the $h_c \times W$ vs. W curve in figure 4-8 to account for hydrodynamic enhancement effects for the yield of interest

D_1 = initial gamma radiation delivered to a surface target at the given range for the given average relative air density by a 1-kt burst (this is obtained directly from figure 4-9)

Example 1.

Given: A 10-kt surface burst, with average relative air density between target and burst of 0.8.

Find: Initial gamma radiation dose delivered to a surface target 1700 yd from the burst.

Solution: From figure 4-9(B), relative air density of 0.8, D_1 at 1700 yd is 15 rads/kt. From figure 4-8, $h_c \times W$ for a 10-kt yield is 10 kt. From table 4-4, f_{tb} for a surface target-surface burst condition is 2/3.

Answer: Therefore the initial gamma radiation delivered to a surface target 1700 yd from a 10-kt surface detonation in an average relative air density of 0.8 is:

$$D_x = (f_{tb})(h_c \times W)(D_1) = (2/3)(10)(15)$$
$$= 100 \text{ rads}$$

Example 2.

Given: A 0.01-kt air burst in an average relative air density of 1.

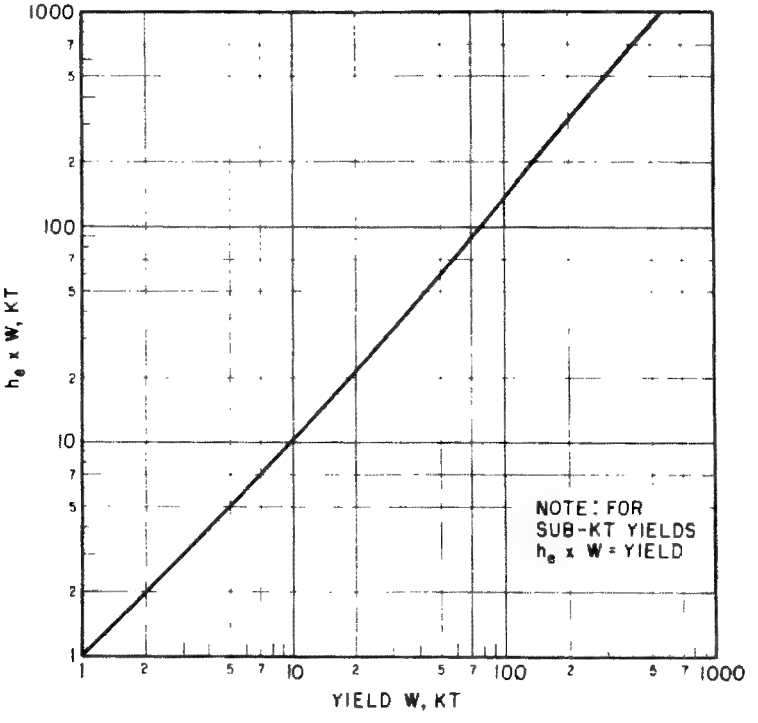

Figure 4-8. Hydrodynamic Scaling Factor Times Yield vs. Yield

[redacted]

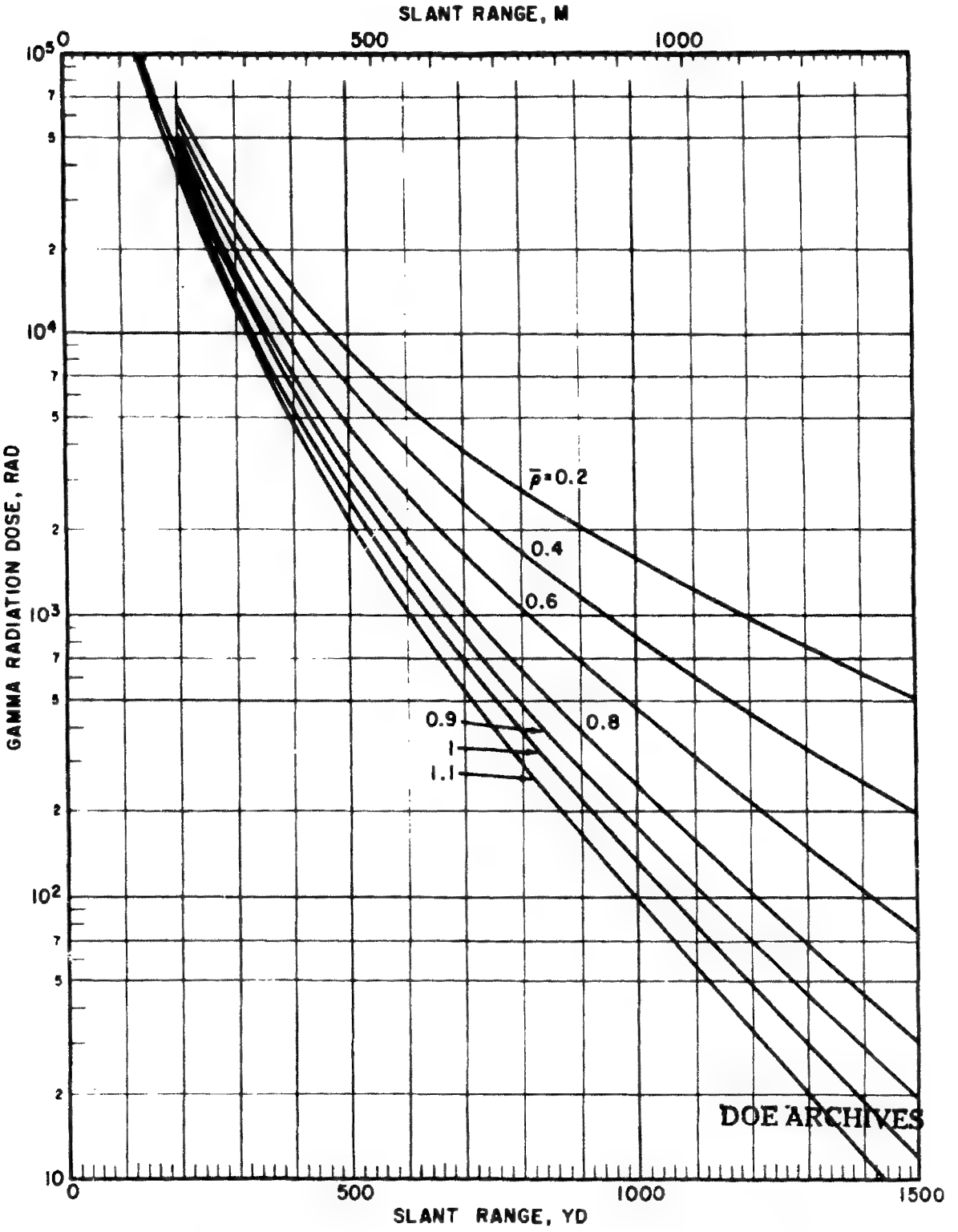

Figure 4-9(A). Initial Gamma Radiation Dose vs. Slant Range (to 1500 yd) for Various Average Relative Air Densities, 1-kt Air Burst-Surface Target

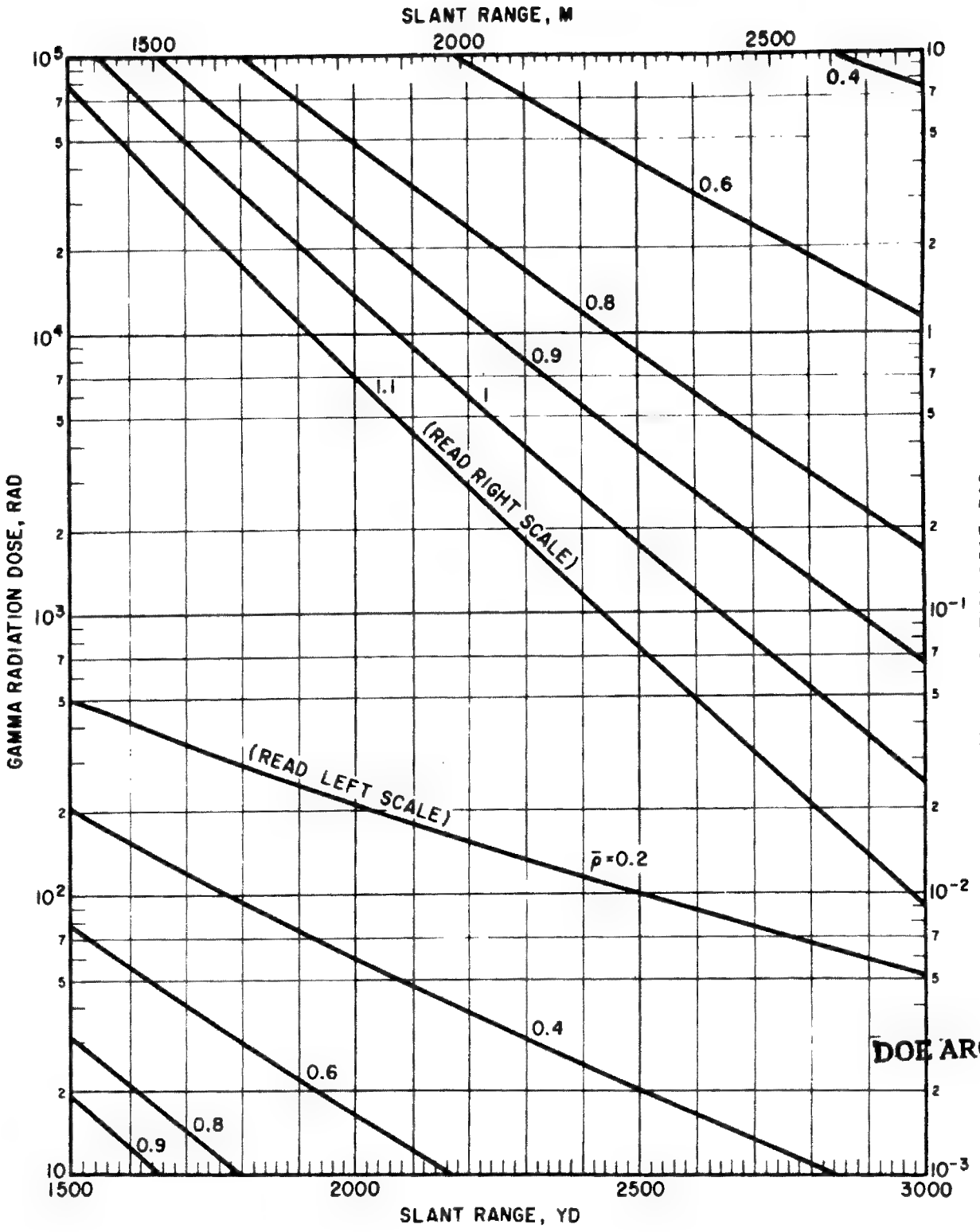

Figure 4-9(B). Initial Gamma Radiation Dose vs. Slant Range (over 1500 yd) for Various Average Relative Air Densities, 1-kt Air Burst-Surface Target

[redacted]

Find: The slant range at which a minimum initial gamma radiation of 500 rads will be received by a surface target.

Solution: From an examination of the equation, note that $D_x = 500$ rads is given.

From figure 4-8, $h_c \times W$ = yield for sub-kiloton yields, therefore $h_c \times W = 0.01$ kt.

From table 4-4, $f_{tb} = 1$ for a surface target-air burst condition.

Therefore $D_1 = D_x/(f_{tb})(h_c \times W) = 500/1 \times 0.01 = 50{,}000$ rads. This is the initial gamma radiation that would be delivered at the same range by a 1-kt air burst.

Answer: Using $D_1 = 50{,}000$ and an average relative air density of 1 enter figure 4-9(A) and read the slant range of approximately 180 yd. This is the slant range at which a minimum initial dose of 500 rads would be delivered to a surface target by a 0.01-kt air burst with an average relative air density of 1.

Example 3.

Given: A 100-kt detonation 4000 ft above the surface with an average relative air density of 0.8.

Find: The initial radiation delivered to a target 1000 ft above the surface and at a slant range of 2000 yd from the detonation.

Solution: The height of burst of 4000 ft is less than $1500\ W^{1/3} = 1500(100)^{1/3} = 7000$ ft (approx). Therefore the burst is in the transition zone and should be treated as a surface burst. Because the target is more than 300 ft above the surface, it should be treated as an air target. From figure 4-9(B), an average relative air density of 0.8, D_1 at 2000 yd is 5 rads/kt.

From figure 4-8, $h_c \times W = 135$ kt.

From table 4-4, f_{tb} for an air target-surface burst condition is 0.87.

Answer: Therefore the initial gamma radiation delivered to an air target 2000 yd from a 100-kt surface detonation with an average relative air density of 0.8 is:

$$D_x = (f_{tb})\ (h_c \times W)\ (D_1) = (0.87)\ (135)\ (5) = 587 \text{ rads}$$

Reliability. For sub-kiloton yields to yields of 100 kt, the doses obtained by use of figures 4-8 and 4-9 and table 4-4 are reliable within a factor of 2. Range obtained for a given dose within this range of yields will be reliable to within ±10 percent.

For yields from 100 kt to 400 kt the doses obtained are reliable within a factor of 5, and the range is reliable to within ±20 percent.

Table 4-4 Target-burst Factors (f_{tb}) for Various Ranges of Yield and Locations of Burst and Target With Respect to Surface

Burst and Target Orientation	Air Burst Surface Target	Air Burst Air Target	Surface Burst Air Target	Surface Burst Surface Target	Sub-surface Burst Surface Target
Yield	Target-burst Factors				
Less than 400 kt	1	1.3	0.87	0.667	Obtain dose or ranges directly from figure 4-10
0.4 mt to less than 10 mt	1	1.3	1.3	1	
10 mt to 20 mt	1 (use with air-burst-surface target curves)	1.3 (use with air burst-surface target curves)	1.3 (use with surface burst-surface target curves)	1 (use with surface burst-surface target curves)	
20 mt to 40 mt	1	1.3			

Note: Extrapolation to surface burst conditions for yields greater than 20 mt and to yields above 40 mt for any burst conditions is unreliable.

Burst Location—considered an air burst when height of burst is greater than $1500\ W^{1/3}$ ft.

Target Position—considered an air target when target location is greater than 300 ft above the surface.

[redacted]

[redacted]

Problem 4-2 Initial Gamma Radiation Dose For an Underground Burst

The curves of figure 4-10 present the initial gamma radiation dose as a function of distance for several air densities for a 1-kt underground detonation at 17 ft. They may also be used for underwater bursts.

Scaling. For other yields at about the same depth and the same relative air density, the dose at a given range is proportional to weapon yield. For relative air density see appendix B.

Example.

Given: A 5-kt burst 15 ft underground with relative air density $\bar{\rho} = 0.9$.

Find: The distance at which 450-rad initial gamma dose is received.

Solution: The quotient 450/5 = 90-rad dose for 1 kt.

Answer: From the curve of $\bar{\rho} = 0.9$, the range at which 90 rads is received is 1100 yd.

Reliability. The curves of figure 4-10 apply to weapons in the yield range from 0.2 kt to 7.5 kt and actual depths of burst from 12 to 22 ft. Used within the prescribed limits, results are good within a factor of 2, provided the soil at the point of burst is not too different from the soil at the Nevada Test Site. The error that would be introduced by a very different soil type is similar in origin, but not necessarily in magnitude, to the error that would be expected from a distinctly different burial depth. At the present time the effect of soil type cannot be estimated. Extrapolation to other yields is unreliable.

Related Material. See paragraph 4-5.

[redacted]

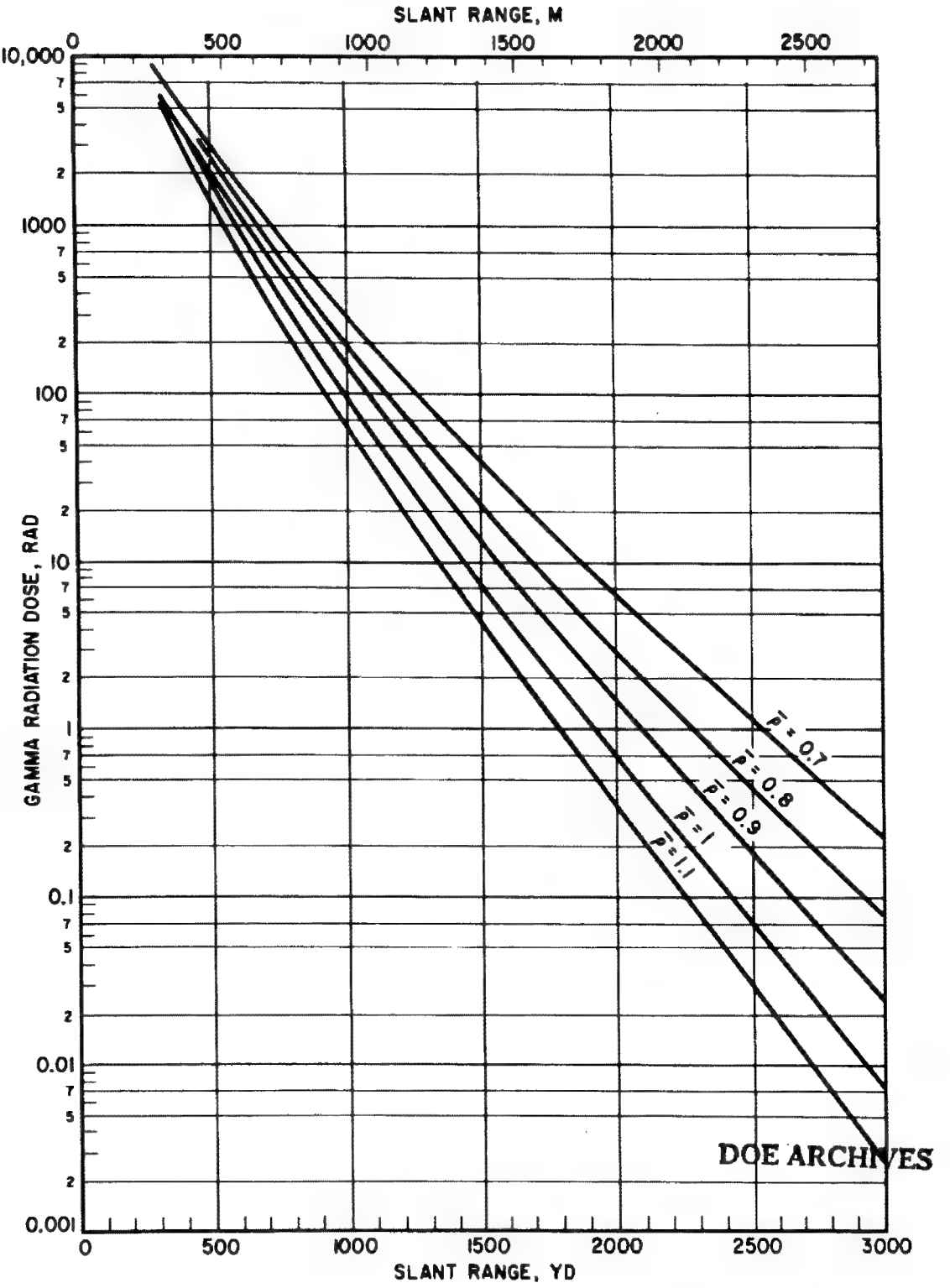

Figure 4-10. Initial Gamma Radiation Dose vs. Slant Range for Various Average Relative Air Densities, 1-kt Underground Burst, Surface Target Depth 17 ft

[redacted]

Problem 4-3 Initial Gamma Radiation Dose For 0.4 to 10-mt Yields

An average hydrodynamic scaling factor cannot adequately represent hydrodynamic enhancement for yields greater than 0.4 mt. For this reason, separate plots of initial gamma radiation versus slant range were drawn taking into consideration hydrodynamic effects for 0.4 mt and other selected megaton yields. Figures 4-11, 4-12, and 4-13 are plots of the initial gamma radiation dose in rads delivered to surface targets versus slant range for several relative air densities from 0.4-, 1-, and 4-mt air bursts, respectively. The radiation delivered by other yields may be obtained by interpolation. One can extrapolate to other burst or target positions relative to the surface through multiplication by an appropriate target-burst factor from table 4-4.

Example.

Given: A 0.4 mt air burst, with average relative air density $\bar{\rho} = 0.4$.

Find: The dose delivered to a target at the same altitude as the burst and at a slant range of 3000 yd.

Solution: From figure 4-11 for average relative air density $\bar{\rho} = 0.4$, the dose $D_{0.4}$ delivered to a surface target at a slant range of 3000 yd from a 0.4-mt air burst is 3100 rads.

From table 4-4, f_{tb} for an air target-air burst situation is 1.3.

Answer: Therefore, the initial gamma radiation delivered to a target at a co-altitude and 3000 yd from a 0.4-mt air burst in air with a relative density of 0.4 is:

$D_x = (f_{tb})(D_{.4}) = (1.3)(3100) = 4000$ rads

Reliability. The doses obtained within the range of yields from 0.4 to 1 mt using figures 4-11 and 4-12 are reliable to within a factor of 5, and ranges obtained for a given dose will be reliable to within ±20 percent.

The doses obtained within the range of yields from 1 to 10 mt are reliable to within a factor of 10 and ranges obtained for a given dose will be reliable to within ±30 percent.

[redacted]

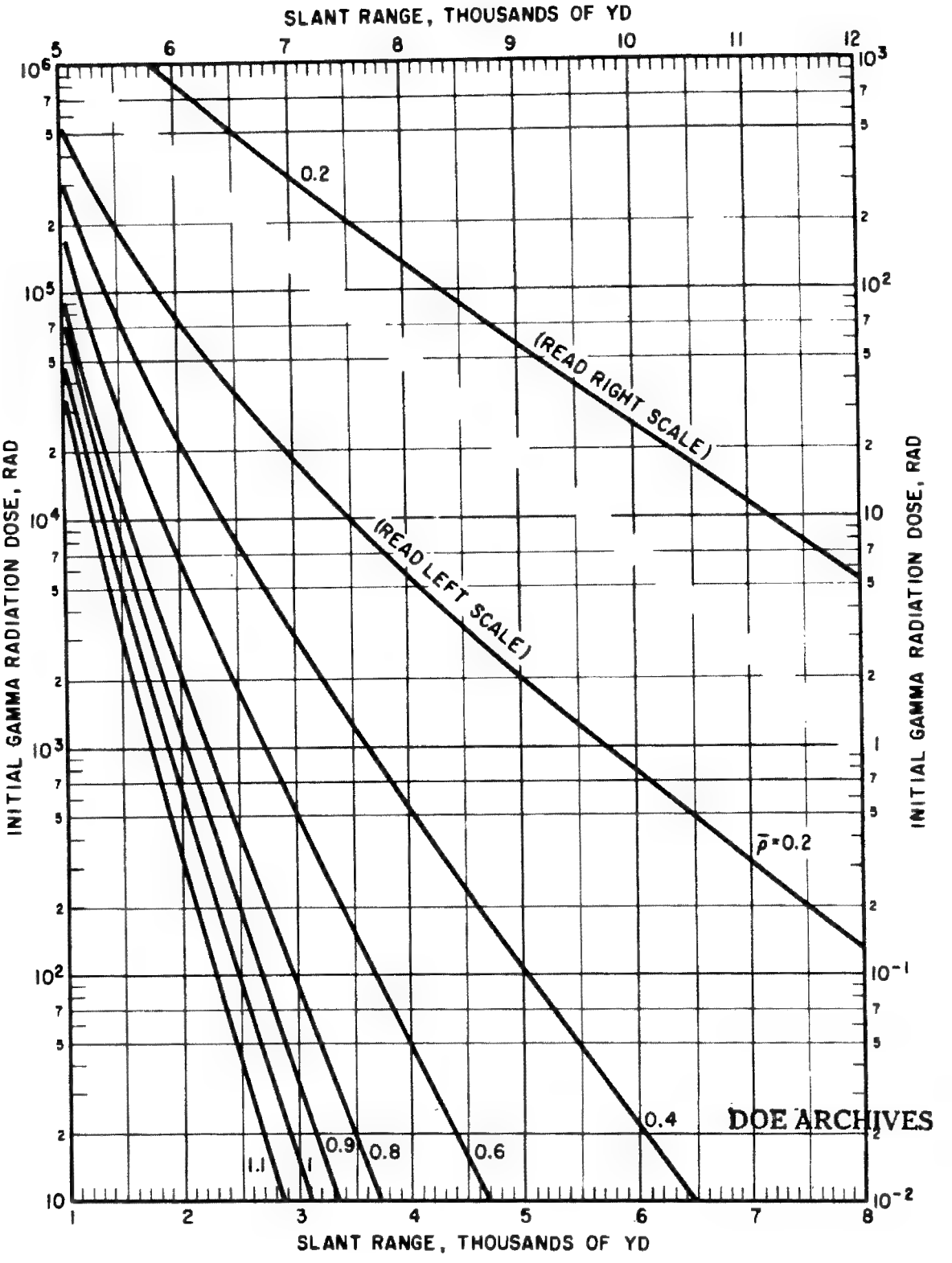

Figure 4-11. Initial Gamma Radiation Dose vs. Slant Range for Various Average Relative Air Densities, 0.4-mt Air Burst-Surface Target

80

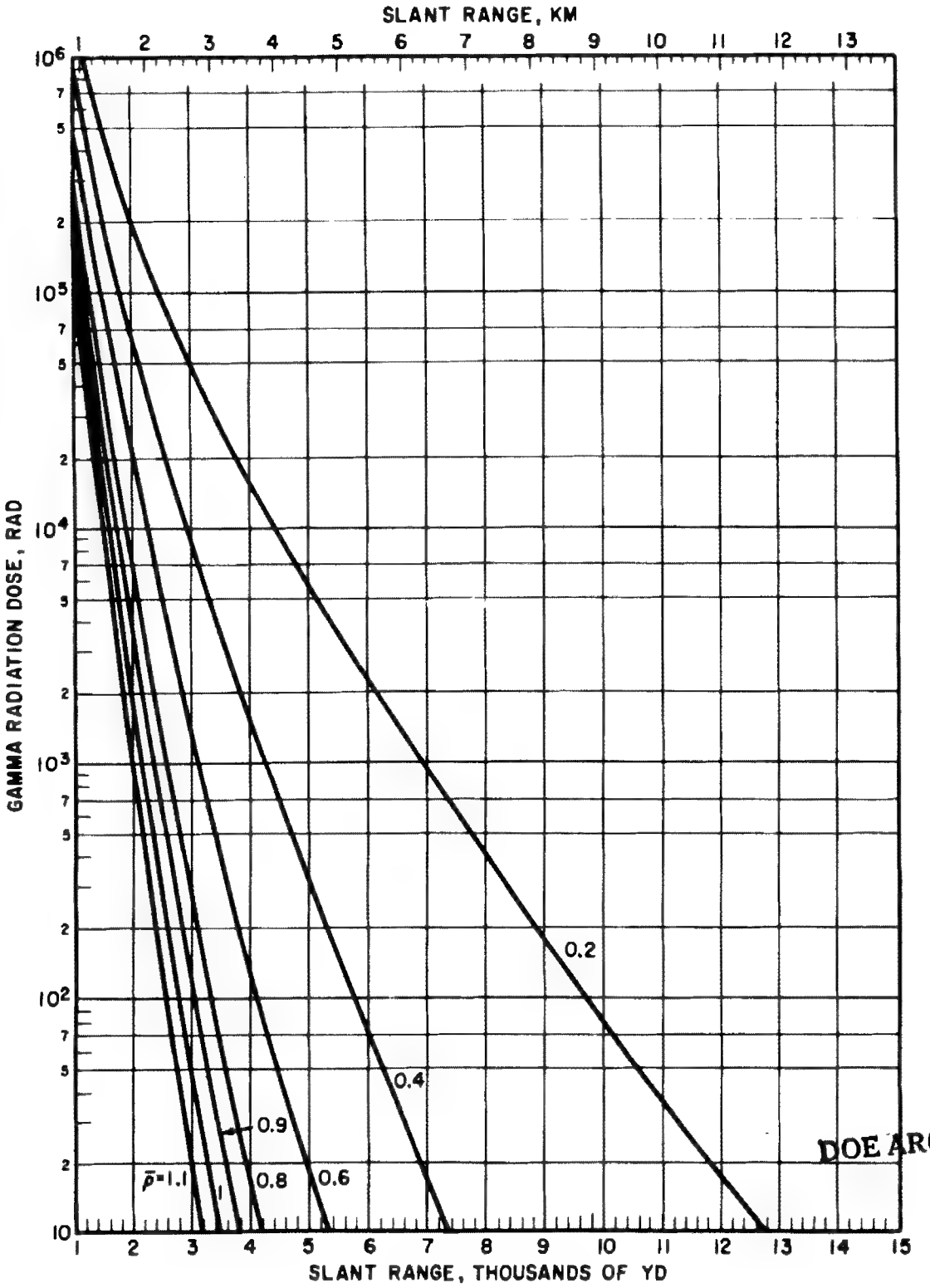

Figure 4-12. Initial Gamma Radiation Dose vs. Slant Range for Various Average Relative Air Densities, 1-mt Air Burst-Surface Target

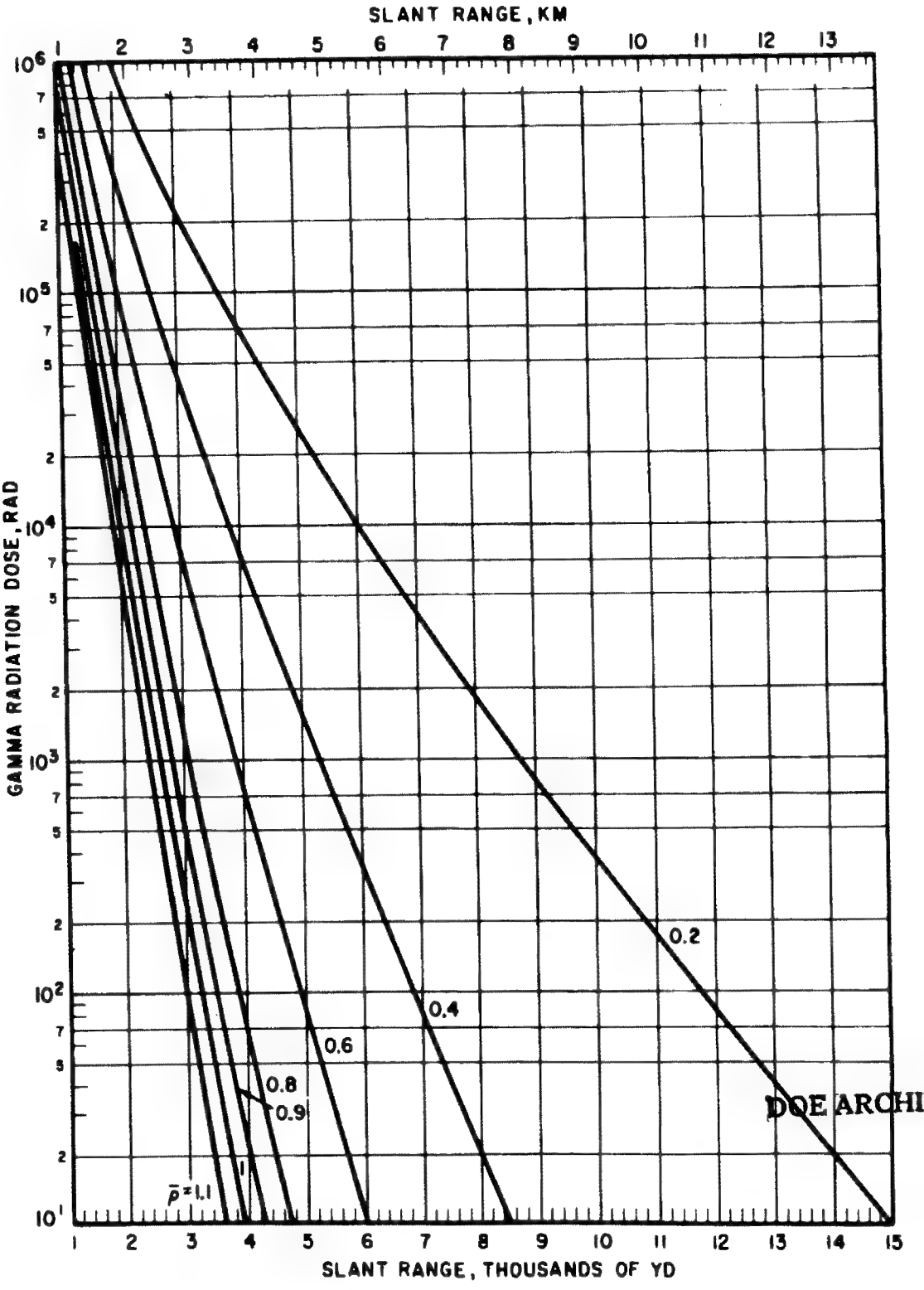

Figure 4-13. Initial Gamma Radiation Dose vs. Slant Range for Various Average Relative Air Densities, 4-mt Air Burst-Surface Target

The effect of the surface, air density, and range on hydrodynamic enhancement is so complex for yields of 10 mt and greater that extrapolation cannot be made, for initial gamma radiation, from air bursts to surface bursts over all ranges of interest by multiplication with a single target-burst factor. For this reason, curves of initial gamma radiation delivered to surface targets versus slant range from surface bursts of 10- and 20-mt weapons are included, along with similar plots for 10- and 20-mt air bursts, in figures 4-14 and 4-15 respectively. Information on yields between 10 mt and 20 mt may be obtained by interpolation. Airborne target situations may be satisfied through use of an appropriate target-burst factor from table 4-4.

Example 1.

Given: A 10-mt surface burst with an average relative air density of 0.8.

Find: The slant range at which a minimum initial gamma dose of 1000 rads would be delivered to a surface target.

Solution: From figure 4-14 and $\bar{\rho} = 0.8$ and a dose of 1000 rads read the slant range using the surface burst-surface target curves.

Answer: Slant range = 4800 yd.

Example 2.

Given: A 10-mt air burst with an average relative air density of 0.3.

Find: The slant range at which a minimum initial gamma dose of 1000 rads would be delivered to an airborne target.

Solution: The curves in figure 4-14 are for delivery of initial gamma radiation by 10-mt air and surface bursts to *surface targets*. The dose received by an airborne target is obtained by multiplying the dose received by a surface target by an appropriate target-burst factor from table 4-4, that is:

$$D_a = (f_{tb})\ (D_s)$$

where

D_a = dose received by airborne target

D_s = dose received by surface target (related to figure 4-14)

f_{tb} = target-burst factor from table 4-4

In this example the dose to be delivered to the airborne target is given: $D_a = 1000$ rads. The target-burst factor f_{tb} for an air burst-air target in the 10- to 20-mt range from table 4-4 is $f_{tb} = 1.3$. Therefore, D_s dose required for entry into figure 4-14 is:

$$D_s = D_a/f_{tb} = 1000/1.3 = 770 \text{ rads}$$

Answer. From figure 4-14 for an initial gamma radiation dose of 770 rads and an average relative air density of 0.3 (interpolate visually, $\bar{\rho} = 0.3$ would be approximately midway between the curves for $\bar{\rho} = 0.4$ and 0.2), read the slant range—approximately 8300 yd. This is the slant range at which a minimum initial gamma dose of 100 rads would be delivered to an airborne target by a 10-mt air burst with an average relative air density of 0.3.

Reliability. The doses obtained within the range of yields covered by figures 4-14 and 4-15 and table 4-4 are reliable to within a factor of 10, and the range for a given dose is reliable to within ±30 percent.

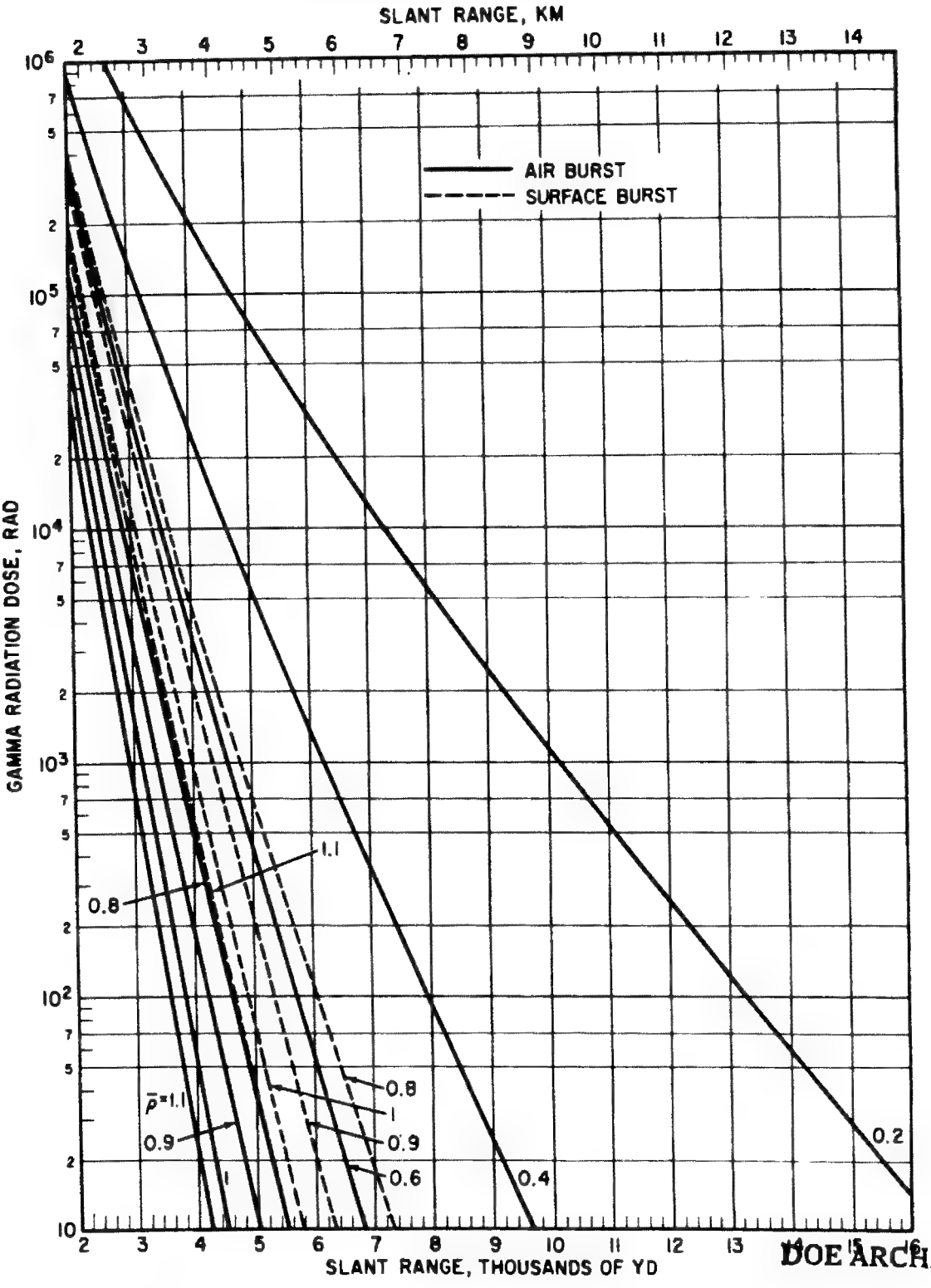

Figure 4-14. Initial Gamma Radiation Dose vs. Slant Range for Various Average Relative Air Densities, 10-mt Air Burst-Surface Target and 10-mt Surface Burst-Surface Target

762-909 O - 65 - 14

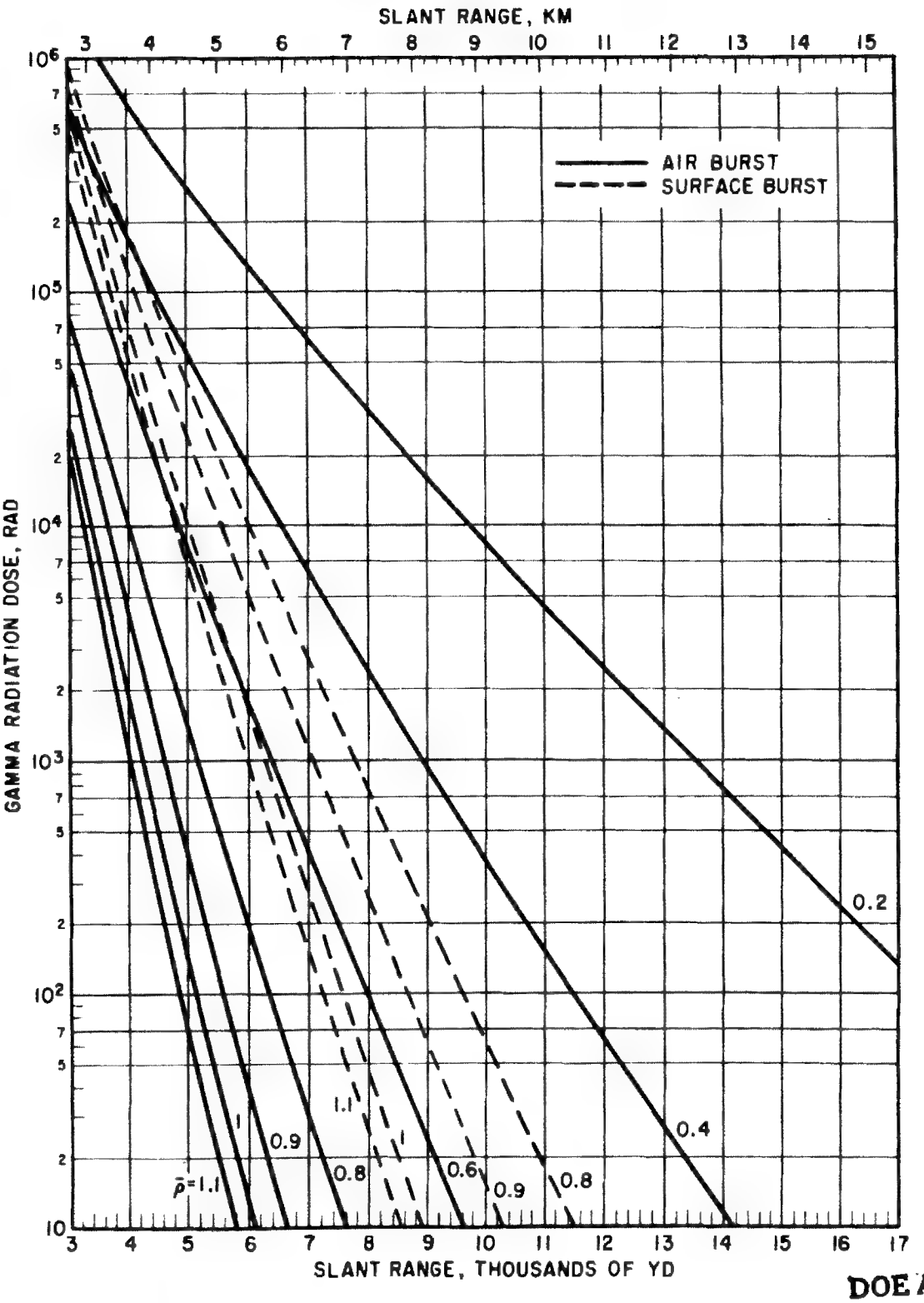

Figure 4-15. Initial Gamma Radiation Dose vs. Slant Range for Various Average Relative Air Densities, 20-mt Air Burst-Surface Target and 20-mt Surface Burst-Surface Target

85

[redacted]

Problem 4-5 Initial Gamma Radiation Dose For 20 to 40-mt Yields

The curves of figure 4-16 present the initial gamma radiation dose in rads delivered to a surface target by a 40-mt air burst. Information for air bursts of yields between 20 and 40 mt may be accomplished by interpolation; however, extrapolation to surface-burst conditions for yields greater than 20 mt and to yields above 40 mt for any burst condition is unreliable. Airborne target situations may be determined by multiplication with an appropriate target-burst factor from table 4-4.

Example.

Given: A 30-mt air burst with an average relative air density of 0.4.

Find: The initial gamma radiation dose delivered to an airborne target at a slant range of 11,000 yd from the detonation.

Solution: Because curves are not available for a 30-mt detonation interpolation will be required from information available in the 40-mt curves (figure 4-16) and 20-mt air burst-surface target curves (figure 4-15). Multiply by an appropriate target-burst factor from table 4-4 to extrapolate from surface target situations to airborne target situations. From figure 4-16, for relative air density of 0.4, the dose, D_{40s} delivered to a surface target 11,000 yd from a 40-mt air burst is 5000 rads. From figure 4-15 for relative air density of 0.4, the dose D_{20s} delivered to a surface target 11,000 yd from a 20-mt air burst is 150 rads. By interpolation, the dose D_{30s} delivered to a surface target 11,000 yd from a 30-mt air burst is approximately 2600 rads. From table 4-4, f_{tb} for an air target-air burst situation is 1.3.

Answer: Therefore, the initial gamma radiation delivered to an air target at an 11,000-yd slant range from a 30-mt air burst with an average relative air density of 0.4 is:

$$D_x = (f_{tb})\ (D_{30s}) = 1.3\ (2600) = 3400 \text{ rads}$$

Reliability. For air bursts, the doses obtained within the range of yields from 20 to 40 mt are reliable to within a factor of 10 and ranges obtained for a given dose will be reliable to within ±30%. Extrapolation to yields greater than 20 mt for surface bursts or 40 mt for air bursts is not recommended.

[redacted]

56

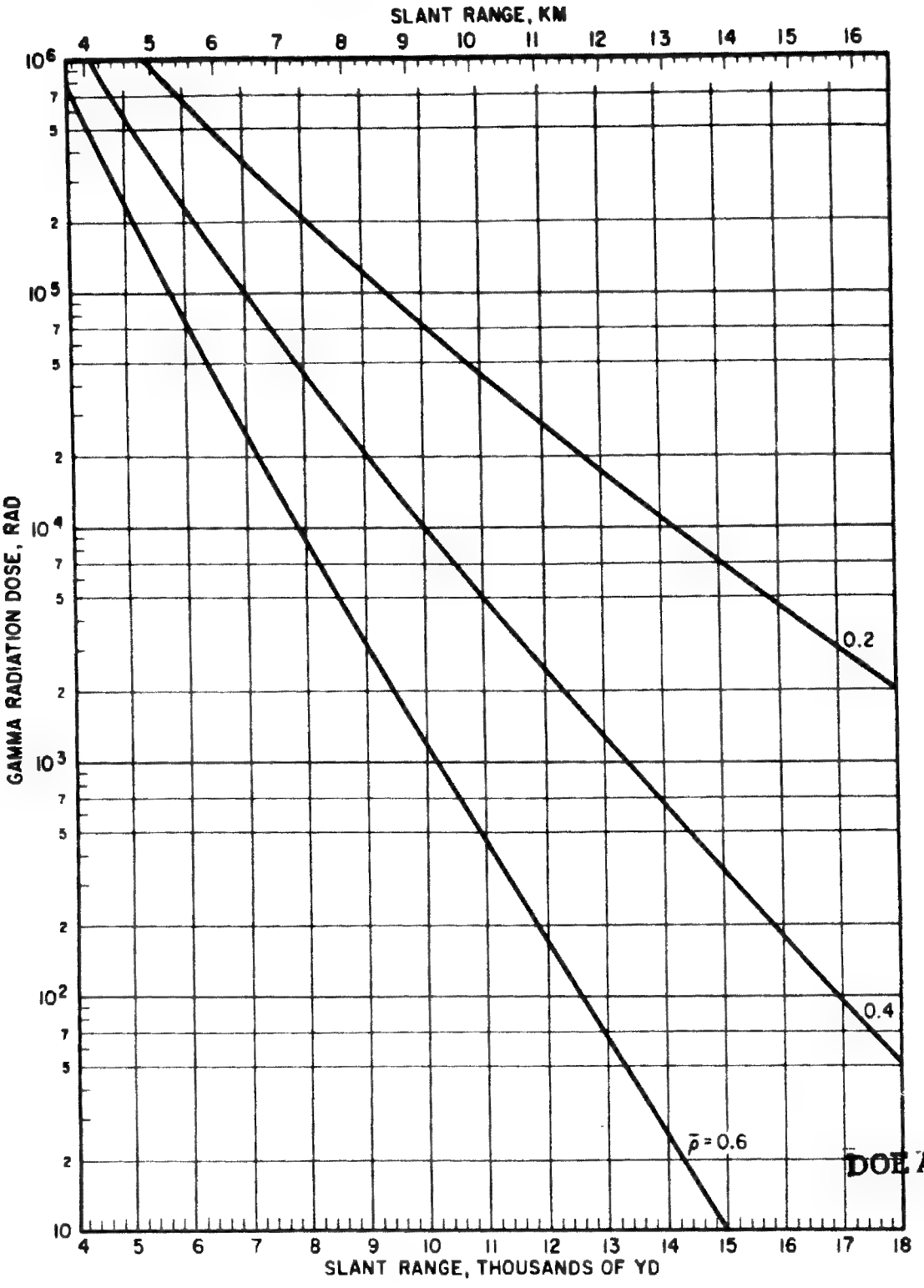

Figure 4-16. Initial Gamma Radiation Dose vs. Slant Range for Various Average Relative Air Densities, 40-mt Air Burst-Surface Target

[redacted]

Problem 4-6 Neutron Radiation Dose

Weapon design strongly influences neutron radiation. Figures 4-17 to 4-20 are given as representative curves applicable to four general weapon categories based upon expected neutron output. Figure 4-17 applies to sub-kiloton yields and the dose is given in units of rads/ton. Figures 4-18 and 4-19 apply to average and high-flux kiloton fission weapons respectively, and the units are in rads/kt. Figure 4-20 applies to fusion weapons and the dose is given in units of rads/mt. From these curves the slant range can be determined at which a weapon of given yield will produce a specified dose; conversely, the yield required to produce a given dose at a desired range can also be found.

Several other factors will influence the dose expected at a given target location. If either the target or the burst is raised above the surface the dose can be expected to increase by approximately 50 percent. If the target is located on the water the dose can be expected to be reduced. Figures 4-17 to 4-19, curves for sub-kiloton and kiloton fission weapons, apply directly to the dose received by a land surface target from a low air burst (fireball does not touch the ground). Figure 4-20 applies directly to the dose received by a land surface target from a surface burst.

Table 4-5 Adjustment Factors for Varying Given Conditions

Condition	Factor
Target location on water surface	0.85
Target location airborne	1.5
Changing burst location from air to surface	0.67
Changing burst location from surface to air	1.5

Scaling. At a given range and relative air density, the neutron dose is proportional to weapon yield. For relative air density, see appendix B.

Example 1.

Given: A high flux 50-kt burst at 2000 ft above a water surface where the average air density between the point of burst and the target location is 0.8.

Find: The maximum neutron dose on the surface of the water at a slant range of 2200 yd.

Solution: From figure 4-19 for $\bar{\rho} = 0.8$ the dose for 1 kt at 2200 yd is 2 rads. The correction factor for the target being on water rather than on land is 0.85.

Answer: Therefore the maximum dose on the surface of the water for 50 kt at 2200-yd slant range and $\bar{\rho} = 0.8$ is $2 \times 50 \times 0.85 = 85$ rads.

Example 2.

Given: A sub-kiloton weapon burst on the ground where the relative air density is 0.9.

Find: The yield required to deliver a neutron dose of 450 rads to the outside of a bunker 500 yd from ground zero.

Solution: From the information given, figure 4-17 (sub-kiloton fission) must be used. Because the given conditions for figure 4-17 are air burst-surface target, the adjustment factor "changing burst location from air to surface—0.67" (see table 4-5) must be used to correct for a surface burst.

Answer: From figure 4-17 for $\bar{\rho} = 0.9$ read 7.2 rads/ton at 500 yd, air burst-surface target.

$$7.2 \text{ rads/ton} \times 0.67 \text{ (adjustment factor)} = 4.82 \text{ rads/ton delivered to target}$$

$$\frac{450 \text{ rads total}}{4.82 \text{ rads/ton}} = 92 \text{ tons}$$

Reliability. Depending upon weapon design, it is estimated that the dose values given in figures 4-17 through 4-20 may be low by as much as a factor of 2 for certain very high flux designs and high by as much as a factor of 5 for some older weapon designs.

Related Material. See paragraph 4-6.

[redacted]

88

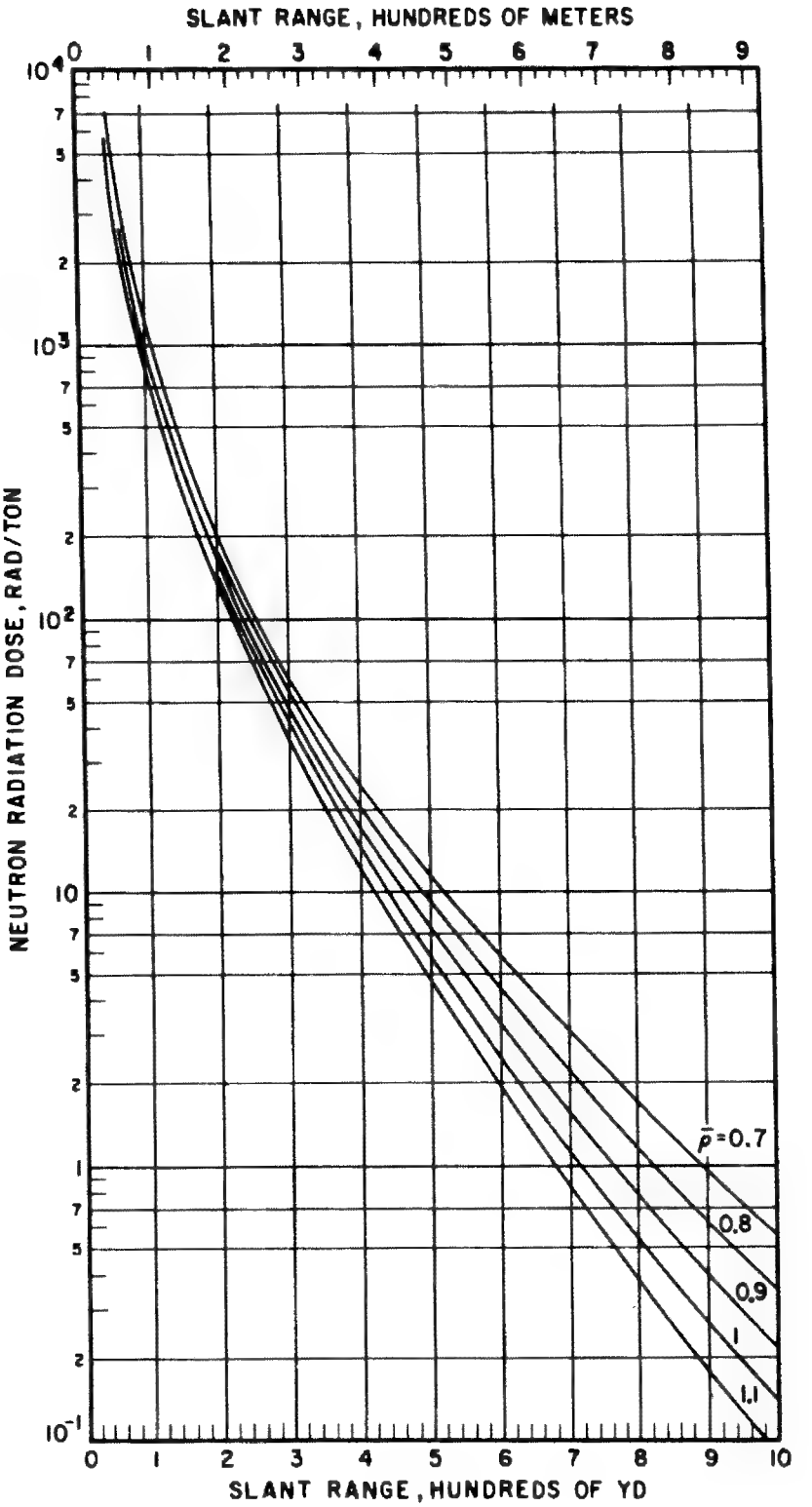

Figure 4-17. Neutron Radiation Dose vs. Slant Range for Various Average Relative Air Densities, 1-ton (Sub-kiliton Fission) Air Burst-Surface Target

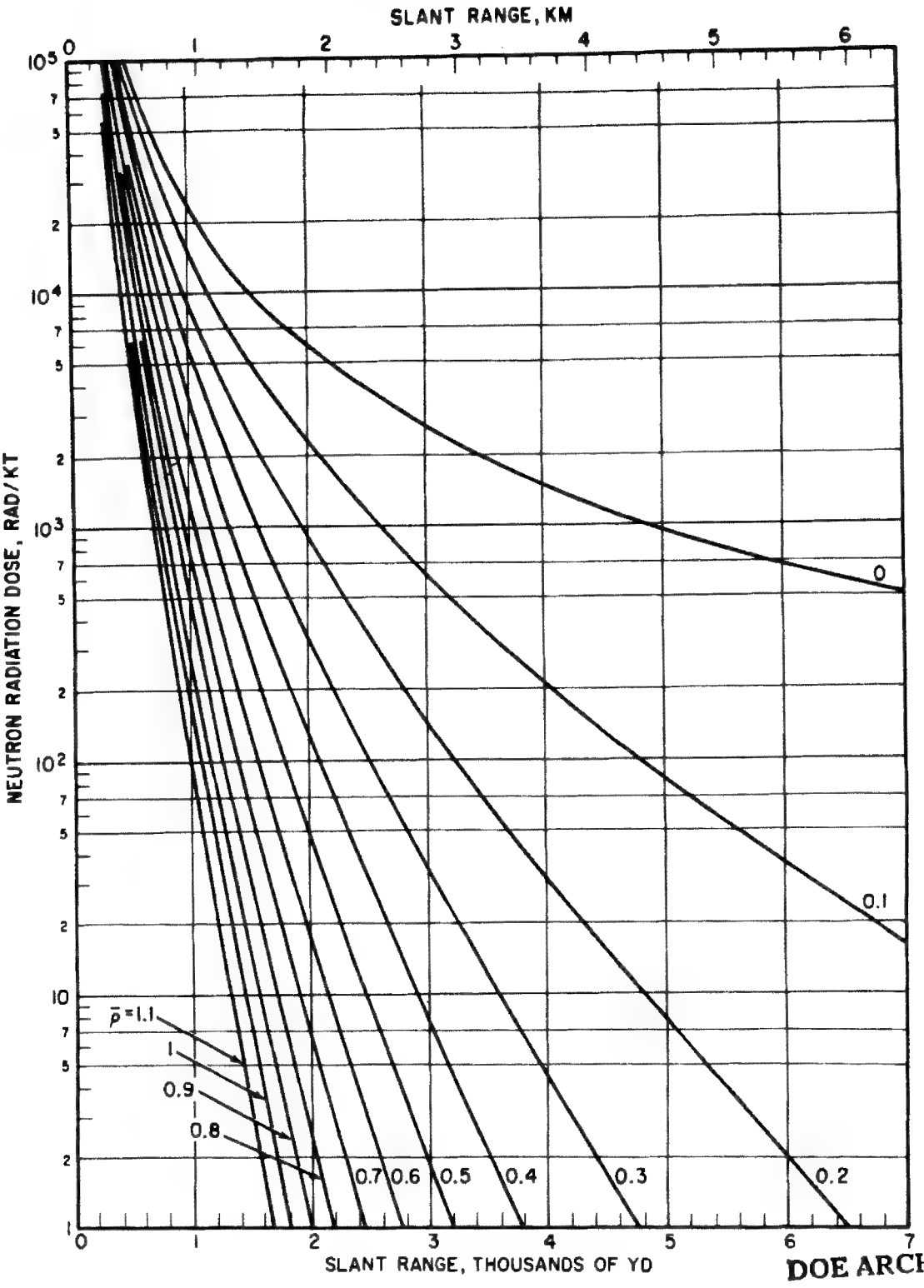

Figure 4-18. Neutron Radiation Dose vs. Slant Range for Various Average Relative Air Densities, 1-kt (Average Flux Fission) Air Burst-Surface Target

[redacted]

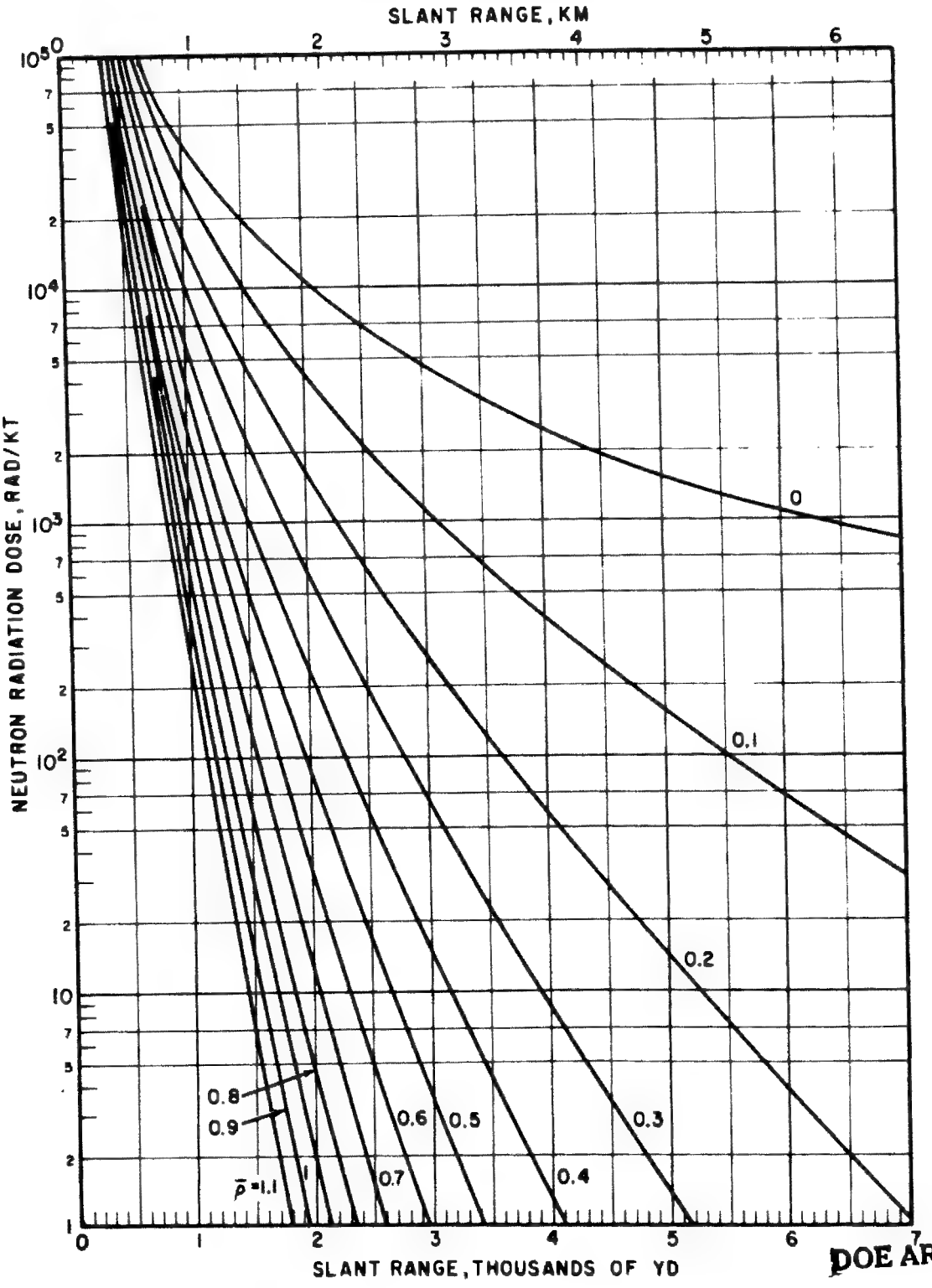

Figure 4-19. Neutron Radiation Dose vs. Slant Range for Various Average Relative Air Densities, 1-kt (High Flux Fission) Air Burst-Surface Target

[redacted]

91

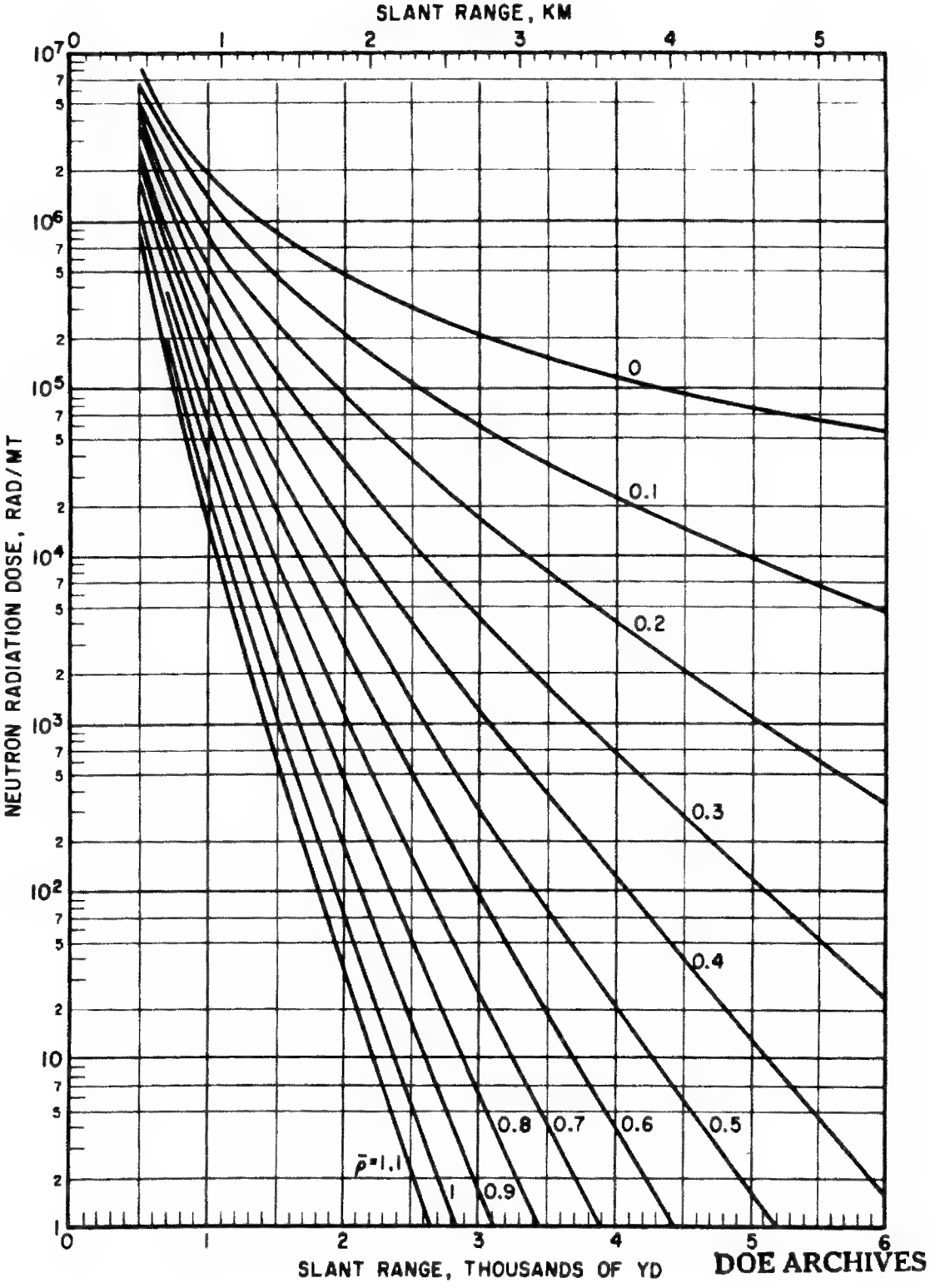

Figure 4-20. Neutron Radiation Dose vs. Slant Range for Various Average Relative Air Densities, 1-mt (Fusion) Surface Burst-Surface Target

From the dose rate at $H + 1$ hr the dose rate at any other time is obtained by forming the product of the appropriate decay factor from figure 4-21 and the 1-hr dose rate.

Example 1.

Given: The dose rate at a given point at 1 hr after detonation is 500 rads/hr.

Find: The dose rate at that point 12 hr after detonation.

Solution: From figure 4-21, the decay factor at 12 hr is 0.05.

Answer: The dose rate at 12 hr is $500 \times 0.05 = 25$ rads/hr.

The decay curve may also be used to determine the value of the dose rate at 1 hr from the dose rate at a later time. In this case, the measured dose rate is divided by the appropriate decay factor.

Example 2.

Given: The dose rate at a given point 10 hr after detonation is 72 rads/hr.

Find: The dose rate at the same point 1 hr after the detonation.

Solution: From the decay factor curve at 10 hr we have a factor of 0.06.

Answer: Therefore, the dose rate at 1 hr is:

$$\frac{72}{0.06} = 1200 \text{ rads/hr}$$

Related Material: See paragraph 4-18. See also figure 4-50.

Figure 4-21. Fission-product Decay Factors Normalized to Unity, 1 hr after Detonation

[redacted]

Problem 4-8 Fallout Gamma Radiation Dose as Function of Time

Figure 4-22 shows integrated gamma dose received in a fallout-contaminated area as a function of time after $H + 1$ hr ($\sim$0.042 day). This curve was generated by integrating a $t^{-1.2}$ decay function normalized to unit dose rate at $H + 1$ hr. The integration was performed over the range $H + 1$ hr and $H+$ 1000 days. If the true dose rate at sometime between $H + 1$ hr and $H + 1000$ days is known, figure 4-22 can be used to estimate the dose accumulated during any time interval in this time range, *provided* the fallout decays as shown in figure 4-21.

Example. At $H + 4$ hr a dose rate of 20 rads/hr exists in a fallout-contaminated area. At $H + 4.8$ hr personnel enter the area and remain 2.5 hr before leaving the area. What is the total dose these personnel can expect to receive?

Solution:

$$H + 4.8\,\text{hr} = H + 0.2\,\text{day}$$

$$(H + 4.8 + 2.5)\,\text{hr} = H + 7.3\,\text{hr}$$

$$= H + 0.304\,\text{day}$$

From figure 4-22, the normalized dose that would be received between $H + 1$ hr and $H +$ 0.304 day is 1.55. Similarly the normalized dose received between $H + 1$ hr and $H + 0.2$ day is 1.3. Therefore, the *normalized* dose received by these personnel between $H + 0.2$ day and $H +$ 0.304 day would be:

$$1.55 - 1.3 = 0.25$$

To convert this to actual dose received, use is made of the $H + 4$-hr dose rate (= 20 rads/hr). Using the dashed curve of figure 4-21, the normalized dose rate at $H + 4$ hr is found to be 0.2, and at $H + 1$ hr it is 1. Then by simple proportion, the actual dose rate at $H + 1$ hr is:

$$\frac{1}{0.2} \times 20\ \text{rads/hr} = 100\ \text{rads/hr}$$

The dose the personnel can expect to receive is found by multiplying the $H + 1$-hr dose rate by the normalized dose obtained from figure 4-22.

Answer: $100 \times 0.25 = 25$ rads

Reliability. For times up to $H + 100$ days figure 4-22 is accurate to within 25 percent provided the decay of the fallout does not differ too radically from a $t^{-1.2}$ law. Under this assumption figure 4-22 will probably give an overestimate of accumulated dose, even for times longer than 100 days.

Related Material. Figures 4-21, 4-50 and 4-55, paragraphs 4-11, 4-12, 4-14, 4-18 and 4-23.

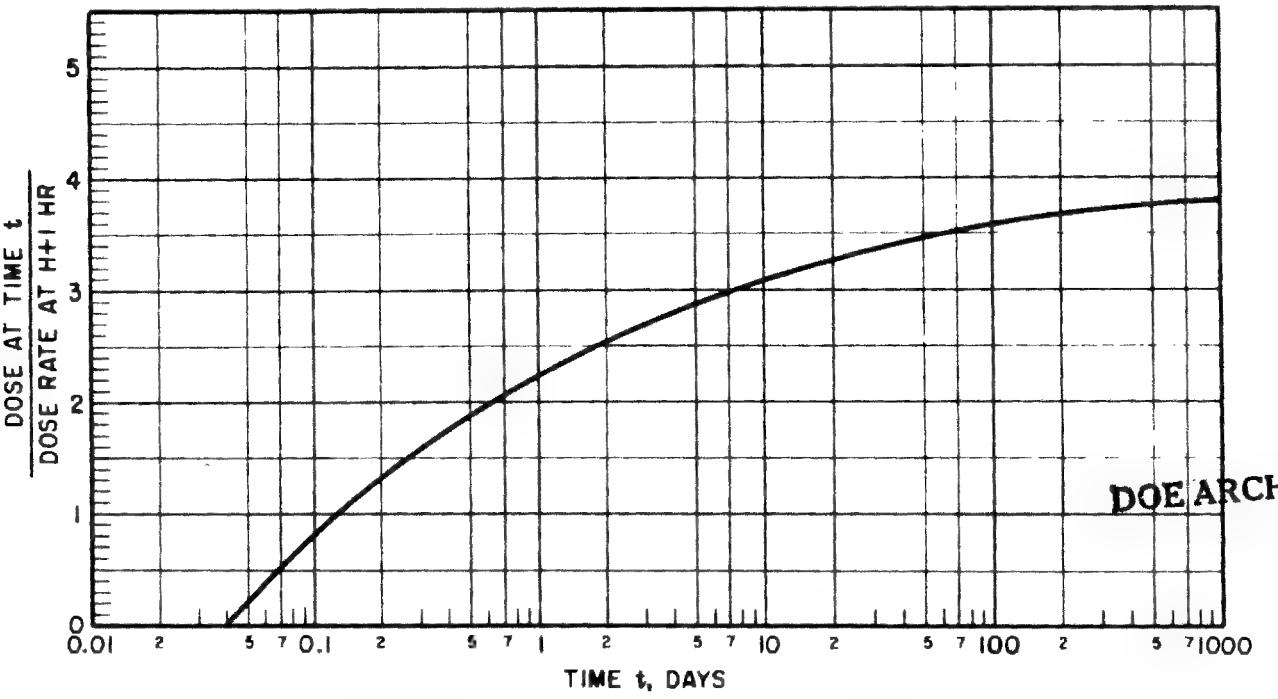

Figure 4-22. Normalized Theoretical Dose Accumulated in a Fallout-contaminated Area from $H + 1$ hr to $H + 1000$ Days

[redacted]

Problem 4-9 Fallout Gamma Radiation From Surface Bursts (Dose-rate-contour Parameters vs. Yield for Various Dose Rates)

Figures 4-23 through 4-42 present idealized dose-rate-contour parameters for residual fallout radiation from surface bursts of weapons with yields between 0.01 kt and 100 mt. The basic data are presented for weapons for which all the yield is due to fission; but, as described below, the data can also be used to obtain fallout contours for weapons for which the fission yield is only a fraction of the total yield, and for which essentially all of the contamination produced (90 percent or more) is due to fission products. The dose-rate values are given for a reference time of $H + 1$ hr. The more distant parts of the larger contours do not exist at $H + 1$ hr, because the fallout that eventually reaches some of these more distant areas is still airborne at that time. The dose-rate contours do exist at later times when fallout is complete, but with dose-rate-contour values reduced according to the appropriate decay factor from figure 4-21. Visual interpolation may be used for dose-rate-contour values between those for which curves are given. Extrapolation to dose-rate-contour values higher or lower than those shown in the families of curves cannot be done accurately and should not be attempted.

An approximate estimate of the area within a particular dose rate contour may be calculated by assuming that the roughly elliptical contour obtained by plotting the parameters given in figures 4-23 through 4-42 is an ellipse. The formula for this area is: Area $= \pi ab/4$ where a is downwind distance plus upwind distance, and b is maximum crosswind distance.

To obtain dose-rate values for times other than $H + 1$ hr, decay factors from figure 4-21 should be used. To obtain contour values for effective winds other than those given in the curves, that is, 10, 20, 40, and 60 knots, linear interpolation may be used. Thus, the downward distance for a 30-knot effective wind speed would be midway between the 20-knot and 40-knot downwind distances.

For a burst in the transition zone, a rough estimate of the resulting fallout-contamination patterns may be made by multiplying the dose-rate-contour values for a contact surface burst weapon of the same yield by an adjustment factor obtained from figure 4-44 for the appropriate yield and height of burst.

Note that the contribution made by neutron-induced activity may be significant compared to the fallout activity in the area near ground zero for weapons burst in the upper quarter of the fallout transition zone. For guidance, a rough estimate of this contribution may be obtained using figures 4-56 through 4-59 together with the discussion in paragraphs 4-8 through 4-10.

Contour shapes and sizes are a function of the total yield of the weapon, whereas the dose-rate-contour values are determined by the fission yield. Thus, if only a fraction of the total yield of the weapon is due to fission, and this fraction is known, figures 4-23 through 4-42 may be used to estimate fallout contours resulting from the detonation of such a weapon. The dose rate for the dimension of interest as read from the figures opposite the total yield must be multiplied by the ratio of fission yield to total yield to obtain the true dose-rate value for that dimension. Similarly, to obtain contour dimensions for a particular dose rate, the value of the desired dose rate must be divided by the ratio of fission to total yield, and the dimension of the resultant dose rate read from the figure opposite the total yield.

Example.

Given. A weapon with a total yield of 600 kt, of which 200 kt is due to fission, is detonated on a land surface under 10-knot effective wind conditions.

Find: (a) Contour parameters for a dose rate of 50 rads/hr at $H + 1$ hr reference time over rough, hilly terrain. (b) If the weapon were burst at a height of 1050 ft above the surface, what dose rate contour would be represented by the 50 rads/hr surface-burst contour solved for in (a)?

Solution: (a) The 50 rads/hr contour for a fission yield to total yield ratio of $200/600 = 1/3$ corresponds to the contour for $50 \div 1/3 = 150$ rads/hr for a weapon of 600-kt fission yield. Table 7-5 shows that the dose rate above contaminated rough and hilly terrain is about one-half that above an ideal smooth plane. Thus the

desired contour parameters can be obtained by entering figures 4-23, 4-27, 4-31, 4-35 and 4-39 at a yield of 600 kt and reading the parameter values corresponding to a $H + 1$ hr dose rate of $2 \times 150 = 300$ rads/hr. (See table 4-6.)

Answer: (b) From figure 4-44, the adjustment factor for a 600-kt burst at a height of 1050 ft is about 0.04, and the contour solved for in (a) corresponds for this burst condition to $0.04 \times 50 = 2$ rads/hr at $H + 1$ hr.

Reliability. The degree to which wind and other meteorological conditions affect these contour parameters cannot be overemphasized. The contours presented in these curves have been idealized in order to make it possible to present average, representative values for planning purposes. Due to these limitations, a meaningful percentage reliability figure cannot be assigned to the idealized fallout pattern. Although the shape of the actual fallout contours cannot be predicted by this method, it nonetheless does provide a fair approximation of the total area affected, as well as identify the general downwind direction.

Table 4-6 Parameter Values for 10-Knot Wind

Parameter	Source figure	Parameter value for 10-knot wind (miles)
Downwind distance	4-23	70
Maximum width	4-27	16
Distance to maximum width	4-35	40
Upwind distance	4-31	3.1
Ground-zero width	4-39	6

Related Material. See paragraphs 4-11 through 4-20. See also figures 4-2, 4-21, 4-22, 4-43, 4-44 and 4-55.

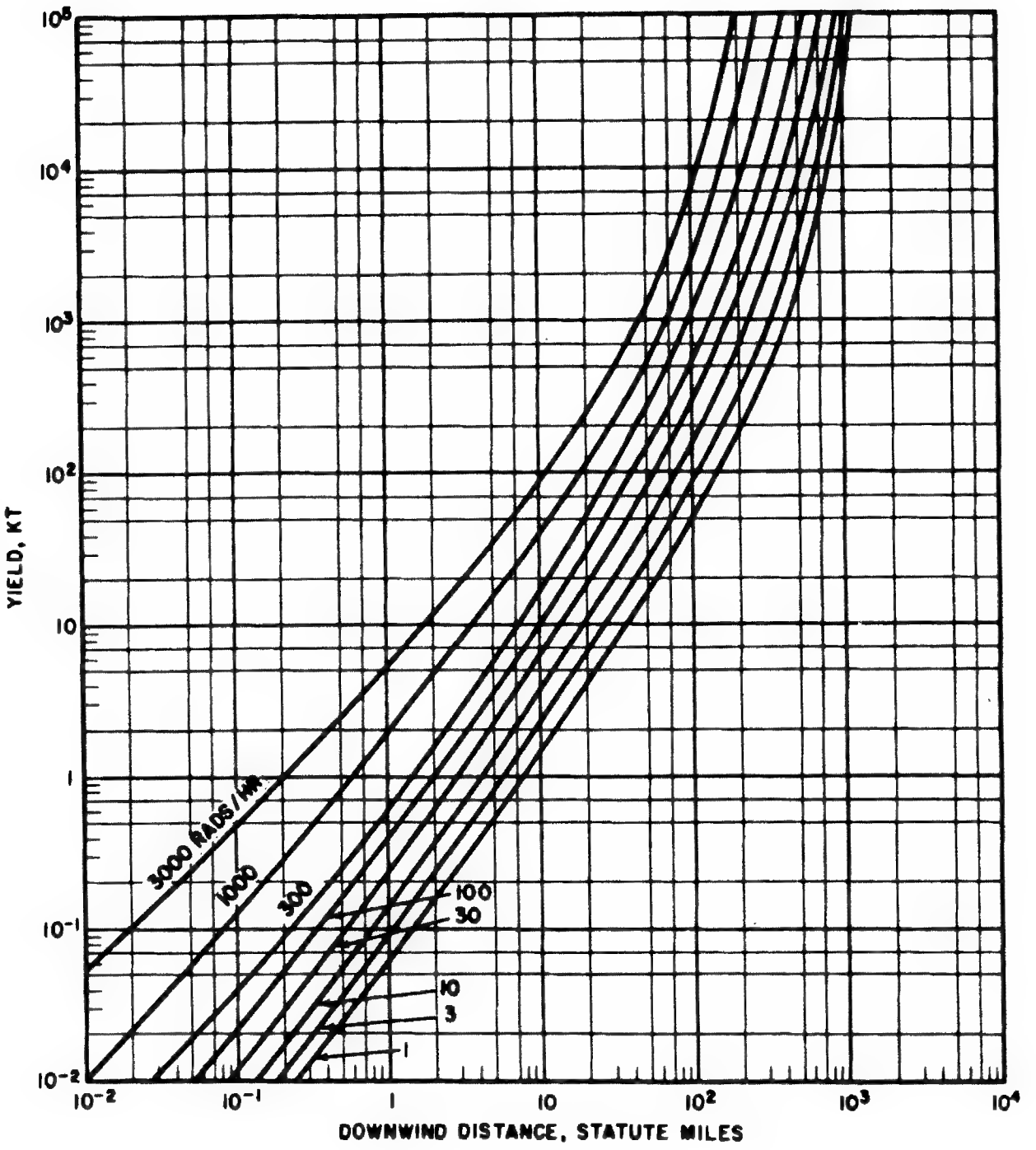

Figure 4-23. Yield vs. Downwind Distance, 10-knot Effective Wind

98

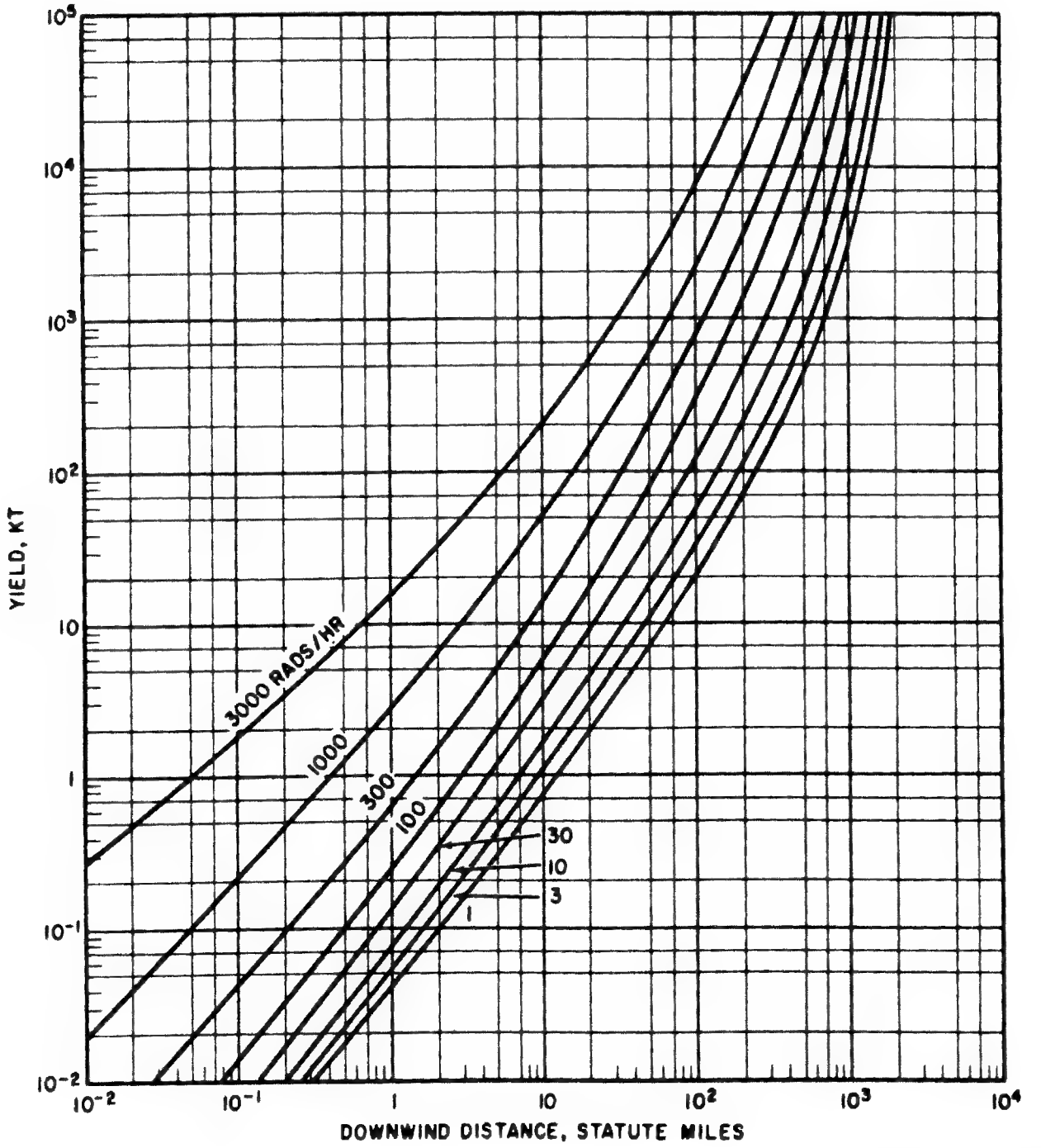

Figure 4-24. Yield vs. Downwind Distance, 20-knot Effective Wind

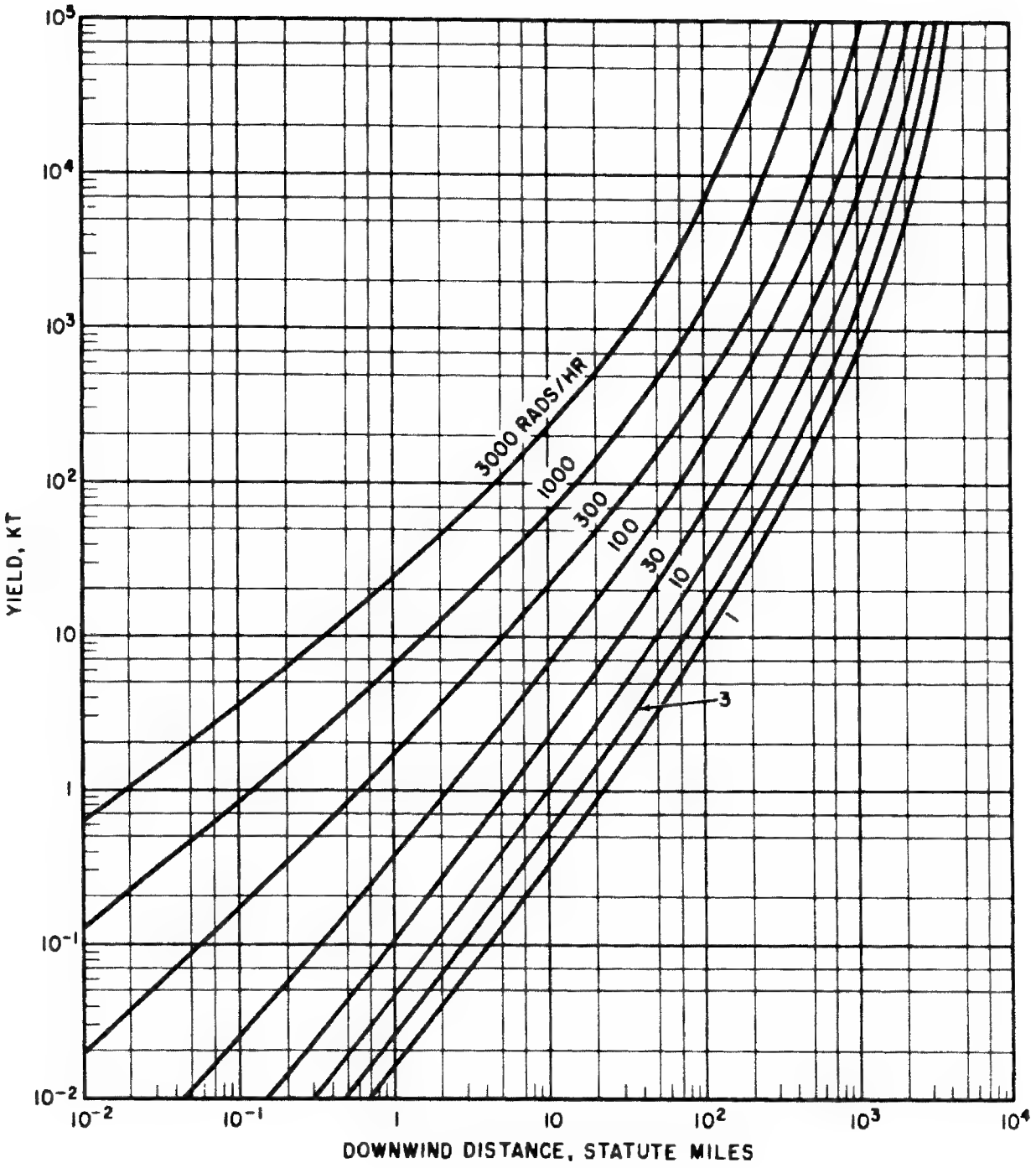

Figure 4-25. Yield vs. Downwind Distance, 40-knot Effective Wind

762-909 O - 65 - 15

100

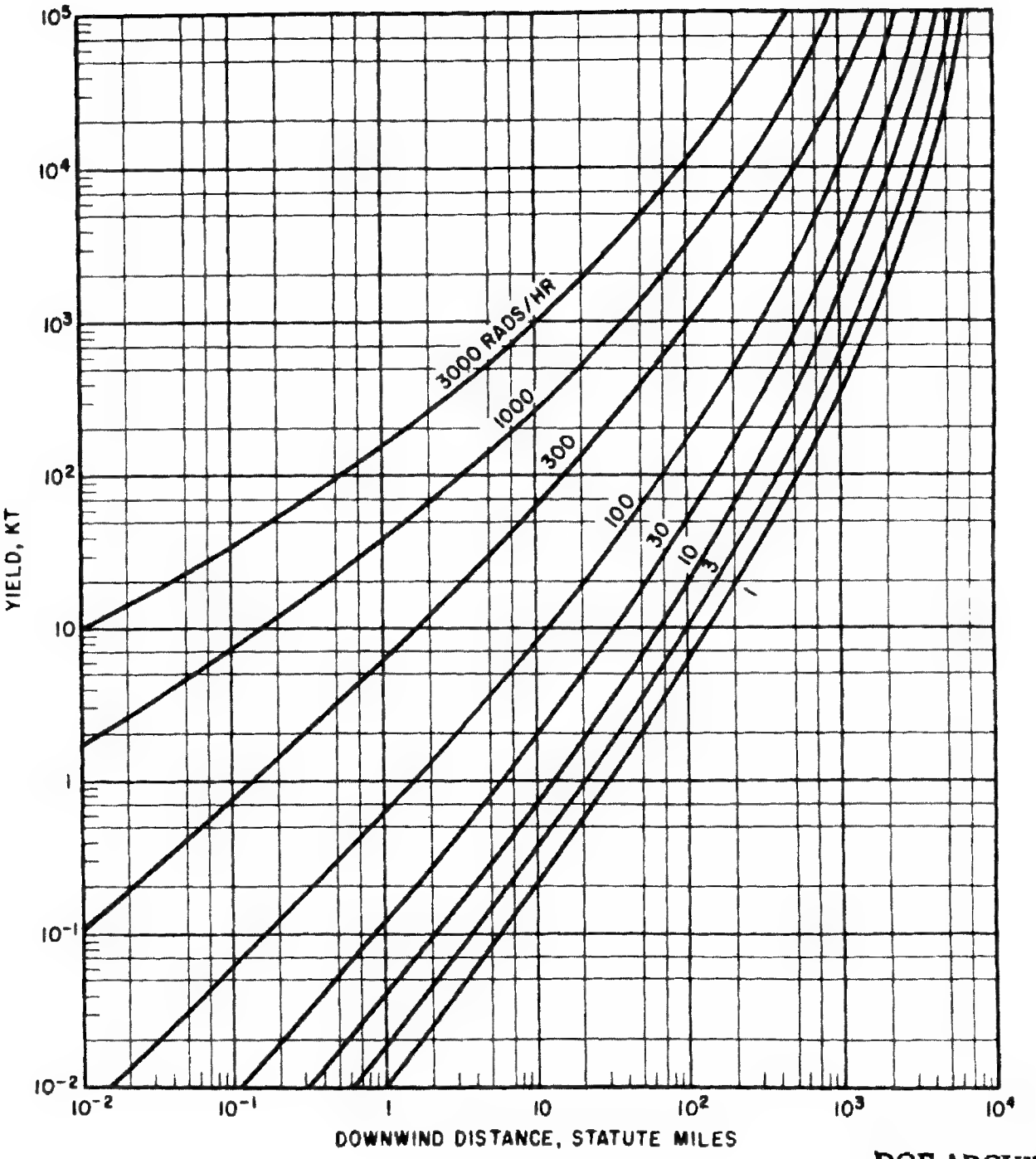

Figure 4-26. Yield vs. Downwind Distance, 80-knot Effective Wind

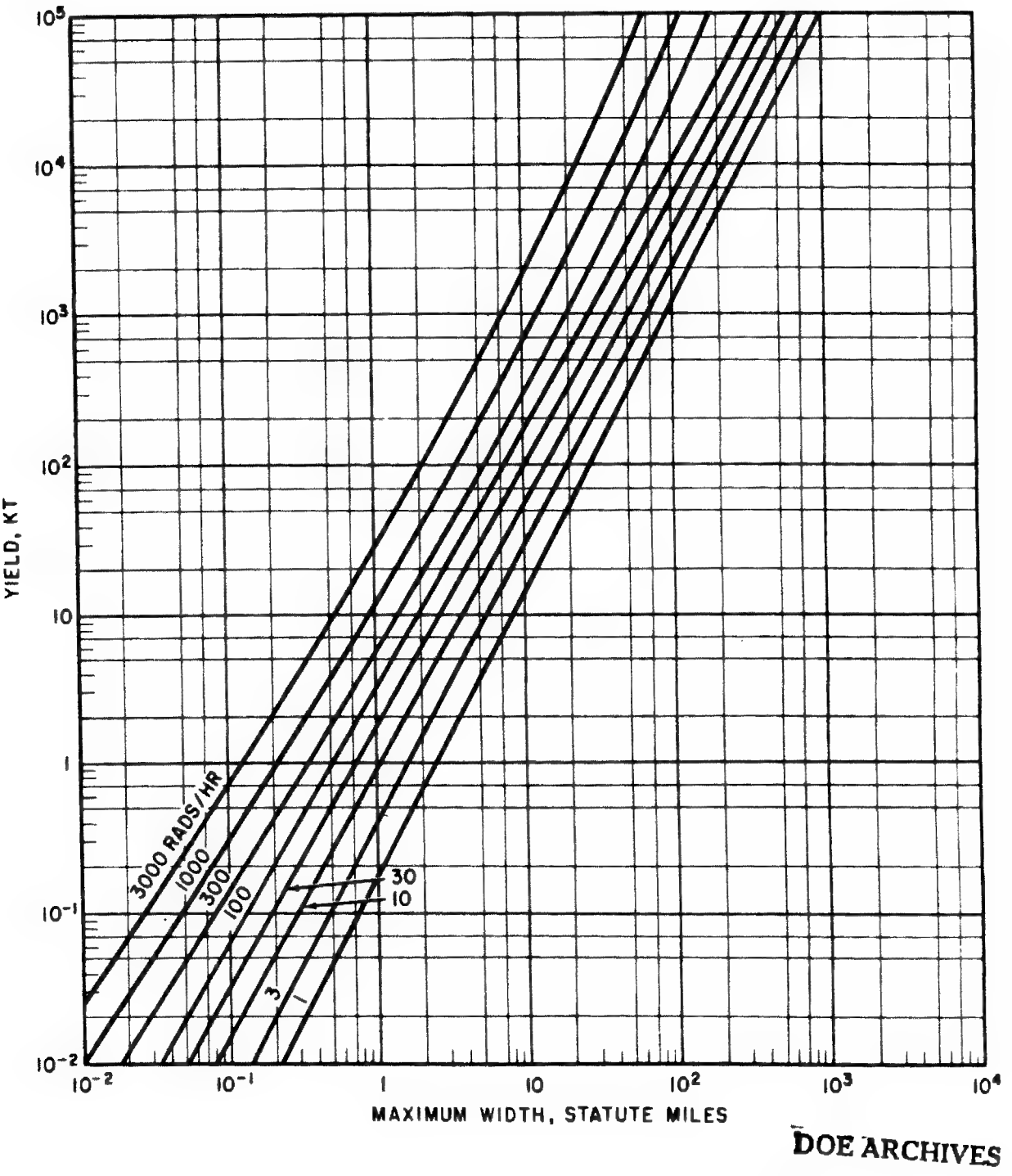

Figure 4-27. Yield vs. Maximum Width, 10-knot Effective Wind

[redacted]

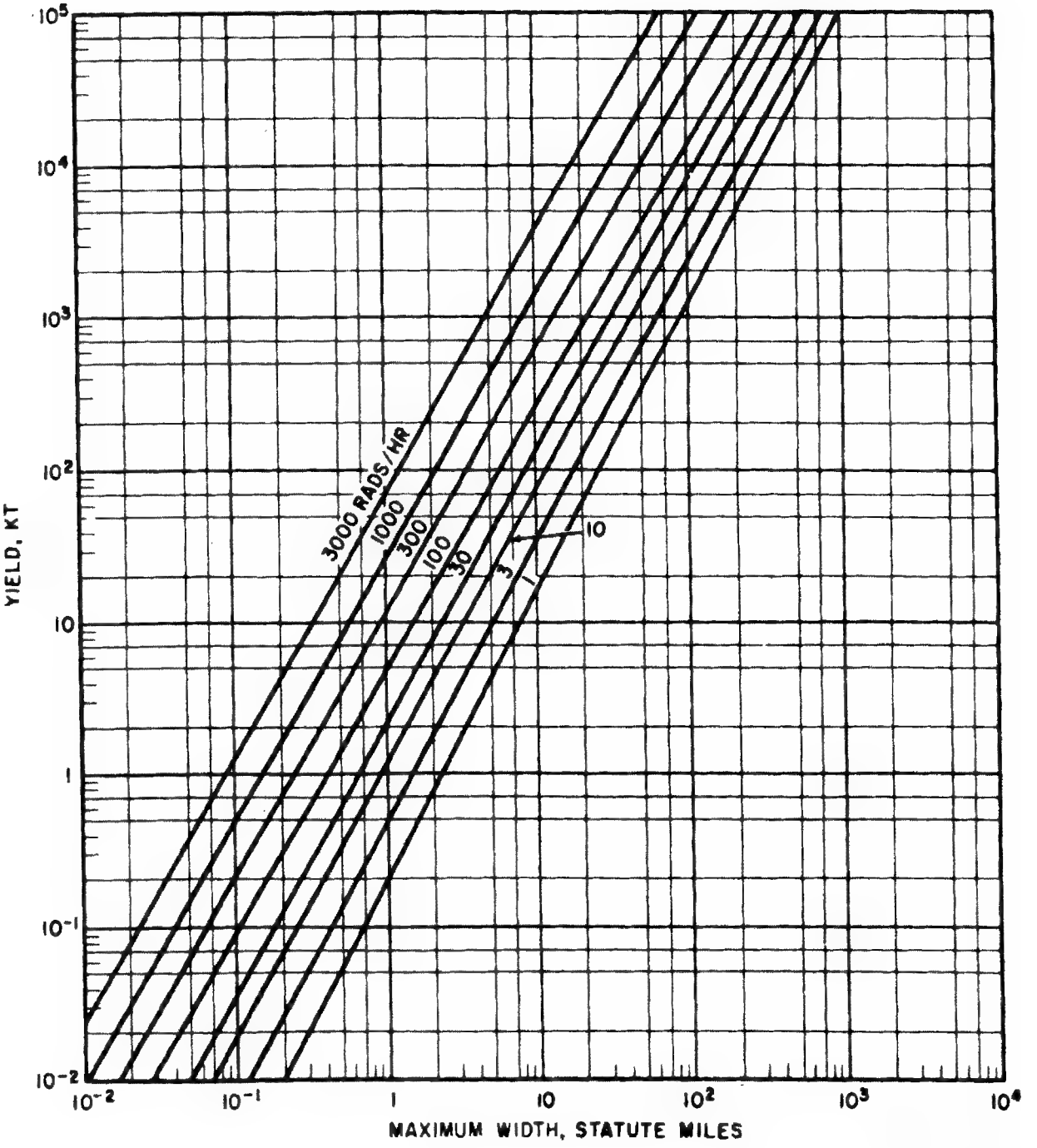

Figure 4-28. Yield vs. Maximum Width, 20-knot Effective Wind

[redacted]

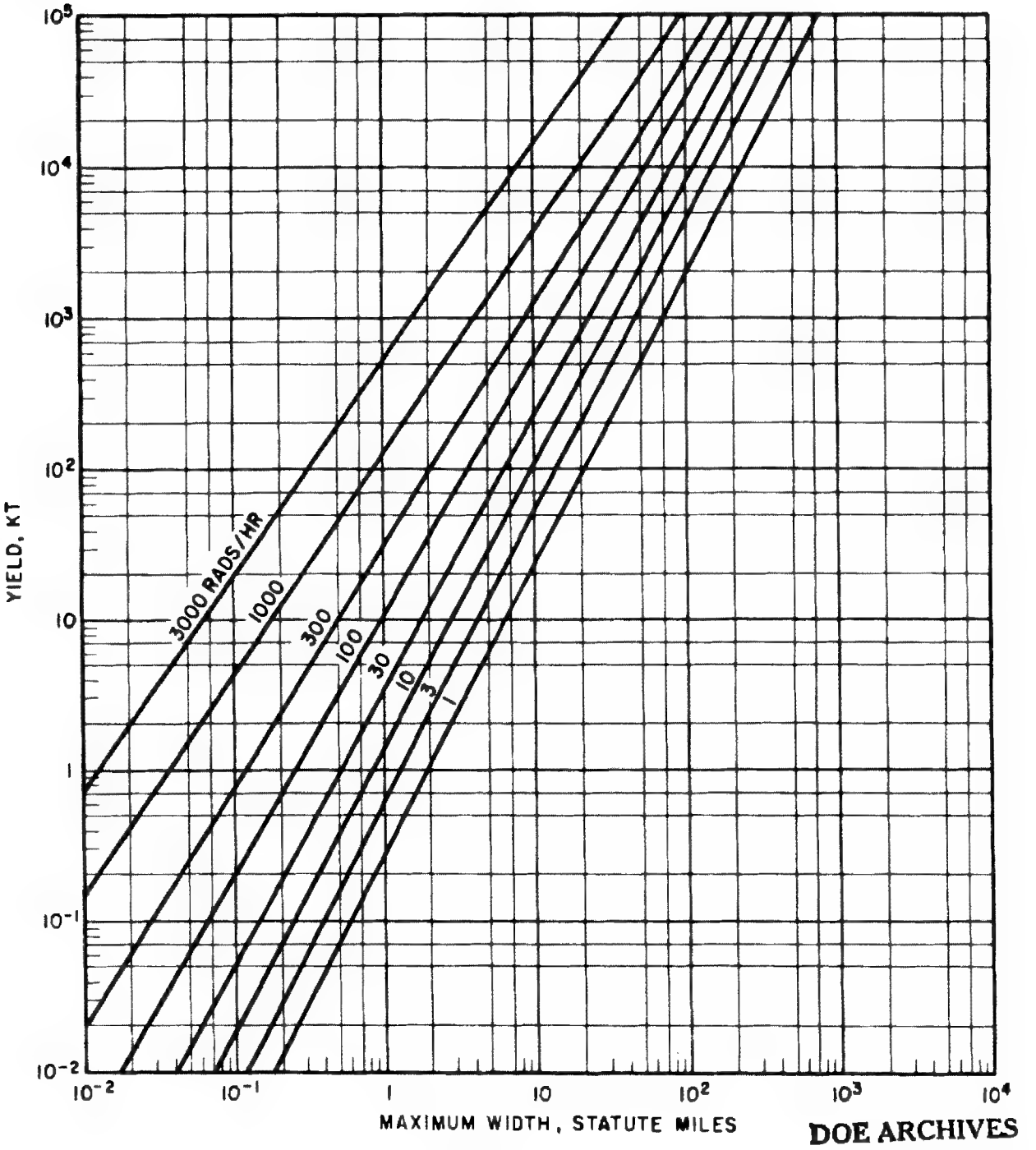

Figure 4-29. Yield vs. Maximum Width, 40-knot Effective Wind

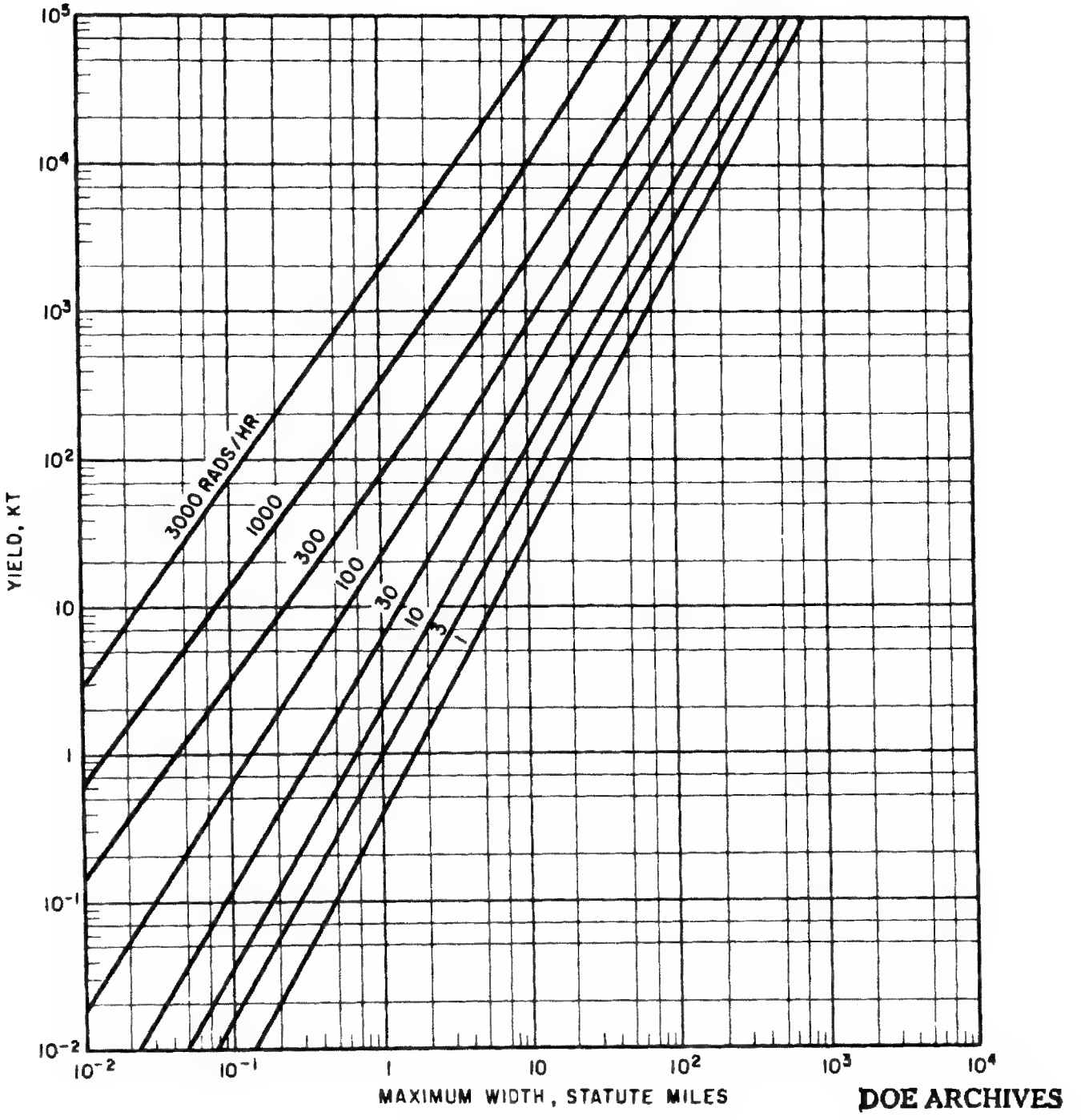

Figure 4-30. Yield vs. Maximum Width, 60-knot Effective Wind

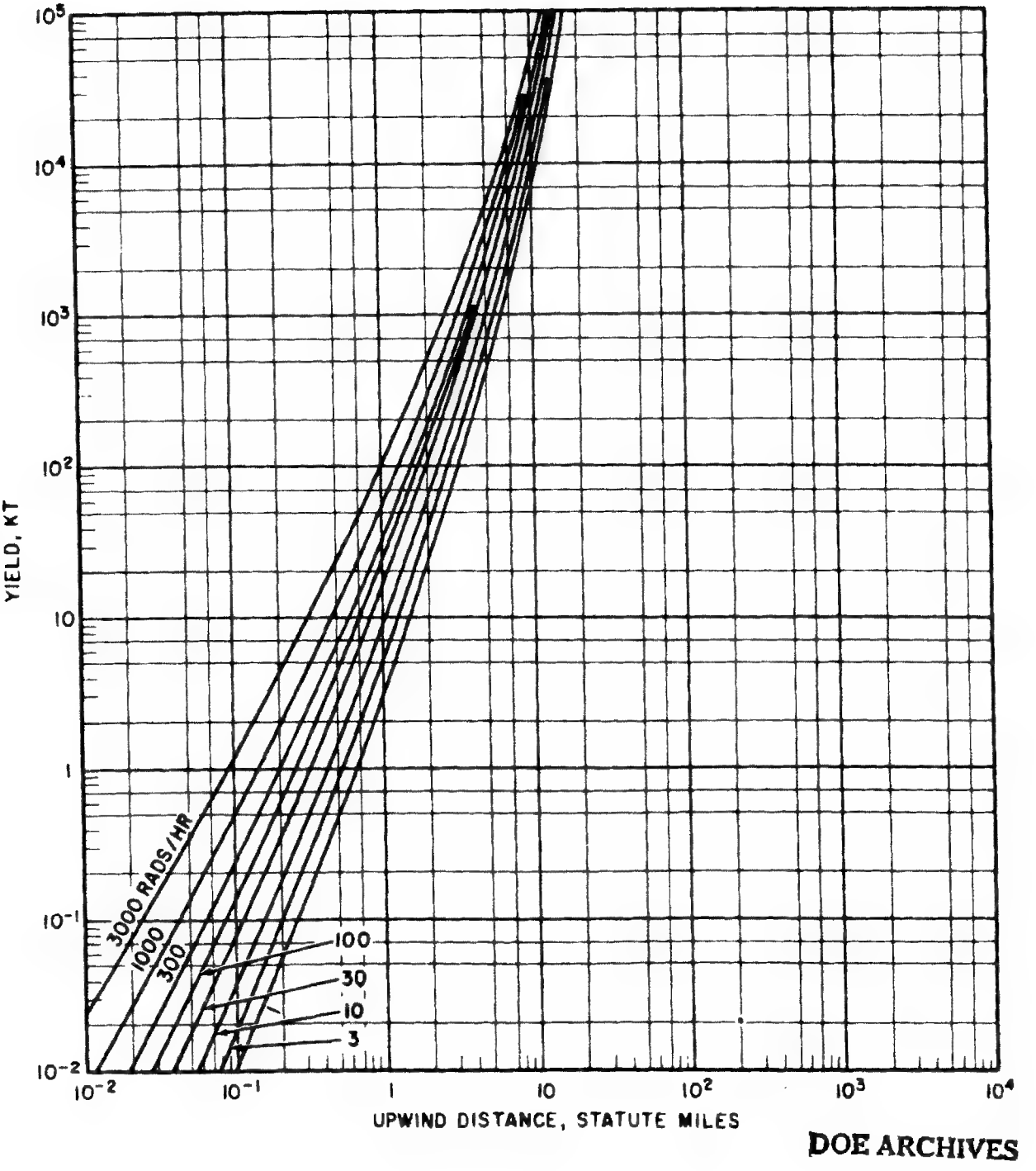

Figure 4-31. Yield vs. Upwind Distance, 10-knot Effective Wind

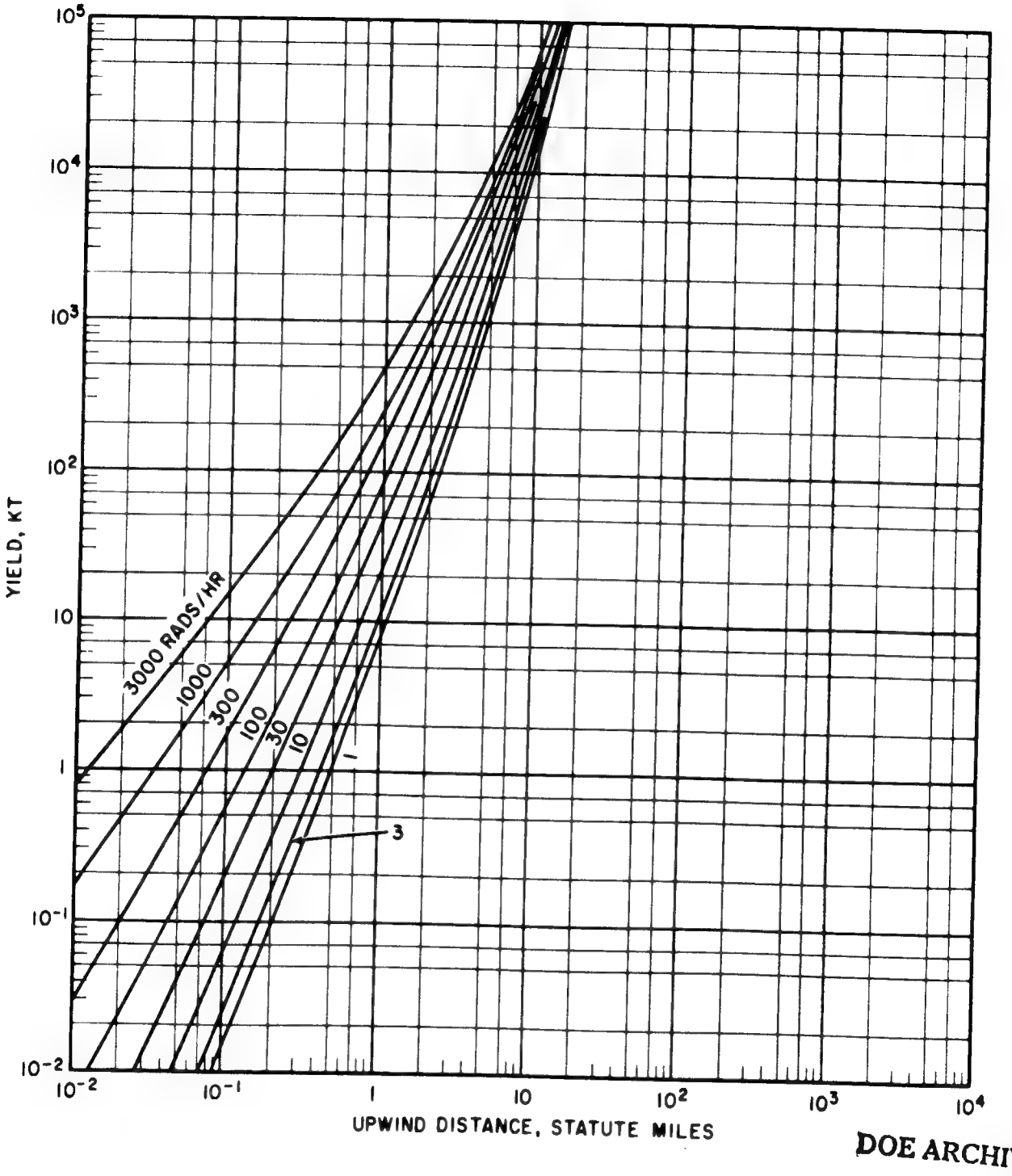

Figure 4-32. Yield vs. Upwind Distance, 20-knot Effective Wind

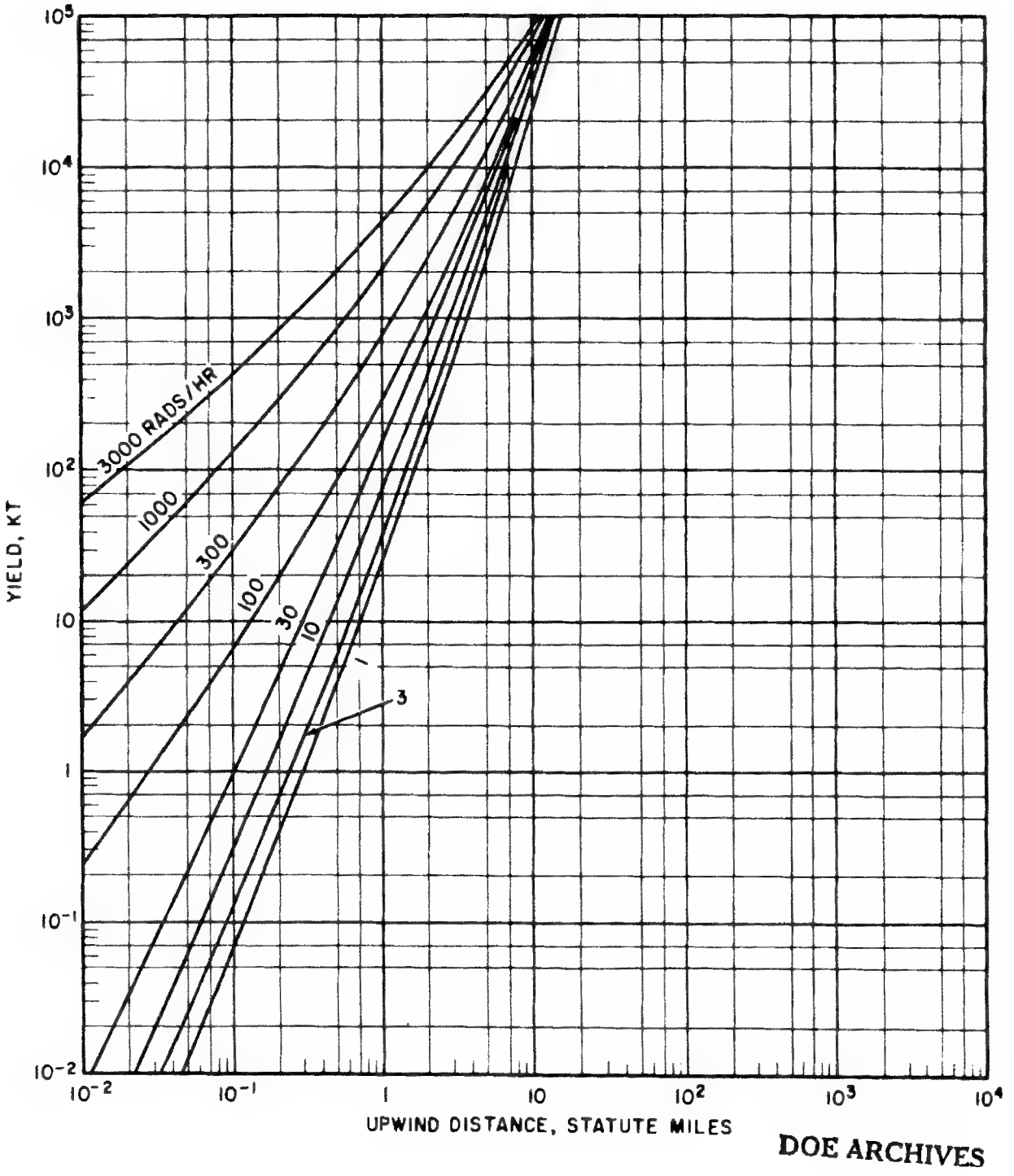

Figure 4-33. Yield vs. Upwind Distance, 40-knot Effective Wind

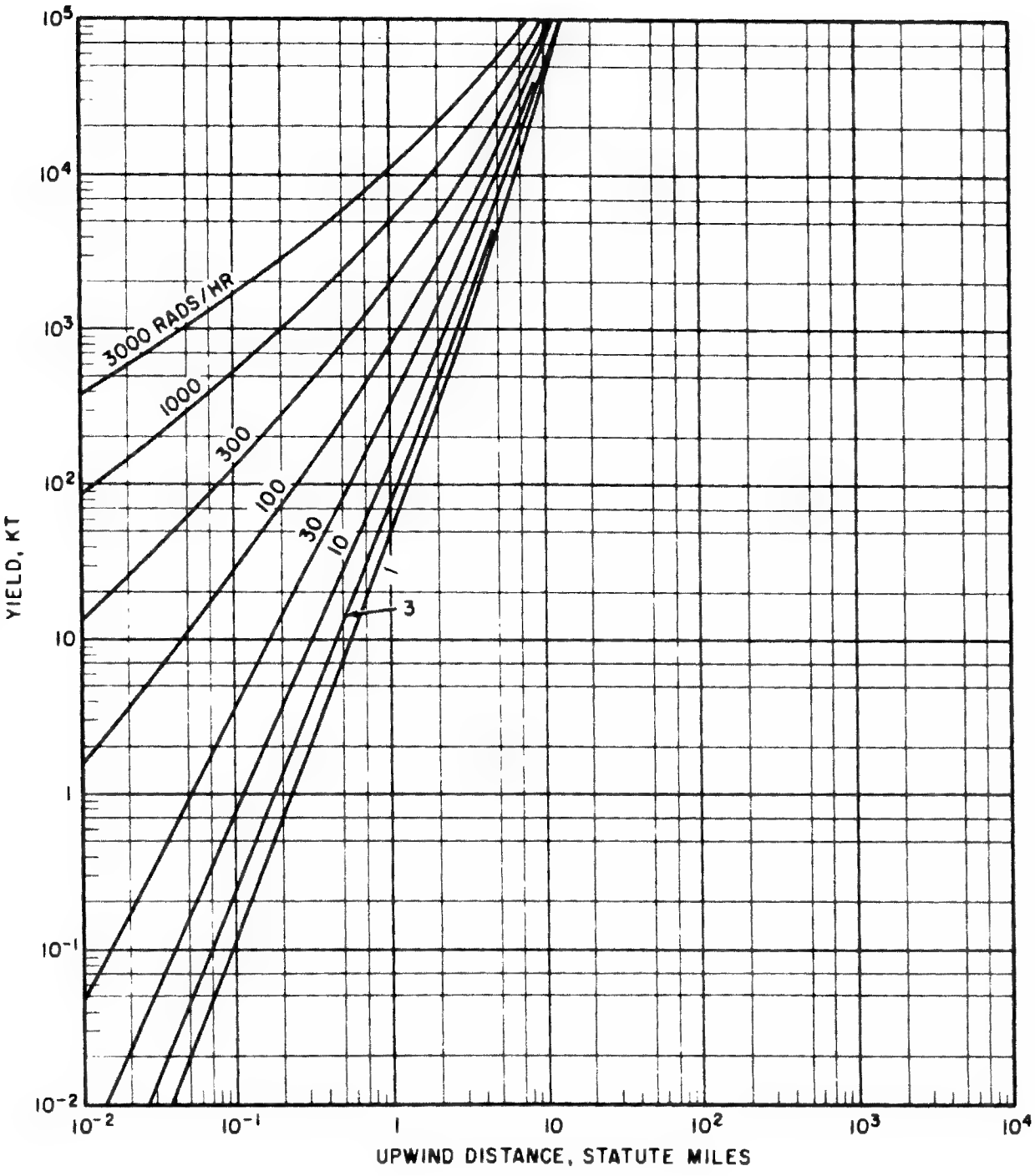

Figure 4-34. Yield vs. Upwind Distance, 60-knot Effective Wind

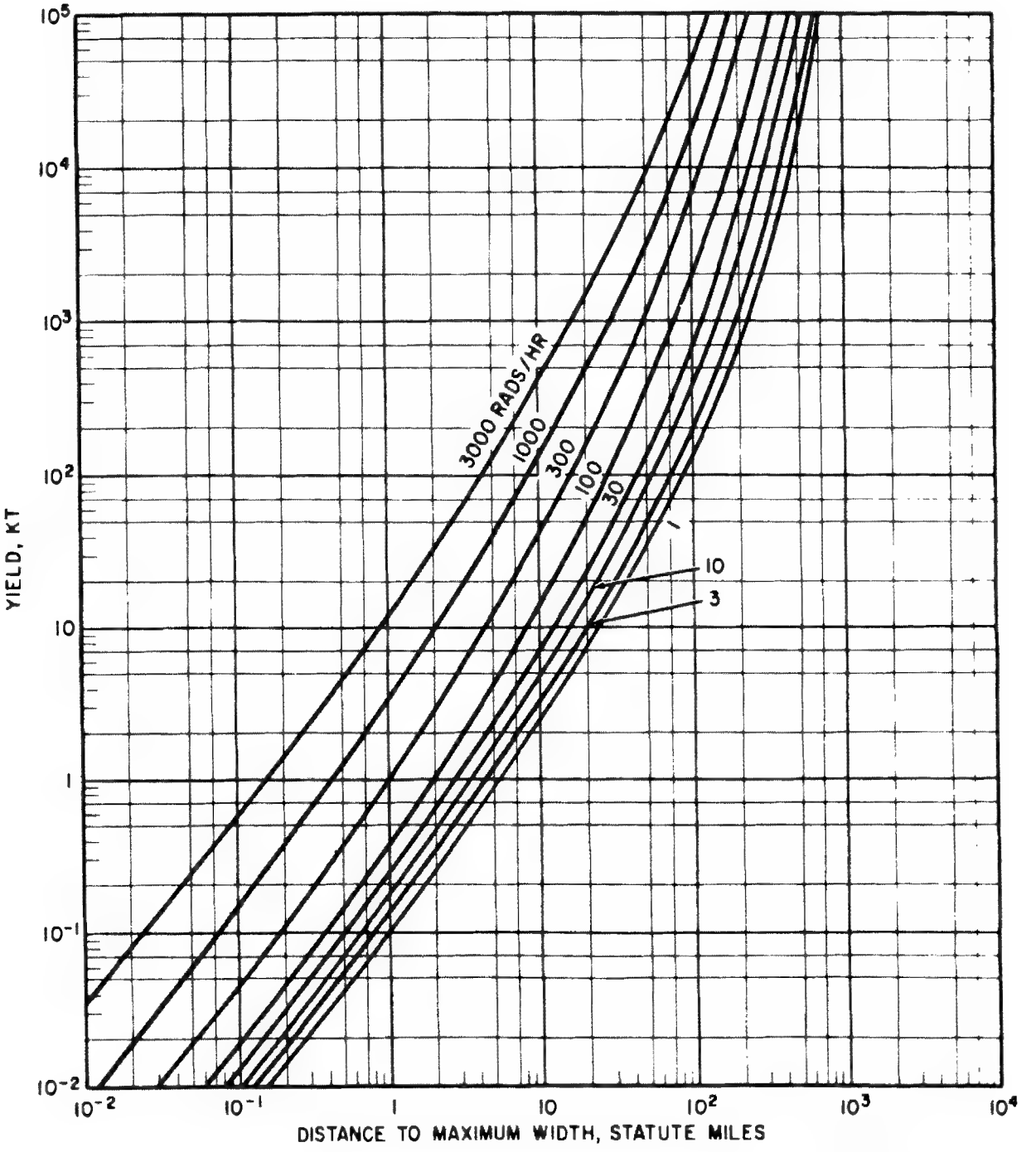

Figure 4-35. Yield vs. Distance to Maximum Width, 10-knot Effective Wind

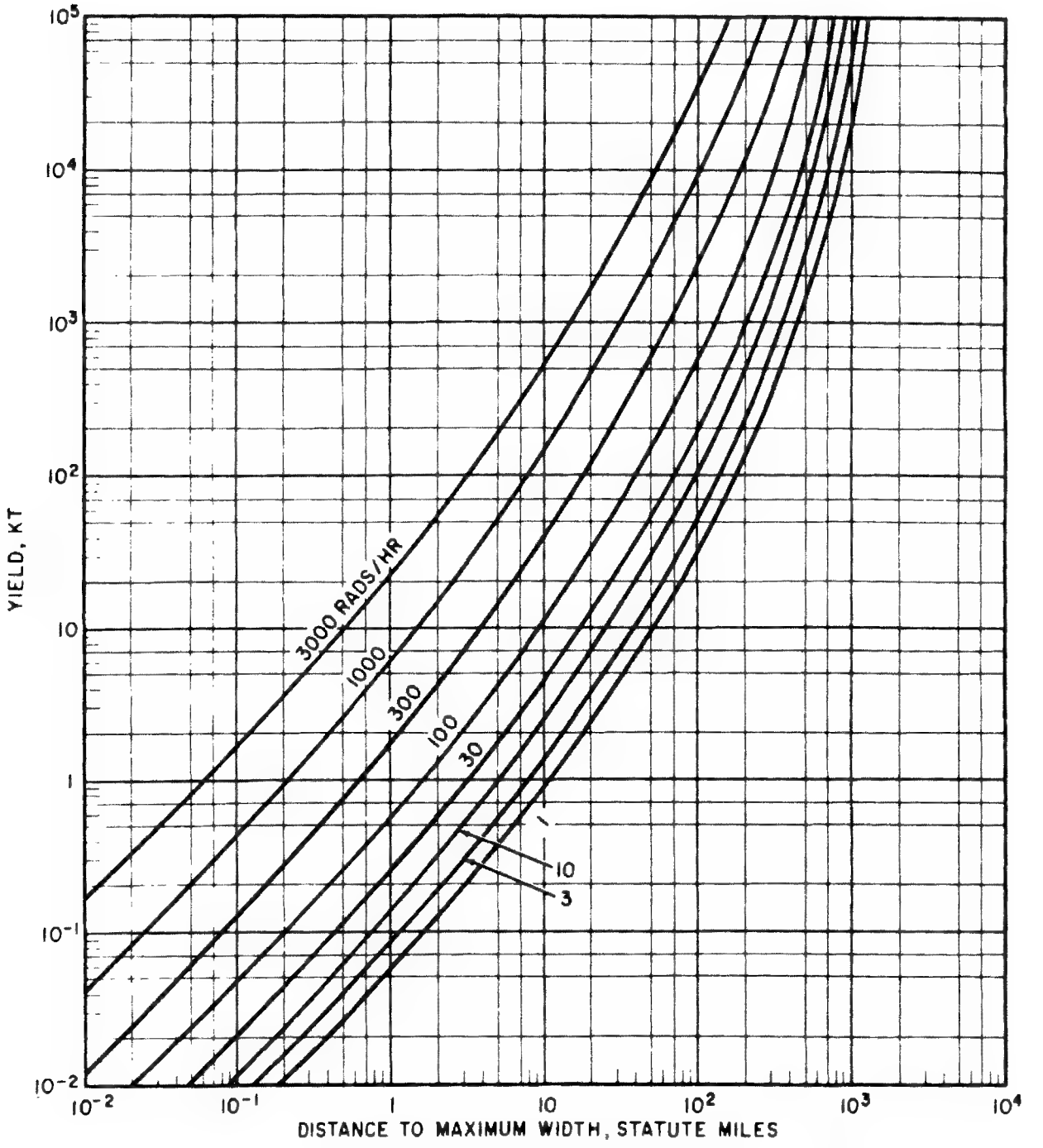

Figure 4-36. Yield vs. Distance to Maximum Width, 20-knot Effective Wind

111

[redacted]

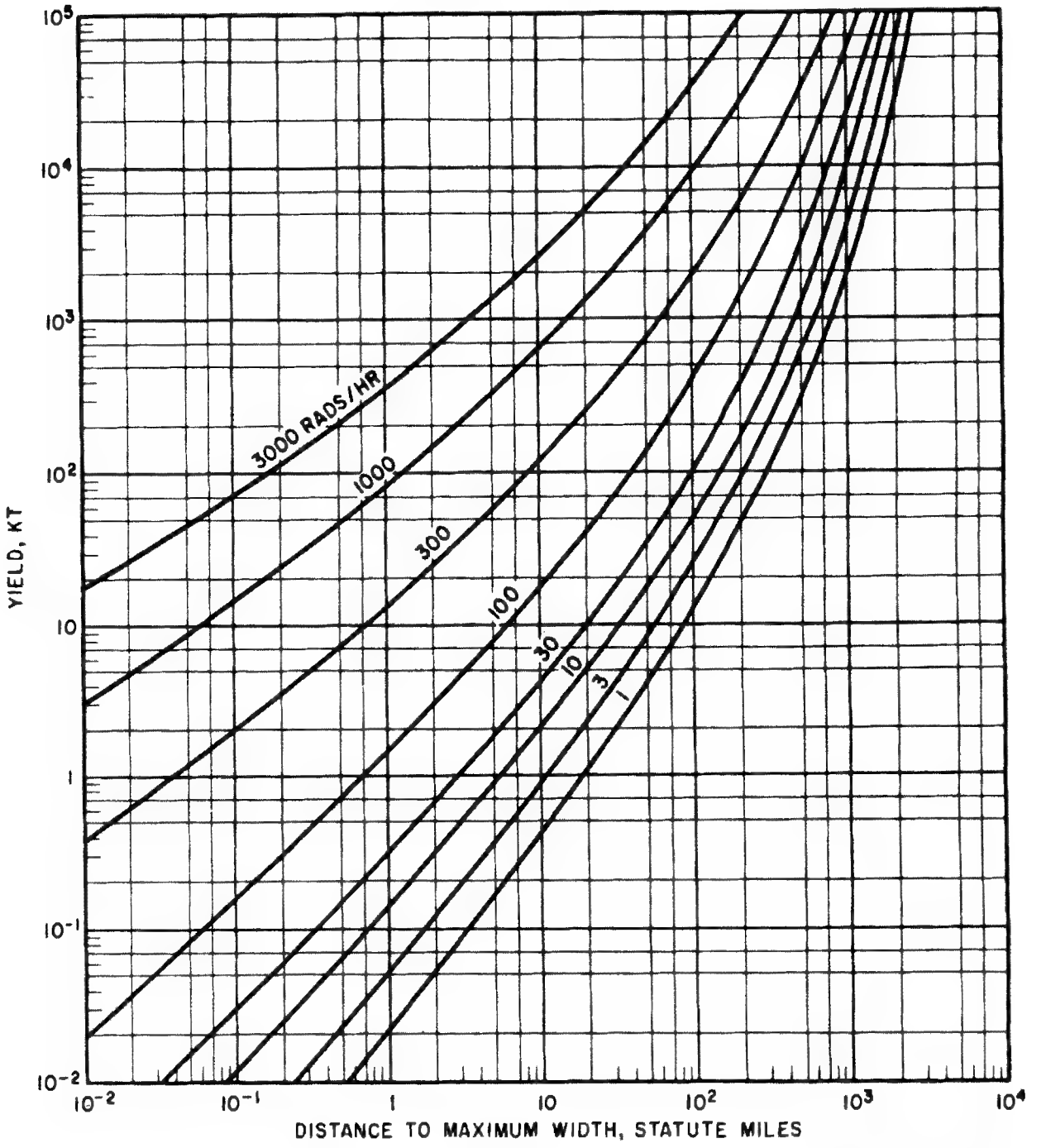

Figure 4-37. Yield vs. Distance to Maximum Width, 40-knot Effective Wind

[redacted]

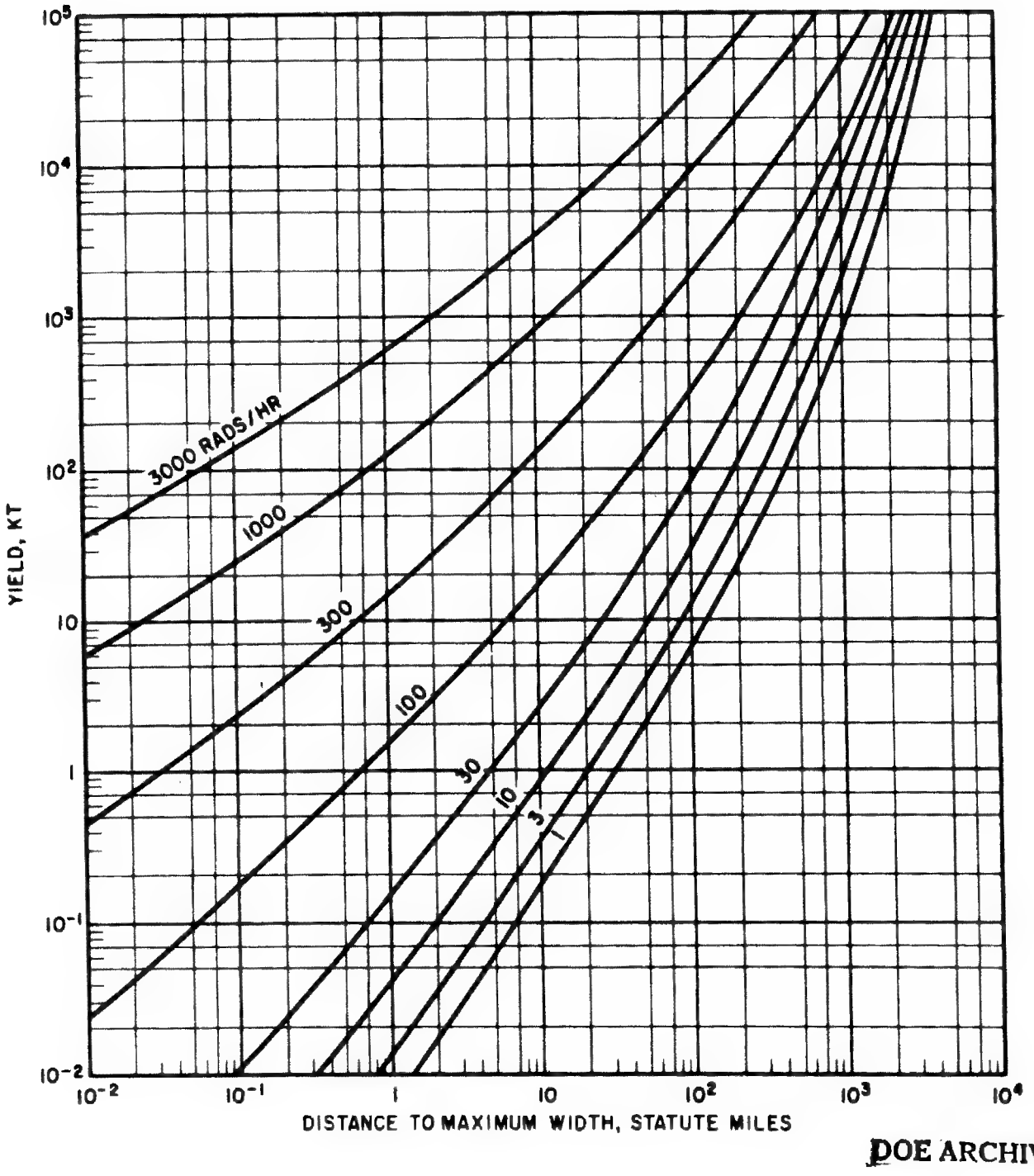

Figure 4-38. Yield vs. Distance to Maximum Width, 60-knot Effective Wind

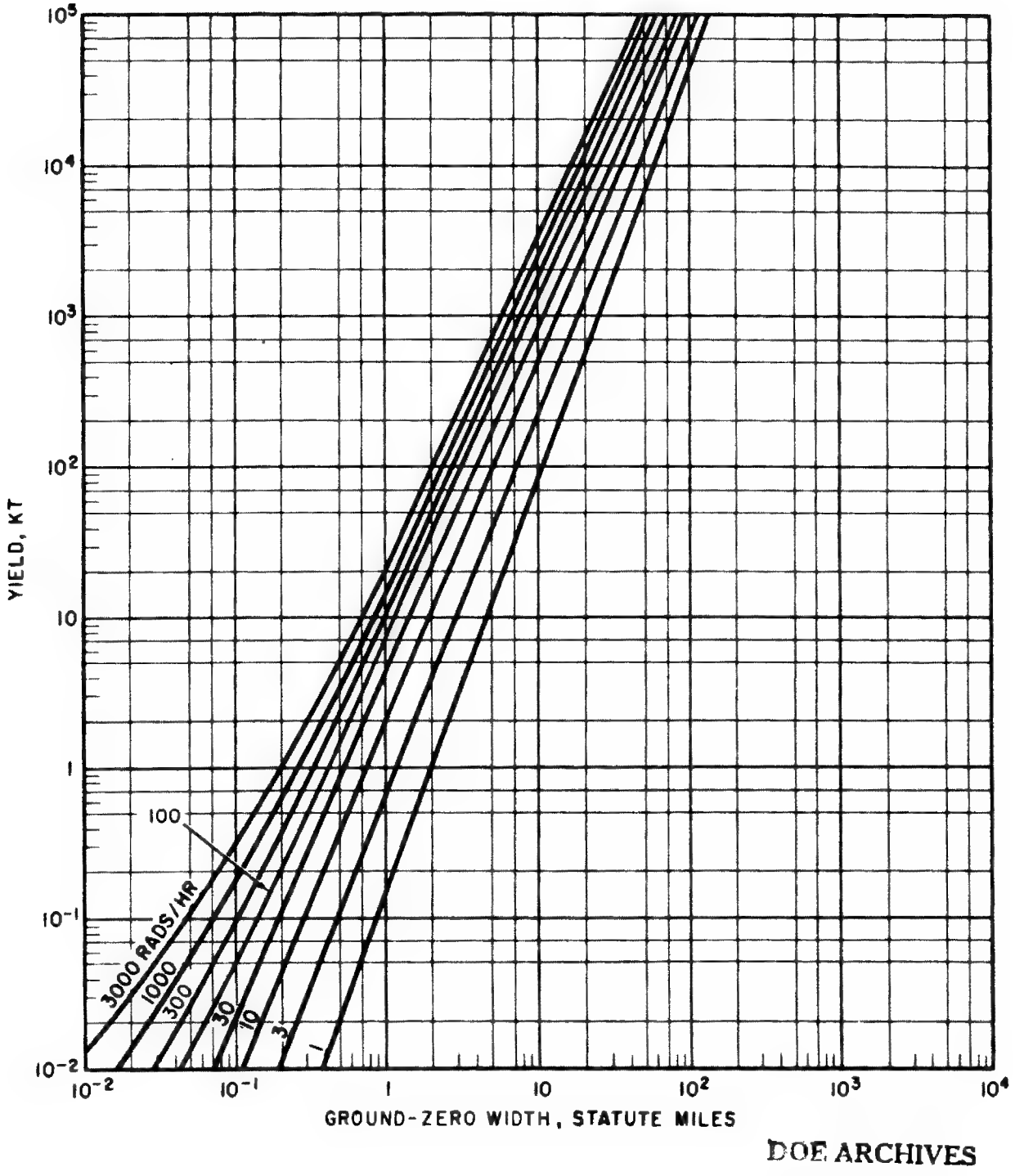

Figure 4-39. Yield vs. Ground-zero Width, 10-knot Effective Wind

[redacted]

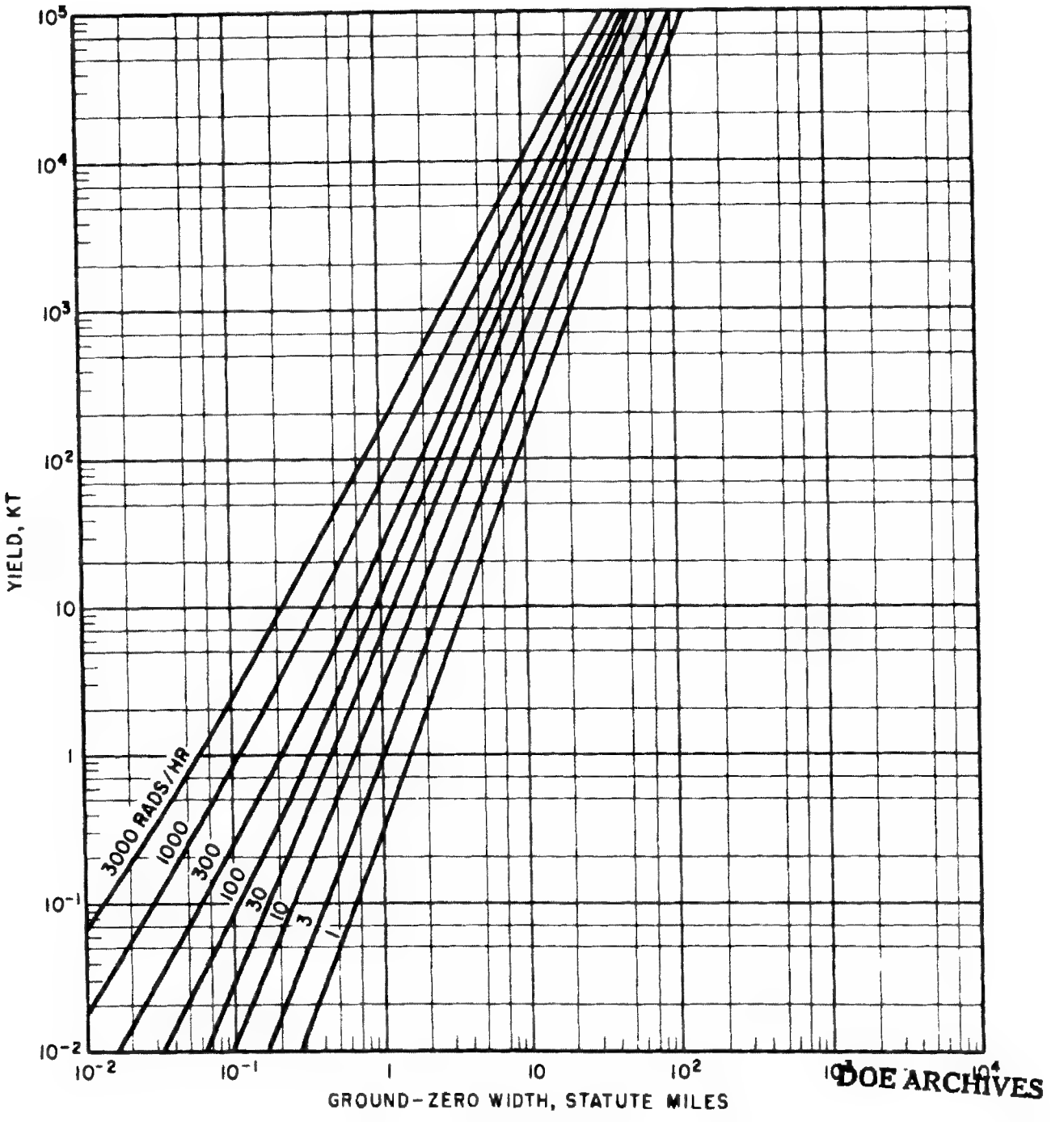

Figure 4-40. Yield vs. Ground-zero Width, 20-knot Effective Wind

[redacted]

115

[redacted]

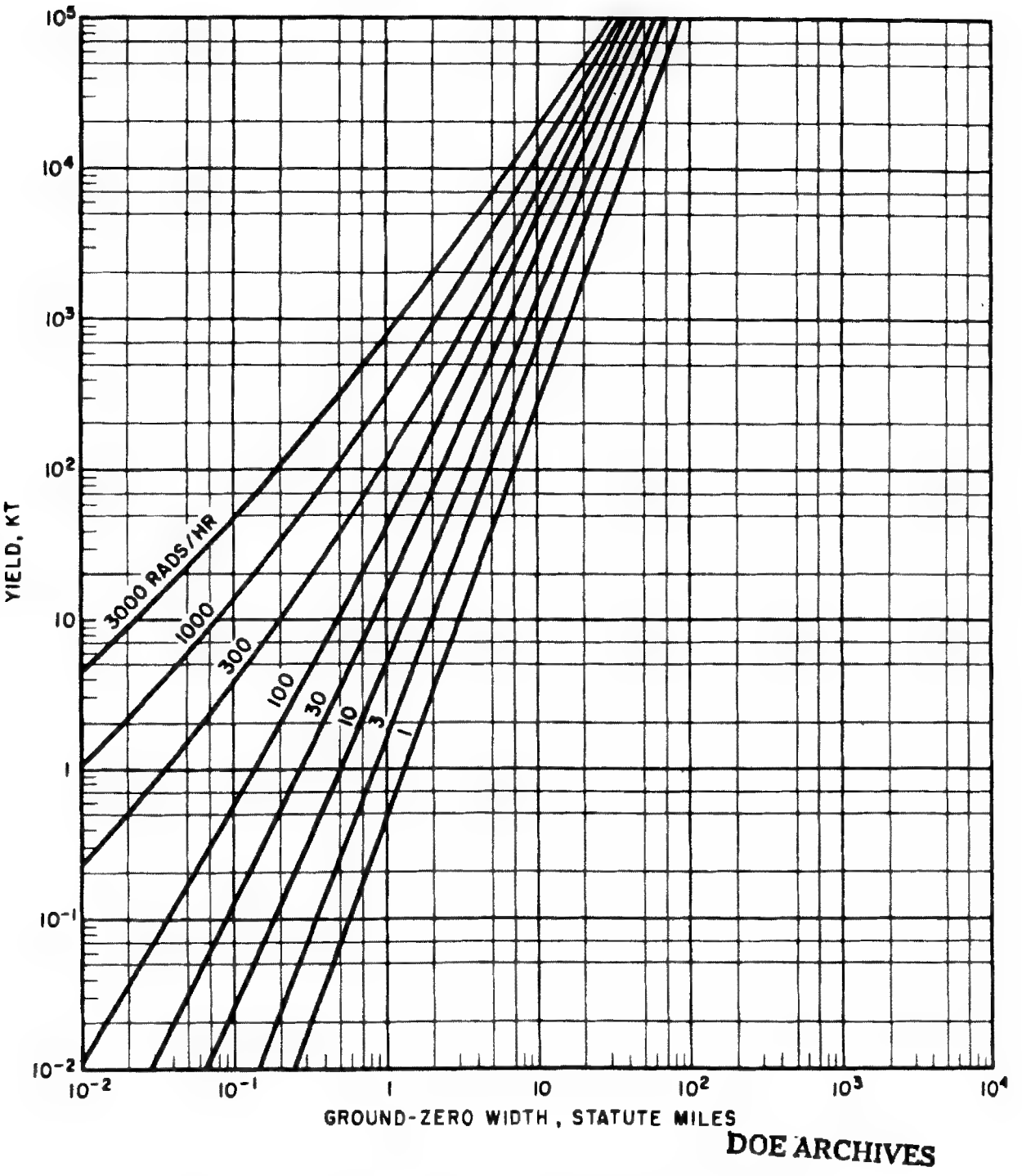

Figure 4-41. Yield vs. Ground-zero Width, 40-knot Effective Wind

[redacted]

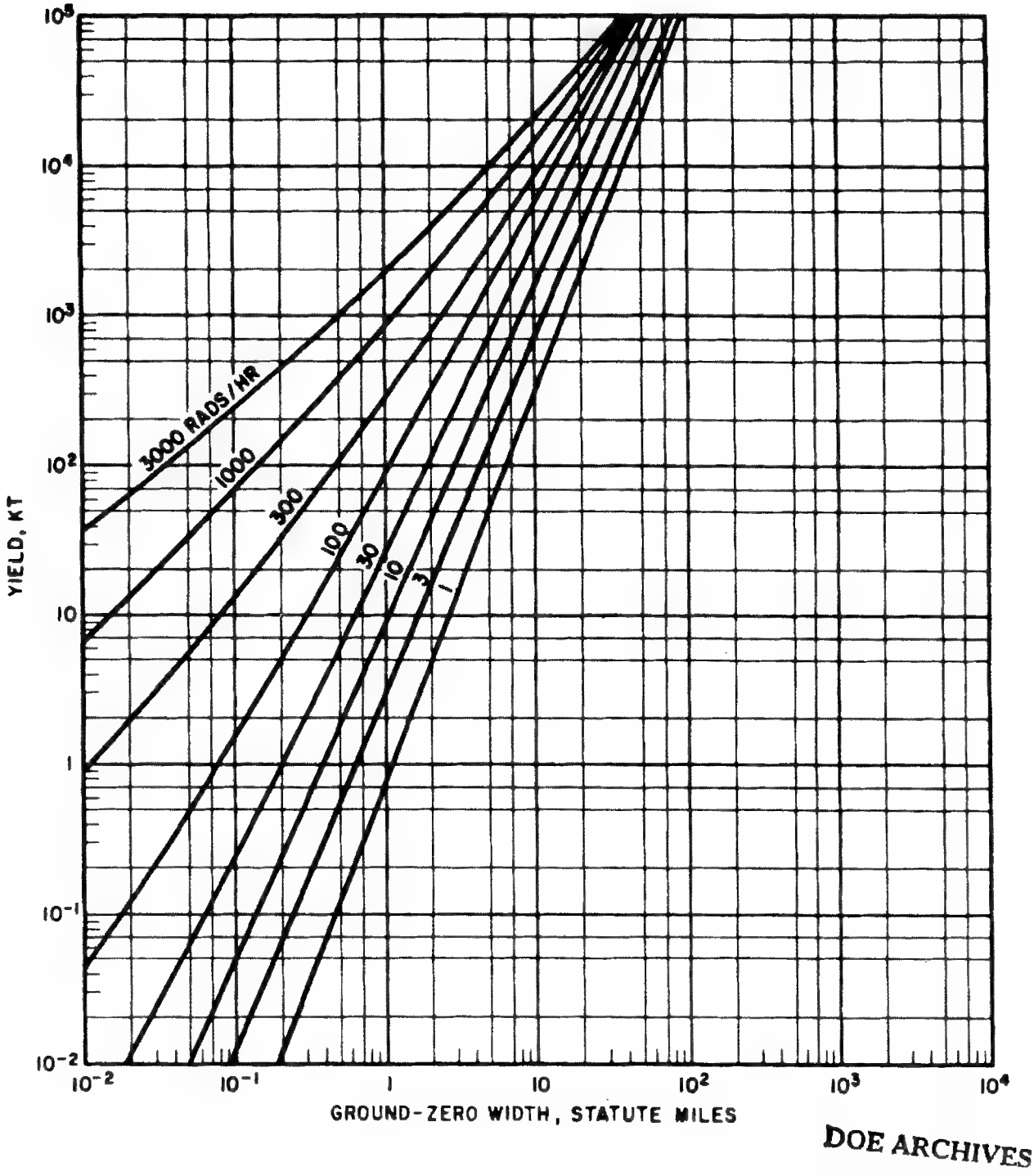

Figure 4-42. Yield vs. Ground-zero Width, 60-knot Effective Wind

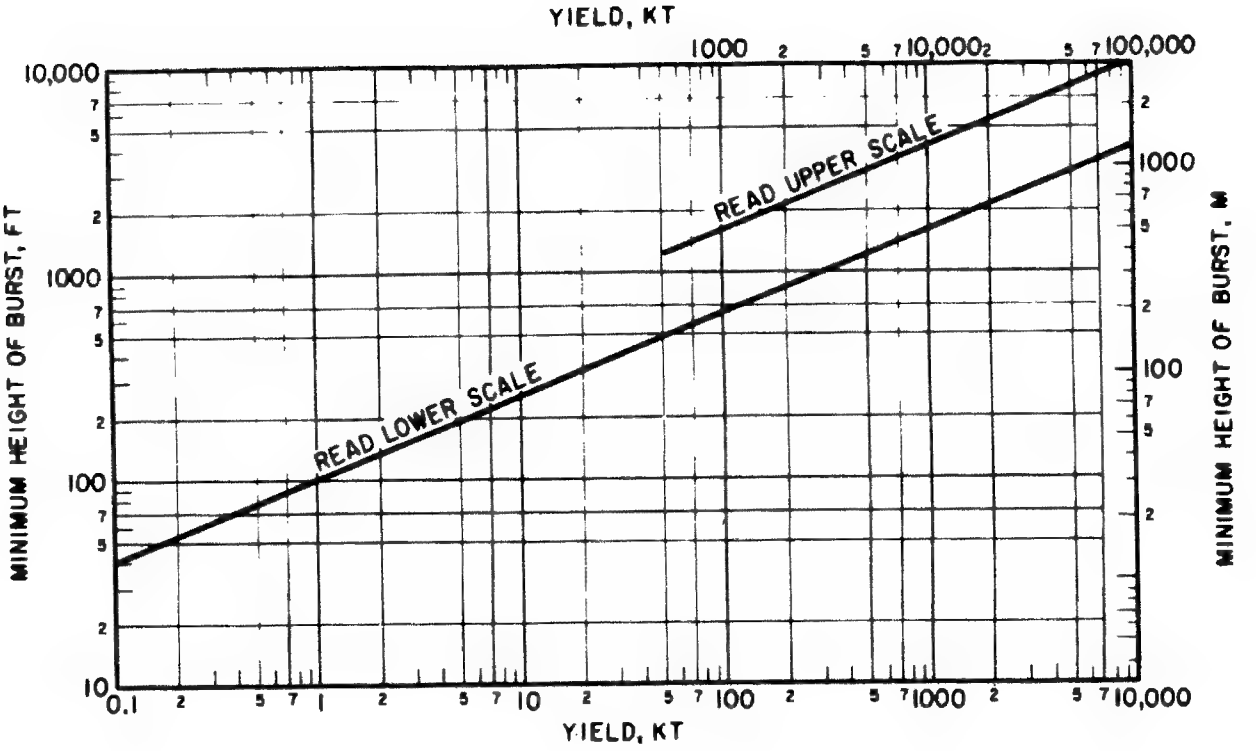

Figure 4-43. Minimum Height of Burst vs. Yield

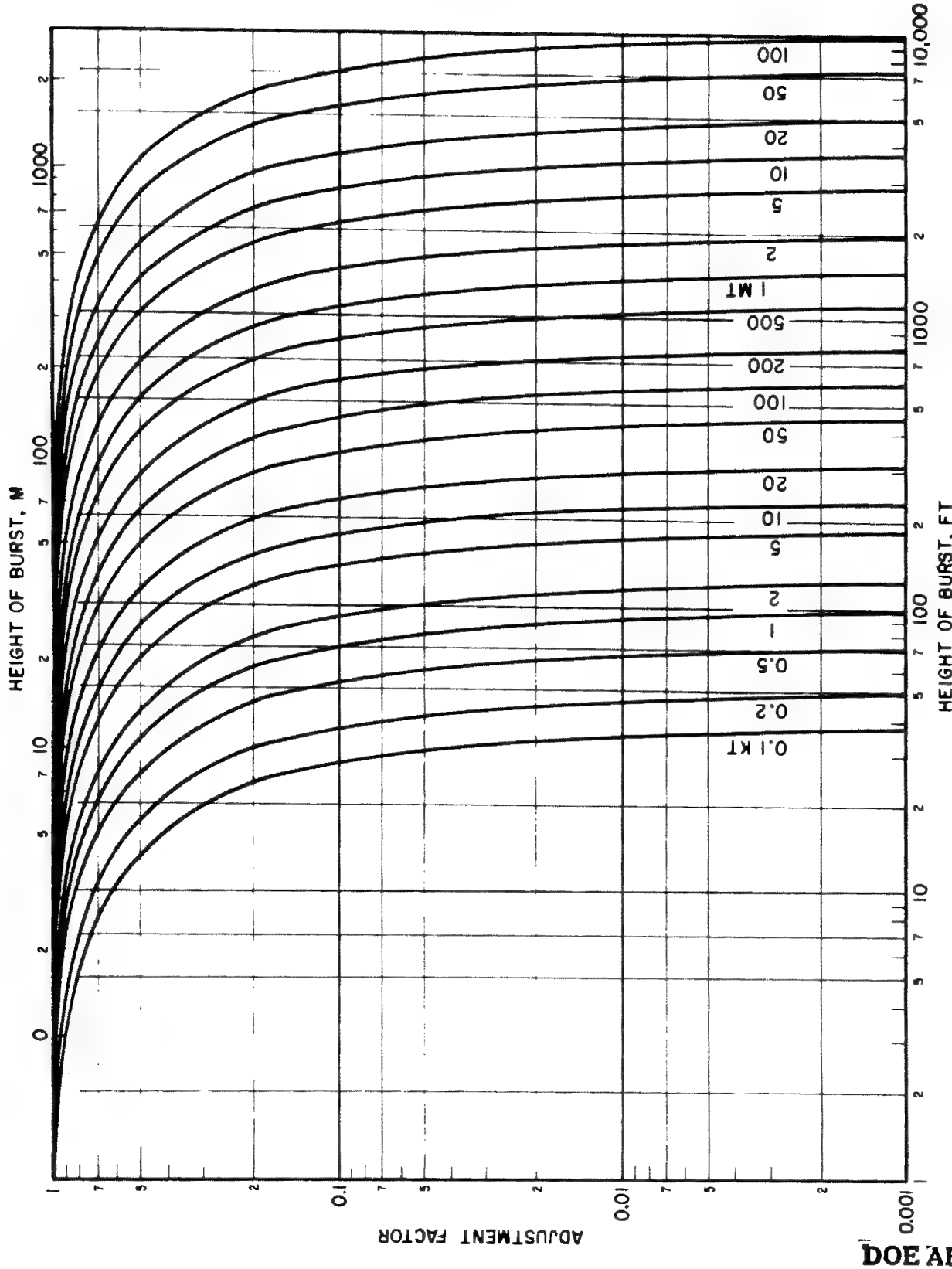

Figure 4-44. Height-of-burst Adjustment Factor for Dose-rate-contour Values Underwater Explosion, 15-knot Wind, Range of Burst Depths, 150 to 1000 ft

[redacted]

Problem 4-10 Residual Gamma Radiation From Underground Bursts (Determination of Fallout Contour Parameters for Underground Bursts)

Figure 4-45 presents depth multiplication factors for the surface-burst-contour parameters in figures 4-23 through 4-42. If the weapon yield and depth of burst are known, a multiplication factor can be determined from this curve. The idealized contour parameters of a surface burst of the same yield are multiplied by this factor to obtain idealized contour parameters for the underground burst.

Figures 4-23 through 4-42 must be used to obtain surface-burst parameters. These curves present idealized contour parameters for various effective wind speeds and for yields from 0.01 kt to 100 mt. These parameters are for a *reference* time of one hour after detonation on an infinite smooth plane. Because these surface-burst parameters must be used in determining contours for underground bursts, all such conditions that apply to figures 4-23 through 4-42 also apply to the resulting underground burst contours. For example, to obtain dose-rate values for times other than $H + 1$ hr, adjustment procedures are the same for underground bursts as those for surface bursts as discussed in the explanatory text for these figures.

The following example illustrates the use of figure 4-45 with figures 4-23 through 4-42 to determine contour parameters for underground bursts.

Example.

Given: A 20-kt weapon burst 128 ft underground under 20-knot effective wind conditions.

Find. Idealized contour parameters for a dose rate of 100 rads/hr at 1 hr after detonation.

Solution: The scaled depth of burst is found as:

$$\frac{(\text{depth in ft})}{(\text{yield in kt})^{1/3.4}} = \frac{128}{(20)^{1/3.4}} = 53 \text{ ft/kt}^{1/3.4}$$

Using figure 4-45, the depth multiplication factor corresponding to this scaled depth is 1.2. Using figures 4-24, 4-28, 4-32, 4-36, and 4-40, the solution is shown in table 4-7.

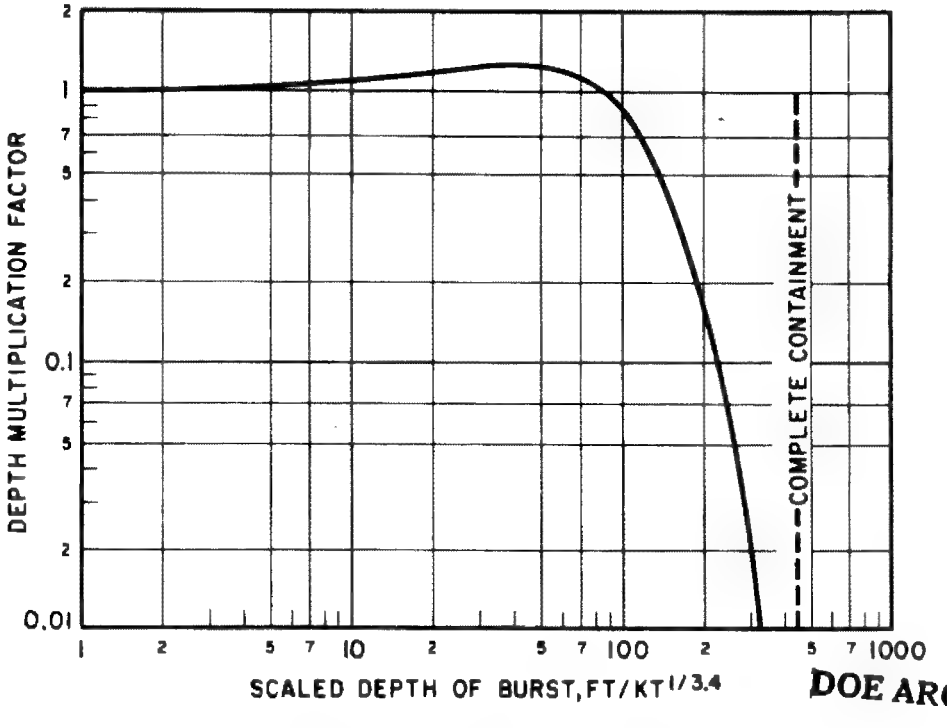

Figure 4-45. Depth Multiplication Factor for Linear Contour Dimensions vs. Scaled Depth of Burst

[redacted]

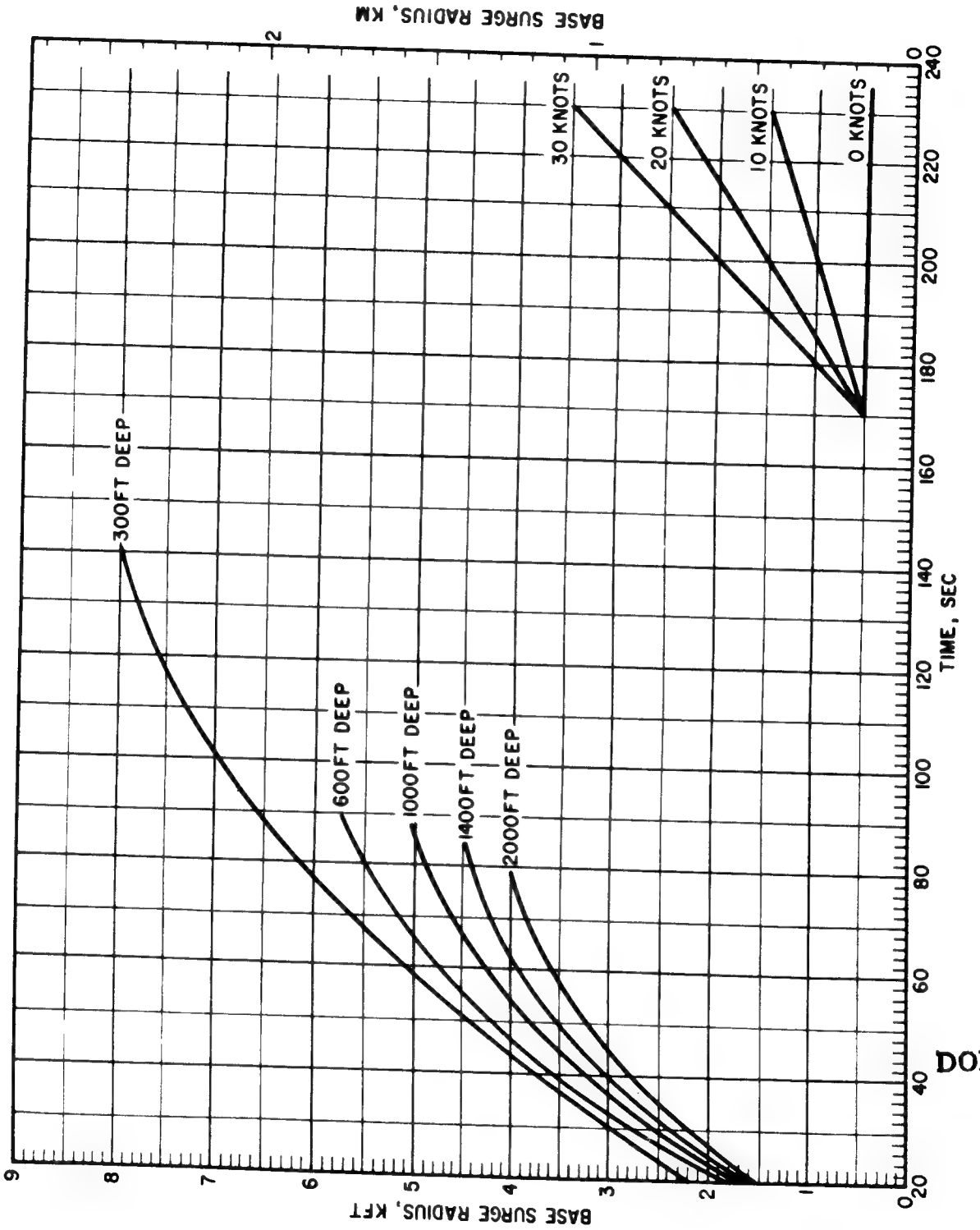

Figure 4-46. Base Surge Radius vs. Time for a 10-kt Yield

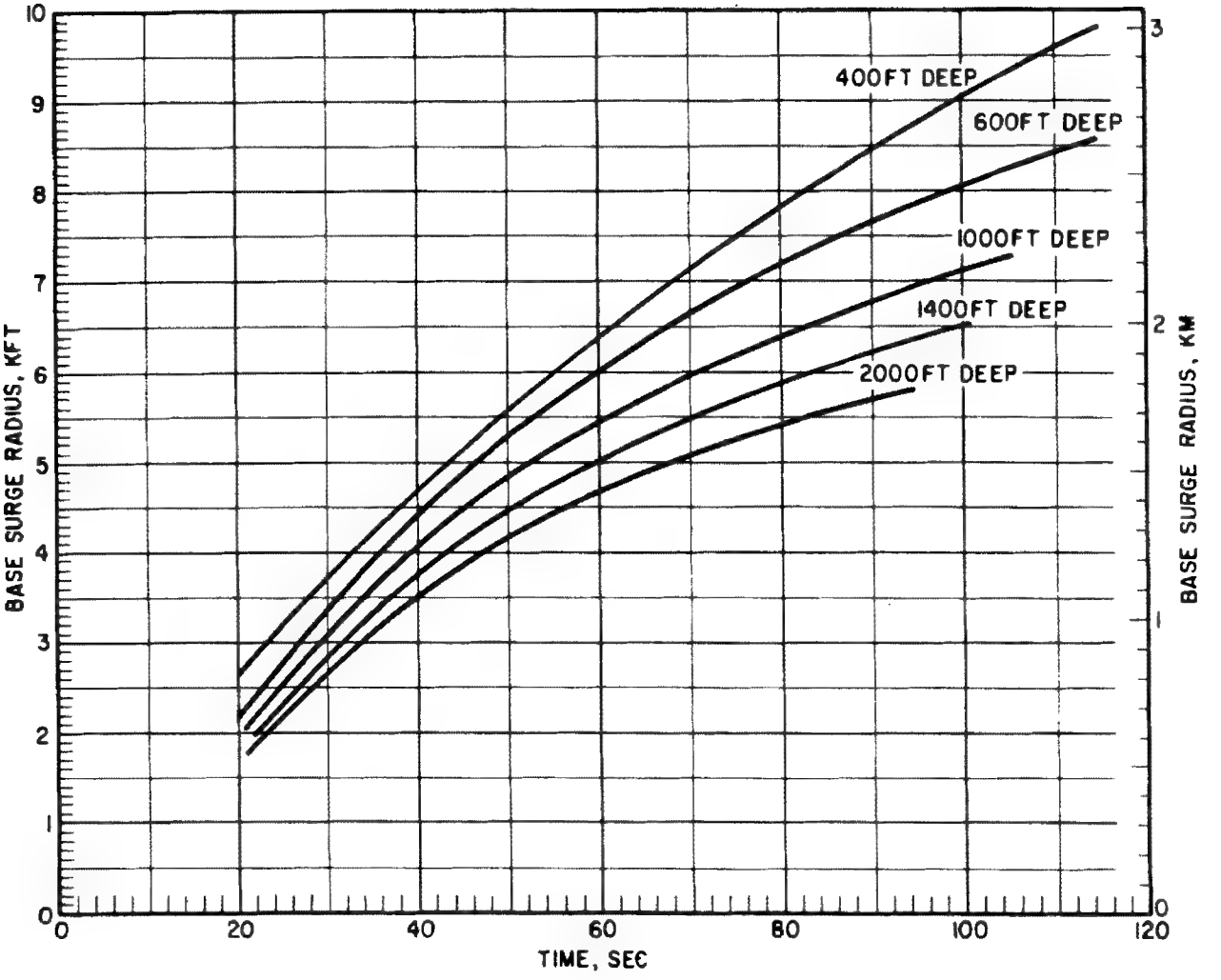

Figure 4-47. Base Surge Radius vs. Time for a 30-kt Yield

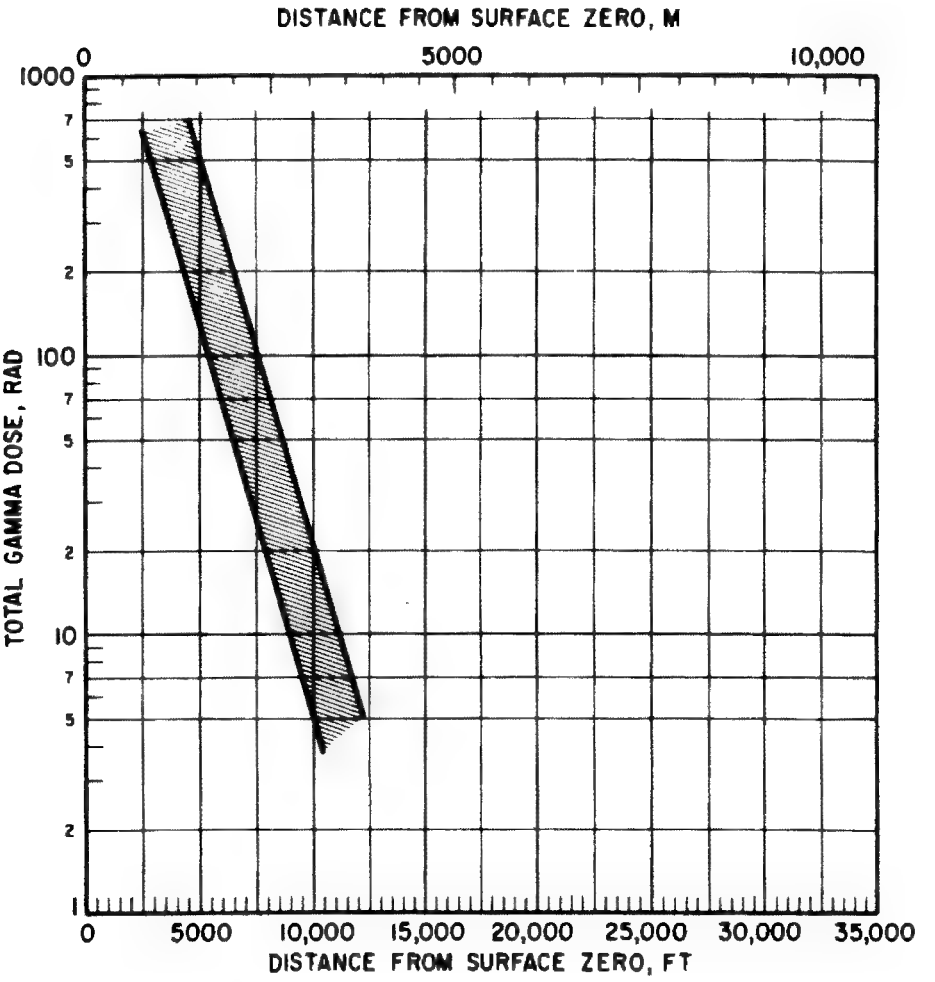

Figure 4-48. Total Dose at the Surface Upwind and Crosswind from a 10-kt

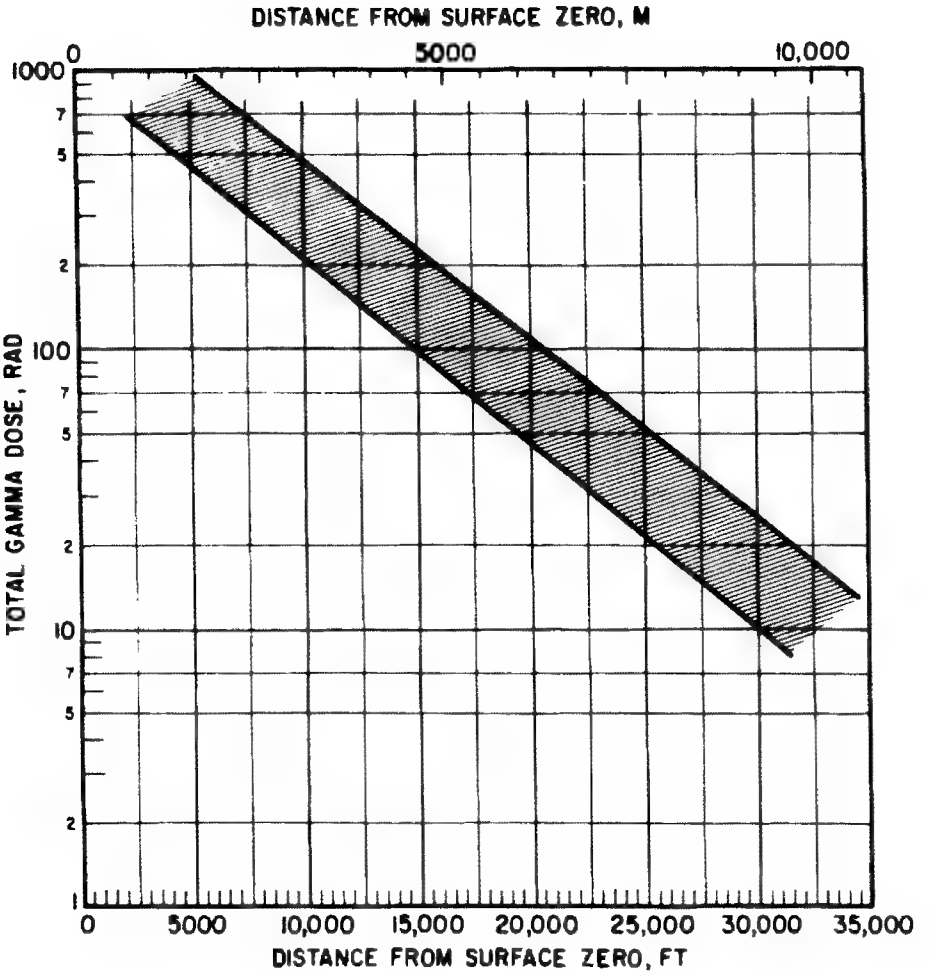

Figure 4-49. Total Dose at the Surface Downwind from a 10-kt Underwater Explosion, 15-knot Wind, Range of Burst Depths, 150 to 1000 ft

[redacted]

Problem 4-12 Total Radiation Dose Received in a Contaminated Area

Figure 4-50 gives the total dose received if one enters a given contaminated area at a specified time and remains for a specified interval of time. The vertical axis gives the accumulated dose for each unit (rads/hr) of dose rate at one hour after the detonation. The various curves represent time of stay in the contaminated area. To get the accumulated dose, a factor is taken from the vertical axis corresponding to the time of entry and the time of stay. The product of this factor and the dose rate at one hour gives this accumulated dose.

Example.

Given: The dose rate in a given area at 1 hr after detonation is 500 rads/hr.

Find: The total dose received by a man entering the area 2 hr after detonation and remaining 4 hr.

Solution: From figure 4-50 the intersection of the line for a time of entry of 2 hr after detonation with the 4-hr curve gives a factor of 0.8.

Answer: Therefore, the accumulated dose is:

$$500 \times 0.8 = 400 \text{ rads}$$

Related Material. See paragraphs 4-19 and 4-23. See also figures 4-21 and 4-22.

[redacted]

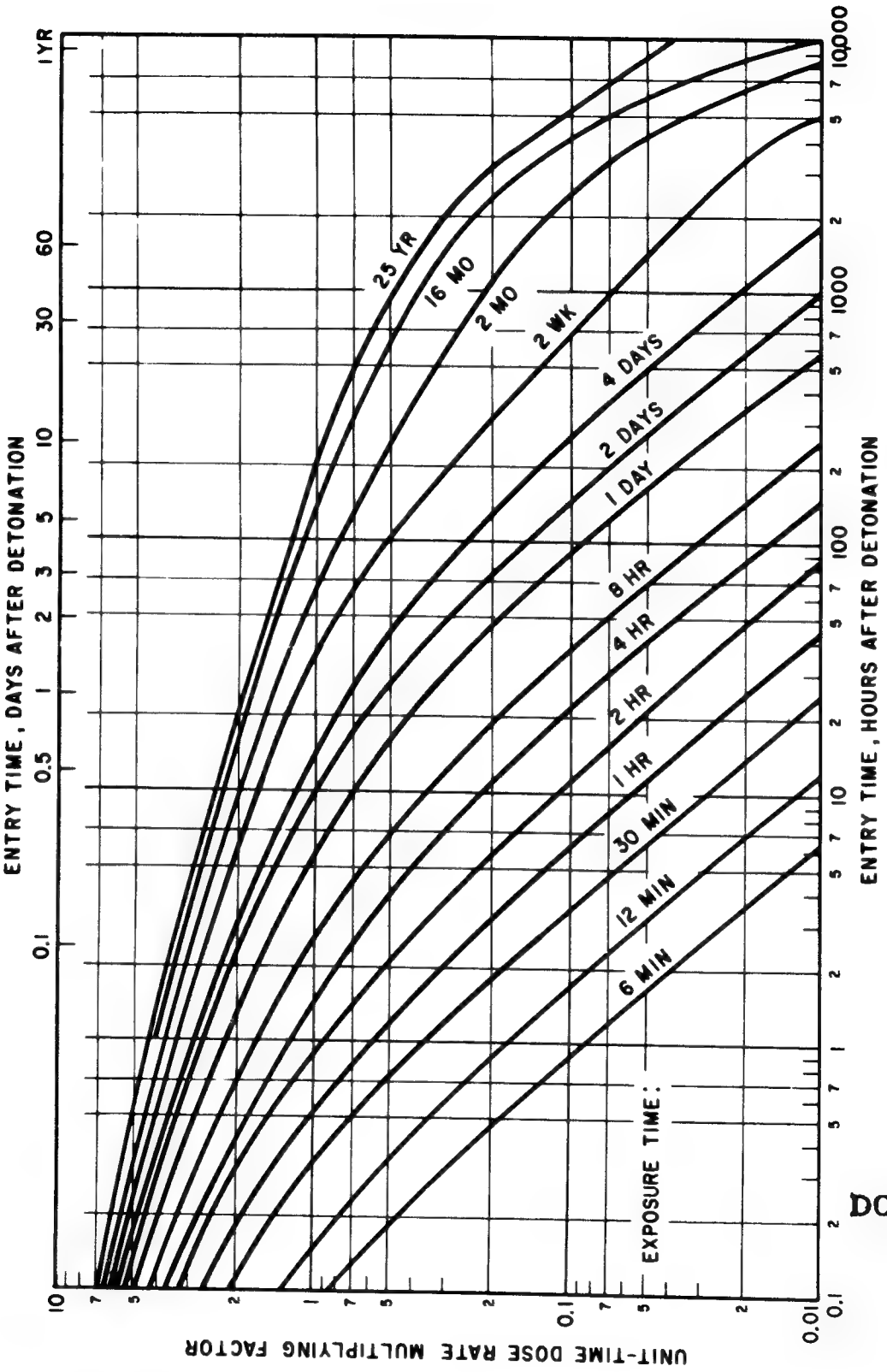

Figure 4-50. Total Radiation Dose from Early Fallout Based on Unit-Time Reference Dose Rate

Problem 4-13 Cloud Height Growth

Figure 4-51 gives the percentage of the maximum height reached by a nuclear cloud as the cloud moves up into the atmosphere for times after detonation up to about 7 min.

Example.

Given: A 5-mt nuclear detonation on a temperate land surface.

Find: The altitude of the cloud top 3 min after detonation.

Solution: From figure 4-51, at 3 min after burst time the cloud has reached 62 percent of its maximum altitude. From figure 4-52, the cloud top maximum altitude is between 60,000 and 70,000 ft.

Answer: Using 65,000 ft as the mean probable altitude, the cloud top at 3 min is:

$$65{,}000 \times 0.62 = 40{,}300 \text{ ft high}$$

Reliability. Figure 4-51 applies to clouds from surface and air bursts of weapons with yields between 0.1 kt and 16 mt. The time to reach a given percentage of the maximum height is believed to be accurate within ±30 percent.

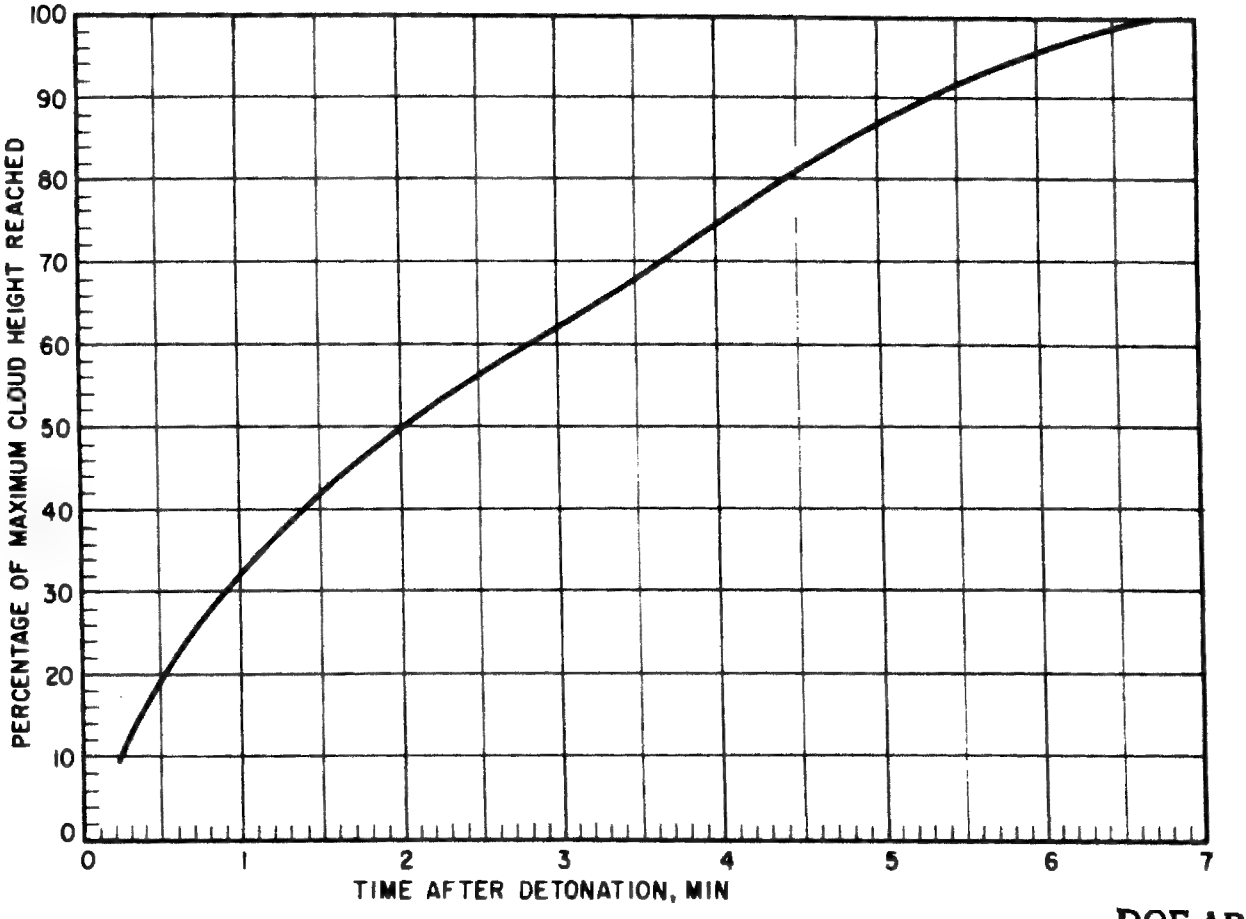

Figure 4-51. Percentage of Maximum Cloud Height Reached vs. Time

[redacted]

Problem 4-14 Stabilized Cloud Altitudes

Figures 4-52 and 4-53 give stabilized altitudes of nuclear cloud tops as a function of yield for various burst conditions and burst altitudes up to about 3000 ft above sea level.

Example.

Given: A 60-kt tropical land surface burst.

Find: The altitude of the top of the cloud after it ceases to rise, that is, when it is stabilized.

Solution: Figure 4-53 is applicable for bursts in tropical climates. The land surface curve shows the altitude for the stabilized cloud of a 60-kt burst to be between 35,000 and 45,000 ft.

Reliability. The breadth of the curves in figures 4-57 and 4-58 delineates the variation in maximum altitude which may be expected. It may be noted, however, that extremes in meteorological conditions, such as winds of 50 knots or more, can cause clouds from weapon yields less than 100 kt to stabilize at altitudes lower than indicated. (See figure 4-54.) Bursts of greater yield are less affected by meteorology with respect to cloud stabilization altitude.

Related Material. See figures 4-51 and 4-54.

[redacted]

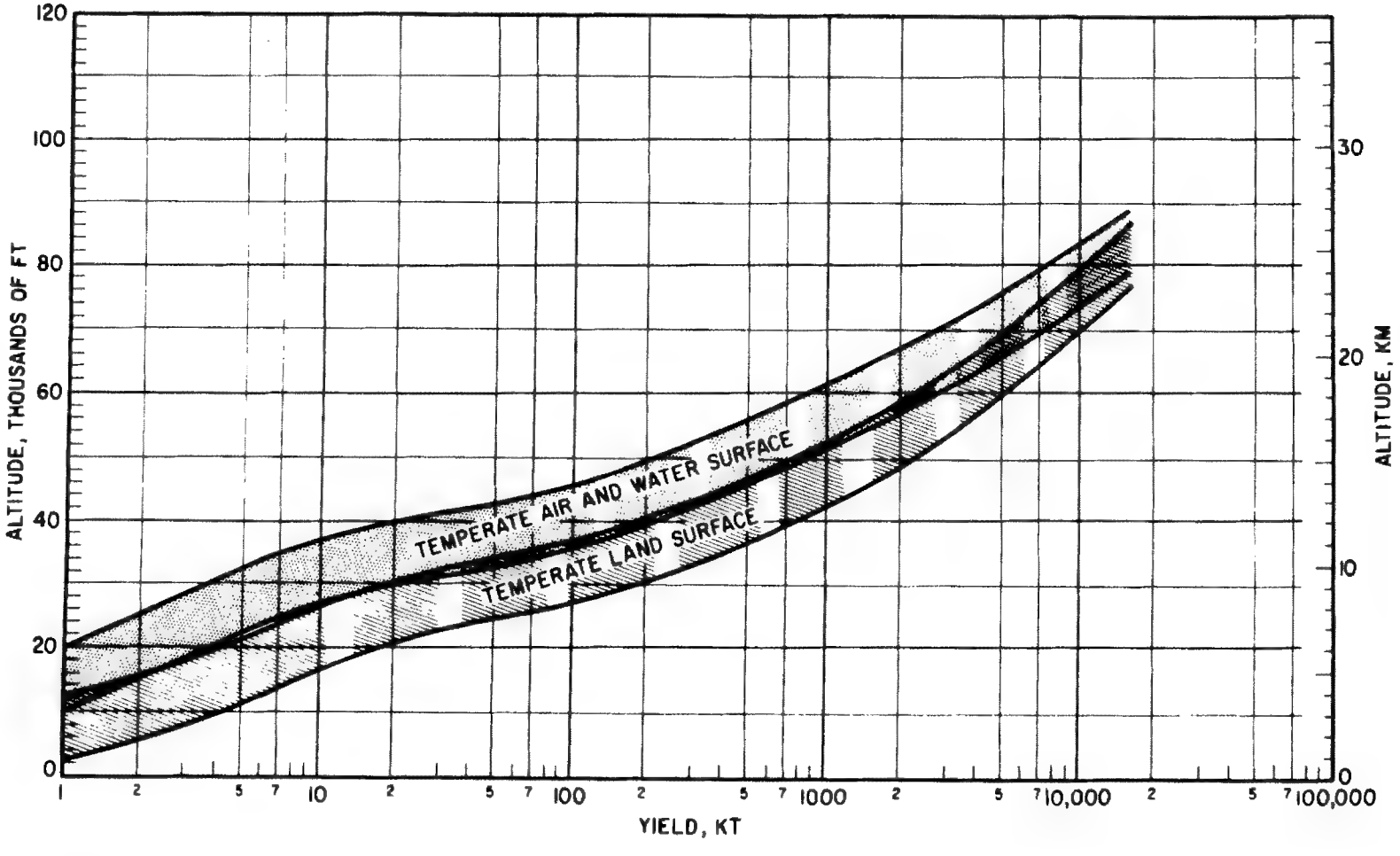

Figure 4-52. Height of Cloud Tops vs. Yield, Temperate Climates

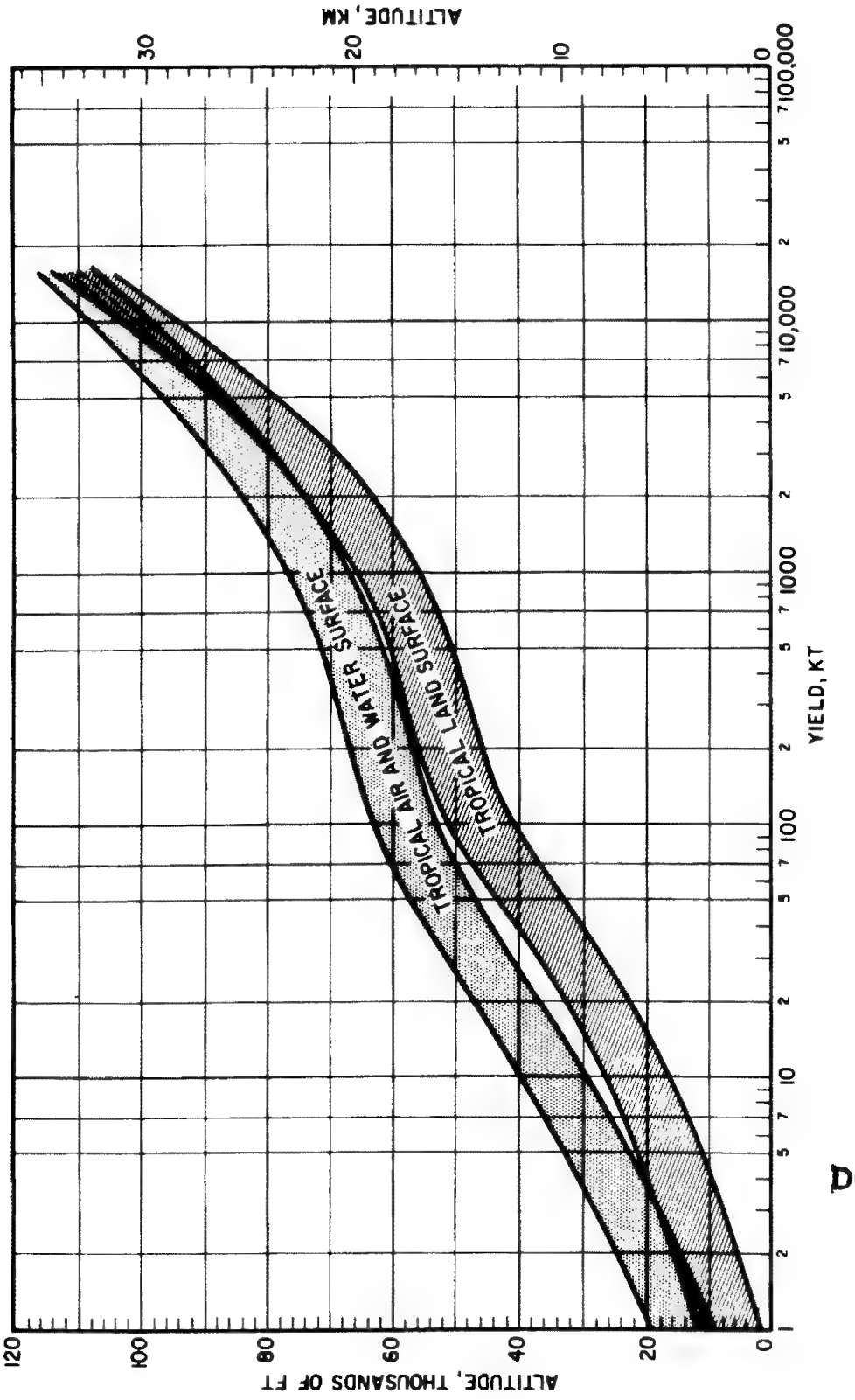

Figure 4-53. Height of Cloud Tops vs. Yield, Tropical Climates

762-909 O - 65 - 17

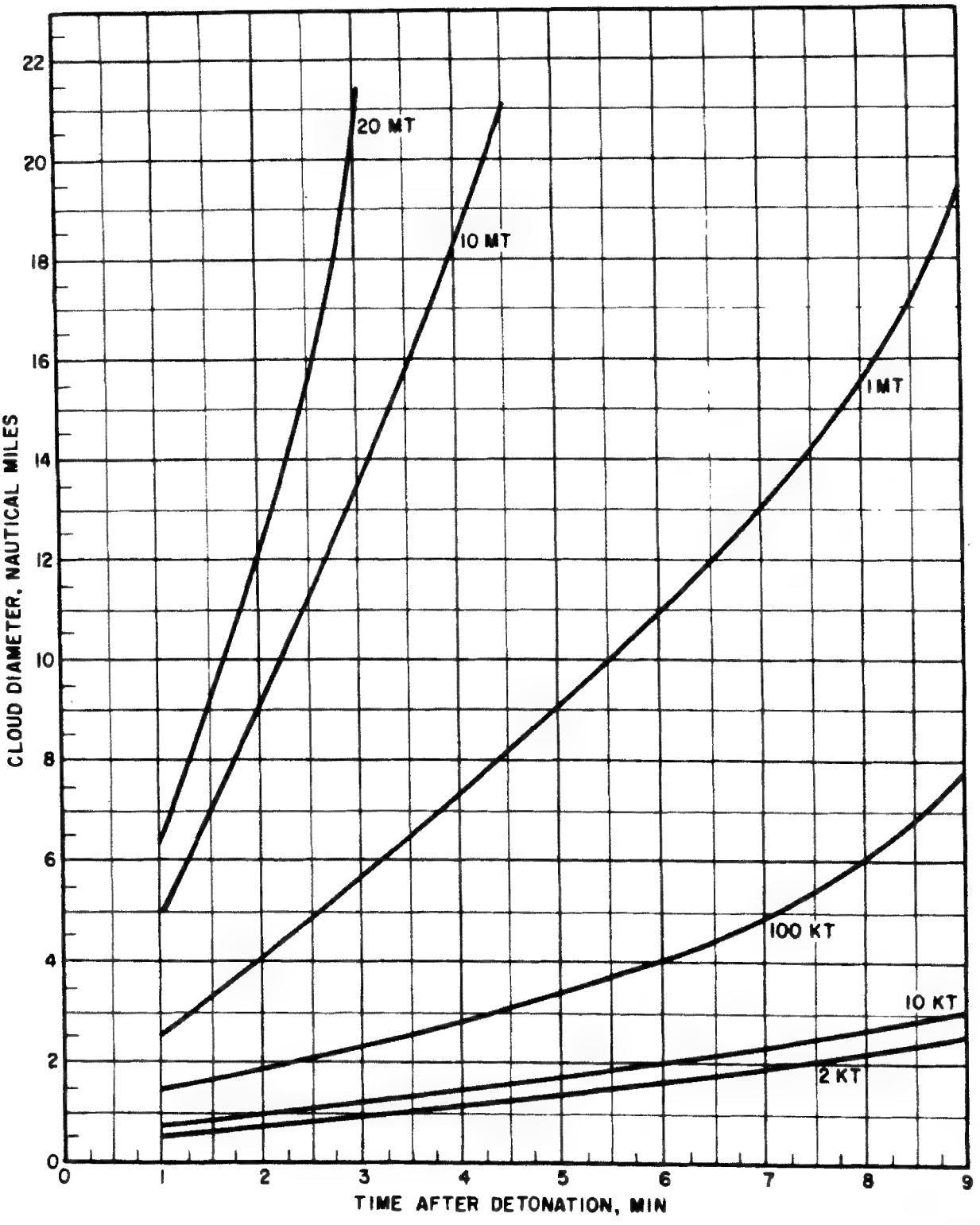

Figure 4-54. Cloud Diameter vs. Time

[redacted]

Problem 4-15 Dose Received While Flying Through a Nuclear Cloud

The curves of figure 4-55 give the total dose received when passing through nuclear clouds at various times after burst. The relative hazard for flight through the stem is not definitely known; however, flight through the stem is considered somewhat less hazardous than flight through the center of the cloud.

Example.

Given: An aircraft flying at an altitude of 22,000 ft with a speed of 310 knots passes through the center of the nuclear cloud from a 50-kt weapon detonated on a temperate land surface.

Find: The maximum and minimum probable radiation doses the aircraft crew may receive.

Solution: From figure 4-52, the cloud will stabilize at an altitude between 24,000 and 34,000 ft. Then 22,000 ft is between 92 percent and 65 percent of the altitude at which the cloud will stabilize. From figure 4-51, the cloud will reach 22,000 ft at a time between 3.2 and 5.5 min after burst. Using figure 4-54 and interpolating for a 50-kt weapon, the cloud diameter will be between 2 and 2.6 nautical miles. Using the aircraft speed of 310 knots, the maximum and minimum transit times through the cloud are:

$$\frac{2.6}{310} = 0.0084 \text{ hr} = 0.5 \text{ min}$$

$$\frac{2}{310} = 0.065 \text{ hr} = 0.4 \text{ min}$$

The probable maximum dose will result with a time of entry of 3.2 min after burst with the applicable transit time of 0.4 min; the minimum with an entry time of 5.5 min after burst and transit time of 0.5 min. Using figure 4-55 these doses are found by interpolating:

Probable maximum dose = 85 rads

Probable minimum dose = 26 rads

It should be understood that the purpose of the above example is primarily to illustrate the use of figure 4-55. However, because figures 4-51, 4-52, and 4-53 were also used in obtaining the solution, the reliability of the solution depends on the combined reliabilities of these figures.

Reliability. The doses indicated by figure 4-55 are considered accurate within a factor of 2 for flight paths passing near the cloud center. For paths close to the cloud boundaries, the predicted dose will probably be higher than the actual dose, although the magnitude of the error is unknown.

Related Material. See figures 4-51 through 4-54.

[redacted]

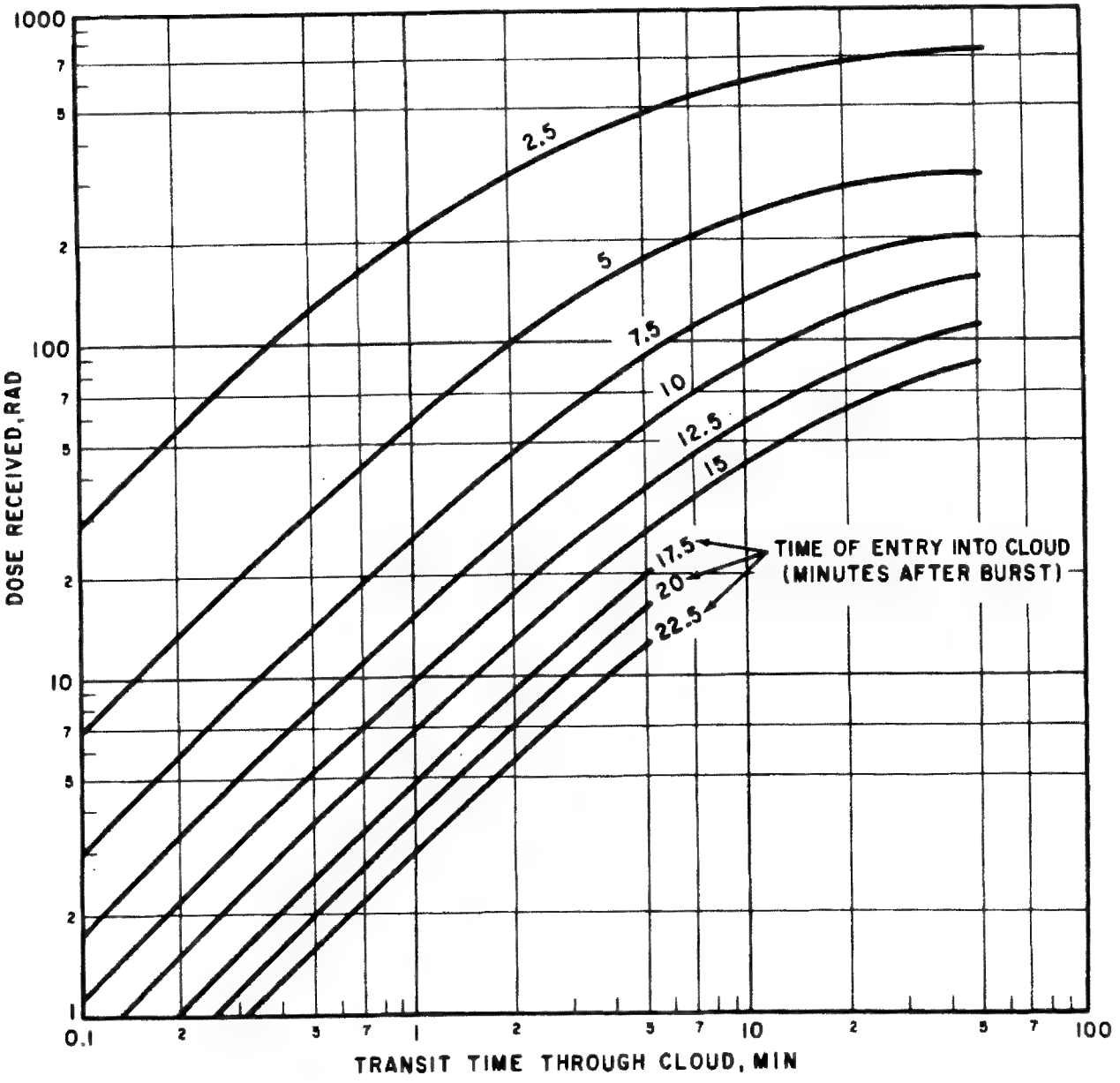

Figure 4-55. Dose Received While Flying Through a Nuclear Cloud vs. Transit Time Through Cloud

[redacted]

Problem 4-16 Neutron-induced Gamma Activity

Given the weapon type and the slant range from the point of burst to the point of interest, the induced-gamma dose rates in the vicinity of ground zero at $H + 1$ hr can be estimated using figures 4-56 to 4-58 for bursts over soils similar in composition to any of the soils illustrated in table 4-1. Figure 4-56 should be used for sub-kiloton fission weapons and is normalized to 1 ton. Figure 4-57 is normalized to 1 kt for use with average and high-flux fission weapons. Figure 4-58, for fusion weapons, is normalized to 1 mt of fission yield. To estimate the dose rate, enter the slant-range axis with the slant distance in yards, read the dose rate for the appropriate weapon type, and multiply this dose rate by the appropriate factor for the soil type of interest from the following:

Soil type	Multiplying factor
I	0.11
II	1
III	12
IV	0.0026

Scaling. For yields other than those for which the curves are normalized, multiply the dose rate from the curve by the yield of the weapon in question in tons, kt, or mt as appropriate.

Example.

Given: An average-neutron-flux 50-kt weapon is burst at a height of 900 ft above soil of type III.

Find: The $H + 1$ hr dose rate at ground zero and at 600 yd from ground zero.

Solution: From the average-neutron-flux weapon curve of figure 4-57 the dose rate at $H + 1$ hr at ground zero (300-yd slant range) is 10 rads/hr/kt of weapon yield. The multiplying factor for soil type III is 12.

Answer: Therefore, the dose rate at ground zero 1 hr after detonation of a 50-kt weapon over soil type III is:

$$50 \times 12 \times 10 = 6000 \text{ rads/hr}$$

At 600 yd from ground zero the slant range is 670 yd. From the curve, the induced gamma intensity is 0.43 rads/hr/kt of weapon yield at this distance.

Answer: Therefore, the dose rate 600 yd from ground zero 1 hr after detonation of a 50-kt weapon over soil type III is:

$$50 \times 12 \times 0.43 = 258 \text{ rads/hr}$$

Reliability. Dose-rate values taken from the curves for the soils presented are correct to within a factor of 5 for the conditions indicated. For other soils, the data will merely furnish an estimate of the magnitude of the hazard.

Related Material. See paragraphs 4-8 to 4-10. See also figures 4-59 through 4-63.

[redacted]

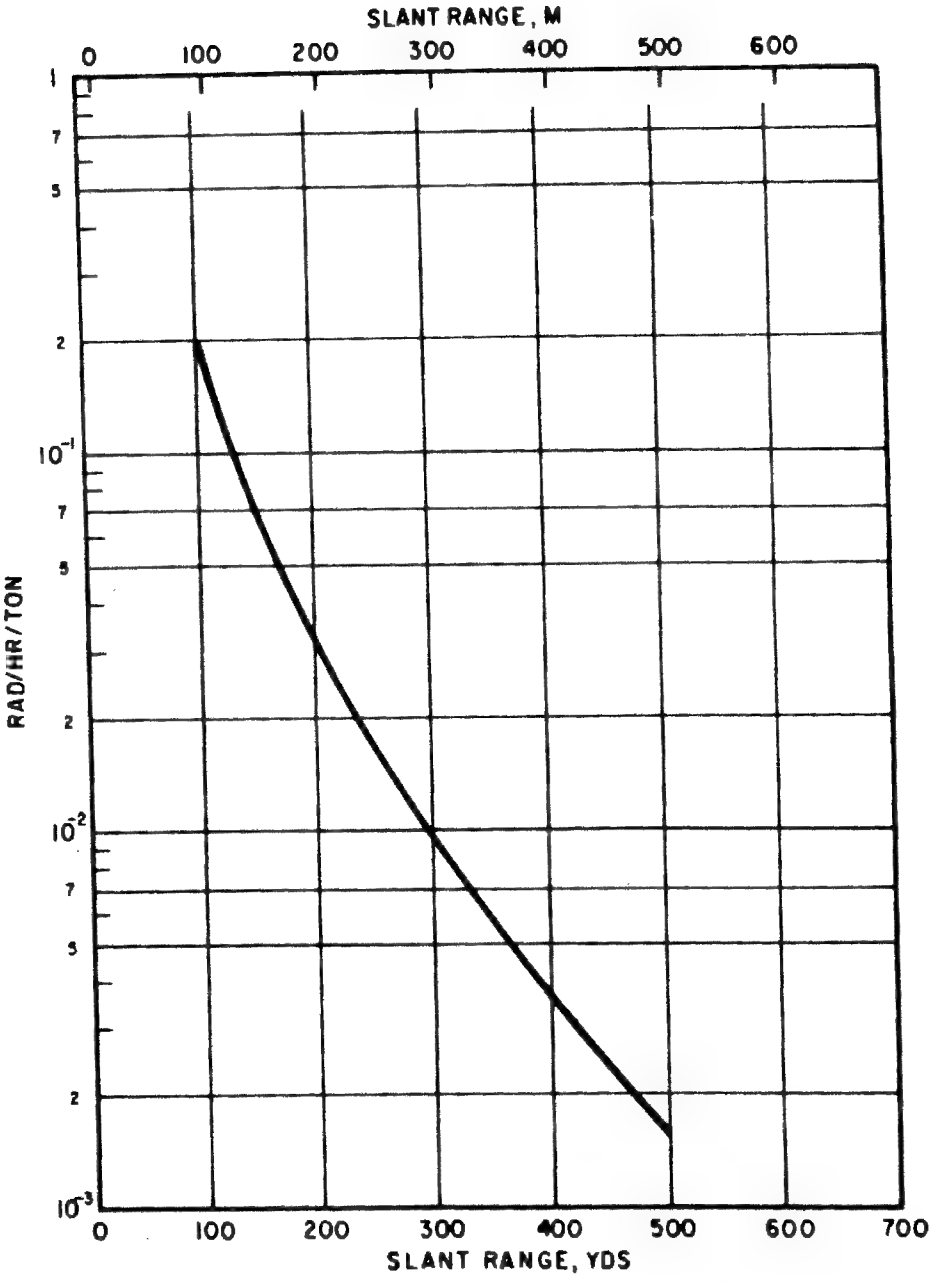

Figure 4-56. Neutron-induced Gamma Activity vs. Slant Range at a Reference Time of 1 hr After Burst, Sub-kiloton Fission Weapons per Ton

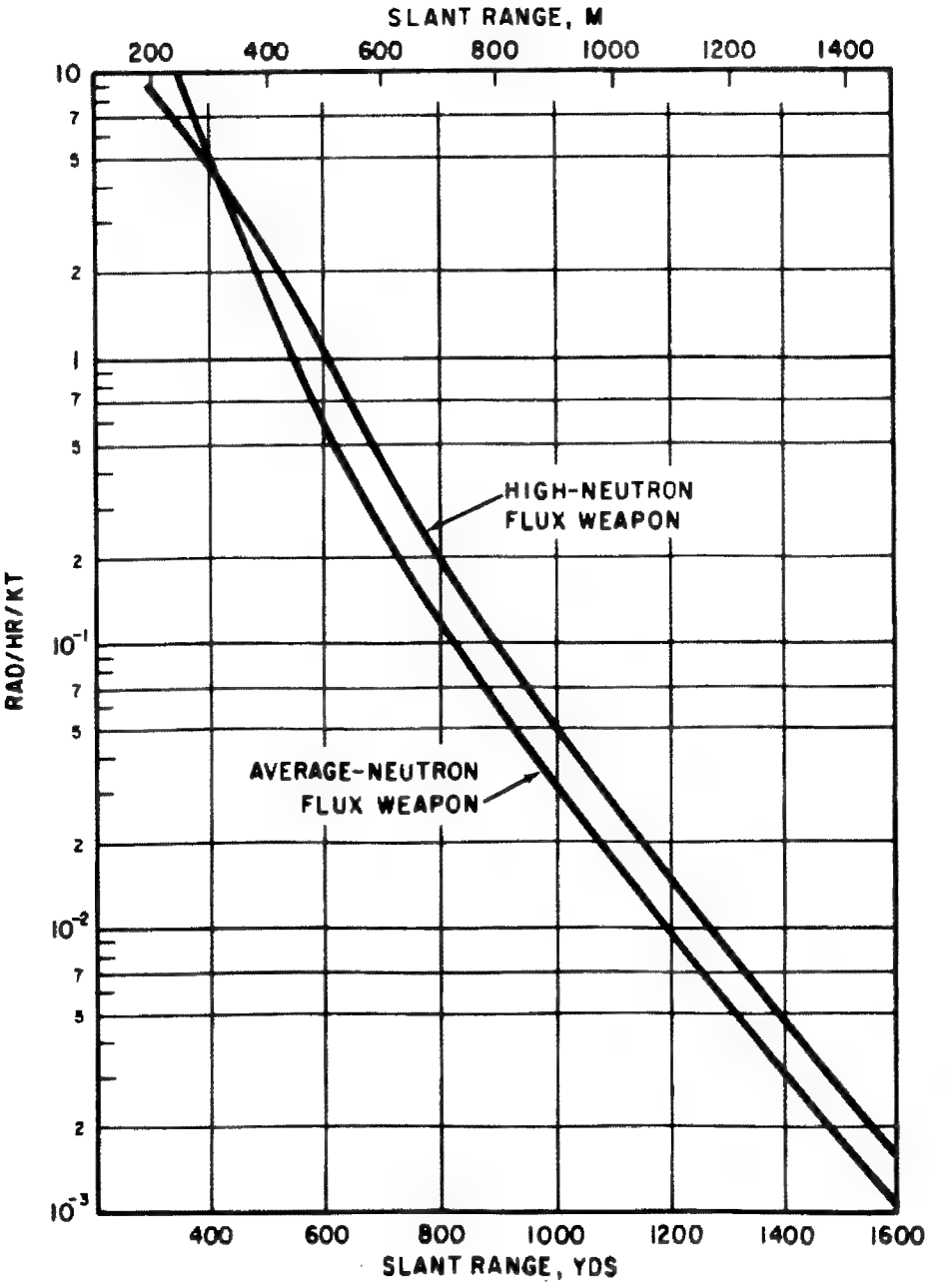

Figure 4-57. Neutron-induced Gamma Activity vs. Slant Range at a Reference Time of 1 hr After Burst, Fission Weapons per kt

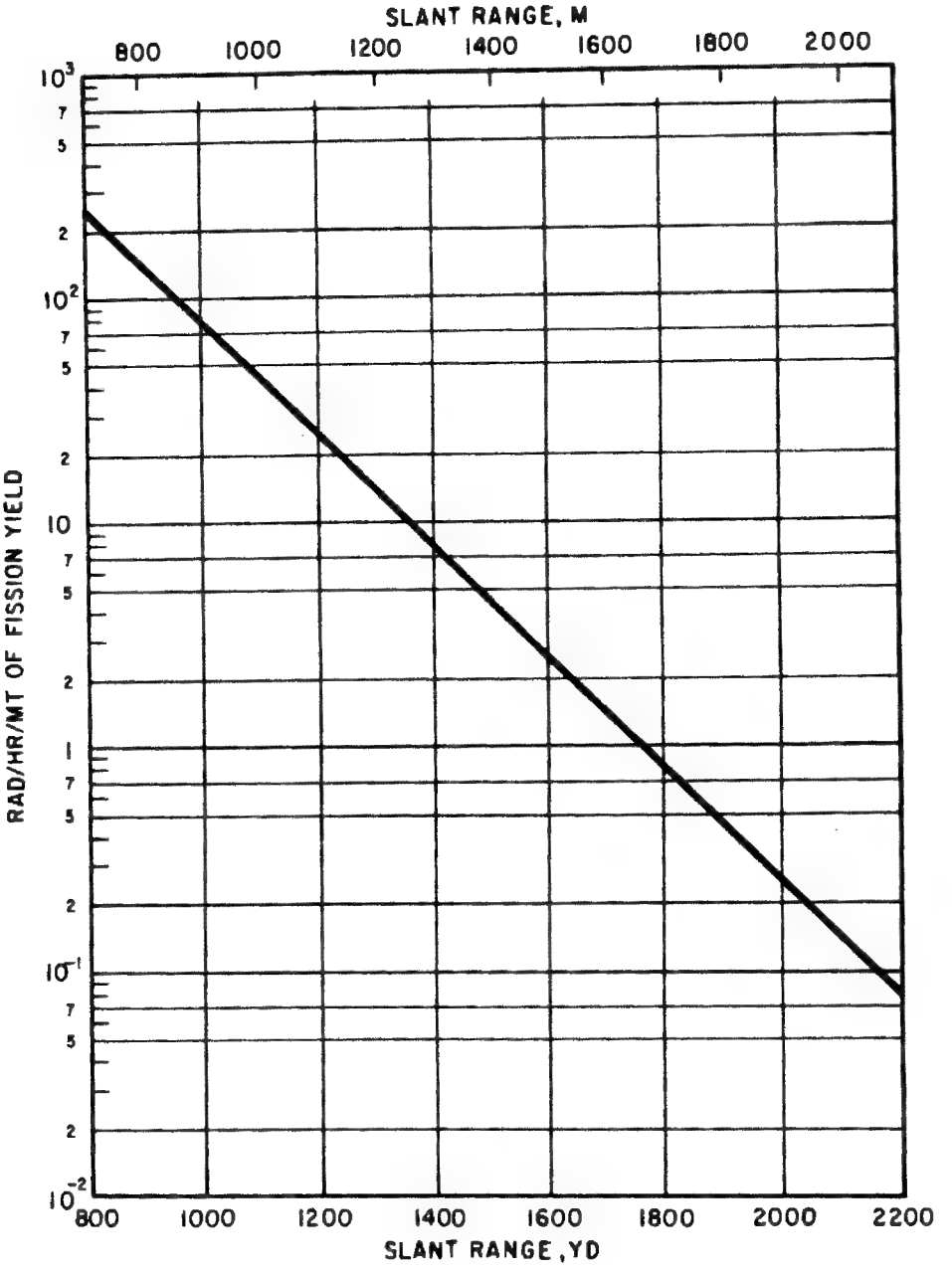

Figure 4-58. Neutron-induced Gamma Activity vs. Slant Range at a Reference Time of 1 hr After Burst, Fusion Weapons per mt of Fission Yield

[redacted]

From the dose rate at $H + 1$ hr, the dose rate at any other time is obtained by computing the product of the appropriate decay factor from figure 4-59 and the 1-hr dose rate.

Example.

Given: The dose rate at a given point on soil type I is 30 rads/hr at $H + 1$ hr.

Find: The dose rate at that point at $H + 1/2$ hr and at $H + 10$ hr.

Solution: From figure 4-59 the decay factors for soil type I for 1/2 hr and 10 hr are 3 and 0.083, respectively.

Answer: The dose rate at 1/2 hr is:

$$30 \times 3 = 90 \text{ rads/hr}$$

and the dose rate at 10 hr is:

$$30 \times 0.083 = 2.5 \text{ rads/hr}$$

The decay curves may also be used to determine the value of the dose rate at $H + 1$ hr from the dose rate at a later time. In this case, the measured dose rate is divided by the appropriate decay factor.

Example.

Given: The dose rate at a given point on soil type II 20 hr after detonation is 100 rads/hr.

Find: The dose rate at the same point 1 hr after the detonation.

Solution: From figure 4-59, the decay factor at 20 hr is 0.24.

Answer: Therefore, the dose rate at 1 hr is:

$$\frac{100}{0.24} = 417 \text{ rads/hr}$$

Reliability. The reliability is the same as for figures 4-56 to 4-58.

Related Material. See paragraphs 4-8 to 4-10. See also figures 4-56 through 4-63.

[redacted]

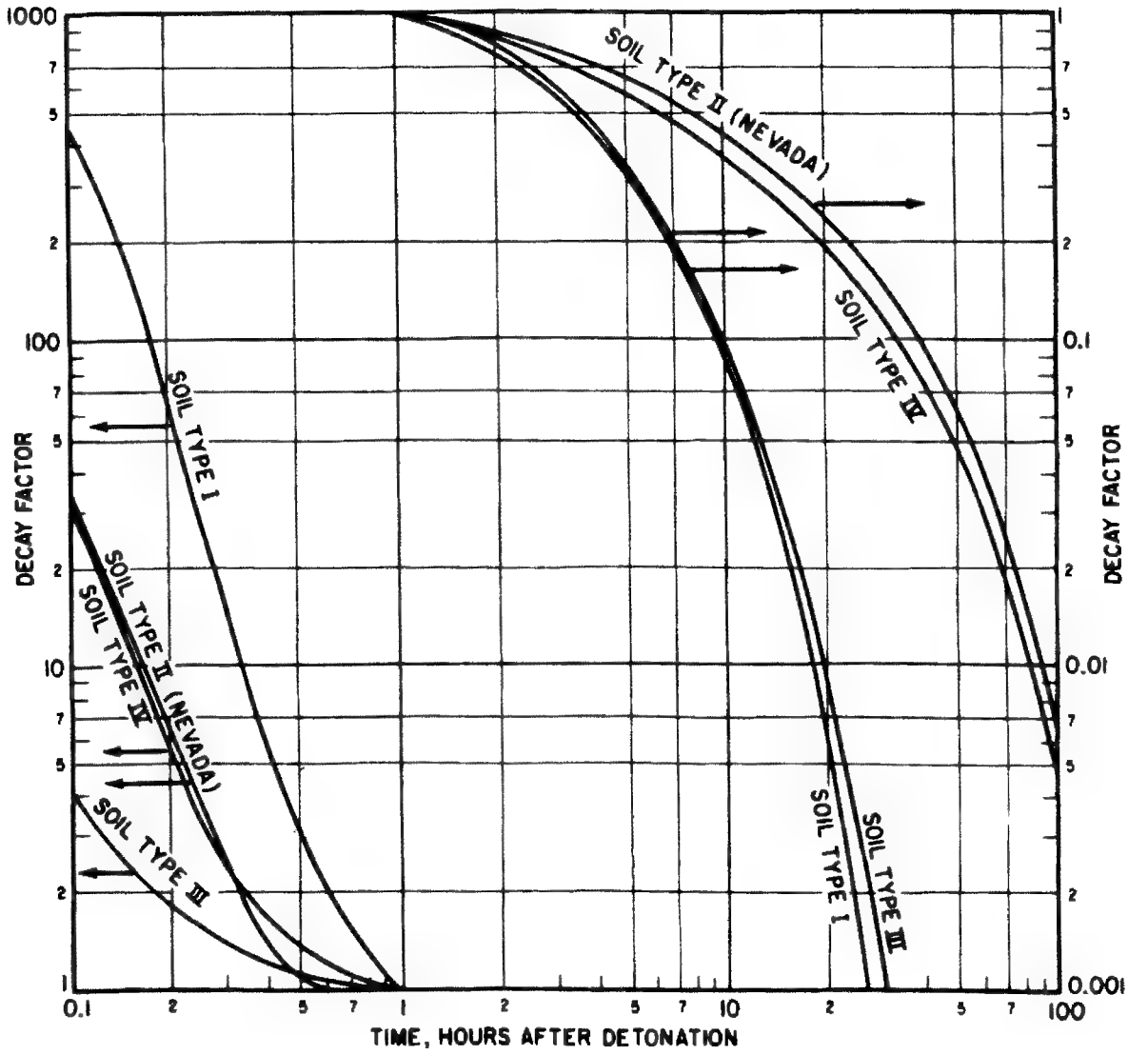

Figure 4-59. Decay Factors for Neutron-induced Gamma Activity

[redacted]

Problem 4-18 Total-neutron Induced Gamma Dose for Various Soil Types

Figures 4-60 through 4-63 give the total dose received on entering a given contaminated area at a specified time and remaining for a specified interval of time. The vertical axes give the accumulated dose for each unit of dose rate (rads/hr) at 1 hr after a detonation over that soil. The various curves represent times of stay in the contaminated area. To get the accumulated dose, a factor is taken from the vertical axis corresponding to the soil type, time of entry, and the time of stay. The product of this factor and the dose rate at 1 hr gives the accumulated dose.

Example.

Given: The dose rate in a given area over soil type III at 1 hr after detonation is 300 rads/hr.

Find: The total dose received by a man entering the area 5 hr after detonation and remaining 1 hr.

Solution: The proper curves for soil type III are found on figure 4-62. From this figure the intersection of the line for a time of entry of 5 hr after detonation with the 1-hr curve gives a factor of 0.3. Therefore, the accumulated dose is $300 \times 0.3 = 90$ rads.

Related Material. See paragraphs 4-8 to 4-10. See also figures 4-56 through 4-59.

[redacted]

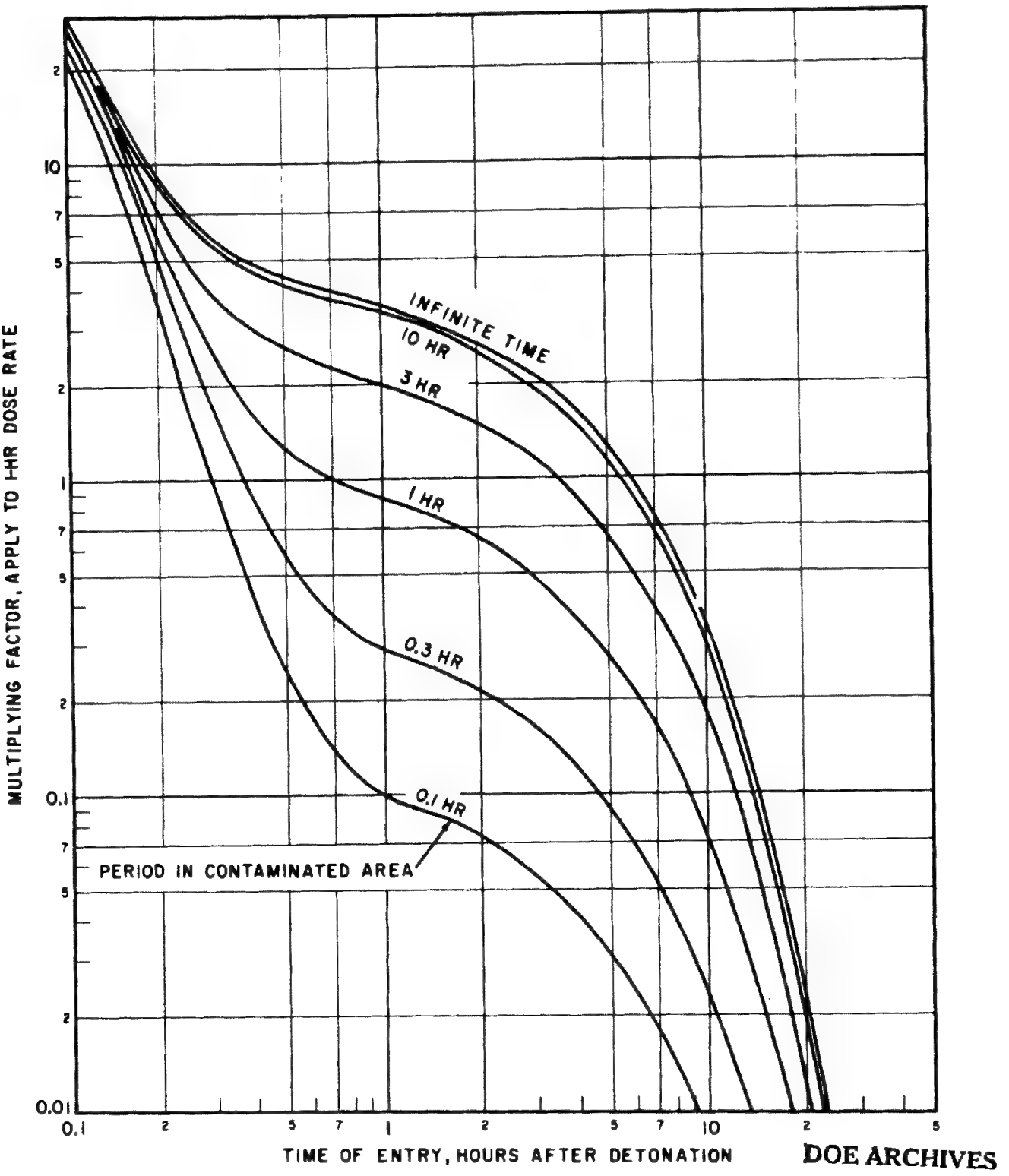

Figure 4-60. Total Radiation Dose Received in an Area Contaminated by Neutron-induced Gamma Activity, Soil Type I

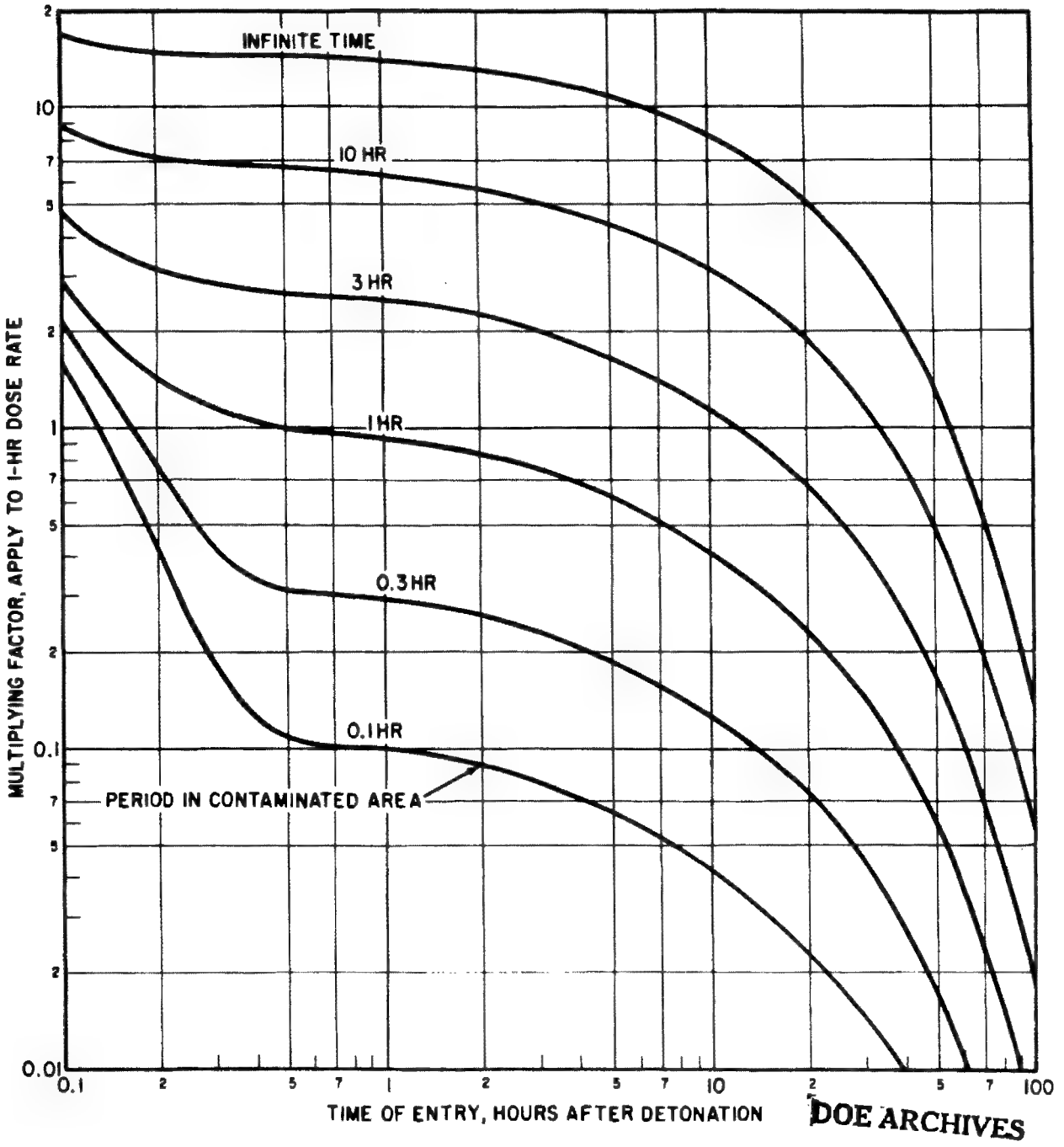

Figure 4-61. Total Radiation Dose Received in an Area Contaminated by Neutron-induced Gamma Activity, Soil Type II

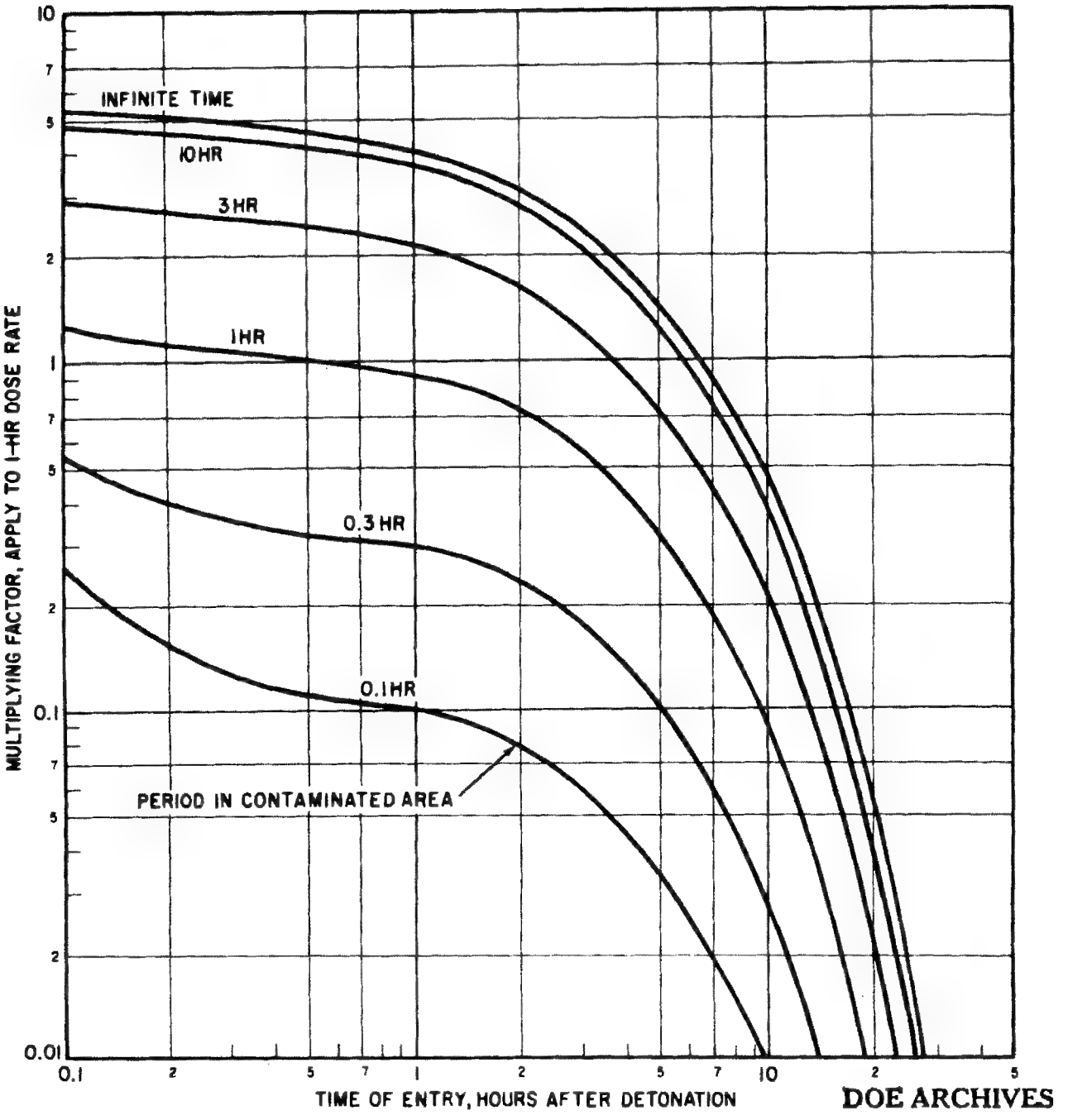

Figure 4-62. Total Radiation Dose Received in an Area Contaminated by Neutron-induced Gamma Activity, Soil Type III

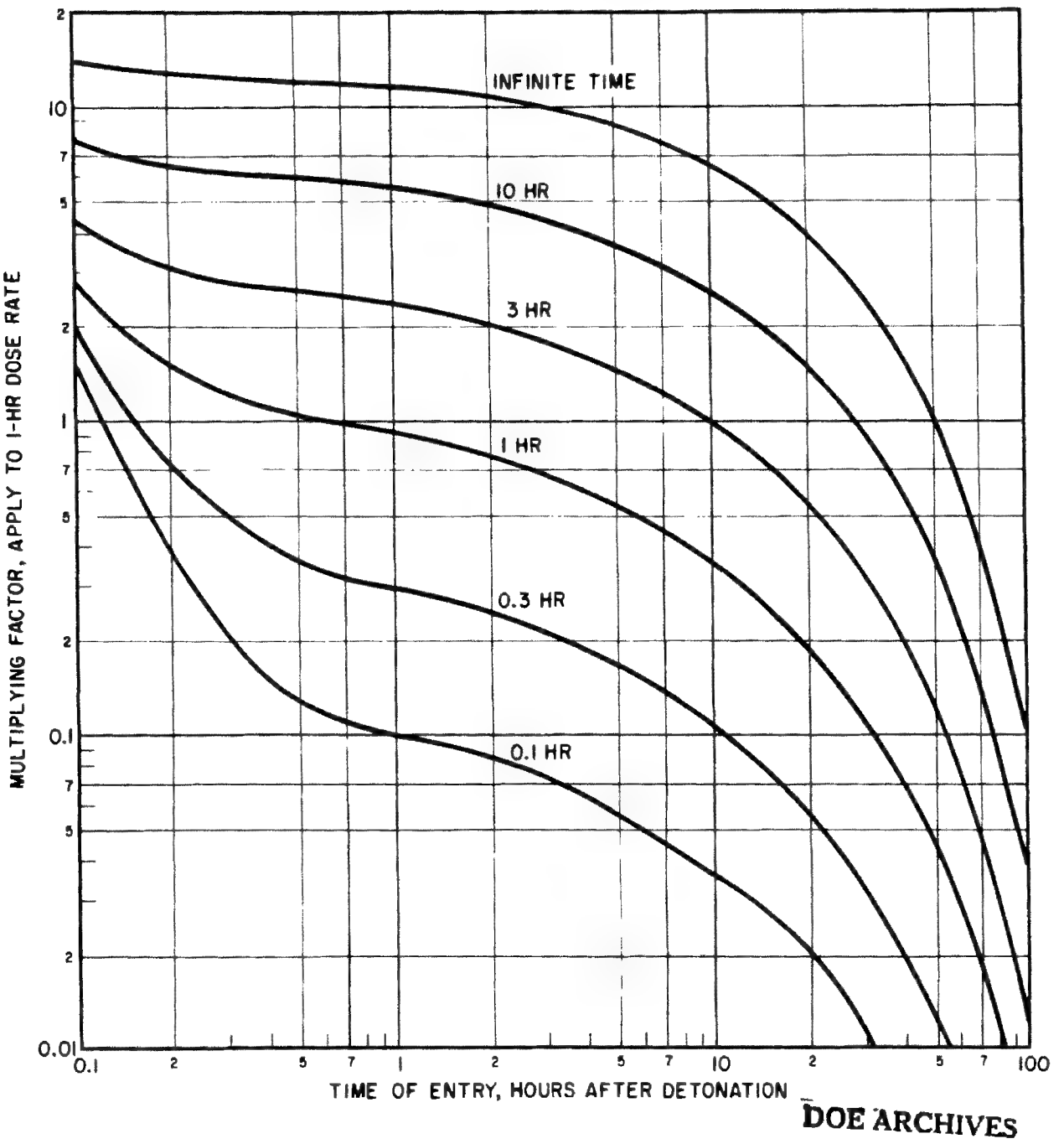

Figure 4-63. Total Radiation Dose Received in an Area Contaminated by Neutron-induced Gamma Activity, Soil Type IV

[redacted]

This page intentionally left blank.

[redacted]

PARTIAL DOCUMENT RECORD SHEET

Parts of this document were judged irrelevant to the CIC collection effort and were not copied:

Pages _____

Enclosures _____

Attachments _____

Other Chapter 5

Title page and table of contents have been copied for reference.

Dick Koogle
signature

9-15-87
date

PART II
DAMAGE CRITERIA

Chapter 6
INTRODUCTION

GENERAL

Part I has described the phenomena associated with a nuclear explosion for various burst conditions. The numerical values of these phenomena must be expressed by degree of damage to targets of military interest. Part II summarizes the aggregate knowledge of nuclear weapons effects on personnel and materiel, and includes statistical and theoretical treatment of data from tests results, weapons dropped on Japan, and laboratory work. Where checkpoints are not available, but reasonable accuracy can be expected, some extrapolation of data is made. The information is presented in a usable form for the atomic weapons staff officer. Graphical presentation is used in preference to tabular presentation wherever possible. Part II is divided into chapters according to types of targets exhibiting similar response characteristics. Further subdivisions within the chapters are generally by phenomena causing the damage. The damage curves presented in Part II are drawn for a probability of 50 percent of inflicting the degree of damage indicated, with curves of 90 and 10 percent probability included where the amount and quality of data available are sufficient to justify it.

BLAST AND SHOCK DAMAGE

6-1 GENERAL. When a blast or shock wave strikes a target, the target may be damaged (distorted sufficiently to impair usefulness) by the blast or shock wave itself, by being translated by the blast wave and striking another object or the ground, or by being struck by another object translated by the blast wave. For example, the air blast wave can shatter windows, dish in walls, collapse roofs, deflect structural frames of buildings, and bend or rupture aircraft panels and frames. Vehicles, tanks, artillery pieces, and personnel can strike other objects on the ground while being hurled through the air or tumbled on the ground by the blast wave. Ship hulls may be split or crushed by the water shock wave. Buried structures or structural foundations can be displaced, collapsed, or ruptured by the ground shock wave. Usually, the degree of damage sustained by a particular target cannot be specifically correlated to a single blast or shock parameter. The total damage received by the target may depend on a combination of air blast and ground or water shock parameters. The orientation of the target with respect to the blast wave, and the type of surface (the topography or the type of soil) associated with the target also determine damage. Paragraphs 6-2 through 6-6 briefly discuss the relationship among loading, response, and damage of various targets. A detailed discussion of blast and shock damage criteria is given in the introductory paragraphs of Chapters 7 through 12.

6-2 LOADING. The blast loading on an object is a function not only of the blast characteristics of the incident wave (rise time, peak overpressure, peak dynamic pressure, decay, and duration), but also of the size, shape, orientation, and response of the object. The influence of the target characteristics on the loading is discussed below, with emphasis on air blast loading.

6-3 Air Blast Loading. The loading on an object exposed to air blast is a combination of the forces exerted by the overpressure and the dynamic pressure of the incident blast wave.

762-909 O - 65 - 19

The loading at any point on a surface of an object can be described as the sum of the dynamic pressure, multiplied by a local drag coefficient, and the overpressure after any initial reflections have cleared the structure. Because the loading changes rapidly while the blast wave is reflecting from the front surfaces and diffracting around the object, loading generally comprises two distinct phases: during the initial diffraction phase; and after the diffraction is complete (i.e., where the obect is completely engulfed by the blast wave). This latter phase approaches a steady state and is usually referred to as the drag phase, because during this phase the drag forces (i.e., the forces resulting from the dynamic pressures) predominate in producing a net translational force on the object. The discussion of the loading process below is based primarily on an ideal blast wave as described in Chapter 2. Where non-ideal blast waves (with slow rise time, irregular shapes, and high dynamic pressures) introduce complications into the loading process, further explanation is given.

a. Diffraction loading. The side of an object facing the shock front of an air blast wave bears overpressures several times that of the incident overpressure because it both receives and reflects the shock. In the Mach reflection region the overpressure incident on the object is actually that of the original free air blast wave which has been reflected from the ground surface to a higher value. The reflection off the object therefore constitutes a second reflection process. In the regular reflection region, the incident overpressure is that of the free air blast wave (see *e* below). The magnitude of this reflected overpressure depends principally on the angle between the shock front and the face of the object, the rise time of the incident blast wave, and the initial incident shock strength. The greatest reflected overpressures occur when the direction of propagation of the shock front is normal to the face of the object, when the rise to the peak overpressure is essentially instantaneous, and when the incident shock strength is high. As the blast wave progresses it bends or diffracts around the object, eventually exerting overpressures on all sides. Before the object is entirely engulfed in the pressure region, however, overpressure is exerted on the front side of the object, whereas only ambient air pressure exists on the back side. During the diffraction phase this pressure differential produces a translational force on the object in the direction of blast wave propagation. When the blast wave has completely surrounded a small object, the transitional force due to diffraction loading is reduced essentially to zero, because the pressures on the front and on the back are almost equal. In the case of long objects or for short duration blast waves, the net force may actually reverse, because the overpressure on the front face may decay to a value lower than that on the rear face. The importance of this translational loading in the production of damage to the target depends on the duration of the loading or on the time required for the shock front to traverse the target and, therefore, on the size of the target. The effects of the translational load decrease as the duration of the load is decreased until, in some instances, translational load effects can be ignored. The overpressures continues on all sides of the object until the positive phase of the blast wave has passed. These pressures may be sufficient to crush an object (a 55-gallon drum may be so damaged in addition to damage incurred by translation). Thus the diffraction phase translational loading depends primarily on the object size and on increases in differential overpressures resulting from reflection on the front face.

b. Drag loading. During the time of diffraction and until the blast wave has passed, the high wind behind the shock front causes dynamic pressures that are also exerted on the object as drag loading. Except for high shock strengths, these pressures are much lower than the reflected overpressures but produce a translational force that the target component receives for the entire positive phase duration of the blast wave. For a given blast wave, the loading resulting from dynamic pressures depends principally on the shape, and orientation of the object, ranging from less than four-tenths the dynamic pressures in the case of a cylinder (when normal to the cylindrical axis), to over twice the dynamic pressures for an irregular, sharp-edged object.

c. Net loading. Net loading denotes the combined load on the element that tends to translate

it in the direction of propagation of the blast wave. Thus the back face loading has been subtracted from the front face loading; the loads on the sides are of no effect.

Figures 6-1(A) and 6-1(B) give representative net loading for two weapon yields on two objects or structural elements, one small and one large. A small element would be an object about the size of a telephone pole or a jeep; and a large object, the size of a house or larger. Because the overpressure being reflected is more than twice the incident pressure on the

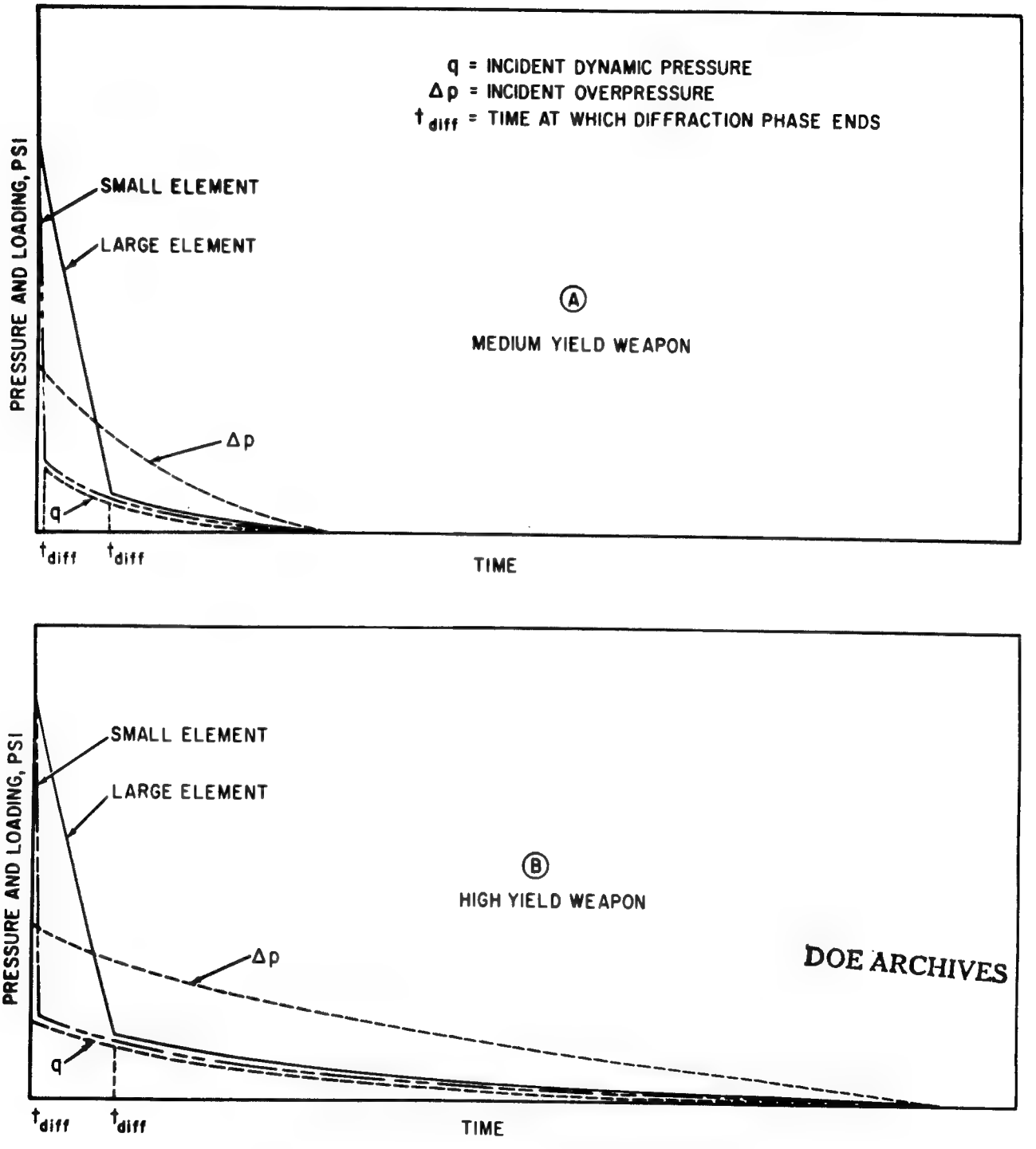

Figure 6-1. Net Blast Loading on Representative Structures

front face of the element, the loading displays an initial peak value. The reflected pressure decays or clears the front face at a time dependent on the size of the element. The rapid decay for the small element may make the reflected pressure spike of no significance, whereas the slow decay for the large element creates a load that may entirely govern the response of the target. For the representative cases indicated, the diffraction phase is shown to terminate at time t_{diff}, the time at which the reflected pressure has decayed to the incident pressure. At this time the drag phase begins, and continues until the end of the positive phase of the incident blast wave. The load during the drag phase is shown as equal to the dynamic pressure (i.e., the drag coefficients of the elements are equal to 1.0). The characteristics of the target element determine whether the response of the element is governed primarily by the diffraction phase or the drag phase. Figures 6-1(A) and 6-1(B) show that for medium and high yield weapons and small elements, a much greater impulse (the area under the loading curve) occurs during the drag phase than during the diffraction phase. As the yield increases, the drag phase impulse increases in predominance. For large elements and large yield weapons, the diffraction phase and drag phase impulses are about equal. In this latter case the drag phase impulse may still be of no importance, because the significant target response may occur during the diffraction phase. The diffraction phase impulses are not changed by the yield of the weapon (this is true for all but very large structures exposed to low yield weapons), whereas the drag phase impulses are directly related to the weapon yield (for the same peak dynamic pressures).

d. Target motion. When air blast loading is considered, the movement of the target component during loading is assumed to have negligible effect on the loading itself. Aircraft and missiles in flight are an exception. Their speed, orientation, and movement during loading assume increased importance. (See Chapter 10.)

e. Regular and Mach reflection. In computing the loading on a target, specific aspects of the blast wave propagation must be considered. The loading of a surface target in the regular reflection region is complicated by the vertical component of the incident blast wave, causing multiple reflections between the ground and the target, and additional reflected pressures on horizontal surfaces. In the Mach reflection region the loading is simplified because the blast wave propagation is horizontal. Near the surface of the ground the vertical component of the drag forces in the regular reflection region is quickly cancelled by the reflected wave, therefore the brief vertical drag loading is ignored except when the target is near the ground zero of an air burst. For aircraft in flight, the loading may be a single horizontal shock from a Mach stem or two separate shocks; the first from the free air wave and the second from the ground reflected wave. In establishing the damage curves for surface targets, the loadings on targets in the regular reflection region during the diffraction phase are considered separately from the loadings on similar targets in the Mach reflection region. The surface conditions are assumed to be average unless otherwise indicated. Objects susceptible primarily to horizontal drag loading if in the Mach region may become primarily susceptible to crushing action if they are in the early regular reflection region.

f. Non-ideal wave forms. As discussed in paragraphs 2-6 and 2-8, ideal wave forms are seldom found along the surface for overpressure levels above 6 psi. The description above of the diffraction and drag phases does not hold true in regions of non-ideal wave forms. If the overpressure wave has a long rise time (30 or 40 msec) to a peak value, full reflection of the wave off the surface of a structure will not occur. At the same time, the relationship between dynamic pressure and overpressure is different from that described for the ideal blast wave, so that during the diffraction phase the drag forces caused by high dynamic pressures may predominate as the damage-producing criteria. Because many conventional surface structures sustain severe damage at low peak overpressure levels, and non-ideal wave forms occur only in the higher overpressure regions, such wave forms have not been considered in determining damage criteria for these structures. For protective shelters designed to withstand high pressures, however, careful consideration must be given to non-ideal wave forms

and the dynamic pressures that are even higher than would be expected if the wave forms were ideal. There are few data on blast loading in the high pressure regions.

6-4 Underwater Shock Wave Loading. The water shock wave is similar in general form to the blast wave in air, although it differs in detail. The peak values in water are higher than at the same distance from an equal explosion in air. But the duration of the shock wave in water is shorter than in air. When the shock wave strikes a rigid, submerged surface, such as the hull of a ship or the sea bottom, reflection occurs as in air. When the shock wave reaches the surface (a less rigid medium), however, a rarefaction (or negative pressure) wave occurs. The combination of the surface reflected shock wave and the direct shock wave produces a sharp decrease or "cutoff" in the water shock overpressure, as shown in Figure 6-2. The impact of a shock wave on a ship or structure produces damage from direct effects and indirect effects resulting from components set in motion by the shock wave.

6-5 Ground Shock Loading. The loading of buried structures by ground shock is intimately tied to the response of the structures. For certain underground structures ground shock has to be so intense to cause serious damage that the damage area for those structures is confined closely to the crater area of a surface or underground burst. Therefore, the ground shock damage is given in terms of the crater radius and not in terms of the shock phenomena of stress (pressure), particle velocity, acceleration, or displacement. Because the analysis of damage for structures buried at great depth (equal to or greater than twice the crater depth for a surface burst) is complex, and not amenable to simple prediction techniques, damage criteria and ranges for these deep structures are not given. For structures near the surface, however, air-blast induced ground shock, transmitted with little attenuation to a depth as great as 8 ft, may cause significant damage to the roofs and walls of shallow buried structures (with less than 15 ft of cover) outside of the crater. The damage to these structures is more closely related to air blast pressures than it is to crater dimensions. Loading pressures are numerically equal to the ground stress normal to the structure. Such pressures do not produce detectable reflected pressures. The pressures exerted on the sides of such structures vary from 15 percent of the air blast pressures for dry soil up to nearly 100 percent for saturated soil. Internal equipment of a structure may be subjected to ground shock accelerations that will severely damage the equipment without damaging the structure. For a discussion of accelerations resulting from ground shock see paragraphs 2-34 through 2-37.

6-6 RESPONSE AND DAMAGE. Damage to a target is closely related to, and is a direct derivative of, its response. For targets anchored to the ground, damage is usually the result of displacement of one part of the target with respect to another part, resulting in permanent distortion, collapse, or toppling. For movable targets, however, the target may be moved by the loading with or without damage resulting. In these cases the damage to the target is governed primarily by the manner in which the moving target comes to rest. Whether drag phase loading or diffraction phase loading causes the greater damage depends on the weapon yield, target characteristics, and the damage level considered.

For large targets, such as buildings that have small window areas for walls that either support the structure or are as strong as the structural frames, the predominant cause of failure occurs because the pressure differential between the front and rear faces exists over a relatively long period of time. If the window area is large, the pressure on each wall is quickly equalized by the entry of the blast wave through the windows. The pressures exerted on the inside of the wall thus reduce the translational force on the wall. This translational force is also reduced because of a smaller wall area on which the pressures can act; however, the force exerted on interior partitions and rear walls tends to offset the reduction in front face loading in production of total damage. When the overpressures causing translational force on the structural component are quickly equalized because of the geometry or construction of the building, the primary damaging forces are the significant damaging forces when

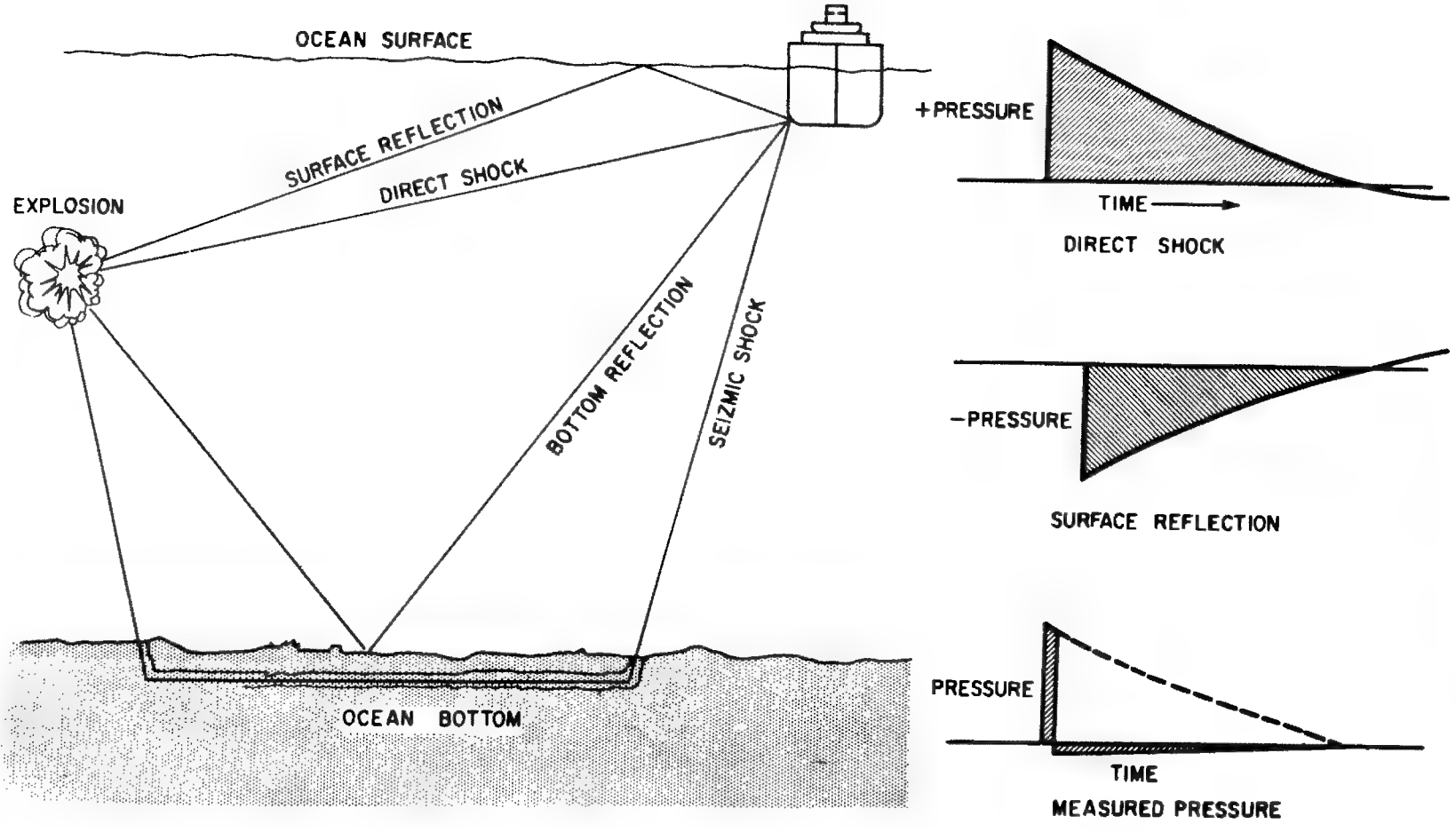

Figure 6-2. Direct and Reflected Shock Waves from an Underwater Burst

the structural components have fairly small cross sections, such as columns and beams. Structures normally damaged by drag forces are smoke stacks, telephone poles, truss bridges, and steel or reinforced concrete frame buildings with light walls. These buildings are drag sensitive because the light walls of corrugated steel, asbestos, or cinder block fail at low reflected pressures, transmitting little load to the structure frame. Then only the frame itself is exposed to the blast and, being composed of small cross section structural elements, is distorted primarily by drag forces. These buildings are not considered severely damaged unless the structural frame has collapsed or is near the point of collapse. A tree is a good example of a drag sensitive target, because the duration of the diffraction phase is extremely short and there is considerable force applied by the high wind velocity drag loading. Most military field equipment is drag sensitive, because damage generally results from the tumbling or overturning caused by the drag forces.

If the target is shielded from the drag forces, or lies within the early regular reflection region, high overpressures may become the damage producing criteria. For blast resistant aboveground structures designed to resist more than 5 to 10 psi overpressure, the distinction between diffraction and drag sensitivity cannot be well defined because full reflection from the surface of the structure does not occur, and dynamic pressures exceed those expected in the case of the wave form. As a result, drag forces may predominate even during the diffraction phase in producing damage.

Aircraft may be damaged by the forces developed in the diffraction phase, in the drag loading phase, or in both. Parked aircraft can receive light, crushing forces corresponding to low overpressures. For example, light skins and frames are easily dished and buckled at relatively low overpressures. At higher overpressure levels, drag loading (referred to as "gust loading" with respect to aircraft) adds to the damage. At these levels, much of the damage may result from translation and overturning of the aircraft. For aircraft in flight, the diffraction and drag forces combine with the existing aerodynamic forces to develop destructive loads on airfoils at low overpressure levels. The diffraction or crushing overpressure effects on the fuselage and other thin skinned components, however, are usually of secondary importance for the in-flight aircraft. (Target response and damage are covered in detail in Chapter 10.)

THERMAL RADIATION DAMAGE

6-7 GENERAL. The two most important effects of thermal radiation on ground targets are injury (burns) to personnel and the setting of fires in the target area. Depending upon the yield and detonation conditions of the weapon, and upon target characteristics, blast effects or nuclear radiation effects may override the thermal effects in importance. Predictions of thermal damage to targets are limited by the precision with which thermal energy may be scaled with yield, height of burst, and slant range. The factors of target geometry, previous precipitation history, prevailing meteorology, and seasonal effects introduce additional uncertainties. The criteria for thermal damage, set forth in Part II in terms of specific radiant exposures required to produce the damage of interest, should be applied with the understanding that significant deviations from the mean values quoted may be experienced in individual cases because of variations in the factors mentioned above.

6-8 ENERGY AND RATE DEPENDENCE. The damage produced by thermal radiation depends upon the energy per unit area incident on the target, and the rate at which the energy is delivered. For convenience, the incident thermal energy per unit area (or *radiant exposure*) has been adopted as the damage criterion when the temporal characteristics of the thermal pulse have been specified. The temporal characteristics for bursts below 20,000 ft are defined by the equations in Chapter 3. The duration of the thermal pulse is related to weapons yield and air density at the altitude of detonation. Since changes in air density below 20,000 ft do not significantly affect the duration of the thermal pulse, below that altitude the thermal pulse duration can be defined simply as a function of weapon yield. The importance of the temporal characteristics of the thermal pulse is emphasized by the following example. It

takes about 4 cal/cm² to produce a second degree burn on bare skin for the rapid pulse of 1 kt detonation, whereas direct sunlight produces this amount of radiation in a little over 2 minutes with no effect. To produce the same thermal effect in a given material, the total amount of thermal energy received per unit area must be larger for a nuclear explosion of high yield than for one of lower yield, because the energy is delivered over a longer period of time; i.e., more slowly, in the former case. Therefore, thermal damage criteria in Part II are given for specified yields, or factors for scaling the criteria with yield are given.

6-9 EFFECT OF INCREASED HEIGHT OF BURST. As the height of burst is increased above 20,000 ft there is a gradual shortening of the duration of the thermal pulse and a deviation from the pulse shape of a near sea-level detonation. Above 200,000 ft the thermal characteristics are changed so that only a single thermal pulse of 1-200 msec duration is emitted for even multi-megaton detonations. For studies of the incendiary effects of large yield weapons detonated above 200,000 ft, the ignition thresholds indicated for a 40 kt sea-level detonation may be used with an uncertainty of $\pm 50\%$. Due to insufficient data in the intermediate altitude regions (20,000 to 200,000 ft) the determination of precise ignition thresholds is not now possible. However, the formula $t_{max} = .04W^{0.4}(\rho/\rho_o)^{0.4}$ may be applied to obtain a time to second maximum which in turn may be used to approximate an equivalent sea level yield ($W = 3.0 \times 10^3 (t_{max}^{2.5})$. Because of the uncertainty in pulse duration and the deviation of the pulse shape from that observed for near sea level detonations, the equivalent yield is believed to be valid to within a factor of 2. Using this equivalent yield, the total thermal energy required for a given effect can then be estimated from sea level radiant exposure values given in Table 13.2.

6-10 Damage Mechanisms. Except for thin materials such as fabrics, newspaper, and leaves, thermal damage to materials is largely confined to changes at shallow depths in the exposed surface. Damage to materials results from raising the temperature of the surface, which, in the case of organic materials, brings about permanent chemical changes or induces ignition of the material. Only the part of the energy absorbed (i.e., neither reflected nor transmitted) by the material is effective in producing thermal damage. Highly reflecting materials or transparent materials are relatively resistant to thermal damage. Light colored objects of a given thickness are more resistant than dark colored objects of the same material and thickness because they reflect more of the incident energy. Color has little effect on the response of materials that blacken readily upon exposure early in the thermal pulse, because the energy delivered during the remainder of the pulse is largely absorbed by the blackened surface. The effect of absorptivity has been included in the derivation of damage criteria.

6-11 EFFECT OF THICKNESS. Thick organic materials such as wood, plastics, and heavy fabrics do not support combustion, but only char as the result of exposure to thermal radiation. During the delivery of the pulse, the surfaces of these materials may flame, but the combustions are not sustained once the radiant pulse has died out. Materials such as light fabrics, newspaper, dried leaves and grass, and dry rotted wood may ignite at energies as low as 3 cal/cm² from a 1-kt detonation. The subsequent arrival of the blast wave at distances corresponding to these low ignition energies frequently fails to extinguish the ignitions and they become possible sources of primary fires. Charring and flaming or disintegration is typical of organic substances. Many of these substances emit jets of flame or smoke during exposure but do not actually ignite. Bare metals are unchanged unless structurally weakened or melted by heat action. The thicker the metal, the more resistant it is to thermal effects.

6-12. Effect of Orientation. Orientation of material is an important factor affecting the thermal damage produced by a weapon detonated in clear atmospheres, because the radiant exposure of a plane surface depends on the angle between the perpendicular to the surface and the direction of the burst. The maximum effect is produced when the incident radiation is perpendicular to the surface. Surfaces that do not receive direct radiation may be exposed

[redacted]

to the lesser amounts of radiation reflected from the ground or from clouds or scattered by haze in the atmosphere. Under hazy conditions at slant ranges greater than half the visibility, much of the energy received is scattered by particles in the atmosphere and comes from all directions. References in table 13-2 to the exposures required to produce various types of damage are based on an alignment perpendicular to the incident beam. For other orientations of the target surface, greater exposures will be required to produce the same degree of damage.

6-13 Effect of Shielding. Except under hazy conditions at greater slant ranges, when the incident radiation is received from all angles, the geometry of the target of interest with respect to nearby objects is of importance, particularly within buildings or in complex target areas. Trees, buildings, foxholes, hills, etc., if in a position to shield the target from the fireball, are effective as thermal shields. The shielding effect of deciduous trees, once the leaves have been shed, is greatly reduced. Reflection of thermal radiation from exposed walls of foxholes is about 5 percent.

6-14 MOISTURE CONTENT. Thermal damage to materials that absorb moisture depends on the percentage of water in such materials. Usually, the moisture content varies with the prevailing relative humidity. Exposure to recent rain, however, may greatly alter the moisture content. Scorching or charring of an organic surface by radiant energy is preceded by vaporization of the water. Because of this effect, more energy is required to produce a given damage effect to wet surfaces or to targets in highly humid atmospheres. Materials located within structures during the latter part of the heating season (late winter and early spring) are more readily damaged by thermal radiation, largely because of decreased interior humidities. But materials exterior to structures are more readily damaged during the summer and fall. Vegetation at the end of the growing season and fallen leaves are classed as ignition sources of greatest potential in the summer and fall. (See Chapter 13.)

6-15 X-ray Effects. When a weapon is burst at altitudes greater than about 250,000 ft, the soft X-rays emitted from such bursts can travel great distances through the rarified air without suffering appreciable attenuation. They can, of course, be stopped by denser materials such as space or re-entry vehicles. This can, under some conditions, have a destructive effect on the material or structure, and is one of the means which might be used for killing an object engaged at these altitudes.

NUCLEAR RADIATION

6-16 BIOLOGICAL HAZARD. Basic nuclear radiation data are presented in previous sections. According to the burst type, initial or residual radiation effects may predominate. With few exceptions (see paragraphs 13-1, 13-2) radiation damage is largely to living organisms. Neutrons and gamma rays constitute the penetrating radiation that results in acute injuries of military concern. Alpha particles from fallout are a hazard only if deposited inside the body, and as such represent a long term problem. Beta radiation from fallout deposited on the skin can cause burns of varying severity, but the burns do not appear for several days, depending on the exposure, and would not immediately affect a military operation.

6-17 CUMULATIVE EFFECTS. Ultimate body damage resulting from nuclear radiation is a function of the rate and type of radiation as well as the total dose. For a discussion of the effects of rate and type of radiation and the concept of biological recovery, see paragraph 7-17.

6-18 SHIELDING. The basic nuclear radiation data presented in Part I apply to completely open and unshielded regions. Reductions in dosage actually received by an individual will occur from the shielding afforded by surrounding structures and terrain elevations. Shielding factors and transmission curves by means of which actual doses behind certain shields can be estimated are given in paragraph 7-26.

[redacted]

[redacted]

This page intentionally left blank.

[redacted]

Chapter 7
PERSONNEL CASUALTIES

AIR BLAST AND MECHANICAL INJURY

7-1 DIRECT BLAST INJURY. One of the ways the air blast from a nuclear detonation may cause casualties among human beings is by direct blast injury. These casualties may result from crushing forces or translational forces.

7-2 Crushing Forces. Although the human body is relatively resistant to the crushing forces from air blast loading, large pressure differences resulting from blast wave overpressures may damage lungs, abdominal organs, and other gas-filled body organs. Experiments on animals indicate that from 45 to 55 psi reflected overpressure from nuclear weapons is required to cause 50 percent mortality in humans, provided no translational motion occurs. For a peak reflected overpressure of less than 35 psi, no crushing injury is expected other than ear drum rupture, which may result from a peak reflected overpressure of 7 psi, although 20 to 30 psi is usually required. The occurrence of ear drum rupture will not seriously hamper the overall effectiveness of a military unit because this injury is not considered disabling. Other damage-producing effects may be more important at pressures above 35 psi, therefore crushing forces as such need not be considered a prime cause of casualties to personnel in the field.

The design of structures such as bomb shelters or permanent type gun emplacements, where adequate shielding exists against thermal and nuclear radiation, may permit the buildup of blast pressure from multiple reflections. Reflected overpressure inside such structures may cause blast injuries even though the free air overpressure outside the structure would not be sufficient to cause injury. In some cases, the inside pressure may be three or four times the outside pressure.

Ear drum rupture and other bodily damage that may result from overpressure depend largely on the characteristics of the shock front. If the rise time is long there is a lower probability of injury because the body organs are subjected to less severe pressure differences, and also are able to adapt themselves better to high overpressure.

7-3 Translational Forces

1. *Mechanisms.* An individual exposed to a blast wave receives translational forces that depend primarily on drag forces. Because the human body is relatively small, and the blast wave almost immediately envelops it, the diffraction process is short. One can predict the translational forces with reasonable accuracy if the burst position, yield, terrain, and the orientation of the human body are known. Because the translational forces applied depend on the exposed frontal surface area of the human body, an individual standing in the open receives much larger translational forces than an individual lying on the ground. Thus, an individual assuming a prone position at the instant a nuclear bomb flash is detected, reduces the likelihood of injuries resulting from bodily translation. The translational forces are also appreciably reduced for an individual behind a building or in a blast-resistant shelter. Although the degree of protection a foxhole gives is not known at present, there is some evidence that foxholes may be dangerous because of reflected pressures. They do, however, provide some protection against blast displacement, thermal radiation, and ionizing radiation.

2. *Criteria for injury.* A direct correlation between translational motion parameters and injury is unknown, but the initial rate of acceleration, the motions of various parts of the body while being translated, and the nature of the impact, all certainly contribute to injury. Most injuries will probably result from impact, with the severity of injury depending on factors such as the objects with which the translated body collides (or objects that collide with

the body), the nature of the impact (whether glancing or solid), and velocity at impact. Some individuals may survive a large translation, whereas others may be severely injured or killed by a relatively small translation. Because increased yield results in increased positive phase duration, attainment of velocities sufficient to cause injury or impact will occur for lower peak pressures. Similarly, the manner of impact depends on the nature of the terrain and surface configuration. If solid impact occurs, a velocity of 10 ft/sec is unlikely to cause a significant number of serious injuries; at 10 to 20 ft/sec some fatalities may occur, and above 20 ft/sec the probability of fatal injury increases rapidly with increasing displacement velocity. Figure 7-3 is a plot of burst height vs. ground range at which 50 percent of standing and prone personnel in the open are expected to become direct blast casualties. The curves are drawn for 1 kt and may be scaled to other yields by multiplying the burst heights by the cube root of the yield and the ground distance by the four-tenths power of the yield.

7-4 INDIRECT BLAST INJURY. Individuals not subject to direct blast may be injured indirectly. Burial by debris from collapsed structures (with attendant fractures and crushing injuries), flying objects placed in motion by the blast wave, or fire or asphyxiation may cause indirect blast casualties.

7-5 Personnel in Structures. Because a major cause of personnel casualties in cities is structural collapse and damage, the number of casualties in a given situation may be reasonably estimated if the structural damage is known. Table 7-1 shows estimates of casualty production in two types of buildings for several damage levels. Data from Chapter 8 may be used to predict the ranges at which specified structural damage occurs. Demolition of a brick house is expected to result in approximately 25 percent mortality, with 20 percent serious injury and 10 percent light injury. About 60 percent of the survivors must be extricated by rescue squads because without rescue they may become fire or asphyxiation casualties, or, in

Table 7-1 Estimated Casualty Production in Structures for Various Degrees of Structural Damage

Structural damage	Killed outright	Serious injury (hospitalization)	Light injury (No hospitalization)
		Percent*	
1-2 story brick homes (high explosive data):			
Severe damage	25	20	10
Moderate damage	<5	10	5
Light damage		<5	<5
Reinforced-concrete buildings (Japanese data, nuclear):			
Severe damage	100		
Moderate damage	10	15	20
Light damage	<5	<5	15

*These percentages do not include the casualties that may result from fires, asphyxiation, and other causes from failure to extricate trapped personnel. The numbers represent the estimated percentage of casualties expected at the maximum range where the specified structural damage occurs. For the distances at which these degrees of damage occur for various yields see Chapter 8.

some cases, receive lethal doses of residual radiation. Reinforced concrete structures, though much more resistant to blast forces, produce almost 100 percent mortality on collapse. The table 7-1 figures for brick homes, which are based on data from British World War II experience, may be assumed reasonably reliable for cases where the population expects bombing, and most personnel have selected the safest places in the buildings as a result of specific air raid warnings. For cases of no warning or preparation, the number of casualties is expected to be considerably higher. To estimate casualties in structures other than those listed in table 7-1, one must consider the type of structural damage that occurs, and the characteristics of the resultant flying objects. Glass breakage may produce large numbers of casualties, particularly for an unwarned population, at overpressure ranges where personnel are relatively safe from other effects. As little as 2 psi overpressure can cause glass fragments to penetrate the abdominal wall, causing life-threatening injury to internal organs.

7-6 Personnel in Vehicles. Personnel in vehicles may be injured as a result of the response of the vehicle to blast forces. Padding where applicable and the use of safety belts, helmets, and harnesses virtually eliminate this source of casualties, at least within armored vehicles. In the absence of these protective devices, impact with sharp projections within the vehicle interior may cause serious lacerations. Comparative numbers of casualties are almost impossible to assess because of the many variables involved.

7-7 Personnel in the Open. Flying objects (or missiles) translated by the blast wave may injure exposed personnel. Low velocity missiles, if of sufficient size, may cause crushing injuries, whereas high velocity missiles may cause penetrating wounds. The missile density and characteristics are largely a function of the target. When the target area is relatively clean, with little material subject to fragmentation and displacement, fewer injuries from missiles are expected in the open than from debris within structures at comparable distances. When the target complex presents many possible sources of missiles this may not be the case. Personnel in a prone position are less likely to be struck by flying missiles than those who remain standing. Those in bunkers, foxholes, or in defilade probably will be almost completely protected from missiles.

THERMAL INJURY

7-8 TARGET AND RADIATION FACTORS. Because of the many factors involved, it is necessary to analyze each particular target situation before attempting to predict the number of thermal casualties that will occur in a given situation. Factors that define the target include the following: the distribution or deployment of personnel within the target area (whether proceeding along a road, in foxholes, standing or prone, in the open or under natural cover); orientation with respect to the bomb; clothing (including number of layers, color, weight, fabric, intervening air spaces between cloth and skin, and whether the uniform includes helmets, gloves, or other protective devices that might protect the bare skin); ambient temperatures; skin temperatures; and natural shielding. Factors that define the source of radiation such as yield of weapon, height of burst, and visibility (as discussed in Chapter 3) must also be considered. In many target complexes, particularly in cities and industrial areas where intervening structures may shield a major part of the direct radiation, secondary burns may cause a large percentage of thermal casualties.

7-9 BURNS TO BARE SKIN. Bare skin burns are related to the total radiant exposure and the rate of delivery of the thermal radiation, both of which depend on yield and height of burst. For a given total exposure, as the weapon yield increases, the thermal radiation is delivered over a longer period of time and thus at a lower rate for explosions within the atmosphere. This allows energy loss from the skin surface by conduction to the deeper layers of the skin and by convection to the air. Figure 7-1 presents critical radiant exposures for the production of first and second degree burns on bare skin as a function of yield for normal incidence of radiation. The shaded areas reflect variations in individual response due to factors such as skin color (for example, darker skin requires less exposure to produce a given

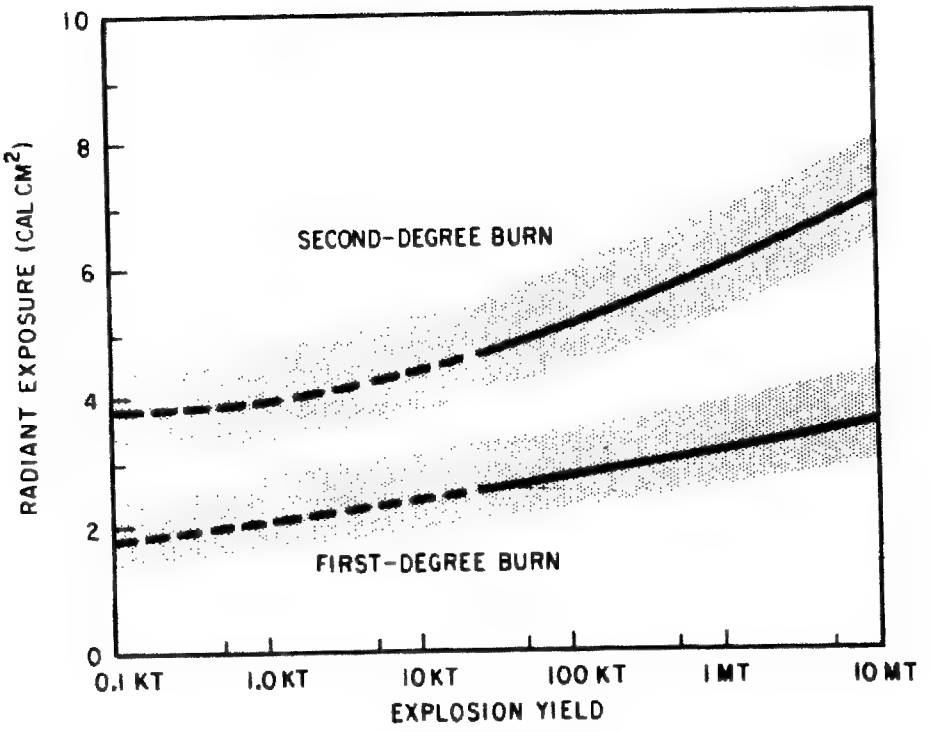

Figure 7-1. Median Effective Radiant Exposure for First and Second Degree Burns on Bare Skin

severity of burn) and skin temperature (for example, colder skin as is found in winter or in arctic climates requires a greater exposure to produce the given burn). A first degree burn is defined as one that shows redness; a second degree burn exhibits partial skin destruction or blistering. The radiant exposures shown in Figure 7-1 were based on experiments with subjects in fixed positions. In an actual situation people may move, turn, cringe, run or take other voluntary or involuntary action. The radiant exposures for which burns occur would then be greater than those indicated in Figure 7-1.

7-10 **BURNS UNDER CLOTHING.** Many factors contribute to the protection clothing gives the underlying skin. For cotton, synthetic, and wool fabrics one of the most important factors is resistance to destruction, because skin burns are seldom seen under undamaged cloth unless the cloth layers are in contact with the skin. For cotton fabric ignition is also important, along with destruction and degree of contact with the skin. Fire retarding treatment does not necessarily increase protection as the greater amount of volatiles released may, in turn, heat the skin and cause burns. Ignition of fabrics will vary with weight, weave, color, amount of contact between fabric layers; wind speed, and direction; initial temperature; degree and type of soiling; and so on. In general, lighter weight clothing offers less protection. Table 7-2 lists the radiant exposure for no burns, and first and second degree burns, for general guidance in estimating the burn hazard. The values are estimates based on the results of the evaluation of many specific clothing assemblies under limited specified conditions. More accurate estimates can be made in those instances in which the clothing assembly and environmental parameters are specified. The radiant exposures given are for fixed exposure. Voluntary and involuntary movement can increase the permissible exposure significantly. Besides the factors listed above, the following conditions will also affect the protection clothing affords: much less energy than given in table 7-2 is required to produce a skin burn under wet clothing; laundering and amount of wear will also change the values given in the table; white or very light colored clothing will increase the exposure required to produce a

[redacted]

Table 7-2 Radiant Exposures for Burns Under Clothing

Clothing	Burn	40 kt	1 mt	10 mt
		Radiant exposures[1,2]		
Bare skin	none	2.0	2.6	2.9
	1°	2.6	3.1	3.5
	2°	4.6	6.3	7.0
Summer uniform (2 layers of light porous fabric)	none	5	6	7
	1°	10	16	21
	2°	12	20	26
Winter uniform (2 to 5 layers of tightly woven fabric)	none	7	10	12
	1°	13	21	29
	2°	16	26	36
Sub-artic and arctic (3 to 8 layers of tightly woven fabric)[3]	none	15	25	40
	1°	15	25	40
	2°	15	25	40

[1] Expressed in cal/cm^2 incident on skin or outer surface of clothing when the inner layer of the clothing is spaced 0.5 cm from the skin and when at least the first 70% of the thermal pulse is received normal to the surface.

[2] These values are sensitively dependent on many variables and are probably correct to within ±50% for the range of normal military situations.

[3] Burns to personnel wearing these heavy uniforms will occur only by contact with flaming or glowing outer garments. Some systems require in excess of 100 cal/cm^2 to produce burns by direct transmission of heat through the fabrics.

burn; and some synthetic materials such as nylon, which do not burn readily, will melt at only moderate energies causing hot droplets that can severely burn bare skin.

7-11 THE COMBAT INEFFECTIVE. A useful term in discussing effects of thermal radiation on personnel is "the combat ineffective." A combat ineffective is defined as a person who, because of his injuries, is no longer capable of carrying out his assigned tasks. This differs from the more common term "casualty," which is defined as an individual whose injuries require medical attention. Damage to certain areas of the body produces a greater number of combat ineffectives than damage to other areas. Burns of any degree in the area surrounding the eyes will cause the eyes to swell shut, and burns to the hands that lead to loss of mobility are particularly apt to cause ineffectiveness.

If a sufficient portion of the total body area is burned, physiological shock follows and the individual becomes a casualty. When more than 10 to 15 percent of the total body area received second degree burns (or worse), shock may be expected. The importance of injuries to the hands and eyes in producing combat ineffectives, coupled with the vulnerability of these parts because of lack of protection under ordinary circumstances, indicates the desirability of providing protection for these areas when nuclear attack is likely.

7-12 THERMAL SHIELDING. Almost any nontransparent material withstands the thermal radiation long enough to afford some shielding. The degree of protection depends on the weight, color, and destruction or ignition level of the covering material. Heavy smoke screens are excellent energy absorbers (see Chapter 3).

7-13 Material Effectiveness. For a prone individual in the open, shielding materials such as those in table 7-3 give increased protection. The figures are for a shield 30 in. high, and for the individual's head at least 6 in. away from the shield material. The same material used for foxholes covers would increase protection.

Because of the ease of complete shielding from thermal radiation, the amount of forewarning, if any, is of utmost importance to exposed personnel. Covered foxholes or bunkers

Table 7-3 Effectiveness of Thermal Shield Materials

Material	1 kt	100 kt	10 mt
		*No burn**	
Vinyl poncho	6	10	18
Neoprene poncho	8	13	23
Cotton sateen, 9 oz	7	12	21
Cotton duck, 12 oz	8	13	23
Wool blanket	14	25	43

*Incident energies expressed in cal/cm^2.

[redacted]

[redacted]

are excellent thermal shields. The degree to which uncovered foxholes protect is related to the height of burst and the distance from ground zero as well as the position of the man within the foxhole. The nearer foxholes offer less protection, because the shadowed portion is a smaller fraction of the total volume. At greater distances from low yield weapons, only those areas subject to the direct radiation produce burns because reflections from the exposed surfaces of the foxholes may be neglected. Under high-megaton-burst conditions, a sufficient amount of thermal radiation may be reflected and produce casualties. In highly scattering atmospheres, such as fog or haze, scatter of the radiation into the foxholes could become an important factor. It is important to note that in targets containing openings such as windows (in buildings and aircraft) and portholes (in tanks and ships), although external thermal radiation may not damage the general target, the openings may allow damaging amounts of thermal radiation to fall on personnel inside.

7-14 Evasive Action. Figure 7-2 demonstrates that evasive action against thermal radiation following the detonation of weapons up to 100 kt is not expected to be successful because of the rapid delivery of the thermal pulse. For weapons in the megaton range within the atmosphere, the thermal pulse is delivered over a period of seconds. Simple evasive action such as covering exposed hands and face, or dropping to the ground or obtaining thermal shelter avoids significant portions of this pulse.

7-15 SPECIFIC EFFECTS ON THE EYE. That visual impairment can be caused by the thermal radiation from nuclear detonations has been well established by investigations during weapons tests and by laboratory experiments. This impairment may be temporary, as in flash-blindness, or permanent, as in chorioretinal burns.

The visual impairment associated with flash-blindness can be so severe as to interfere seriously with the ability to pilot aircraft, operate vehicles, or perform other tasks requiring high visual acuity. The loss of visual acuity is immediate upon exposure to the nuclear flash and may last from a few seconds to several hours. The return to normal is gradual and the recovery time depends upon the magnitude of the causative stimulus and ambient light conditions.

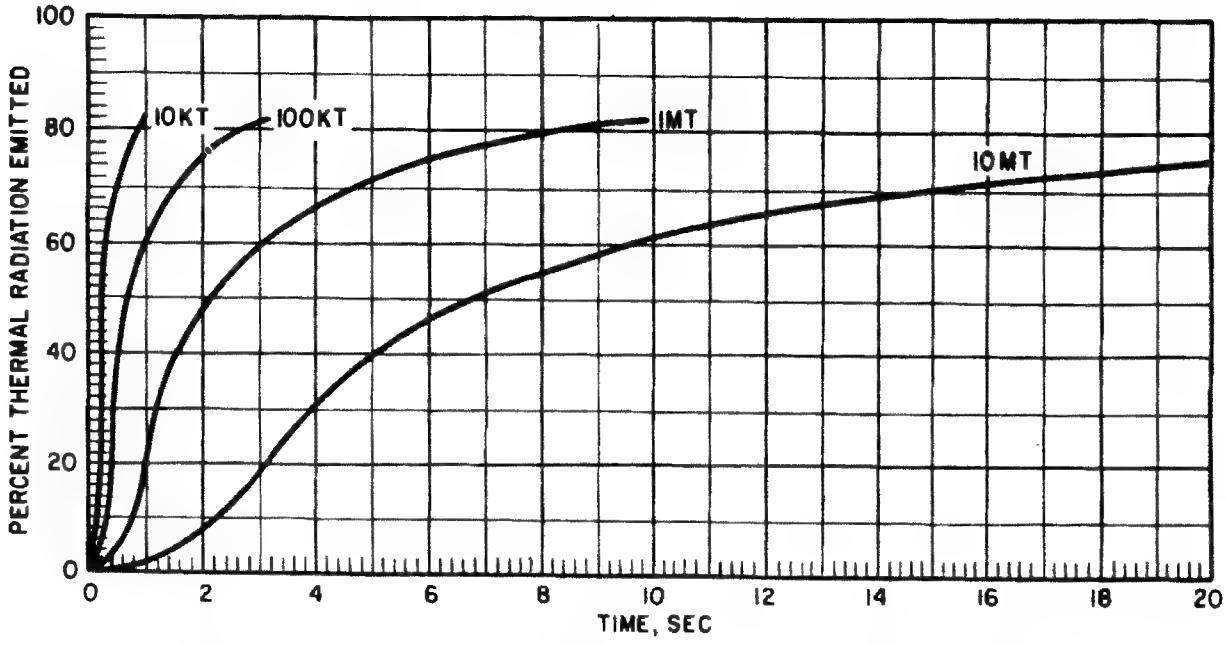

Figure 7-2. Percent Thermal Radiation Emitted vs. Time for Detonations Within the Atmosphere

[redacted]

[redacted]

The visual acuity lost in a chorioretinal burn, however, is not recovered. The significance of this loss depends upon the size and location of the burn on the retina. The decrement is immediate upon exposure to the nuclear flash but is probably dual in nature. During the first few hours following exposure, loss of vision is undoubtedly due to a combination of flashblindness and the pathological change of the retinal burn. Indeed, if the burn is small and located near the periphery of the retina, temporary flashblindness may well represent the only significant loss of vision.

The distances at which visual impairment can occur are much greater than the distances at which ionizing radiation and blast damage are problems. Retinal burns have been found in animals exposed as far as 300 nautical miles from a nuclear detonation.

If the nuclear detonation is not in the field of vision and is not reflected to the eye from an image forming surface, then retinal burns are not a hazard under either daytime or night time conditions. Flashblindness, also, would not be a hazard under these conditions in daytime. At night, however, dark adaption would be lost and recovery of vision required to read instruments or identify targets with low levels of illumination might require several minutes.

Nuclear detonations occurring in the field of vision present much more serious problems. Retinal burns can occur under the conditions and at the distances indicated by the curves in Figures 7-3 through 7-8 for low altitude detonations. In addition, high altitude atmospheric detonations can produce retinal burns at much greater distances than those predicted for the low altitude detonations. The loss of vision associated with these burns will depend on the size and location on the retina. Detonations outside the sensible atmosphere will not cause retinal burns.

Flashblindness will result from a nuclear detonation in the field of vision. This blindness will be most severe and of longest duration if the flash occurs at night and is viewed directly —that is, if the fireball is in the field of maximum visual acuity. Under such conditions, afterimages and visual impairment may persist for hours.

On the other hand, if the flash occurs during daylight hours and near the periphery of vision, any flashblindness which might occur probably would not interfere with useful vision for more than a few seconds. Direct viewing of the fireball during daylight could result in flashblindness lasting for several minutes.

The curves in Figures 7-3 through 7-8 indicate the predicted maximum distances at which retinal burns can be formed under the conditions listed. These curves were calculated and are believed to be conservative for the conditions given. Calculations were based on an average blink reflex time of 150 msec. If blink occurs at later times, then retinal burns will occur at greater distances for detonations above 25 kt.

7-16 SECONDARY FLAME BURNS AND CONFLAGRATION. Secondary flame burns and conflagration effects may cause further casualties. Secondary flame burns of the hands and face may occur from ignition of clothing. In areas where conflagrations are likely to result from the detonation, large numbers of burn casualties may occur among individuals trapped in the wreckage of burning buildings or structures, or in forest fires. Under circumstances where conflagrations can occur, individuals in shelters may die of asphyxiation even though protected from the other casualty producing effects of the nuclear detonation. After a firestorm or a large-scale conflagration begins, it would be virtually impossible for an individual to leave the shelter and reach safety through the streets of a burning city.

NUCLEAR RADIATION INJURY

7-17 EFFECTS. The radiation exposure of a nuclear explosion is divided into two categories: (1) external radiation (from gamma rays, beta particles, and neutrons); and (2) internal radiation (from gamma rays, and alpha and beta particles). The end result in cells receiving doses of these nuclear radiations is qualitatively the same. Although the effects may be acute or delayed, only acute effects will be considered here. Delayed effects, though important, may not be manifest for years and thus will not affect the immediate military situation.

[redacted]

762-909 O - 65 - 20

[redacted]

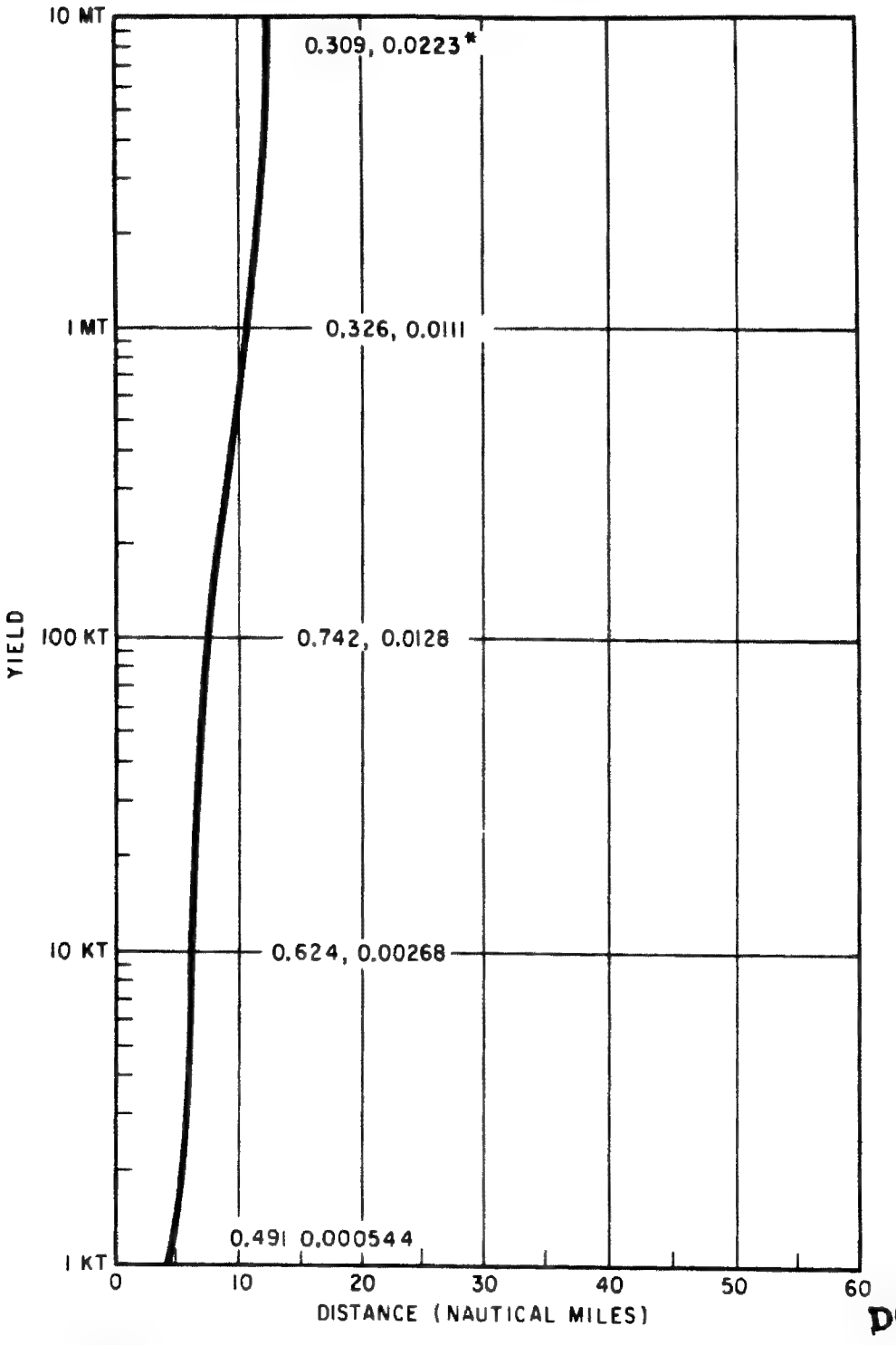

*EACH PAIR OF VALUES INDICATE, RESPECTIVELY, CALORIES AT THE CENTER OF THE IMAGE AND CALORIES ON THE LENS SURFACE

SEA LEVEL (BURST AND OBSERVER)
WATER VAPOR PRESSURE: 5mm HG
PUPILLARY DIAMETER: 3mm

Figure 7-3. Yield vs. Maximum Distance at which a Retinal Burn will be Formed. Visibility 10 Statute Miles; Standard Normal Day, and Daytime Adapted Eye

[redacted]

[redacted]

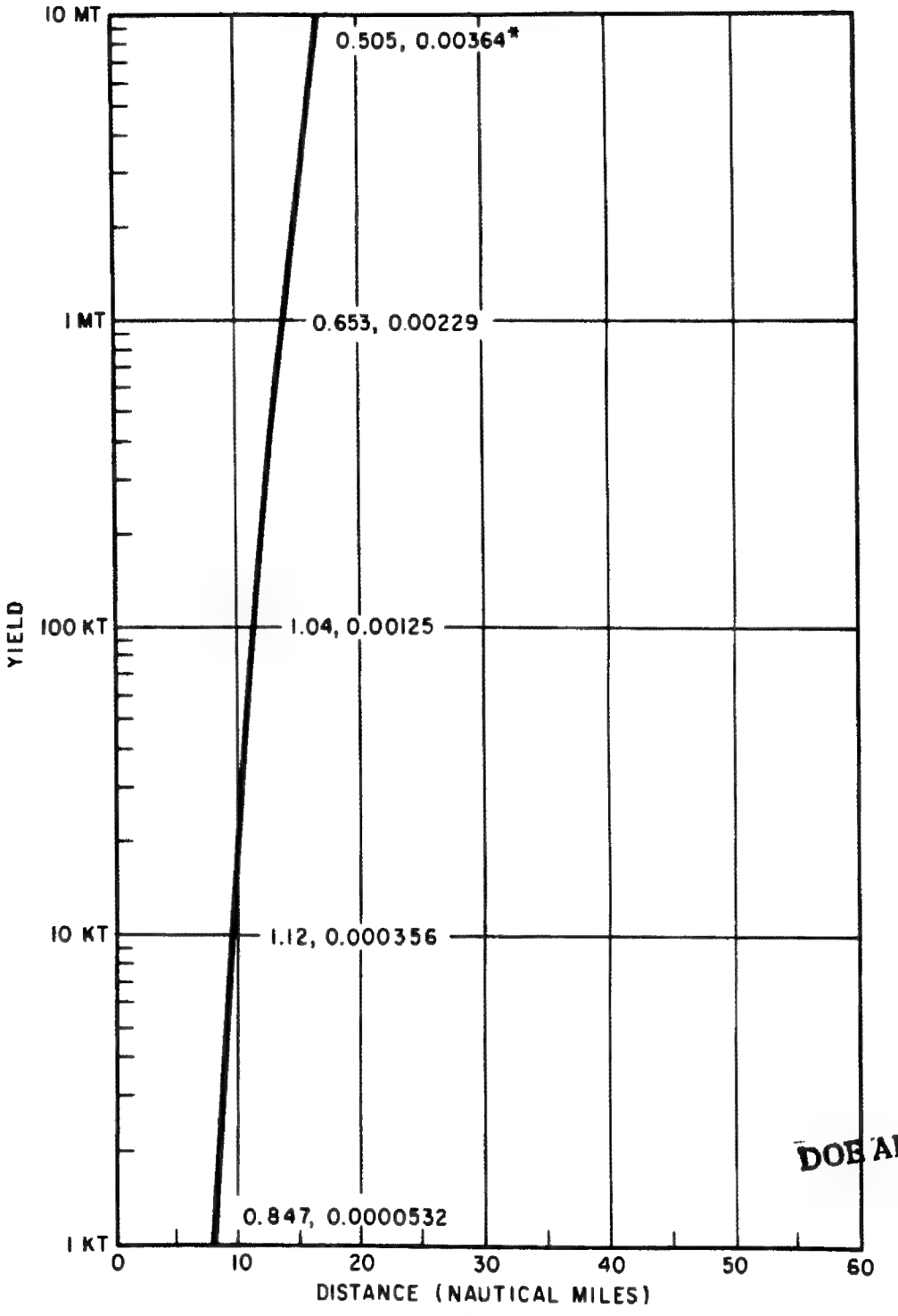

*EACH PAIR OF VALUES INDICATE, RESPECTIVELY, CALORIES AT THE CENTER OF THE IMAGE AND CALORIES ON THE LENS SURFACE

SEA LEVEL (BURST AND OBSERVER)
WATER VAPOR PRESSURE: 5mm HG
PUPILLARY DIAMETER: 7mm

Figure 7-4. Yield vs. Maximum Distance at which a Retinal Burn will be Formed. Visibility 10 Statute Miles, Standard Normal Day, Dark Adapted Eye

[redacted]

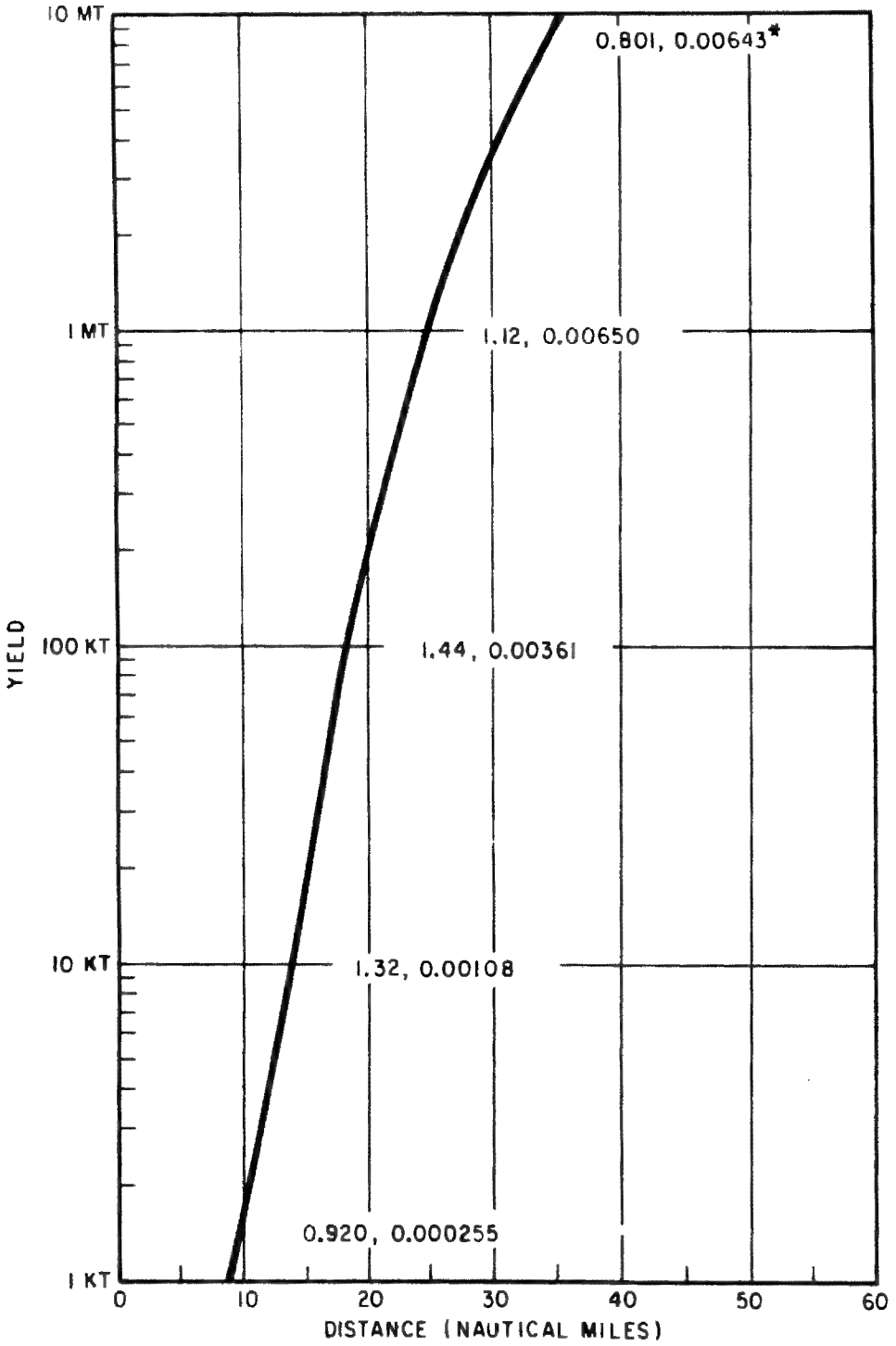

*EACH PAIR OF VALUES INDICATE, RESPECTIVELY, CALORIES AT THE CENTER OF THE IMAGE AND CALORIES ON THE LENS SURFACE

SEA LEVEL (BURST AND OBSERVER)
WATER VAPOR PRESSURE: 2mm HG
PUPILLARY DIAMETER: 3mm

Figure 7-5. Yield vs. Maximum Distance at which a Retinal Burn will be Formed. Visibility 35 Statute Miles, Standard Abnormal Day, Daytime Adapted Eye

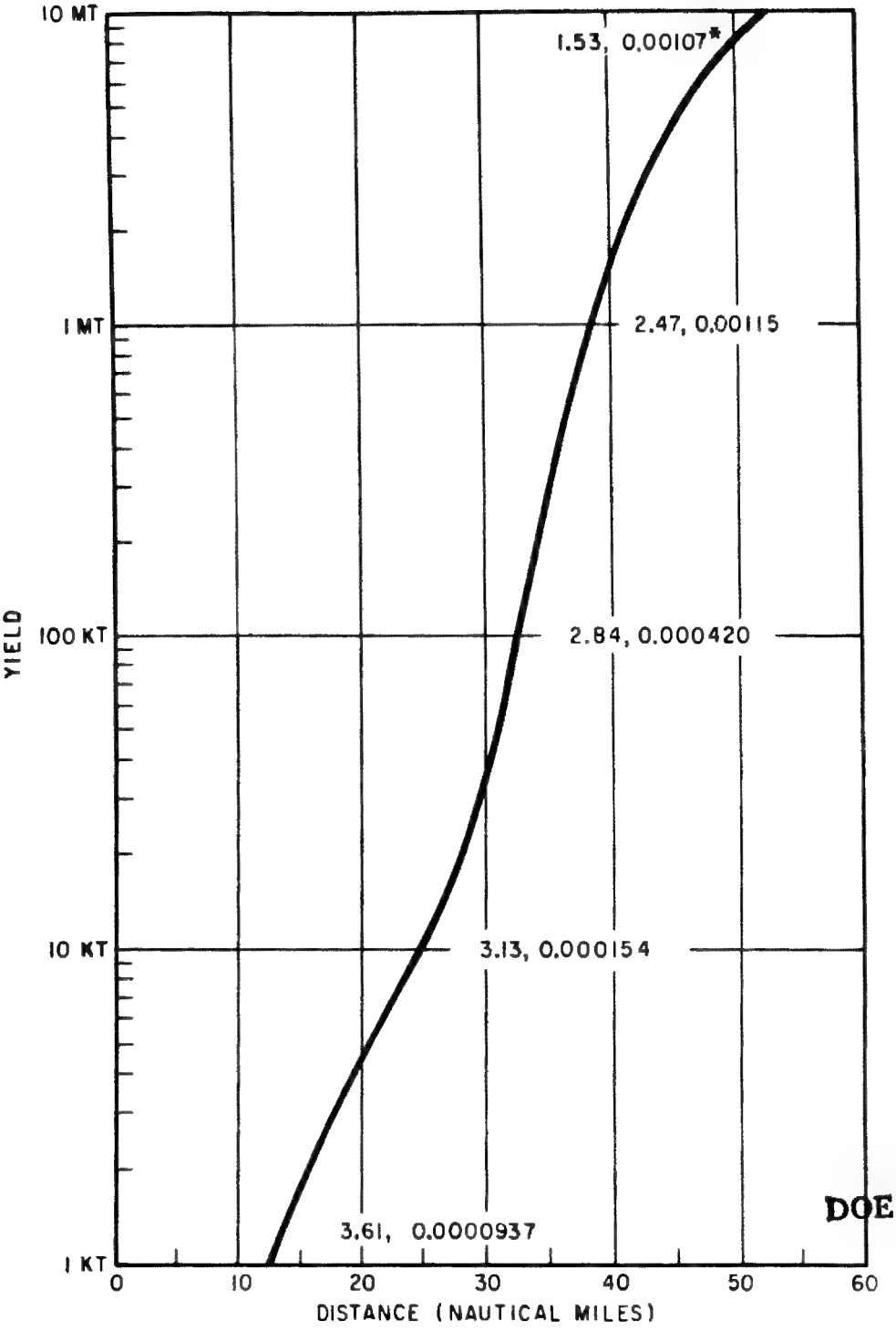

*EACH PAIR OF VALUES INDICATE, RESPECTIVELY, CALORIES AT THE CENTER OF THE IMAGE AND CALORIES ON THE LENS SURFACE

SEA LEVEL (BURST AND OBSERVER)
WATER VAPOR PRESSURE: 2mm HG
PUPILLARY DIAMETER: 7mm

Figure 7-6. Yield vs. Maximum Distance at which a Retinal Burn will be Formed. Visibility 35 Statute Miles, Standard Abnormal Day, Dark Adapted Eye

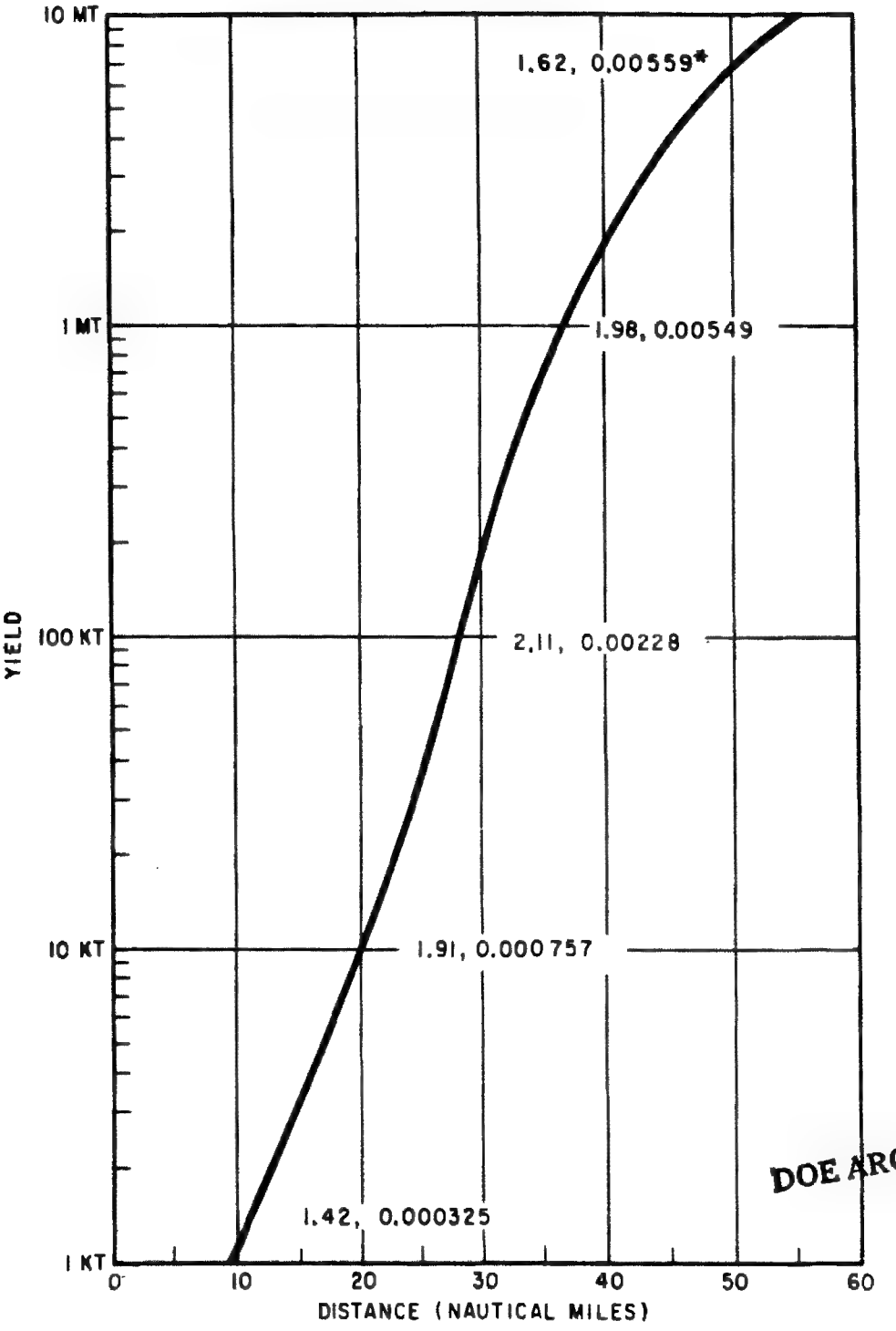

*EACH PAIR OF VALUES INDICATE, RESPECTIVELY, CALORIES AT THE CENTER OF THE IMAGE AND CALORIES ON THE LENS SURFACE

SEA LEVEL (BURST AND OBSERVER)
PUPILLARY DIAMETER: 3 mm

Figure 7-7. Yield vs. Maximum Distance at which a Retinal Burn will be Formed. Visibility 60 Statute Miles, Standard Abnormal Day, Daytime Adapted Eye

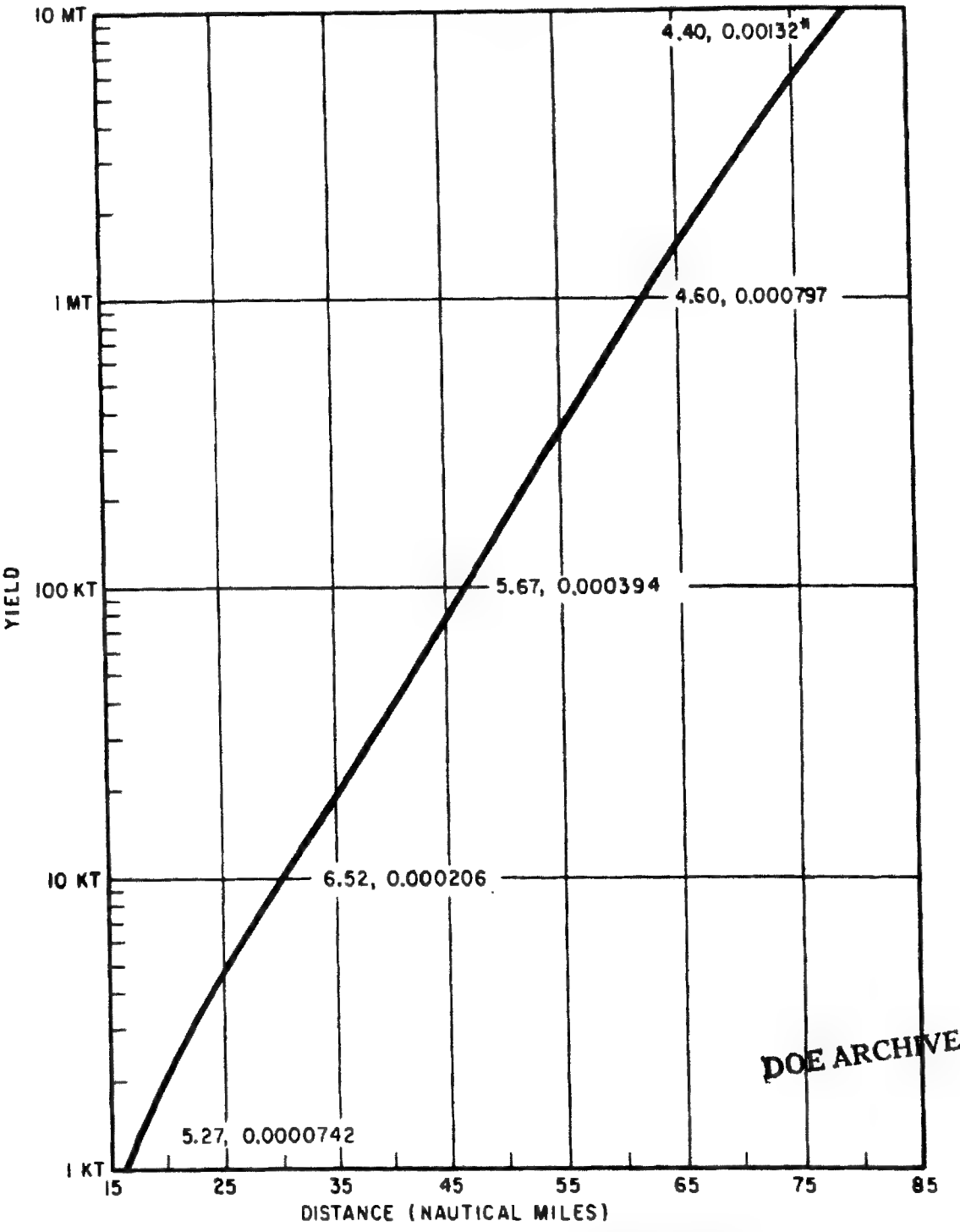

*EACH PAIR OF VALUES INDICATE, RESPECTIVELY, CALORIES AT THE CENTER OF THE IMAGE AND CALORIES ON THE LENS SURFACE

SEA LEVEL (BURST AND OBSERVER)
PUPILLARY DIAMETER: 7mm

Figure 7-8. Yield vs. Maximum Distance at which a Retinal Burn will be Formed. Visibility 60 Statute Miles, Standard Abnormal Day, Dark Adapted Eye

[redacted]

Injury from ionizing radiation obtains from the delivery of the radiation to sensitive body tissues. External beta radiation affects only the skin and closely adjacent tissues, whereas the penetrating gamma rays and neutrons affect tissues throughout the body. With penetrating radiation from external sources the biological effect varies according to the amount of shielding interposed between the source and the critical tissues. In fact, the body itself may shield internal organs from external radiation of low energy, or from a single direction.

Radiation can be received in a short time or over an extended period. When received in a short time (that is, within a few days) the effect is essentially independent of dose rate based upon animal experimentation data. (See paragraph 7-25 on immediate incapacitation.) When radiation is received over a long period of time, either continuously or in repeated doses, apparent biological recovery takes place, although this recovery may not be complete. It is not possible to specify for the whole body a definite biological recovery rate or a percentage of irreparable residual damage, because different tissues have different repair rates and different sensitivities to radiation. Because in the mid-lethal range the state of the blood forming tissues is directly related to survival, one may consider blood cell counting determinations as an index representing the whole body response.

7-18 EXTERNAL RADIATION HAZARD. The only external radiations of significance are gamma rays and neutrons, and under special circumstances, beta particles. During a nuclear explosion the gamma rays and neutrons alone are important, whereas in a residual fallout field gamma rays and sometimes beta particles must be considered.

7-19 Gamma Rays. Gamma radiation received at the time of detonation is essentially from a point source. The exposure dose decreases as the inverse square of the distance from the burst, plus losses because of atmospheric absorption and scattering. For small yield low-altitude bursts, radiation from gamma rays and neutrons constitutes the predominating personnel hazard.

7-20 Neutrons. Neutrons, like the gamma rays are delivered essentially instantaneously at the time of a nuclear explosion. There is some evidence that in animals the size of a man, neutrons are less effective than formerly thought. This may be a result of rapid absorption in superficial tissues. In the past, it had been generally accepted that rad for rad, neutrons caused more damage than gamma rays both for delayed effects and acute effects. It now appears that rad for rad they are the same as gamma radiation, or both have a relative biological effectiveness (RBE) of 1 *for acute effects only*. The RBE is a number assigned to a particular type of radiation to relate its physical units to the effect they produce in the human or animal when compared to the effect produced by the same amount of X-ray or gamma radiation of a certain energy. The unit that is used for neutron and gamma radiation measurements is the rad. To account for situations where the radiation RBE is greater than 1, the roentgen equivalent man (rem) was introduced.

$$\text{rad} \times \text{RBE} = \text{rem}$$

The rem, calculated for each type of ionizing radiation, may be added to obtain the total radiation dose to the point under consideration. Because the RBE for gamma rays and neutrons is 1, an acute exposure dose would be the same given in either rad or rem. By convention, however, rem is commonly used when discussing biological effect.

The curves of gamma radiation and neutron dose given in figures 4-14 through 4-17, which give the dose in rads, may be used with table 7-4 to estimate the probable overall effects of the immediate nuclear radiations.

7-21 Beta Particles. Beta particles, as well as gamma rays, constitute an external hazard from residual contamination. In an extended field of fallout radiation the gamma hazard generally far outweighs that from beta particles. The beta hazard, however, may become important in those circumstances where personnel receive fallout particles on the body surface.

a. Effect. Beta particle penetration is limited and may be partially blocked by thin absorbers such as clothing. Because of the limited range of beta radiation, the skin is the tissue

[redacted]

primarily affected. It has been estimated that a man would require tens of thousands of rems over his whole body surface before reaching a lethal range from purely beta external exposure.

It should be pointed out, however, that the LD50 (the dose lethal to 50 percent of the test population) is a poor end point for evaluation of a skin damaging process, because critical area injuries would be highly incapacitating, though not necessarily fatal, within a relatively short period of time, for example, if the eyes are swollen shut or the hands become inoperative because of pain or swelling. A total body surface beta injury is unlikely. The typical human beta injuries from residual contamination

Table 7-4 Summary of Clinical Effects of Acute Ionizing Radiation Dose

		Therapeutic range			Lethal range	
		100-200 rems	200-600 rems	600-1000 rems	1000-5000 rems	Over 5000 rems
Range	Subclinical range	Clinical surveillance	Therapy effective	Therapy promising	Therapy palliative	
Incidence of vomiting	None	100 rems: 5% 200 rem:: 50%	300 rems: 100%	100%	Up to 100%	
Delay time	——	3 hours	2 hours	1 hour	30 minutes	
Leading organ	None	Hematopoietic tissue			Gastro-intestinal tract	Central nervous system
Characteristic signs	None	Moderate leukopenia	Severe leukopenia; purpura; hemorrhage; infection. Epilation above 300 rems.		Diarrhea; fever; disturbance of electrolyte balance	Convulsions; tremor; ataxia; lethargy
Critical period postexposure	——	——	4 to 6 weeks		5 to 14 days	1 to 48 hours
Therapy	Reassurance	Reassurance, hematologic surveillance	Blood transfusion; antibiotics	Consider bone marrow transplantation	Maintenance of electrolyte balance	Sedatives
Prognosis	Excellent	Excellent	Good	Guarded	Hopeless	
Convalescent period	None	Several weeks	1-12 months	Long		
Incidence of death	None	None	0-80% (variable)	80-100% (variable)	95-100%	
Death occurs within	——	——	2 months		2 weeks	2 days
Cause of death	——	——	Hemorrhage; infection		Circulatory collapse	Respiratory failure; brain edema

are multiple ones, on surfaces directly exposed to the material. Direct contact is necessary for this type of "beta burn."

b. Decontamination. Where personnel have been exposed to direct contact with radioactive fallout particles, a few simple measures greatly reduce the probability of development of beta burns. Immediate showering, bathing, or simple removal by brushing off the particulate matter, accompanied by securing shelter and donning clothing of a protective nature (long-sleeved shirts, coveralls, shoes) afford sufficient protection against the beta burn hazard. The longer the fallout remains in contact with the skin, the more severe and extensive the effect is likely to be.

7-22 INTERNAL RADIATION HAZARD. The hazard associated with the intake of radioactive material into the body is present only in cases where fallout occurs. In such instances radioactive elements may be breathed into the lungs or may be swallowed and absorbed from food and water. The vast majority of the radioactive elements inhaled do not remain in the lungs, but are expectorated. Of the particles retained by the lungs, only a small fraction of the particles are likely to be concentrated and fixed in the lungs. Swallowing and inhaled elements must be soluble to become absorbed by the body. Once absorbed, they are metabolized in the same manner as corresponding nonradioactive elements. It is this prolonged retention of some radioactive fission products that characterizes internal radiation hazard.

7-23 Importance. The immediate effects of internal radiation are negligible. Therefore the external gamma hazard in the residual field of fallout contamination is the controlling factor in determining the danger to personnel. The same holds for the passage of aircraft through a radioactive cloud. The contaminating incident in the Marshall Islands in March 1954, produced data on the contamination associated with internal sources. Although the people on the Islands lived under conditions where the maximum probability of contamination of food and water supplies existed, and they took no steps to protect themselves, the degree of significant internal contamination due to fallout was small.

7-24 Protective Measures. Gas masks, air filters, or even handkerchiefs are effective in removing the particulate matter from inhaled air. Various methods of water decontamination such as distillation, coagulation, filtration, absorption, and ion exchange may all be used advantageously. The Army Engineers' Erdlator units (Mobile Water Purification Units) are of particular value. This equipment, which uses the processes of coagulation, diatomic filtration, and disinfection, is ordinarily used to treat and purify surface waters in the field. When used for radioactive decontamination, a 50 to 85 percent removal of dissolved gross fission products may be expected when the unit is operated in conventional fashion. The removal can be increased to 93 percent with an ion exchange posttreatment. The Erdlator may be expected to remove essentially all of the radioactivity present in the form of turbidity or particulates. Fallout does not directly contaminate canned and covered food and water. Surface contaminated food may be used when necessary by cutting or scraping off the outer layers.

7-25 INCAPACITATION. Direct effects of massive, rapidly administered doses of external radiation result in loss of ability to perform purposeful actions because of lack of coordination and imbalance. Nausea and vomiting may be clinical manifestations and may be sufficiently severe to incapacitate an individual to such a degree that he is not able to perform his duties. Experimental data on monkeys indicate that incapacitation (immobilization) within 2-3 seconds occurs following radiation doses in the order of 100,000 rads when delivered extremely rapidly (10-15 microseconds) as would happen with a nuclear explosion. Times up to several minutes may elapse before loss of coordination is observed with doses more than 50,000 rads. Following doses of 15,000 to 35,000 rad, monkeys were observed to show an initial decrement in functional capacity starting within a few minutes following dosage and lasting up to about an hour. The animals then regained apparent normal functional capacity for a matter of several hours before lapsing into a coma and death. Most monkeys showed little loss of functional capacity for a matter of more than 10-15 hours following exposure of 3000 rads to

about 10,000 rads. Extrapolation of these data to man is extremely difficult but the above figures should give a feeling for the magnitude of the radiation dose necessary to produce clinical effect. It should be pointed out that incapacitation (i.e. inability to perform any useful or purposeful action), and not death, is the endpoint of import to the field commander. Any combination of sublethal exposures to thermal or nuclear radiations or blast injury is expected to produce more casualties than any effect considered singly, because of additive or mutually reinforcing effects. Figure 7-10 represents a comparison of the ranges of the three effects considered individually in one situation. Insufficient knowledge precludes the presentation of any summation curve related to predictions of casualties from combined injury modalities.

NUCLEAR RADIATION SHIELDING

7-26 DOSAGE. The gamma radiation dosage received by an individual is reduced if absorbing material is interposed between the individual and the point of detonation. The dose received by a person behind a building, in a field fortification, in a tank, or in a ship is less, and in some cases much less, than that which would be received in an exposed free field position at the same distance from the detonation. The shielding designated in terms of a "dose transmission factor," defined as the ratio of the dose measured behind shielding material to the dose that would be measured in the absence of the shielding.

7-27 INITIAL RADIATION. The determining factors in the effectiveness of shielding are the total mass of the material between the source of radiation and the target; the energy distribution of the gamma radiation at the target; the distance from the source, which partly determines the gamma energy distribution; the angle of the incident radiation; and the geometry of the shielding. Figure 7-11 combines some of these parameters to give a series of curves of the dose transmission factor as a function of shielding thickness for various materials. The curves assume that the radiation is perpendicular to the slab of shielding material. Because air scatters gamma rays significantly, the resultant dose transmission factor holds strictly only for direct incident radiation. To insure protection against scattered radiation incident from all directions, optimum various shielding material thickness should be used for all directional surfaces. The curves of figure 7-11 are applicable for yields between 0.1 kt and 100 kt. Table 7-5 gives dose transmission factors for particular situations such as personnel in tanks, foxholes, houses, buildings, and basements.

7-28 RESIDUAL RADIATION. Residual radiation is somewhat less penetrating than initial radiation, as can be seen from the dose transmission curves for residual radiation in figure 7-12. In the case of residual radiation from a contaminated ground surface, the most effective location for shielding material is between the receiver and the contaminated ground, such as the floor of a tank, or the ceiling of an underground shelter. Walls also give some shielding against residual radiation because part of the radiation received can come horizontally from points up to several hundred yards from the receiver. A methodology is available for determining the shielding factors of structures located in a residual radiation field. This technique is presented in detail in "Structure Shielding Against Fallout Radiation From Nuclear Weapons," L. V. Spencer, National Bureau of Standards Monograph 42, Jun. 62.

[redacted]

Table 7-5 Dose Transmission Factors (Interior Dose/Exterior Dose)

Geometry	*Gamma rays* Initial	*Gamma rays* Residual	*Neutrons*[1]
Foxholes[2]	0.20	0.10	0.30
Underground—3 ft	0.04-0.05	0.0002	0.002-0.01
Builtup city area (in open)	—	0.70	—
Frame house	0.80	0.30-0.60	0.3-0.8
Basement	0.05-0.5	0.05-0.1	0.1-0.8
Multistory building:			
Upper	0.9	0.01	0.9-1.0
Lower	0.3-0.6	0.1	0.9-1.0
Blockhouse walls:			
9 in	0.1	0.007-0.09	0.3-0.5
12 in	0.05-0.09	0.001-0.03	0.2-0.4
24 in	0.01-0.03	0.0001-0.002	0.1-0.2
Factory, 200 x 200 ft	—	0.1-0.2	—
Shelter, partly above grade:			
With earth cover—2 ft	0.02-0.04	0.005-0.02	0.02-0.08
With earth cover—3 ft	0.01-0.02	0.001-0.005	0.01-0.05
Rough Terrain	—	0.4-0.8	—
Tanks: M-24, M-41, Tank Recov. Vehicle M-51, M-74	0.3-0.5	0.2	0.5-0.7
Tanks: M-26, M-47, M-48, T-43E1; Eng. Armd. Vehicles, T-39E2	0.2-0.4	0.1	0.3-0.6
Tractor, crawler, D8 w/blade	1.0	0.4	1.0
1/4-ton truck	1.0	0.8	1.0
3/4-ton truck	1.0	0.6	1.0
2-1/2-ton truck	1.0	0.5-0.6	1.0
Armd. Inf. Vehicle M-59, M-75. and 8P Twin 40mm Gun M-42	0.8-1.2	0.2-0.6	0.8-1.0
SP 105-mm howitzer M-52	0.6-0.8	0.4-0.6	0.8-1.0
Cruisers[3]			
Navigating Bridge	0.12-0.35	0.005-0.2	0.75
Superstructure Deck	0.008-0.25	0.0001-0.1	0.7
Main Deck	0.005-0.25	0.00003-0.1	0.7
Second Deck	0.0002-0.2	0-0.07	0.6
First Platform	0.0002-0.2	0-0.07	0.2-0.3
Second Platform	0.0001-0.10	0-0.01	0.05-0.15
Destroyer[3]			
Navigating Bridge	0.25-0.40	0.1-0.2	0.85
Superstructure Deck	0.015-0.40	0.00025-0.2	0.8-0.85
Main Deck	0.008-0.34	0.0001-0.2	0.75-0.8
First Platform	0.001-0.25	0-0.1	0.75-0.8
Second Platform	0.0005-0.20	0-0.07	0.5-0.75

[1] Estimated values.

[2] No line-of-sight radiation received.

[3] Assuming a beam-on orientation.

[redacted]

[redacted]

Problem 7-1 Direct Blast Casualties for Personnel in the Open

Figure 7-9 is a plot of burst height vs. ground range for 50 percent probability of producing direct blast casualties to personnel in the open as a result of translational motion. The curves are drawn for a 1-kt detonation.

Scaling.

$$\frac{h_1}{h_2} = \frac{W_1^{1/3}}{W_2^{1/3}} \text{ and } \frac{d_1}{d_2} = \frac{W_1^{0.4}}{W_2^{0.4}}$$

where h_1 and d_1 are the burst height and ground distance for yield W_1, and h_2 and d_2 are the burst height and ground distance for yield W_2.

Example.

Given: A 20-kt weapon burst at a height of 500 ft over open terrain.

Find: The distance at which there is a 50 percent probability of producing direct blast casualties to standing personnel as a result of translational motion.

Solution: The corresponding burst height for

$$1 \text{ kt is } \frac{500}{(20)^{1/3}} = 185 \text{ ft}$$

From figure 7-9 at a burst height of 185 ft, ground distance for 50 percent probability of direct blast casualties to standing personnel as a result of translational motion is 1275 ft.

Answer: The corresponding ground distance for 20 kt is $1275 \times (20)^{0.4} = 4220$ ft.

Reliability. Based primarily upon observed results of disasters involving humans and experiments with small animals, together with theoretical calculations.

Related Material. See paragraph 7-1. See also figure 7-1 and table 7-2 for thermal casualty data; and table 7-4 for nuclear radiation casualty data.

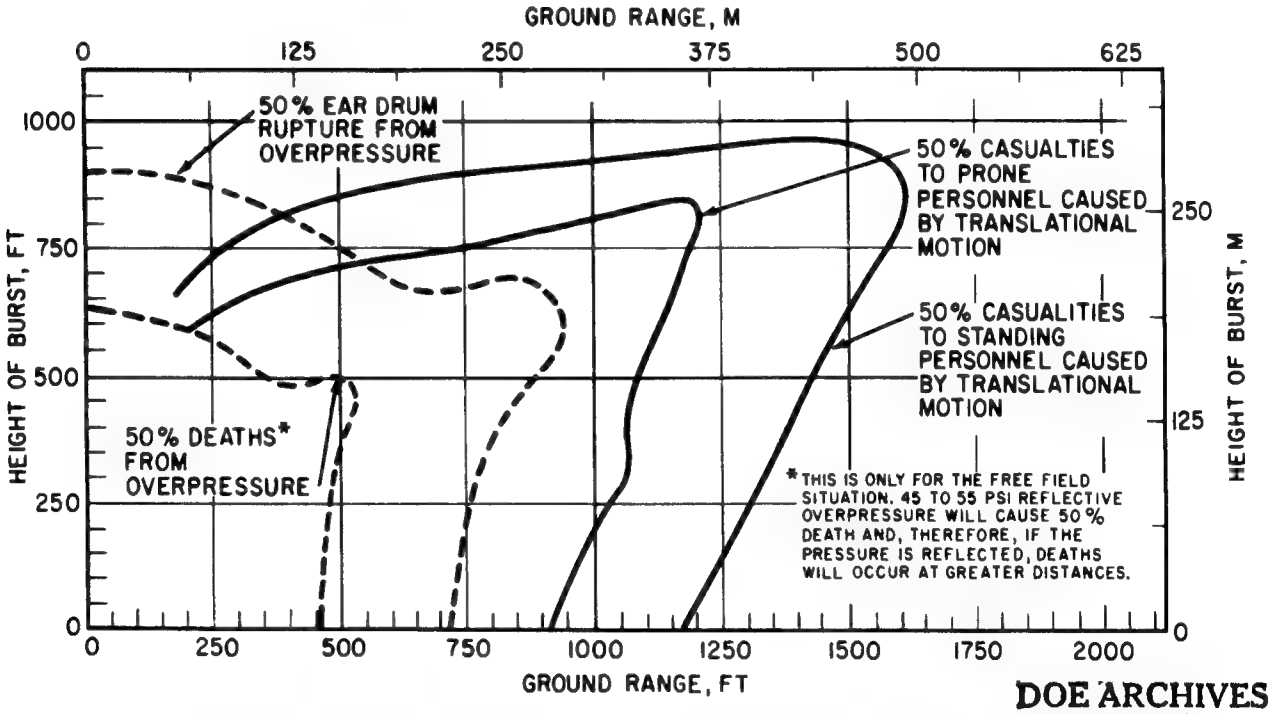

Figure 7-9. Direct Blast Casualties as a Function of Height of Burst and Ground Range for Personnel in the Open Exposed to a 1-kt Burst

[redacted]

Figure 7-10 represents a comparison of the ranges of the three casualty-producing effects of various nuclear weapons when detonated at a scaled height of burst of 300 ft in a clear atmosphere in which the visibility is 50 miles. These casualty predictions are based on the assumption, which will not be true in the majority of cases, that personnel receive a given dose or amount of a single effect only, and that this single effect will produce casualties without assistance from the other effects. There is some reason for believing that ionizing radiation and thermal radiation are synergistic; that is to say, that sub-injury levels of each, delivered simultaneously to the same person, could easily cause serious injury or death. There is no satisfactory way, however, of estimating the extent to which combined injuries can cause ineffectiveness, and figure 7-10 is designed as illustrative of the relative injury-producing capacities of the separate effects acting independently.

Related Material. See COMBINED INJURY.

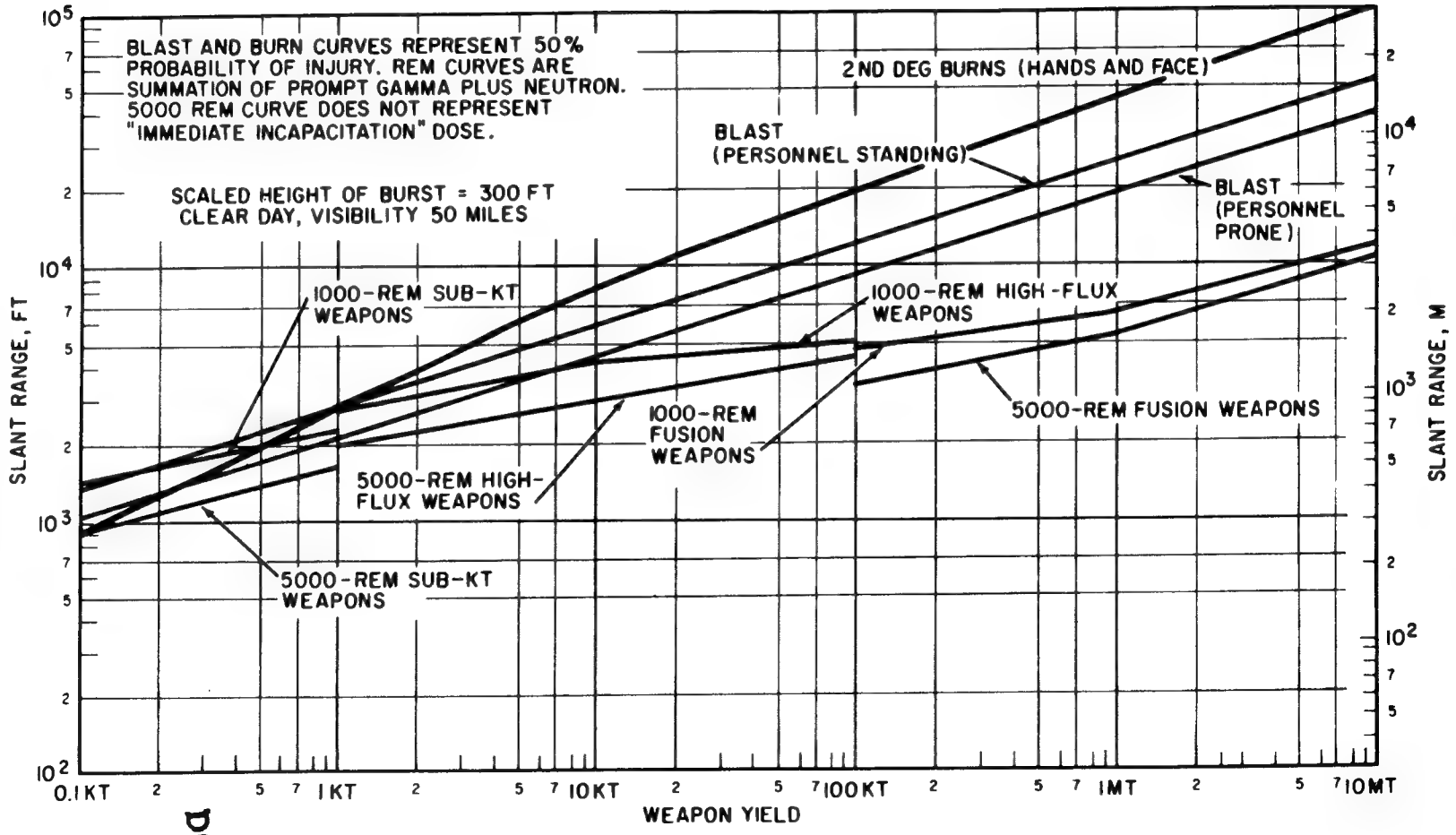

Figure 7-10. Casualties with Troops in the Open as a Function of Slant Range and Yield

[redacted]

Problem 7-3 Shielding from Initial and Residual Gamma Radiation

The curves in figures 7-11 and 7-12 indicate dose transmission factors for both initial and residual gamma radiation, respectively, perpendicularly incident upon various thicknesses of earth, water, concrete, iron, and lead. For other materials of known density, the transmission factor may be estimated by interpolation, on a density basis, between the curves given. (See table 7-6)

Example.

Find: How much concrete would be required to reduce the dose from initial radiation to one one-hundredth the unshielded dose?

Solution: Examine the curve for concrete of figure 7-11.

Answer: The thickness of a slab of concrete required to reduce the dose to 0.01 of its former value is 34 in.

Reliability. Thicknesses indicated for a given transmission factor are considered reliable within ±20 percent, for conditions outlined in paragraph 7-26.

Related Material. See paragraph 7-26. (For radiation input data, see Chapter 4.)

Table 7-6 Densities of Common Materials

	Lb per cu ft
Brick, common	120
Clay, dry	63
Clay, damp, plastic	110
Clay and gravel, dry	100
Coal, piled	40-50
Earth, dry, loose	76
Earth, dry, packed	95
Earth, moist, loose	78
Earth, moist, packed	96
Earth, mud, packed	115
Fuel oil	54
Granite	175
Limestone	165
Masonry, stone	150
Sand, gravel, dry packed	100-120
Fir	34
Hemlock	29
Oak	46
Pine, white	26
Pine, yellow	40

[redacted]

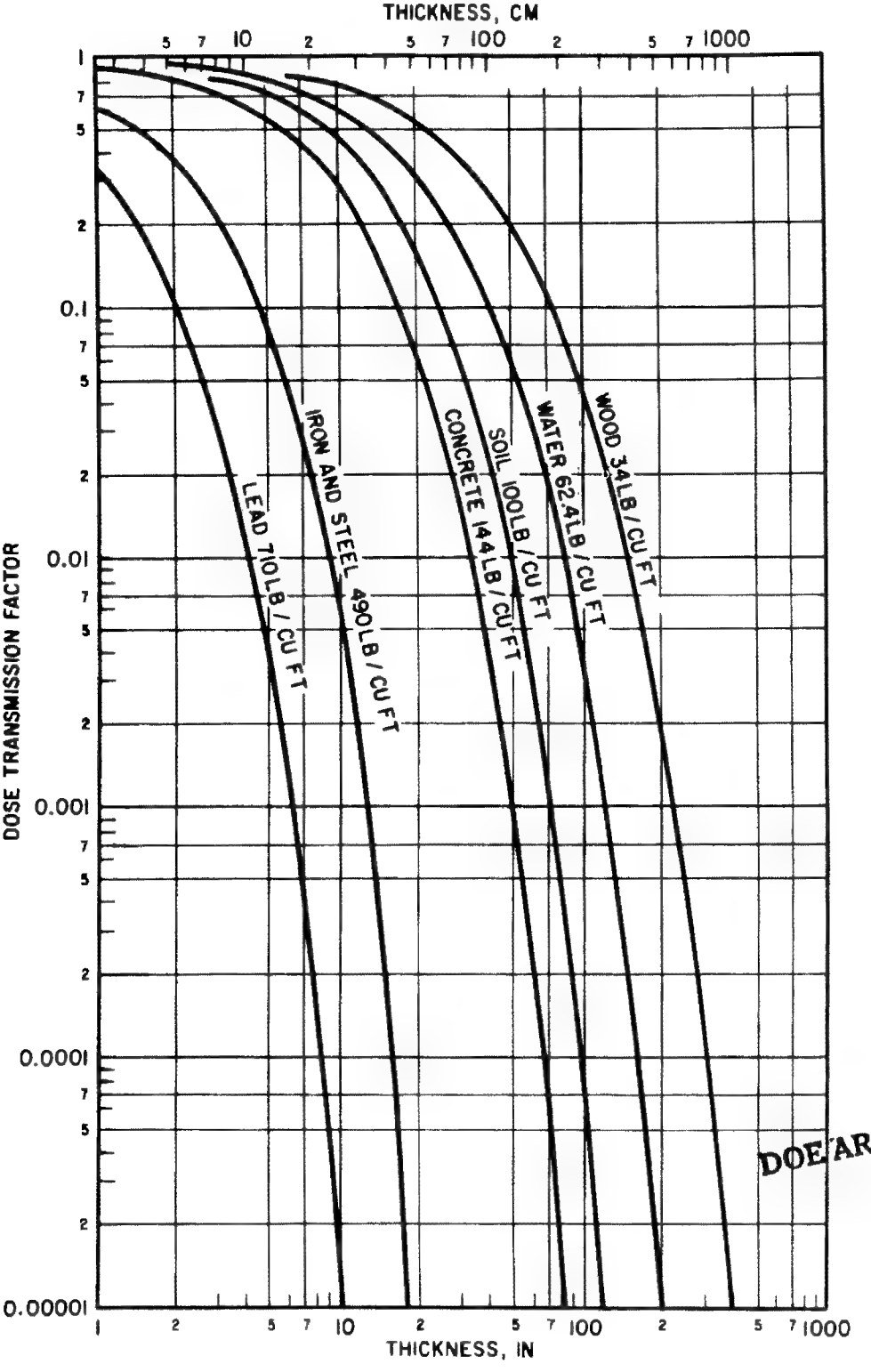

Figure 7-11. Shielding from Initial Gamma Radiation

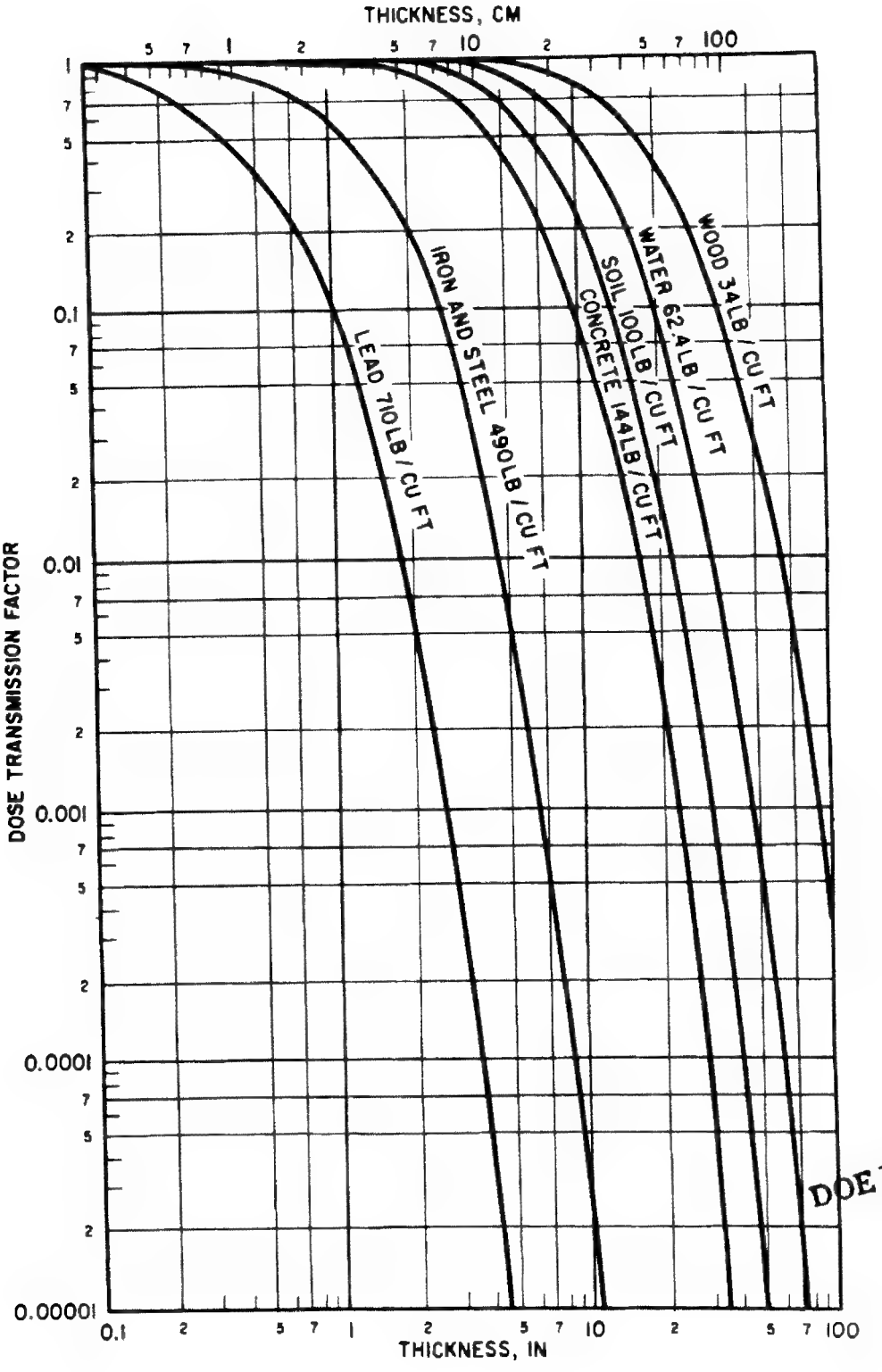

Figure 7-12. Shielding from Residual Gamma Radiation

2/21/85

PARTIAL DOCUMENT RECORD SHEET

Parts of this document were judged irrelevant to the CIC collection effort and were not copied:

Pages _____

Enclosures _____

Attachments _____

Other Chapters 8-9-10-11-12

Title page and table of contents have been copied for reference.

Dick Kongle
signature

9-15-87
date

Chapter 13
RADIATION DAMAGE

NUCLEAR RADIATION DAMAGE

There are two areas besides the biological effect in which initial nuclear radiation damage is militarily significant. These are the exposure of photographic film and the effects on electronic systems.

13-1 PHOTOGRAPHIC FILM. Photographic film is clouded by the interaction of both neutrons and gamma rays with the particles in the photographic emulsion. Actually, the sensitivity of film to radiation is often used to advantage to obtain total neutron or gamma flux measurements in a radiation environment.

13-2 ELECTRONIC SYSTEMS. Radiation effects on electronics may be transient or permanent.

13-3 Transient Effects. Radiation induced transient effects are generated by ionization, electron excitation, charge emission or collection, and the creation of leakage paths between piece parts. The induced signal surges through the circuitry, producing effects ranging from minor current fluctuations to complete destruction of sensitive piece parts through overloading. The exact nature and seriousness of the effect encountered depend on the proximity of the equipment to the point of detonation, the circuit design, and the vulnerability of the circuit piece parts to transients.

Induced transients depend on the rate at which the radiation is received, although sometimes they involve a complex interaction between the radiation rate and the total dose received. In most cases the higher the radiation rate and the longer the time constant of the circuit, the greater will be the magnitude of the induced transient. Also, although transients in sensitive circuits may disappear rapidly with decreasing radiation rate, secondary effects created in a system may persist for a relatively long period.

The range of transient effects for a given yield increases with altitude. Under extra-atmospheric conditions such effects may be significant at ranges up to and perhaps exceeding 100 miles.

13-4 Permanent Effects. Permanent damage to electronic equipment is caused by the displacement of atoms from their normal positions in the lattice structure of a material. Fast neutrons are almost entirely responsible for this effect. The severity of the damage depends on the neutron energy spectrum (that is, the higher the neutron energy, the greater the damage), and is directly proportional to the magnitude of the radiation dose received. The atom displacement produces a change in the basic electrical response characteristics of the material. Although some annealing occurs with time, the damage is never permanently corrected. Between various electronic materials the dose levels that cause such damage vary widely. Circuits using solid-state devices seem most susceptible.

To illustrate the dependence of transient effects on radiation rate as distinguished from total radiation dose, effects have been known to occur from gamma rates of 10^7 rads/sec when the total dose delivered was only 0.1 rad. The threshold for the most sensitive electronic piece parts and circuits for the onset of transient effects generally occurs at rates from 10^8 to 10^4 rads/sec.

Threshold levels for the onset of permanent damage to the most sensitive electronic components generally begin at 10^{10} to 10^{11} n/cm^2. The curves in figure 13-7 show the total number of fast neutrons per square centimeter expected per kiloton of yield at various horizontal distances from typical airburst fission weapons detonated at altitudes up to 100,000 ft MSL. These curves give results correct within a factor of five.

There is no clear line of demarcation between transient effects and permanent damage because classification of effect varies with circuit design and mission of the system involved. For

762-909 O - 65 - 30

example, although such effects as capacitor discharge are usually referred to as transient effects, the time constant for recovery of the capacitor to its normal operating potential may be so long that recovery may not be effected before the mission of the system involved is complete. In this instance the effect would be classified as permanent damage even though the capacitor itself would have eventually completely recovered.

ELECTROMAGNETIC PULSE RADIATION DAMAGE

a. General. Permanent damage due to overheating or puncturing of insulation is possible where the electromagnetic pulse energy is high, where the induced voltage triggers an electrical fault and the damage energy is supplied by the affected system, or where the electromagnetic pulse energy is carried for some distance along a cable or line as a power surge.

Interruption of service may occur where the voltage induced in a cable or line causes fuses to blow or circuit breakers to trip. This may take place many miles away from the point of detonation due to transmission of the surge. An interruption could also result if an electronically stored program were subjected to a strong enough transient electromagnetic field to scramble it.

Transient disturbances to electronic systems may occur in several ways. The electromagnetic pulse may be received via the signal or power lines acting as antennae. Or, the low frequency portion of the pulse may penetrate the enclosures and directly induce transient signals in the circuits.

Many instances of all three kinds of damage, i.e., permanent, interruptive and transient, have been experienced. So far, little if any, correlation of damage with measured electromagnetic field strengths has been established. This has been the result of factors previously described, and of uncertainty of the point where electromagnetic pulse pickup actually occurred in cases where many cables and lines were in use for power, signal, control and mechanical purposes.

b. Power System Damage. Very regular zero-time tripping of power circuit breakers at a substation more than 30 miles away was observed on one series of tests. Standby personnel were always posted to reset the breakers to keep electrical equipment functioning. Within a mile of ground zero, pinholes in underground cable insulation have frequently been found. Such cables carried up to 4160 volts.

At power distribution stations, porcelain cutouts have been observed to arc over and the fuses have often blown. At other stations power transformers have been shorted internally or have had insulating bushings destroyed. Ordinary lightning protective devices provided inadequate protection against the electromagnetic pulse, in those cases.

c. Signal System Damage. Damage to signal systems has also been frequent in the form of burned or fused relays, potentiometers, cable insulation and conductors, as well as blown or damaged meters. In many instances, reviews of the circuits have shown that induced energy caused the damage, rather than triggered system energy. Free ends of cable pairs have often arced and melted.

d. Electronic System Damage. Oscilloscope presentations have frequently been disturbed or obliterated, even as far as 11 miles from ground zero.

Pulse counters in a timing circuit have been scrambled directly by the induced field (this effect has actually been duplicated in a simulation test in which a 1 mfd capacitor was charged to several thousand volts, then discharged into 10 turns of wire wound around the cabinet). Memory circuits employing magnetic elements may be vulnerable to the magnetic field, H, in a direct manner, as well as to the time derivative of the field.

Elaborate protective measures against electromagnetic effects have been devised, on occasion, such as extensive grounding plate systems, double-walled screen rooms, precautions against forming loops, and special bonding. These measures appeared effective on certain occasions, but on others, when higher yield weapons were tested, the precautions did not always suffice.

General recommendations for protection against electromagnetic pulse radiation damage cannot yet be made. Protective measures to be taken will depend principally upon the nature of the target and the degree of protection required.

13-5 FIRE IN URBAN AREAS. The employment of an air burst weapon over urban areas may produce, besides blast damage, mass fires which, under proper conditions, materially increase the degree and extent of damage. The behavior of such fires, whether they are of primary or secondary origin, follows the pattern of fires in forest and wildland areas. The burning potential for urban areas varies with weather conditions, much as for wildlands; however, the fire season as such is not as pronounced as in wildlands. During those seasons when weather conditions may reduce exterior potentials to zero, dwellings are usually heated, so that interior fuels are dried out. Fire incidence and subsequent fire buildup depend also upon the amount and distribution of flammable material used in interior furnishing and building construction, the incidence of interior kindling fuels, and the relative cleanliness of the living habits of the population.

13-6 Ignition Points. A survey of metropolitan areas in the United States indicates that the incidence of exterior ignition points can be correlated with urban land use. Table 13-1 presents a relative tabulation based on exterior kindling fuels. Newspapers and other paper products account for 70 percent of the total, and dry grass and leaves account for another 10 percent in residential areas. Most other exterior kindling fuels are present in small percentages or require radiant exposures in excess of 10 cal/cm^2 for ignition. Weathered and badly checked fences and building exteriors that contain appreciable dry rot constitute an ignition hazard. The tabulation presented in table 13-1 is not representative of European cities and other areas where fuel is at a premium, or where extensive use is made of stone, brick, masonry, and heavy timber construction. Multistory buildings and narrow streets reduce both interior and exterior primary ignitions, because such ignitions are proportional to the amount of sky seen from the location of the probable ignition point.

13-7 Humidity Effects. Because paper is the major exterior kindling fuel and is also an important interior fuel, the extent of ignitions

Table 13-1 Relative Incidence of Ignitions in Metropolitan Areas of the United States by Land Use (Based on Exterior Kindling Fuels).

Land use	Relative incidence
Downtown retail	1.0
Large manufacturing*	1.4
Good residential	1.6
Small manufacturing	3.8
Poor residential	5.2
Neighborhood retail	5.5
Waterfront areas	8.0
Slum residential	11.7
Wholesaler	15.1

* May be likened to a typical fixed military installation in the Z.1.

may be estimated from the minimum radiant exposure requirements for newspaper. Figure 13-1 shows the radiant exposure required to ignite darkly printed picture areas and printed text areas of newspaper at 50% relative humidity. The effect of relative humidity on the ignition of this cellulosic fuel can be estimated by multiplying the ignition radiant exposures for the dry material by the factor, $1 + 0.005\,H$, where H is the relative humidity in percent. Maximum fire effects occur during daily periods of lowest relative humidity, usually mid-afternoon. Guides for estimating urban burning potentials are given in figures 13-2 and 13-3. Figure 13-2, which gives burning potential for urban areas when central heating is not in use, represents approximate values of wind speed and average daytime relative humidity conditions corresponding to low, dangerous, and critical burning potentials according to the following definitions:

Low. Slow burning fires; fire can be controlled at will. Control action can be on unit structure basis.

Dangerous. Fires burn rapidly; individual building fires combine to form an area fire. Organized action needed to confine fire to area originally ignited.

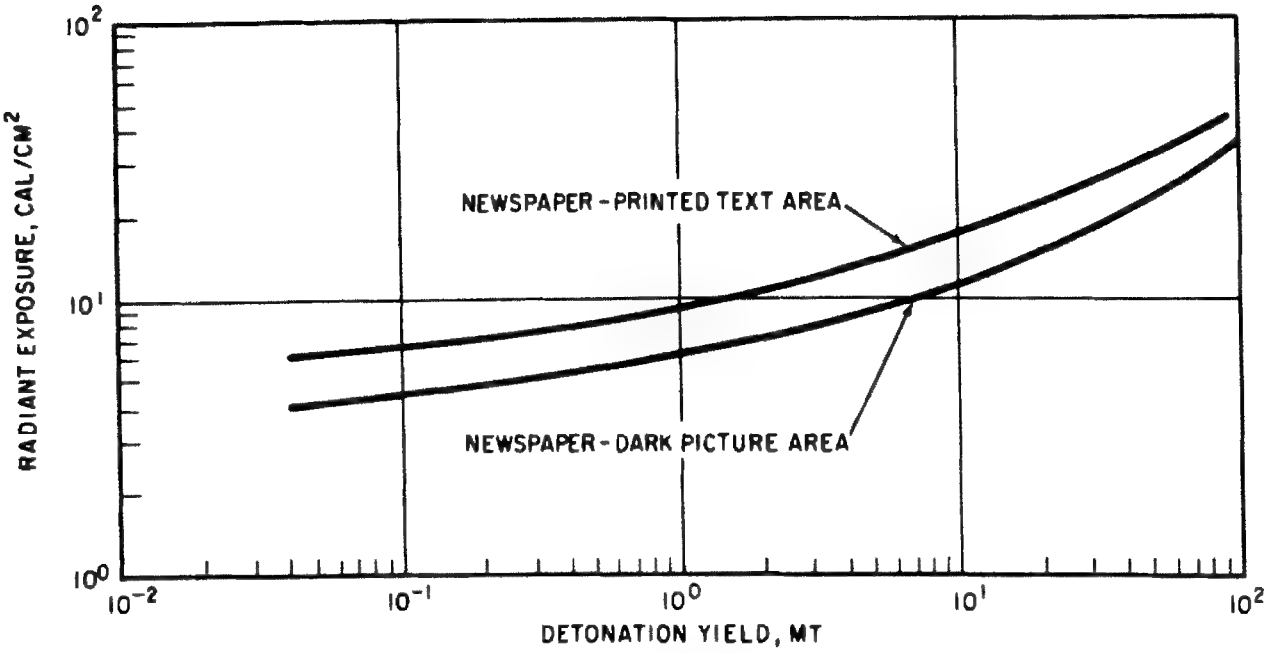

Figure 13-1. Radiant Exposures for Ignition of Newspaper (Relative Humidity—50 Percent)

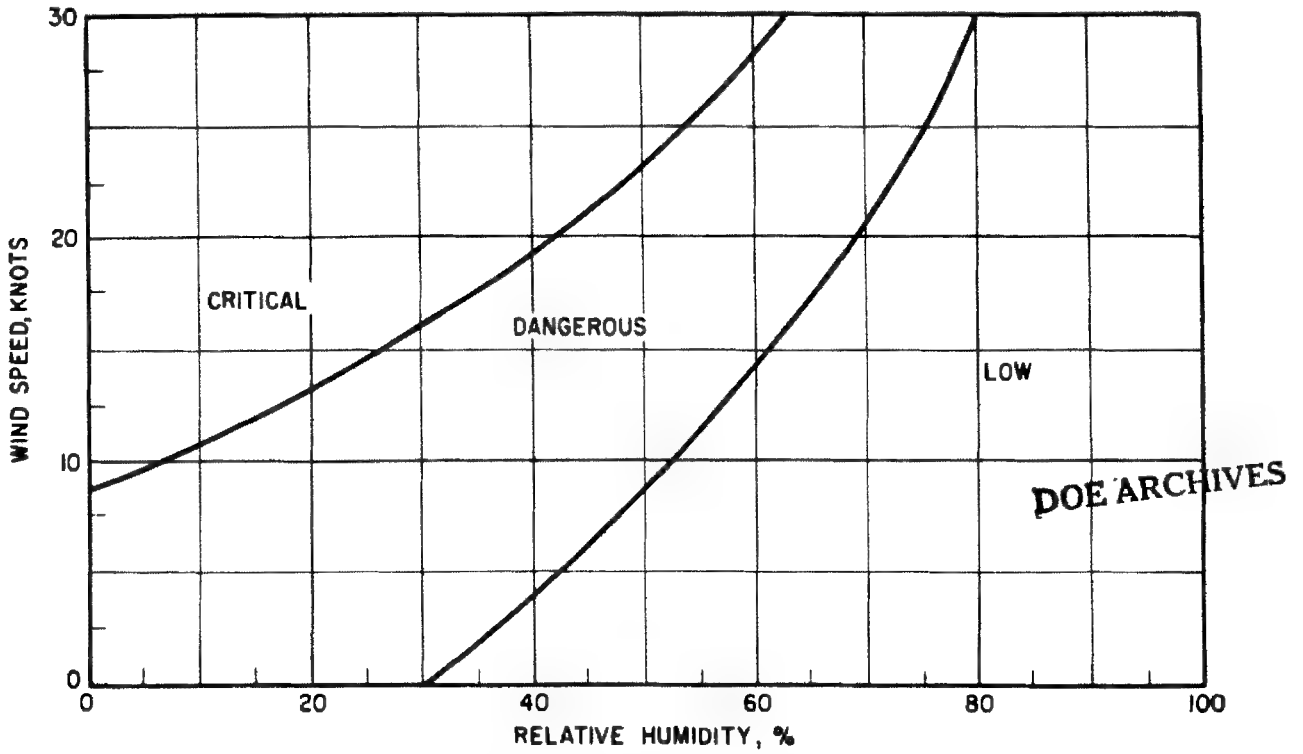

Figure 13-2. Burning Potential for Urban Areas (Central Heating not in Use)

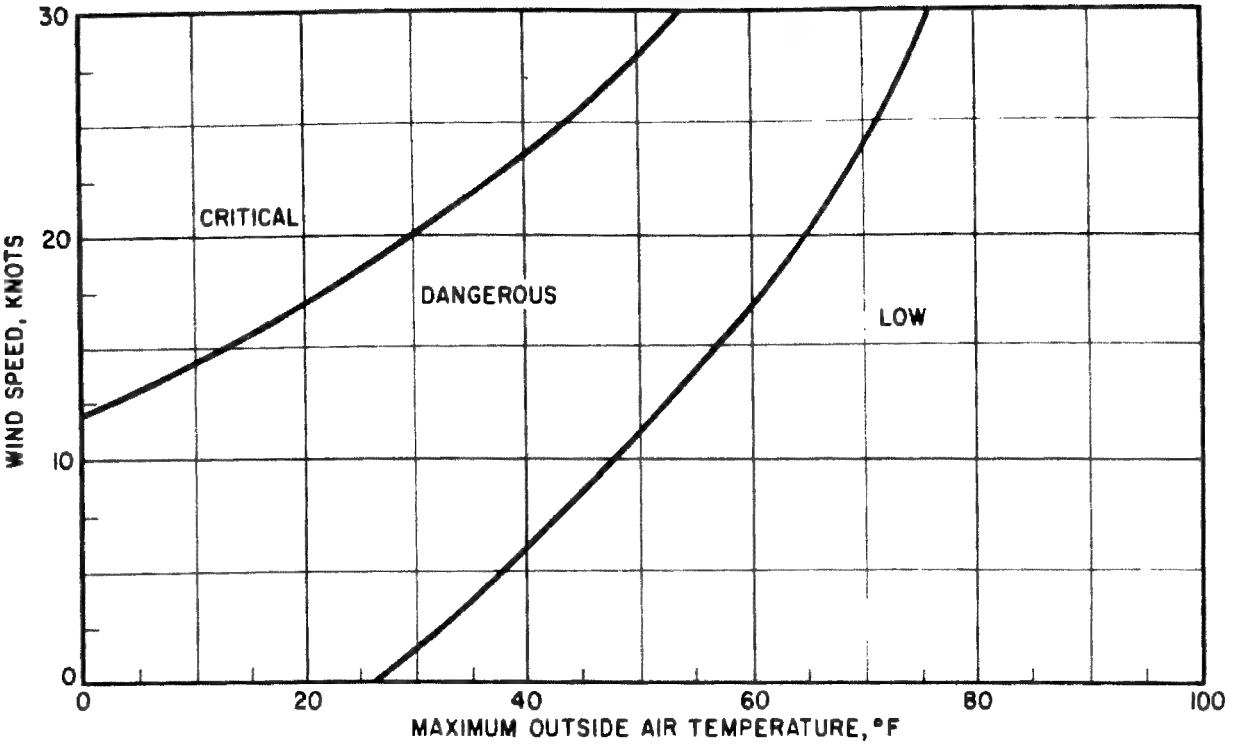

Figure 13-3. Burning Potential for Urban Areas (Central Heating in Use)

Critical. Rapid buildup into conflagration-type fires, high probability of fire storm spotting frequent and severe. Requires evacuation of firefighting equipment and personnel; control action effective only at critical breaks in building continuity or density.

With central heating, interiors are much drier than indicated by exterior relative humidities and temperatures. Based on United States experience, interior heating becomes an important factor when the maximum daily temperature drops below 70°F. Where fuel is scarce or expensive, this temperature may drop to 60°F, or even lower. Figure 13-3, which gives burning potential for urban areas when central heating is in use, shows approximate values of wind speed and maximum outside air temperature conditions corresponding to low, dangerous, and critical burning potentials. These burning potentials are defined in the same way as those in figure 13-2.

13-8 Fire Spread. The rate of fire buildup in urban areas is expected to be slower than for wildlands. The time to maximum fire intensity is less for the relatively high ignition incidence areas of table 13-1 than for those of lower ignition incidence. Besides weather conditions, the principal factors that influence fire spread are the continuity, size, and combustibility of buildings; fuel value of building contents; and topography. When strong convective action develops and spotting is frequent, the flammability of roof material is important in spread. Spread of the fire front generally occurs by radiation from adjacent buildings; hence, fire stops only when the building spacing becomes great enough to reduce this radiation level below a critical value. This critical spacing is greater for multistory buildings and varies with building combustibility, but on the average is about 50 to 100 ft.

13-9 THERMAL DAMAGE TO VARIOUS MATERIALS. In table 13-2 the critical radiant exposures for specified damage to various materials are shown for three weapon yields. The values presented for fabrics apply for an ambient relative humidity of 65 percent and an ambient temperature of 20°C. For extremely

[redacted]

Table 13-2 Critical Radiant Exposures for Damage to Various Materials

Material	Weight (oz/sq yd)	Color	Effect on Material	Radiant Exposure (cal/cm²) 40 kt	1 mt	10 mt
Clothing Fabrics						
Cotton	8	White	Ignites	32	48	85
		Khaki	Tears on flexing	17	27	34
			Ignites	20	30	39
		Olive	Tears on flexing	9	14	21
			Ignites	14	19	21
		Dark Blue	Tears on flexing	11	14	17
			Ignites	14	19	21
Cotton-nylon Mixture	5	Olive	Tears on flexing	8	15	17
			Ignites	12	28	53
Wool	8	White	Tears on flexing	14	25	38
		Khaki	Tears on flexing	14	24	34
		Olive	Tears on flexing	9	13	19
		Dark Blue	Tears on flexing	8	12	18
	20	Dark Blue	Tears on flexing	14	20	26
Rainwear (double neo-prene coated nylon twill)	9	Olive	Begins to melt	5	9	13
			Tears on flexing	8	14	22
Tinder Materials						
Paper, bond, typing, new (white)			Ignites	24	30	50
Newspaper, printed text			Ignites	6	8	15
Newsprint, dark picture area			Ignites	5	7	12
Paper, kraft, single sheet (tan)			Ignites	10	13	20
Rags (black, cotton)			Ignites	10	15	20
Rags (black, rayon)			Ignites	9	14	21
Tent Material						
Canvas, white, 12 oz/sq yd			Ignites	13	28	51
Canvas, OD, 12 oz/sq yd			Ignites	12	18	28
Aluminum aircraft Skin (0.020 in. thick) coated with 0.002 in. of standard white aircraft paint			Blisters	15	30	40
Sandbags, cotton, canvas, dry, filled			Failure	10	18	32
Construction Materials						
Roll Roofing, mineral surface			Ignites	—	>34	>116
Roll Roofing, smooth surface			Ignites	—	30	77
Plywood, douglas fir			Flaming during exposure	9	16	20
Sand, coral			Explosion*	15	27	47
Sand, siliceous			Explosion*	11	19	35
Rubber, pale latex			Ignites	50	80	110
Rubber, black			Ignites	10	20	25

* Popcorning

[redacted]

[redacted]

Notes for Table 13-2

a. The critical radiant exposures for damage to clothing fabrics refer only to the damage to the outer garment on which the radiation is incident. They are not generally applicable to predicting skin burns to the wearer, values for which are given in another chapter. When the outergarment ignites, however, the probability of skin burns should be considered because of contact of unclothed parts of the body with flaming or glowing materials.

b. The effect, "tears on flexing," indicates the radiant exposure level at which the outergarment ceases to serve as a reliable barrier to the environment. Under certain environmental conditions the garment would require immediate replacement.

c. Cotton or rayon fabrics generally can be ignited by exposure to thermal radiation. Nylons, dacrons, and similar synthetics are generally not ignited but melt at relatively low radiant exposures. Woolens do not ignite, but the fibers scorch and coalesce. When a sufficient thickness of the woolen fabric is scorched it becomes brittle and can be readily torn or crumbled.

d. Most thick, dense materials that ordinarily are considered inflammable do not ignite to persistent flaming ignition when exposed to transient thermal radiation pulses. Wood, in the form of siding or beams, may flame during the exposure but the flame is extinguished as soon as the exposure ceases.

---

dry conditions the values shown for fabrics should be reduced by 20 percent. For extremely high relative humidities, near 100 percent (at 20°C), the values for fabrics should be increased by 25 percent. If the fabrics are water-soaked, the critical radiant exposures should be increased by 300 percent.

The values in table 13-2 for uniforms refer to damage to the material itself and are not applicable for predicting skin burns under uniforms. The table also does not include the damage to materials when they come in contact with or are enveloped by the fireball. The heat input under these conditions is many orders of magnitude higher than the cases just discussed. Several of the variables considered as influential factors in determining the amount of surface material lost by an object exposed within a fireball include: type of material, surface curvature, orientation, thermal attenuation by the metallic vapors given off by the object, and spallation. Figures 13-4 and 13-5 give the material loss from spheres of various materials because of ablation or scaling off of the surface material from contact with or envelopment by the fireball. Data for three types of 10-in. diameter spheres are shown; solid steel, solid aluminum, and solid aluminum with small cylindrical wells filled with ceramic inserts. The one curve in figure 13-4 represents all three types.

ELECTROMAGNETIC DISTURBANCES

13-10 GENERAL. Military systems, such as some communication circuits and radars, whose use involves the propagation of electromagnetic waves through the ionosphere, may undergo severe performance degradation following the explosion of a high-altitude nuclear weapon. After such a nuclear explosion, immediate radiation partially or completely dissociates and ionizes the atmospheric gases around the burst. The increased electron content modifies the propagation characteristics of the ionosphere to the extent that radio waves incident on it are strongly absorbed. Near the periphery of the highly ionized region absorption effects become less important and refraction or bending of the incident wave may be a significant effect. Moreover, the debris from the burst remains radioactive for some time and provides a continuous source of ionizing radiation that exerts a profound influence on the lower ionosphere from about 30 to 100 km altitude. Secondary effects of the burst are increased turbulence in the ionosphere, which produces angular scintillation and backscatter, and synchrotron noise, which may cause increased noise levels.

Paragraph 13-12 presents a quantitative description of the major damage mechanisms.

[redacted]

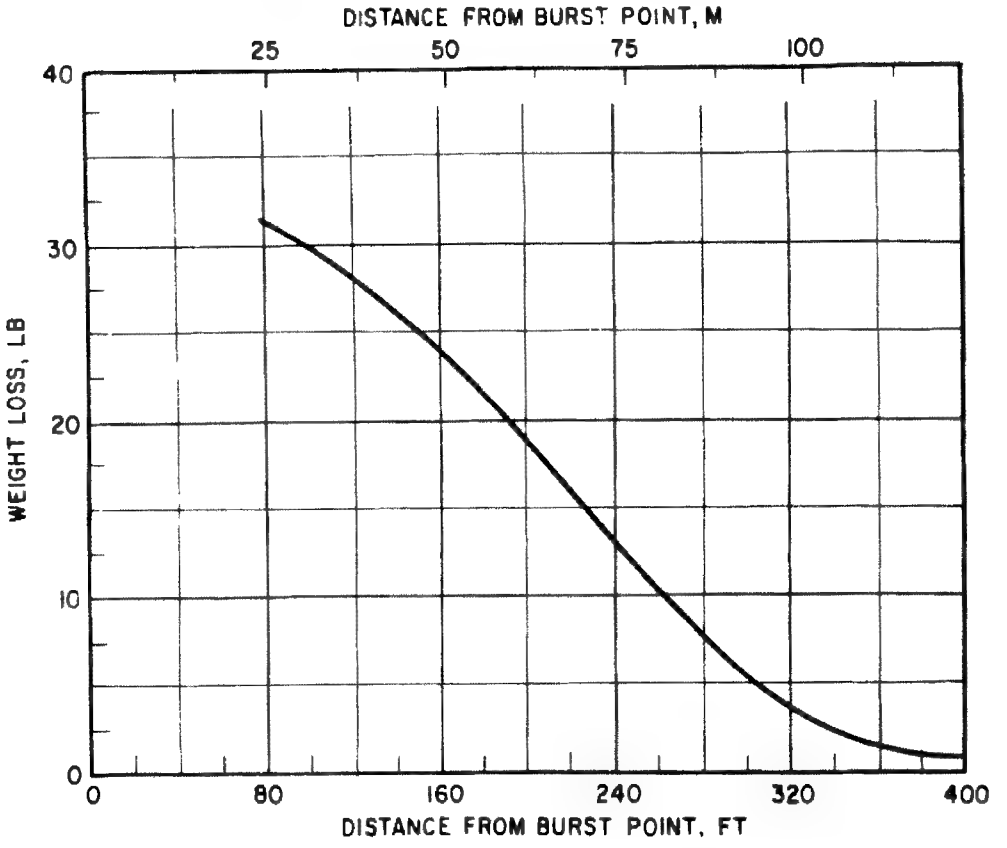

Figure 13-4. Weight Loss with Distance from a 23-kt Burst for Aluminum, Steel, and Ceramic Insert Spheres

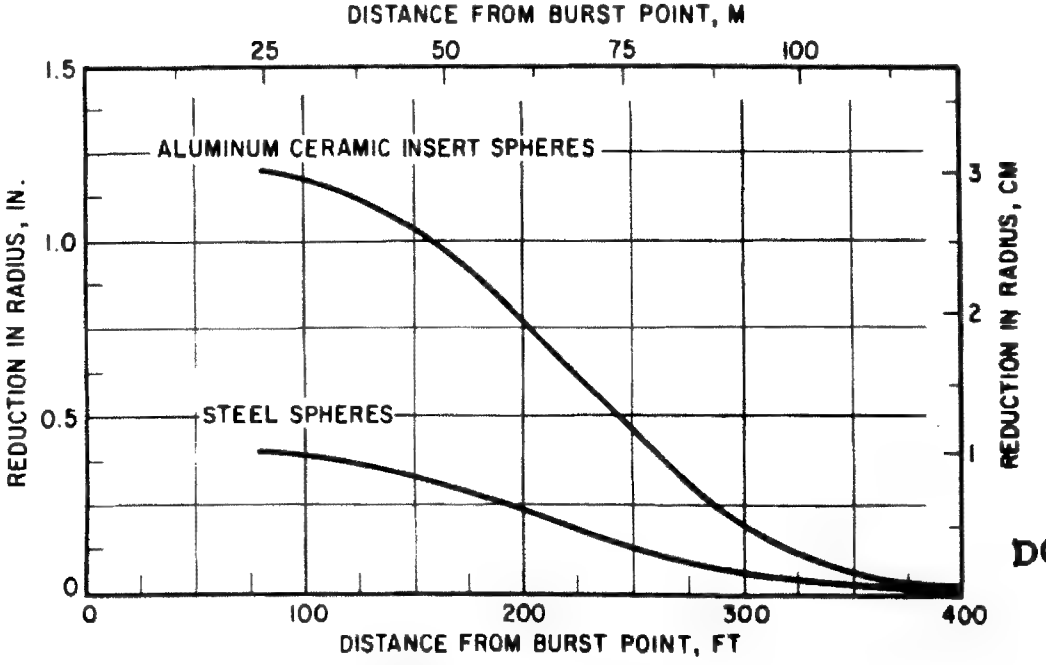

Figure 13-5. Reduction of Sphere Radius with Distance from a 23-kt Burst for Aluminum, Steel, and Ceramic Insert Spheres

These data may be used to assess the damage to military systems using electromagnetic propagation when the system parameters and propagation conditions prior to the burst are known. Paragraphs 13-15 through 13-20 summarize the effects on communication and radar systems .Where possible, assumptions have been made with respect to "typical" system performance criteria to present system degradation directly. Although the assumptions of system criteria are broad, the uncertainties associated with the burst phenomena are such that for many cases further refinement is probably not justified.

13-11 DAMAGE MECHANISMS. The electric field of a propagating electromagnetic wave exerts a force on charged particles (ions and electrons) in the propagation medium. This process results in the interchange of energy between the wave and the ions and electrons. Because electrons are many orders of magnitude lighter than positive or negative ions, they are more readily accelerated by the electric field.

13-12 Absorption. When electrons collide with, or are scattered by, other particles before returning their increased energy to the wave, the energy is dissipated as heat, and the wave attenuated. Exact expressions for the absorption or energy loss are complex, involving the components of earth's magnetic field as well as electron density, collision frequency (number of collisions an electron makes per second) and wave frequency. For frequencies above about 10 mc and when bending of the wave is negligible, the incremental path absorption can be found from:

$$a = 4.62 \times 10^4 \frac{N_e \nu}{w^2 + \nu^2} \text{ db/km}$$

where

N_e = electron density—electrons/centimeter^3
ν = collision frequency
w = wave frequency $= 2\pi f$

In the D region of the ionosphere, collision frequency is proportional to neutral particle density. At higher altitudes where neutral particle density is low, the effect of electron-ion collisions becomes increasingly important. Figure 13-6 (A) shows the incremental path absorption per electron per cubic centimeter as a function of altitude applicable in the D region. At higher altitudes, figure 13-6 (B) applies, and shows incremental absorption as a function of electron density for a temperature of 1400°K. The incremental absorption is proportional to $\left(\frac{1400}{T}\right)^{3.2}$ for other temperatures. The dotted portion of the curves indicates where the electron density causes considerable bending of the wave requiring a more detailed solution for absorption. Figure 13-6 can be used with estimates of electron density as a function of burst parameters to determine incremental path absorption. The integral of the incremental path absorption along the wave path gives the total path loss.

(a) Immediate radiation. Outside of the dissociated region, the ionization created by immediate radiation decays rapidly. Further, near the burst (but outside of the dissociated region) the electron density after about 1 sec, is essentially independent of the initial ionization. Figure 13-8 shows the one-way vertical absorption for the above condition as a function of time following the burst. The daytime curve is to be used when the time of propagation (not the time of the nuclear explosion) through the absorption region is between sunrise and sunset. The nighttime curve is to be used where the time of propagation is between a half hour after sunset and a half hour before sunrise at ground level. Almost complete transition between the day and night curves will probably occur during the half-hour gaps thus allowed. The absorption shown scales inversely with frequency squared for frequencies above about 10 mc. Figure 13-8 is an upper limit for the absorption caused by immediate radiation outside of the dissociated region and is useful in estimating the duration of immediate radiation effects and determining when they can be neglected in comparison with debris radiation discussed below. Within the dissociated region the electron density decay after a few seconds is primarily caused by expansion of the region. The absorption that would be experienced by a single traversal through the center of the dissociated region is shown in figure 13-9 as a function of burst altitude for dissociated region expansion

[redacted]

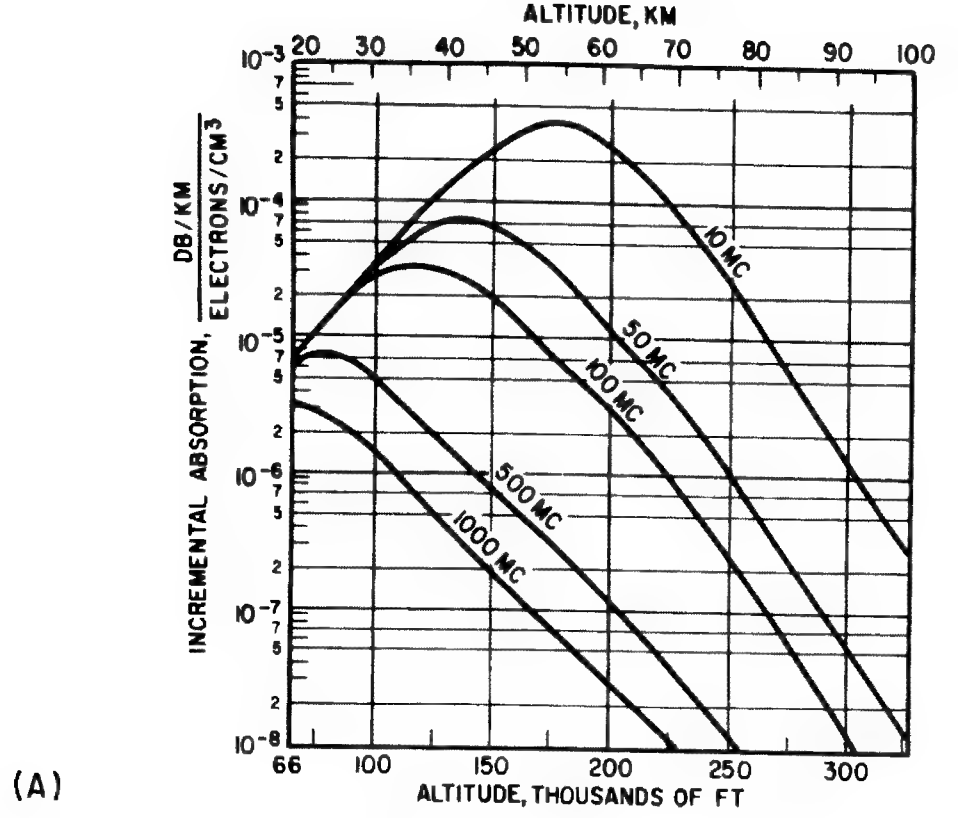

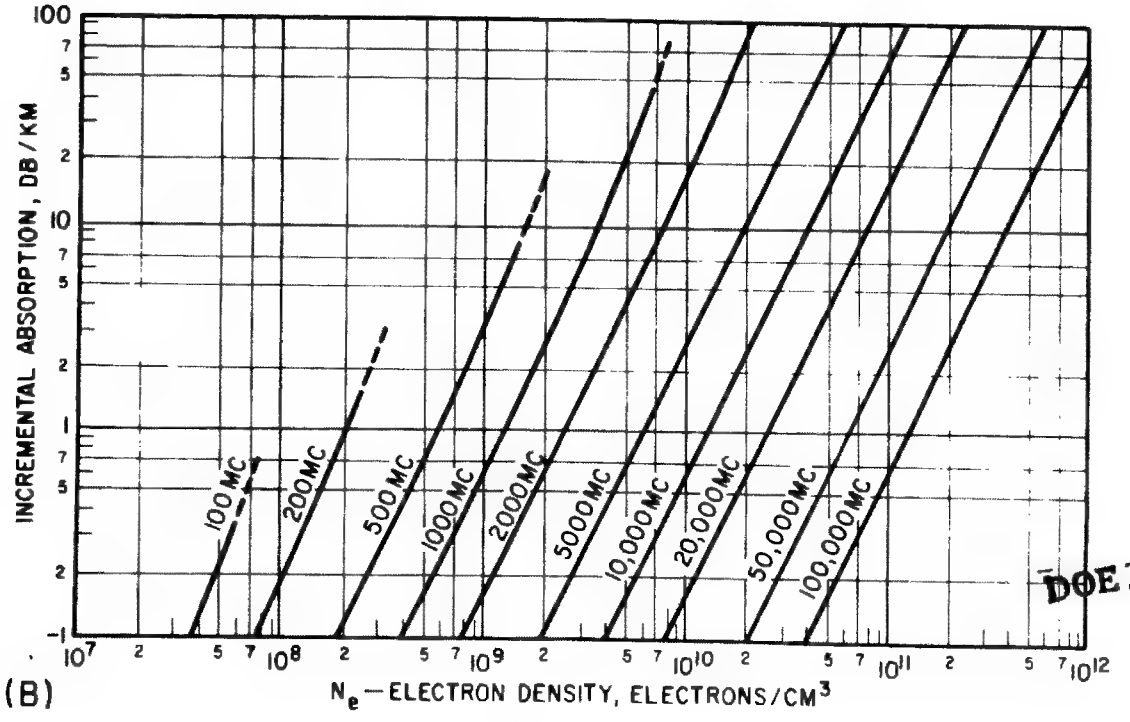

Figure 13-6. Incremental Path Absorption

[redacted]

defined by the expansion velocity scaling factor $F = 1$.

$$F = \frac{W^n}{W_o} \frac{\rho_o{}^m}{\rho}$$

where W_o and ρ_o are the total yield and air density at burst altitude for a reference burst, and W and ρ are total yield and air density for the condition to be scaled. The best estimated values for n and m are $n = 0.8$ $(+0.2, -0.4)$, $m = 0.4$ (± 0.1). For times greater than a few seconds the absorption scales directly with parameter F. Because of uncertainties of magnitude and distribution of electron density, temperature, and size of the dissociated region, the data in figure 13-9 are uncertain as indicated by the error limit bars. Although the magnitude of absorption at a specific time following the burst may be uncertain by several orders of magnitude, the duration of a given level of absorption is uncertain only to about a factor of three. Absorption within the dissociated region also scales inversely with frequency squared. For frequencies equal to or below the plasma frequency, however, approximately given by $9 \times 10^3 N_e{}^{1/2}$ where N_e is the electron density in electrons/centimeter^3, reflection of the wave will occur. Ray paths near the edge of the dissociated region may also be refracted or bent away from the absorption region if they are near the plasma frequency (see paragraph 13-13).

(*b*) *Debris radiation.* Beta and gamma radiation from the debris produces maximum ionization in the D region of the ionosphere. Here the collision frequency of free electrons with air molecules is high enough to cause significant absorption. The electron density, the collision frequency and, therefore, the absorption vary greatly with altitude. The calculation of the total path absorption, which is the quantity generally desired, is aided by expressing the ionization in terms of the radiation intensity I_β and I_γ of beta and gamma radiation emitted by the fission debris. These parameters determine the electron density as a function of altitude. Thus, the absorption may be expressed as a function of the radiation intensity.

Figures 13-10 and 13-11 show the total one-way vertical path attenuation due to absorption as a function of radiation intensity and frequency. Figure 13-10 applies where beta rays are incident on the D region. It applies both at a magnetic conjugate point where there will be only beta radiation and beneath the debris where there is both beta and gamma radiation. The net effect of the gamma radiation superimposed on the beta radiation is negligible. The altitude distribution of beta ray ionization is a function of the earth's magnetic field. Figure 13-10 was prepared for a dip angle of 30 degrees, but the vertical path absorption given is not changed more than 10 percent for dip angles between 20 and 90 degrees.

Figure 13-11 applies when absorption is caused by gamma rays outside of the region beneath the debris. The radiation intensity to be used is that determined for the point source approximation from Part I.

For oblique paths through the D region, if the distribution of debris radiation is uniform, the absorption varies as the secant of the angle θ between the vertical and the ray path. The multiplying factor, secant θ, is given in figure 13-12. To determine the absorption for a particular ray path it is necessary to locate where the ray path penetrates the D region at about 70 km altitude where most of the absorption from debris radiation will be experienced. These penetration points will be termed absorption control points and can be determined from figure 13-3 if the location of the terminal points of the ray path are known. For multiple hop HF links there will be several absorption control points depending on the number of hops (see paragraph 13-17).

Theoretical studies of ionization, deionization, and absorption processes indicate that for a given radiation intensity the absorption results may be in error by a factor of three. For example, if the absorption in figure 13-10 is 30 db, it may be as much as 90 db or as little as 10 db. Also, there are uncertainties in the radiation intensity at a specified time after burst because of uncertainties in the size and distribution of the fission debris. When all of these factors are considered individually, the uncertainty in absorption following a particular burst may be a factor of 10 or more. Predictions of the size and distribution of the debris region, however, are in part determined from absorption

data measured following the TEAK and ORANGE bursts, so that the combined effect of the various uncertainties should be less than their product. During the first 1000 sec after a burst, upper and lower limits for the absorption can be estimated by multiplying the nominal value of absorption by 2.5 $(F_{max}/F_{nom})^{1.4}$ and 1/2.5 $(F_{min}/F_{nom})^{1.4}$ where F_{max}, F_{nom}, and F_{min} are the maximum, nominal, and minimum values of the scaling parameter F, respectively. Thus, if the nominal value of absorption is 30 db and the nominal value of F is 2 with upper and lower limits of 3 and 1.5, the upper and lower limits for the absorption are

$$30 \times 2.5 \left(\frac{3}{1.5}\right)^{1.4} = 198 \text{ db}$$

$$\text{and } 30 \times \frac{1}{2.5}\left(\frac{1.5}{3}\right)^{1.4} = 4.5 \text{ db}$$

For time later than 1000 sec the uncertainty increases and may be twice as large 12 hr after the burst.

13-13 Refraction. The change in the index of refraction caused by free electrons also affects the direction and velocity of propagation of electromagnetic waves. Bending of the ray path results from changes in electron density. The ray bends toward the highest index of refraction or away from the highest electron density. Large electron density gradients can produce angular path changes of many degrees, which can seriously hamper or prevent radar detection, acquisition, or tracking. Accompanying lesser electron density gradients on the fringes of an ionized region will be lesser angular errors or bearing errors of the order of milliradians. However, these errors can seriously degrade tracking radars. Besides angular errors, there are range errors resulting principally from the altered propagation velocity of the radar wave along the ray path. Rate errors are introduced if the angular and range errors change with time. Because the propagation path from a radar to a moving target will traverse different portions of an ionized region as a function of time, significant rate errors can be introduced.

(*a*) *Amount of bending.* In the D region where electron collisions with neutral particles are high, appreciable refraction is accompanied by large absorption. Thus, refraction is of primary interest when it occurs in the lower E region (90 km) or higher. But even here absorption may become important when the electron density is large enough to cause refraction of very high frequencies. This absorption results from collisions of electrons with positive and negative ions as discussed in paragraph 13-12.

If the electron density is arbitrarily distributed, ray tracing procedures must be used to determine the amount of bending. When the electron density distribution can be approximated by simple models, approximations can be used to estimate refraction. Because of the exponential density variation of the atmosphere and the expansion of the initially ionized region, a spheroidal stratification with essentially uniform center is considered typical of the ionization caused by immediate radiation. Refraction errors are presented below for a specific geometry of propagation through a particular spheroidal model depicting electron density caused by immediate radiation. Although the model presented is based on a consideration of physical phenomena, the electron density distribution within the dissociated region and particularly near the fringes of the dissociated region is speculative. Further, there is considerable uncertainty about the magnitudes of electron density and temperature and the size of the dissociated region as a function of time. Useful estimates can be obtained from the model presented, however, by determining upper and lower limits for refraction from appropriate scaling laws. Because absorption may be the limiting factor in determining system performance, absorption data for the model are also presented.

(*b*) *Refraction model.* Figure 13-14 shows the relative location of the radar site and ionization model used in computing refraction. The projection of several ray paths in the zero azimuth plane for 1 kilomegacycle propagation is also shown. Rays A and C show the most deflected rays above and below the ionization center, respectively. Ray B shows that for paths nearly through the center of the model assumed, there is little deflection. Ray D shows that deflection becomes small again below Ray C. In

figure 13-15, contours of constant elevation and azimuth errors are shown as a function of the radar elevation and azimuth angle. Because of symmetry in azimuth, the errors for negative azimuth angles are the mirror image of those shown. Figure 13-16 shows contours of constant range error and contours of constant absorption for the same conditions. The absorption contours are for a temperature of 1400°K. For other temperatures the absorption scales as $\left(\frac{1400}{T}\right)^{3/2}$.

For small refractive errors (less than about 10 degrees) the bearing errors scale as N_e/f^2 where N_e is the maximum electron density along the ray path and f is the propagating frequency. Scaling the size of the model will not change the bearing errors if the electron density remains the same and the ray path traverses the same contours, that is, has the same relative position with respect to the model. Absorption caused by electron-ion collisions scales as N_e^2/f^2 for small refraction errors in which the path through the model is essentially unchanged. The path length and thus the absorption scales proportionally to the size of the model. For the same conditions, range errors scale as N_e/f^2 and are also proportional to the size of the model so that reducing the size of the model will reduce the absorption and range error but leave the bearing errors unchanged.

The bearing errors shown in figure 13-15 are for a target at 1200 km slant range. For targets at other distances the bearing errors scale roughly as $2\left(1 - \frac{600}{R_T}\right)$ where R_T is the slant range to the target if the target lies outside of the ionization region.

The size of the dissociated region, roughly corresponds to the central constant density region of the model. The electron density and temperature data given as a function of burst altitude in Chapter 5 are for this region. Using these data and the scaling laws given above, the bearing errors, range errors, and absorption can be scaled to estimate the conditions following a specific burst of interest. By using upper and lower limits for the size, electron density, and temperature of the model, estimates of the uncertainty of refraction, and absorption may be obtained.

Bearing rate errors and range rate errors are caused when the bearing and range errors change with time, such as in tracking a moving target, or when the electron density changes with time. A crude estimate of the rate errors caused by a moving target can be obtained from figure 13-15 by considering the time to go from one bearing error to another. For example, if the change with time of the elevation and azimuth angles at the radar are estimated, the target path in elevation and azimuth can be traced on figure 13-15. By dividing the difference in bearing or azimuth errors by the time required to change the error, the error rate can be found. A similar procedure using figure 13-16 can be used to estimate range errors.

13-14 Other Effects. Besides absorption and refraction, degradation to electronic systems using electromagnetic radiation may be caused by disturbances in the F region due to the expansion of the ionospheric wave and dissociated region, backscatter and angular scintillation due to field aligned electrons, and synchrotron noise due to electrons trapped in the earth's magnetic field. These effects are not well understood.

The expansion of the ionospheric wave and the dissociated region affects the distribution and magnitude of the electron density in the F region of the ionosphere. These changes can seriously degrade systems dependent upon ionospheric reflections such as HF communication systems.

Angular scintillation, the auroral-like disturbances that accompany a high-altitude nuclear explosion, presumably is associated with "tubes" of free electrons aligned with the earth's magnetic field. A wave propagating through such a medium should suffer random anisotropic refraction (or shimmer) that varies more or less rapidly with time depending on the exact statistical properties of the medium.

Backscatter clutter can affect all classes of radars and may be one of the most damaging repercussions of a high-altitude nuclear explosion for systems where propagation path is below the ionosphere. Radar backscatter was observed at all five high-altitude shots—ARGUS

I, II, III, TEAK, and ORANGE. At least two mechanisms are involved, providing two distinct stages of clutter. The first source of clutter is the intensely ionized fireball itself. This source caused clutter only for a few minutes for TEAK and ORANGE. The second stage apparently involved field aligned electrons, as the echoes received were similar to auroral echoes, coming only from directions such that the direction of propagation was perpendicular to the earth's magnetic field in the reflecting region that is apparently located between 90 and 160 km altitude. These effects are frequency sensitive, being most serious at VHF and low UHF frequencies. Radars operating above L band will probably be little affected.

Synchrotron noise can be caused by trapped beta rays (Argus noise) or from untrapped beta rays emitted by the fission debris. The radiated noise is essentially isotropic for HF, becoming highly directional for UHF. For HF circuits, synchrotron noise caused by beta rays traveling upwards from the debris to the magnetic conjugate point can cause noise levels 30 to 40 db above the background noise if the receiving antenna is located so that the noise reaches the receiving antenna without passing through the beta ray absorption regions. Argus noise may not be serious for HF circuits because of reflection from the F layer; however, satellite systems could be degraded. UHF radars at magnetic latitudes greater than about 30 degrees will not experience Argus noise if the earth's magnetic field lines are not distorted. Argus noise may cause a persistent source of degradation at lower latitudes. Distortion of the magnetic field lines by the burst may result in brief degradation at higher latitudes. Synchrotron noise from the decay of the fission debris may cause degradation for a minute or so depending on the orientation of the radar and fission cloud.

13-15 COMMUNICATION SYSTEMS. Military communication systems use frequencies from VLF to UHF in a variety of propagation modes. Long distance communications between ground stations and communication between ground stations and satellite or space vehicles which use the ionosphere as a propagation medium, may be affected by the artificial electron clouds created by high-altitude nuclear bursts. Even in the absence of nuclear bursts the determination of communication system performance is difficult, involving factors such as modulation, power, antennas, noise, and the changing nature of the "normal" ionosphere.

The following paragraphs summarize major effects of high-altitude nuclear bursts on several classes of communication systems. Where possible, simplified system performance criteria have been assumed in order to present directly the duration of system degradation. These data only indicate the effects of high-altitude nuclear bursts for use in rapidly assessing order of magnitude effects. For a detailed analysis see *Electromagnetic Blackout Guide* (DASA 1229), and *Electromagnetic Blackout Handbook* (DASA 1280).

13-16 VLF and MF Communications. Long range ELF and VLF propagation (below 30 kc) confines the electromagnetic radiation between the conducting earth and the conducting ionosphere. Very low electron densities are adequate to produce the ionospheric reflection at these frequencies. The altitude of reflection moves downward in the daytime as the sun's action causes D-layer ionization. Similarly, the major effect of increased ionization from high-altitude nuclear explosions will be to lower the height of reflection. This will be particularly noticeable at night, when the normal reflecting level is high. Lowering the reflection height can cause a loss of about 20 db for frequencies below 10 kc. In the region of 10-30 kc the amplitude effects are small and on some circuits an actual increase in signal strength may occur.

Atmospherics are the principal causes of noise in the ELF and the VLF bands. Because part of the atmospheric noise is propagated from distant thunderstorms, modification of the ionospheric reflection height may also modify the external noise level at the receiver at the same time that signal strength is modified. The system degradation or improvement will depend on the relative location of signal source, noise source, and burst produced ionization.

Rapid changes in the reflection layer height will cause phase shifts because of the change in propagation path length. This can affect synchronous systems or navigation systems that

rely on phase measurements. Besides the region of the ionosphere, which is line of sight to the burst, a much larger region is affected by these transient phase shifts. This may result from neutrons that travel far into space, decay into ionized particles, then spiral into the ionosphere far beyond the burst horizon.

MF communications that use sky wave propagation will be degraded by absorption following a high-altitude nuclear explosion, just as they are by the normal D-layer ionization.

13-17 HF Communications. In the HF band (3-30 mc) the major propagation path is by sky wave modes reflected from the E and F regions of the ionosphere. Absorption effects caused by a high-altitude nuclear burst will seriously degrade these circuits if the propagation path passes through the absorption region. Outages may be encountered on HF circuits for many hours because of debris radiation for propagation paths traversing a region several thousands of kilometers in diameter. Ionospheric waves and expansion of the dissociated region caused by immediate radiation will also cause degradation by modifying the normal ionization of the upper ionosphere.

Typical HF circuits may have one or more reflections or hops between the E or F region depending on the total path length, operating frequency, and electron density in the E and F regions. The various modes penetrate the D region at oblique angles such that secant θ is as given by figure 13-12. There will be two regions of penetration of the D region for each hop. By use of figure 13-10, it is necessary to find the absorption at each D-region penetration point, add such absorptions and compare with the circuit margin. The total path absorption can be used to determine predicted outage times for a particular circuit frequency and set of burst parameters, the LUF (lowest usable frequency), LRRP (lowest required radiated power), or the remaining circuit margin, if the communication system parameters and propagation conditions prior to the burst are known.

For transmission distances greater than about 4000 km, many alternate modes may connect the terminals. Reflections between the E and F regions may allow some of the D-region penetration points of normal multihop modes between the earth and the ionosphere to be bypassed so that communication may be possible even if blackout absorption is predicted over part of the path. If the absorption region is near the receiver terminal, noise reaching the receiver by ionospheric propagation may also be reduced by absorption, so there may be the same signal-to-noise ratio even though the signal is reduced. Of course, reduction of the signal below the receiver set noise or local noise will break the link.

13-18 VHF Communications. For frequencies above HF, long-range communication between ground terminals depends on scattering modes. In the lower part of the VHF band (about 50 mc), scattering takes place in the upper part of the D region from ionization irregularities caused by turbulence or meteor trails. Because scattering from meteor trails occurs at 90 km or higher, the ray path must pass through the region of maximum debris radiation absorption caused by a nuclear burst. Also, meteor scatter circuits normally operate with fairly small margins so that absorption effects will cause severe degradation for long periods of time. Scattering from irregularities in electron density caused by turbulence may be enhanced by the increased ionization caused by the burst, but absorption will reduce the scattering from the normal scatter heights to a negligible magnitude for short periods of time. Scattering may take place with approximately normal magnitude or greater from the bottom of the artificial ionosphere. Thus, a scatter signal may be present after a burst but from a lower altitude than normal. Long ionospheric scatter links, where the minimum altitude usable to both transmitter and receiver antennas is above the scatter altitude, can be broken.

See DASA 1229 for duration of outage for a 50 mc ionospheric scatter link as a function of the transmission distance of the link.

13-19 UHF Communications. Scattering used at UHF (300-3000 mc) takes place in the troposphere from irregularities caused by turbulence in the air density and water vapor content. Because the scatter occurs below the region affected by the burst, the normal propagation path is not affected. A possible degradation

to tropospheric scatter circuits is an interfering signal reflected from the increased ionization in the ionosphere. A reflection may occur if the ionization is high enough to allow total reflection, approximately 10^8 to 10^9 electrons/centimeter^3 for the UHF band, or if scatter occurs from ionization aligned along the magnetic field. This second possibility is similar to auroral scattering. For short tropospheric scatter, loss from an auroral scatter mode is about the same or larger than the normal tropospheric scatter loss; therefore, when the directivity of the antennas is considered the interfering signal is too small to cause interference. Auroral type scatter may cause an interference signal on larger links of magnitude similar to the normal signal. Even for these links, however, the interference will be negligible unless the geometry of the propagation path of the ionospheric mode makes this path perpendicular to the magnetic field lines.

The high electron density necessary to cause specular reflection also causes absorption along the interfering path, reducing interference on short tropospheric scatter links. Interference on longer links from specular reflection may occur for a few minutes, depending on the duration of electron densities necessary for reflection, antenna directivity characteristics, and normal scatter losses on the troposphere.

Propagation from ground stations to communication satellites will pass through the altitude regions affected by debric radiation and thus, depending on frequency, can be degraded. For frequencies in the UHF band or higher, degradation longer than a few minutes is not likely. Propagation between satellites or vehicles above the ionization caused by the burst may be affected by reflection for particular geometries but, as in the case of tropospheric scatter, the magnitude of the reflected signal will normally be much smaller than the desired signal.

Electron densities high enough to cause widespread degradation of UHF satellite transmission may be encountered within the dissociated region. Theoretical analysis indicates that significant absorption could be experienced at kilomegacycle frequencies for at least several minutes. Refractive errors large enough to make tracking and acquisition of satellites difficult are also possible.

13-20 RADAR SYSTEMS. Radar systems that must see through the ionosphere can suffer serious degradation of performance following a high-altitude nuclear explosion. Included in this class of radars are missile detection radars such as those of BMEWS (FPS-49, FPS-50), missile guidance radars (ATLAS), anti-ICBM radars (NIKE-ZEUS), and satellite detection radars. Also, as discussed in paragraph 13-19, communications to or by means of artificial earth satellites can suffer the same effects as radar. Degrading effects include increased absorption, refraction, clutter, and noise. Although many radars need not look through the ionosphere they still may be subject to clutter and noise that can interfere with their performance.

There are two gross physical features of the disturbance caused by a high-altitude nuclear burst that may degrade radar systems. The first is the dissociated region in which intense, persistent ionization can cause refraction and absorption of radar signals; the second is D-region absorption produced by debris radiation. This latter region can black out radars, which must see through it for time periods ranging from a few seconds to many minutes, depending on specific burst and radar parameters.

Although the effect of absorption on detection is of great interest, the effects on tracking accuracy may be no less important. The errors in radar measurements caused by receiver noise (thermal noise errors) are inversely proportional to the square root of power signal-to-noise ratio. Thus, a reduction of 6 db in signal-to-noise ratio can double the tracking errors of radar. This may or may not be important depending on how much accuracy margin the system has, and on whether or not thermal noise errors override the other errors (such as glint). Losses that appear as "light" when considering detection may be "severe" when considering tracking accuracy. Also, the time duration and spatial extent of the absorbing region that causes light damage is substantially greater than that for moderate or severe damage. This fact tends to increase the importance of relatively small losses—on the order of a few db.

[redacted]

Problem 13-1 Neutron Flux for a Typical Fission Weapon

The curves in figure 13-7 show the number of neutrons per square centimeter per kiloton at various horizontal ranges for different heights of burst of typical fission weapons. The curves are for standard atmospheric conditions. Data are presented in AFSWP-1100, published with a higher security classification, from which neutron flux for specific weapons may be computed.

Scaling. At a given horizontal range and altitude, the neutron flux is proportional to the yield of the weapon.

Example.

Given: A 100-kt air burst at 20,000 ft.

Find: The number of neutrons per square centimeter at a horizontal range of 3400 yd.

Solution: Reading directly from figure 13-7, the neutron flux from a 1-kt weapon is [redacted]

Answer: Since this is a 100-kt burst, 100 × [redacted] square centimeter.

Reliability. Neutron flux is dependent upon weapon design. For most fission weapons the curves of figure 13-7 are considered reliable within a factor of 5.

[redacted]

762-909 O - 65 - 31

[redacted]

BURST ALTITUDE, M

HORIZONTAL RANGE AT BURST ALTITUDE, M

DELETED

Figure 13-7. Neutron Flux from Typical Fission Weapons for a 1-kt Burst in a Standard Atmosphere as a Function of Burst Altitude and Horizontal Range

BURST ALTITUDE, FT

[redacted]

[redacted]

Problem 13-2 D-Region Absorption Due to Immediate Radiation Outside of Dissociated Region

ABSORPTION DUE TO PROPAGATION THROUGH DISSOCIATED REGION

Figure 13-8 gives the maximum D-region one-way vertical absorption caused by immediate radiation outside of the dissociated region. The daytime curve is to be used when the time of propagation is between one-half hour before sunrise to one-half hour after sunset. Figure 13-9 gives the absorption at 1 kilomegacycle caused by a single traversal through the center of the dissociated region as a function of burst altitude for dissociated region expansion defined by $F = 1$.

Scaling. The absorption in figure 13-8 scales inversely with frequency squared for frequencies above about 10 mc. The absorption in figure 13-9 also scales inversely with frequency squared for frequencies greater than about $1.3 \times 10^4 N_e^{1/2}$ cycles where N_e is in electrons/centimeter^3. Tick marks labeled by frequency are shown on the curves of figure 13-9 to indicate the shortest time for which scaling from the 1 kilomegacycle absorption is possible. For example, the absorption for the 60-km burst should not be scaled to frequencies equal to or below 500 mc before 40 sec after burst. For burst parameters such that scaling parameter F is other than one, the absorption scales directly with F after a few seconds.

Example.

Given: A 2-mt burst detonated at 60 km altitude.

Find: The upper limit for daytime absorption outside of the dissociated region 10 sec after burst for a frequency of 500 mc. Determine the absorption for a single traversal through the center of the dissociated region 30 sec after burst for a frequency of 1 kilomegacycle.

Solution: From figure 13-8 for a time of 10 sec, the limit for daytime absorption outside of the dissociated region at 100 mc is 10 db. Scaling inversely with frequency squared gives $10 \times (100/500)^2 = 0.4$ db.

Answer. (See reliability.) The F parameter for a 2-mt burst at 60 km is 1/4. From figure 13-9, for a time of 30 sec and a burst altitude of 60 km, the absorption at 1 kilomegacycle is 75 db. (Scaling directly with parameter F gives $75 \times 1/4 = 19$ db.)

Reliability. The absorption outside of the dissociation region is termed maximum because of the assumption that it is independent of the initial ionization. Uncertainties in atmospheric reaction rates make this "maximum" uncertain by a factor of 10. Uncertainty in absorption in the dissociated region is given by error limit bars.

Related Material. See paragraph 13-12.

[redacted]

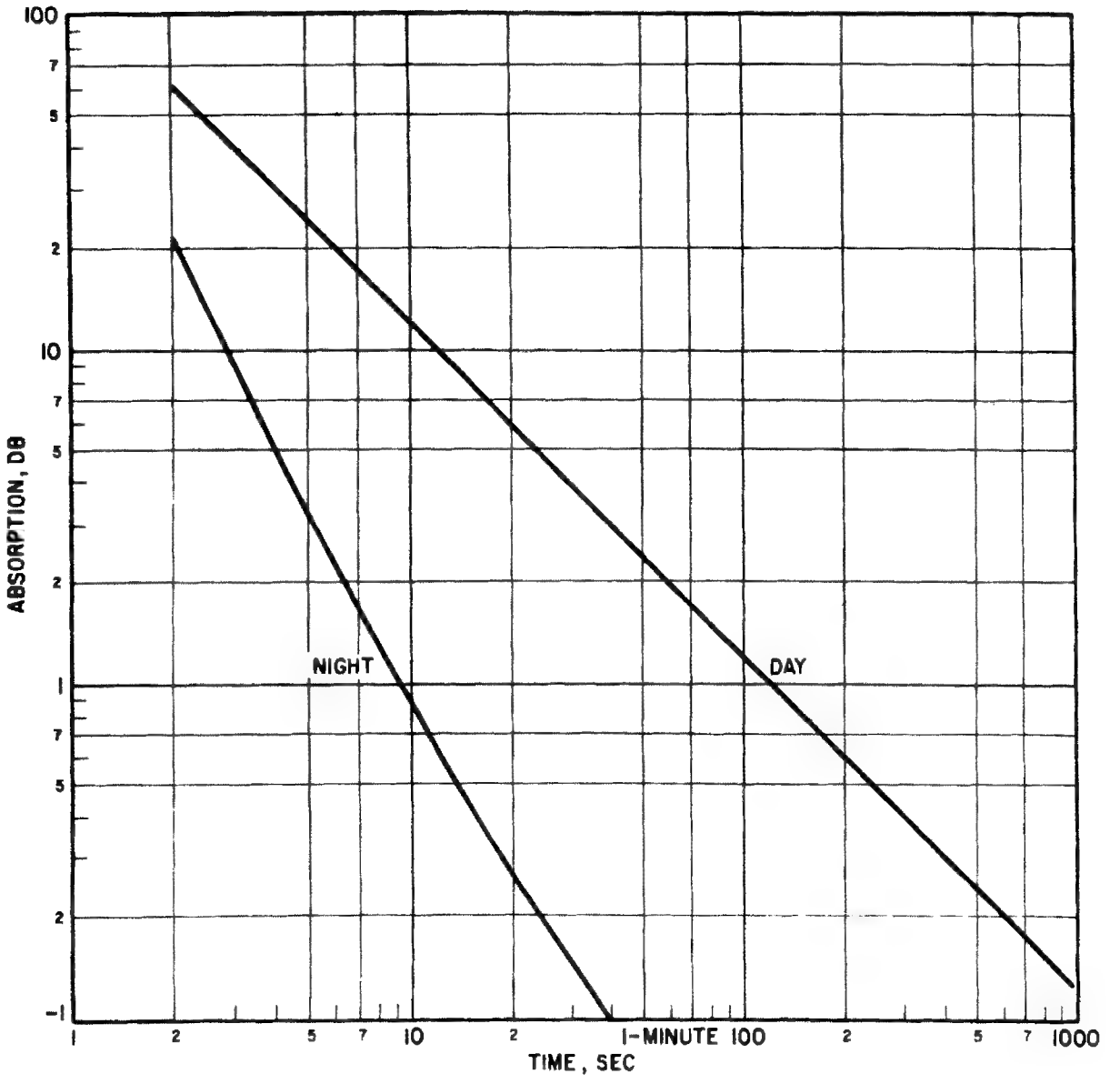

Figure 13-8. Maximum D-Region Vertical Absorption due to Immediate Radiation Outside of Dissociated Region, $f = 100$ mc

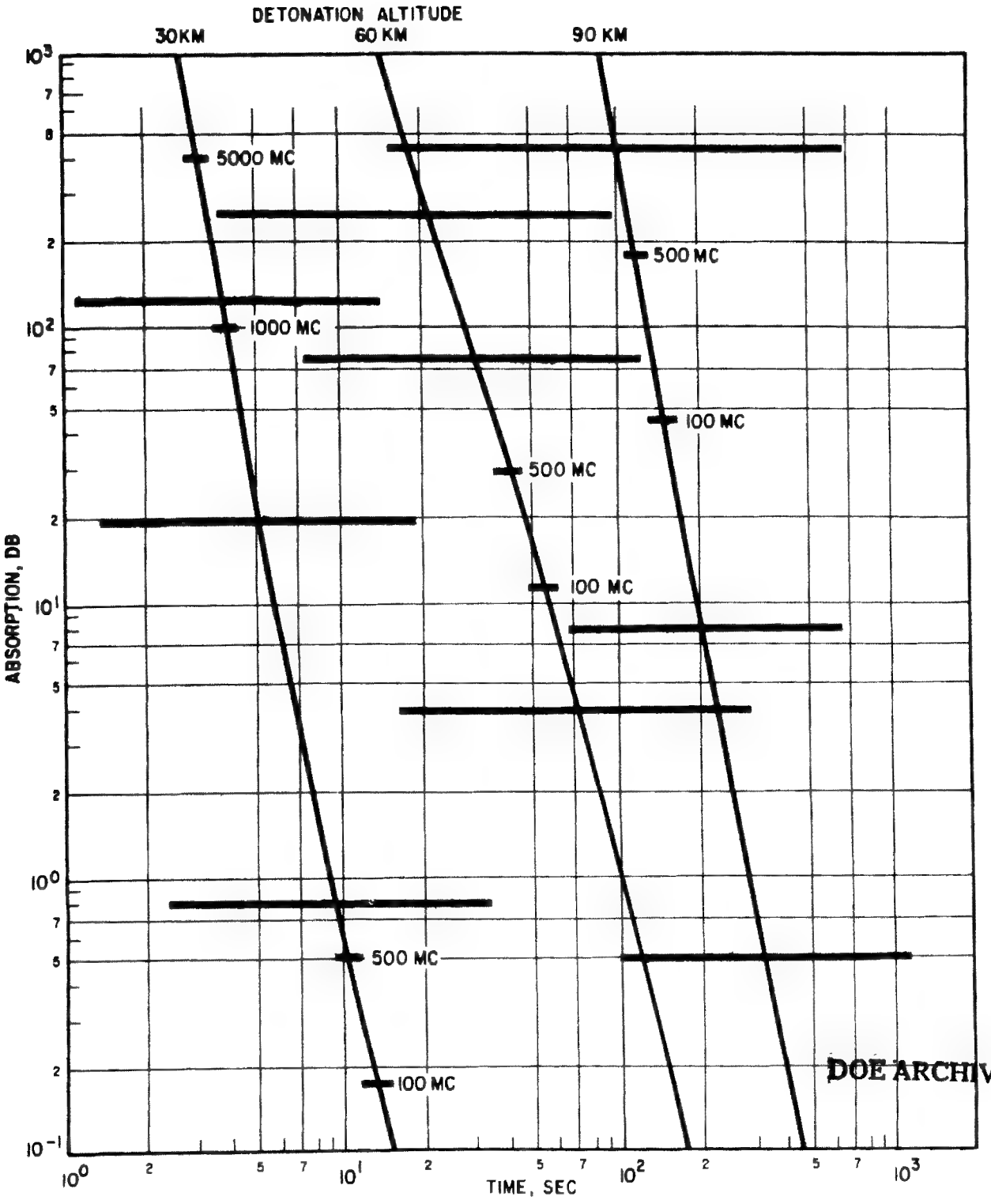

Figure 13-9. One-way Path Absorption Through Dissociated Region
1 Kilomegacycle, $F = 1$

[redacted]

Problem 13-3 One-way Vertical Path Absorption Due to Debris Radiation

Figures 13-10 and 13-11 give the one-way vertical path absorption due to beta and gamma rays from the fission debris as a function of radiation intensity and frequency. The daytime curves are to be used one-half hour before sunrise to one-half hour after sunset.

Scaling. Scaling with burst parameters is accomplished through the radiation intensity parameter.

Example.

Given: A beta radiation intensity of 10^{-3} watts/meter^2.

Find: The one-way vertical path absorption for a frequency of 30 mc.

Solution: From figure 13-10 at a radiation intensity of 10^{-3} watts/meter^2 the one-way vertical path absorption for daytime conditions is 20 db.

Answer. The one-way vertical path absorption at night is 2 db.

Example.

Given: A gamma radiation intensity of 3×10^{-3} watts/meter^2.

Find: The one-way vertical path absorption for a frequency of 30 mc.

Solution: From figure 13-11 at a radiation intensity of 3×10^{-3} watts/meter^2 the one-way vertical path absorption for daytime conditions is 7 db.

Answer. The one-way vertical path absorption at night is 0.5 db.

Reliability. For a given radiation intensity the absorption data are believed accurate within a factor of three. See paragraph 13-12(b) for consideration of uncertainty following a specific burst for which radiation intensity as a function of time is also uncertain.

[redacted]

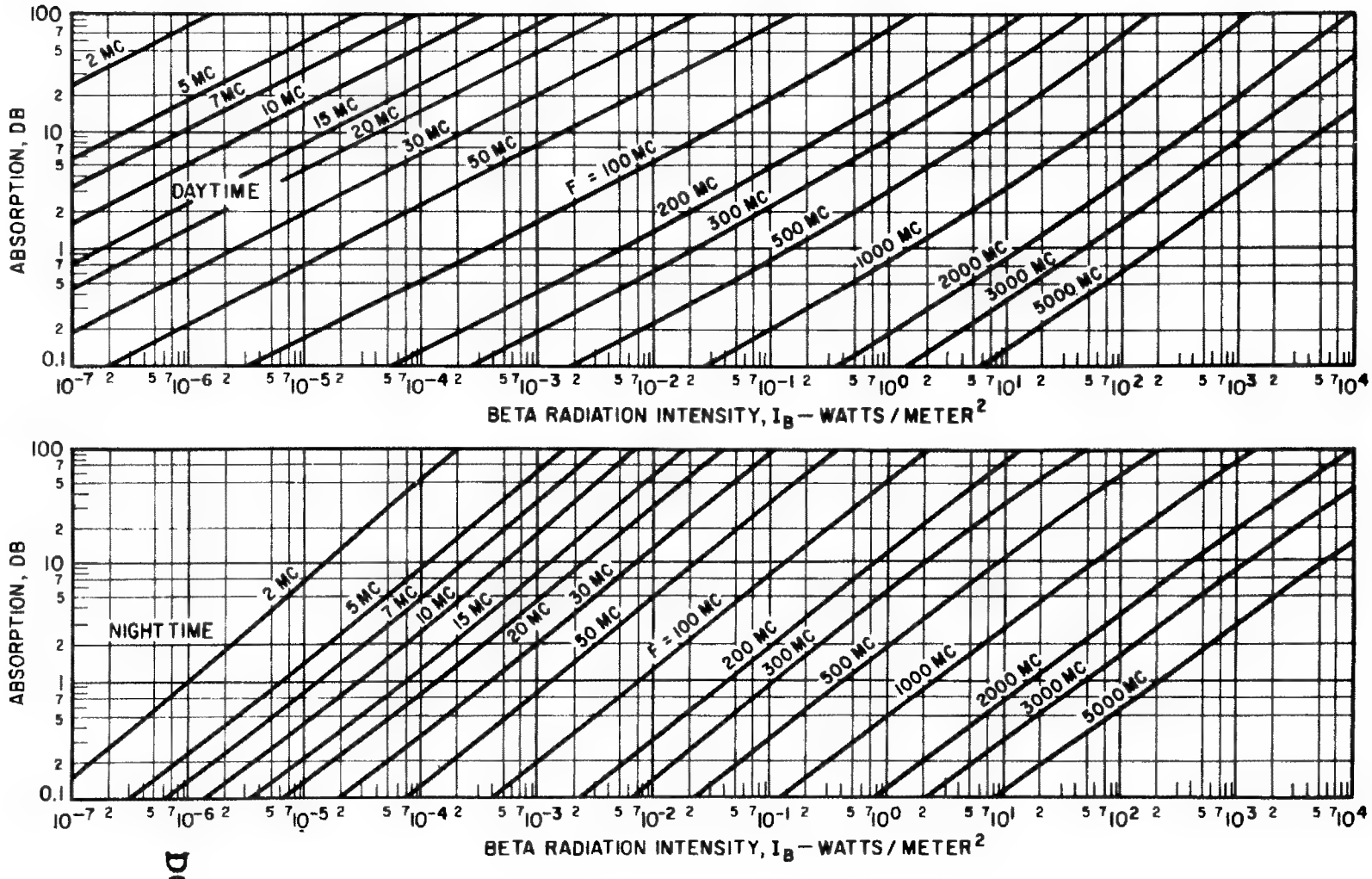

Figure 13-10. One-way Vertical Path Absorption due to Beta Rays

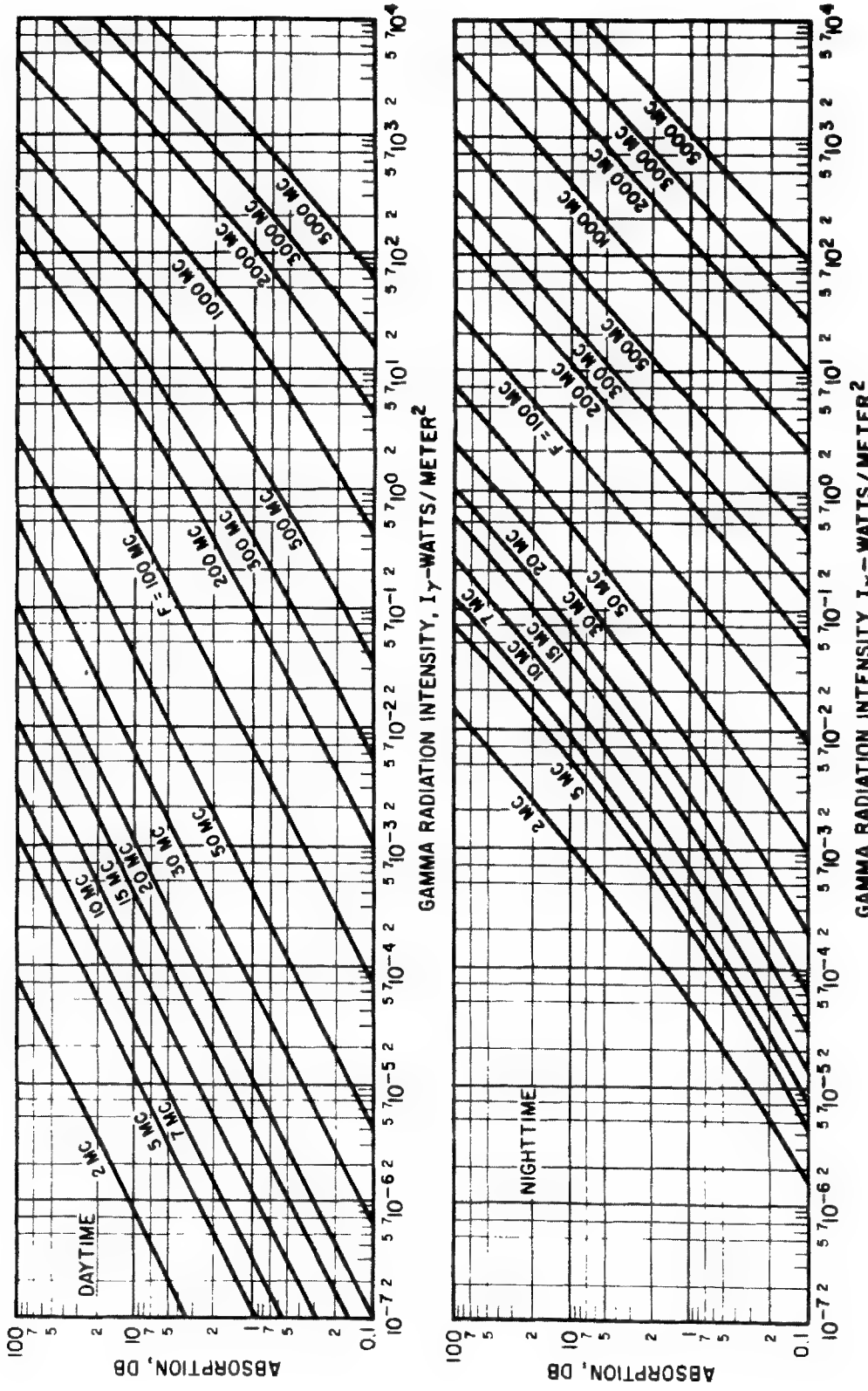

Figure 13-11. One-way Vertical Path Absorption due to Gamma Rays

[redacted]

Problem 13-4 Absorption Multiplication Factor Distance to Absorption Control Point

Figure 13-12 gives the multiplication factor, secant θ, for use in converting the one-way vertical absorption of figures 13-10 and 13-11 to that for an oblique path through the absorption region. Figure 13-13 gives the distance to the absorption control point from a ground terminal of the ray path measured along the earth's surface. Secant θ and distance to absorption control point are shown as a function of elevation angle for communication links that pass through the ionosphere, such as satellite links and for transionospheric radar systems. Secant θ and distance to the absorption control point are also shown as a function of transmission distance and type of reflection mode for analysis of ionospheric reflection propagation such as HF skywave modes.

Example.

Given: A radar system for which the elevation angle is 20 degrees.

Find: The absorption multiplication factor and distance to the absorption control point.

Solution: From figure 13-12, at an elevation angle of 20 degrees the absorption multiplication factor is 2.7.

Answer. From figure 13-13, at an elevation angle of 20 degrees the distance to the absorption control point measured along the earth's surface from the radar site is 180 km.

Example.

Given: An HF communication link 3000 km in length using a 1-hop F mode.

Find: The absorption multiplication factor and distance to the absorption control points.

Solution: From figure 13-12, at a transmission distance of 3000 km and for a 1-hop F mode the multiplication factor is 5.8.

Answer. From figure 13-13, at a transmission distance of 3000 km and for a 1-hop F mode the distance to the absorption control points measured along the earth's surface from the ground terminals is about 525 km.

Reliability. The absorption multiplication factor and distance to the absorption control point are accurate when the absorption takes place in a narrow altitude region at about 70 km. Errors due to the finite distribution of absorption in altitude are included in the absorption data.

Related Material.

See paragraph 13-12(b).

[redacted]

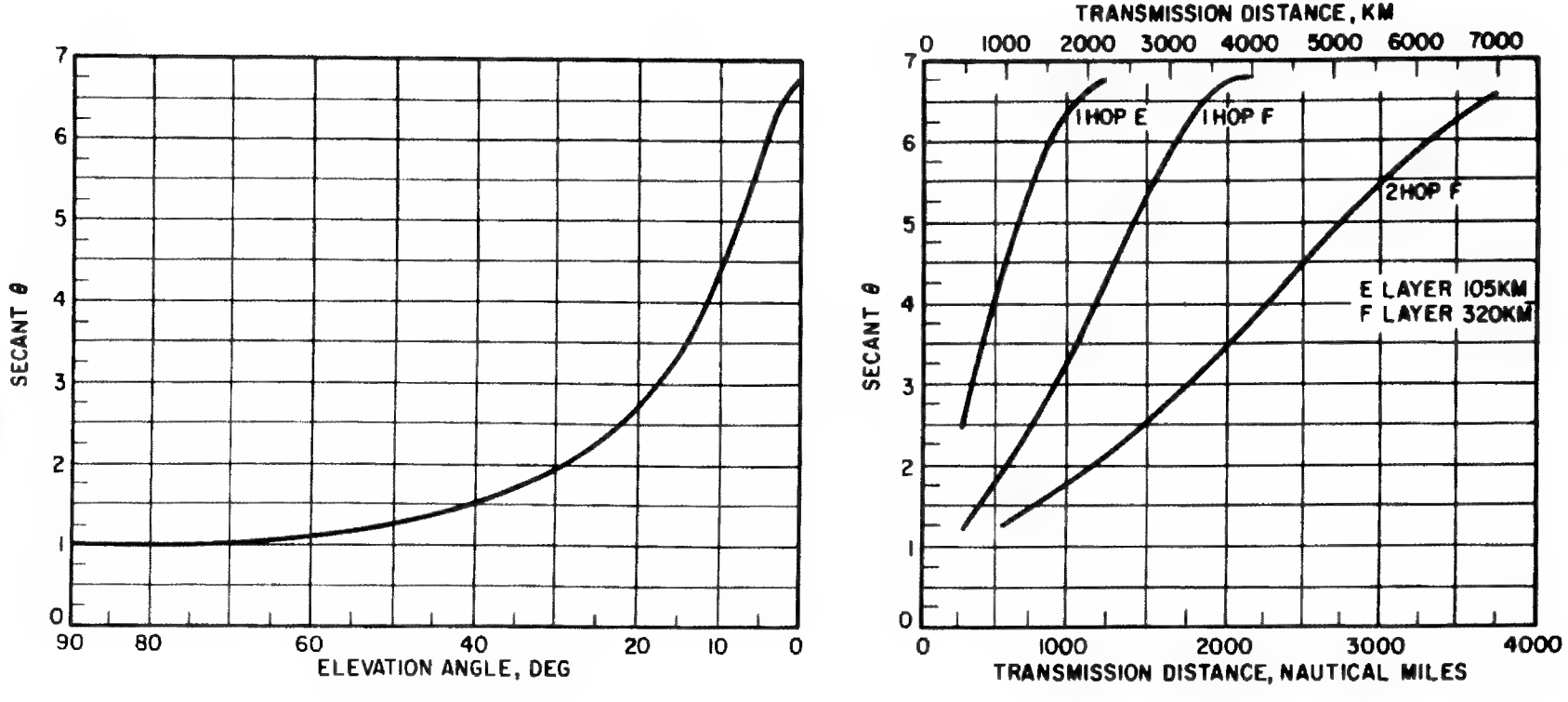

Figure 13-12. Absorption Multiplication Factor

[redacted]

Figure 13-13. Distance to Absorption Control Point from Ground Terminal Measured Along Earth's Surface

[redacted]

[redacted]

Problem 13-5 Refraction and Absorption Through Spheroidal Model

Figures 13-15 and 13-16 give refraction and absorption for propagation of a 1 kilomegacycle wave through the model shown in figure 13-14. Figure 13-15 shows elevation and azimuth bearing errors and figure 13-15 shows range errors and one-way absorption as a function of elevation and azimuth angle measured at the radar site. Because of symmetry in azimuth the errors for negative azimuth angles are the mirror image of those shown.

Scaling: For small refractive errors (less than about 10 degrees): Bearing errors scale as N_e/f^2 and are independent of size scale of model, range errors scale as N_e/f^2 and are proportional to the size scale of model, and absorption scales as $(N_e/f)^2$ and as $(1400/T)^{3/2}$ for temperatures other than 1400°K and is proportional to the size scale of the model. The bearing errors shown are for a target at 1200 km slant range. For targets at other distances the bearing errors scale roughly as $2\ (1 - 600/R_T)$, where R_T is the slant range to the target if the target lies outside of the ionized region. The electron density, temperature, and size of the dissociated region, which corresponds to the central region of the model (approximately 150 km radius), as a function of burst parameters are given in Part I.

Example.

Given: A burst for which the electron density, temperature, and radius of the dissociated region are 2×10^9 electrons/centimeter^3, 2000 °K, and 50 km, respectively.

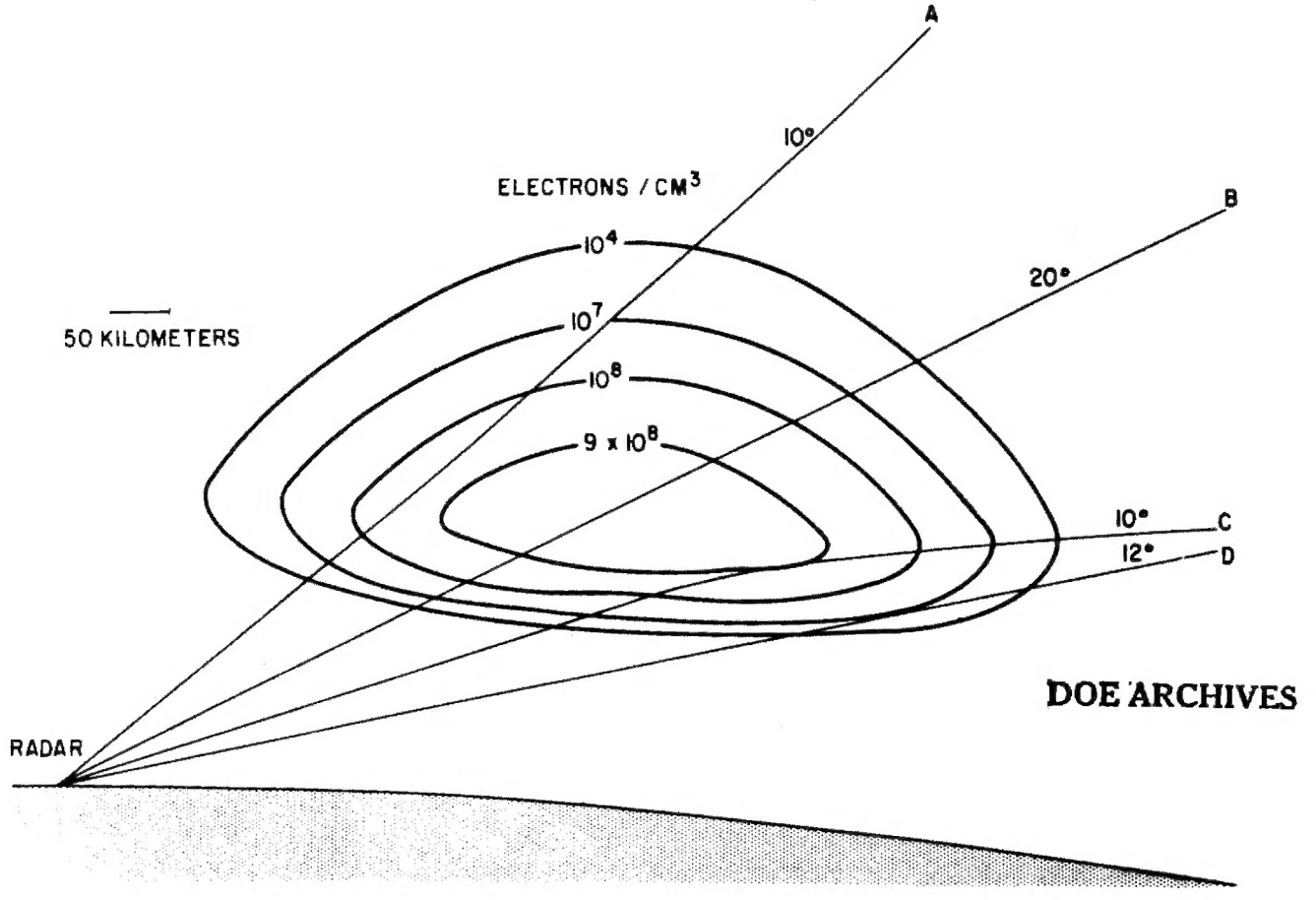

Figure 13-14. Refraction Through Model of Elecrton Density Distribution, $f = 1$ kmc

[redacted]

[redacted]

Find: The bearing errors, range error, and absorption for a zero azimuth ray at an elevation angle of 27 degrees for a frequency of 2 kilomegacycles.

Solution: For 27 degrees elevation, 0 degrees azimuth, the azimuth error is zero and the elevation error is 20 milliradians (figure 13-15); the range error is 15 km (figure 13-16), and the one-way absorption is approximately 150 db (figure 13-16). Scaling the bearing errors as N_e/f^2 gives $20 \times 2/2^2 = 10$ milliradians elevation error.

Answer. The bearing errors scale as N_e/f^2 or if E is the bearing error then E is proportional to $20\ N_e/f^2$. Let N_{e2} be the electron density of the given burst (2×10^9 electrons/centimeter^3), N_{e1} be the maximum electron density of the model (1×10^9 electrons/centimeter^3), $f_1 = 1$ kmc and $f_2 = 2$ kmc. Then $E = 20 \times N_{e2}/N_{e1} \times f_1^2/f_2^2 = 20 \times 2 \times 1/2^2 = 10$ milliradians. Similarly scaling the range error with N_e/f^2 and the change in size of the model gives $15 \times 2/2^2 \times 50/150 = 2.5$ km. Scaling the absorption with $(N_e/f)^2$, $(1400/T)^{3/2}$ and the change in size of the model gives $150 \times (2/2)^2 \times (1400/2000)^{3/2} \times 50/150 = 30$ db.

Example.

Given: A burst for which the electron density, temperature, and radius of the dissociated region are 5×10^8 electrons/centimeter^3, 1400 °K, and 50 km, respectively.

Find: The bearing errors, range error and absorption for a zero azimuth ray at an elevation angle of 18 degrees for a frequency of 1 kilomegacycle .

Solution: For 18 degrees elevation, 0 degrees azimuth, the azimuth error is zero and the elevation error is 100 milliradians (figure 13-15); the range error is approximately 5 km (figure 13-16); and the one-way absorption is approximately 28 db (figure 13-16).

Answer: Scaling the bearing errors as in the previous example gives $100 \times 1/2 = 50$ milliradians. The range error is $5 \times 1/2 \times 50/150$

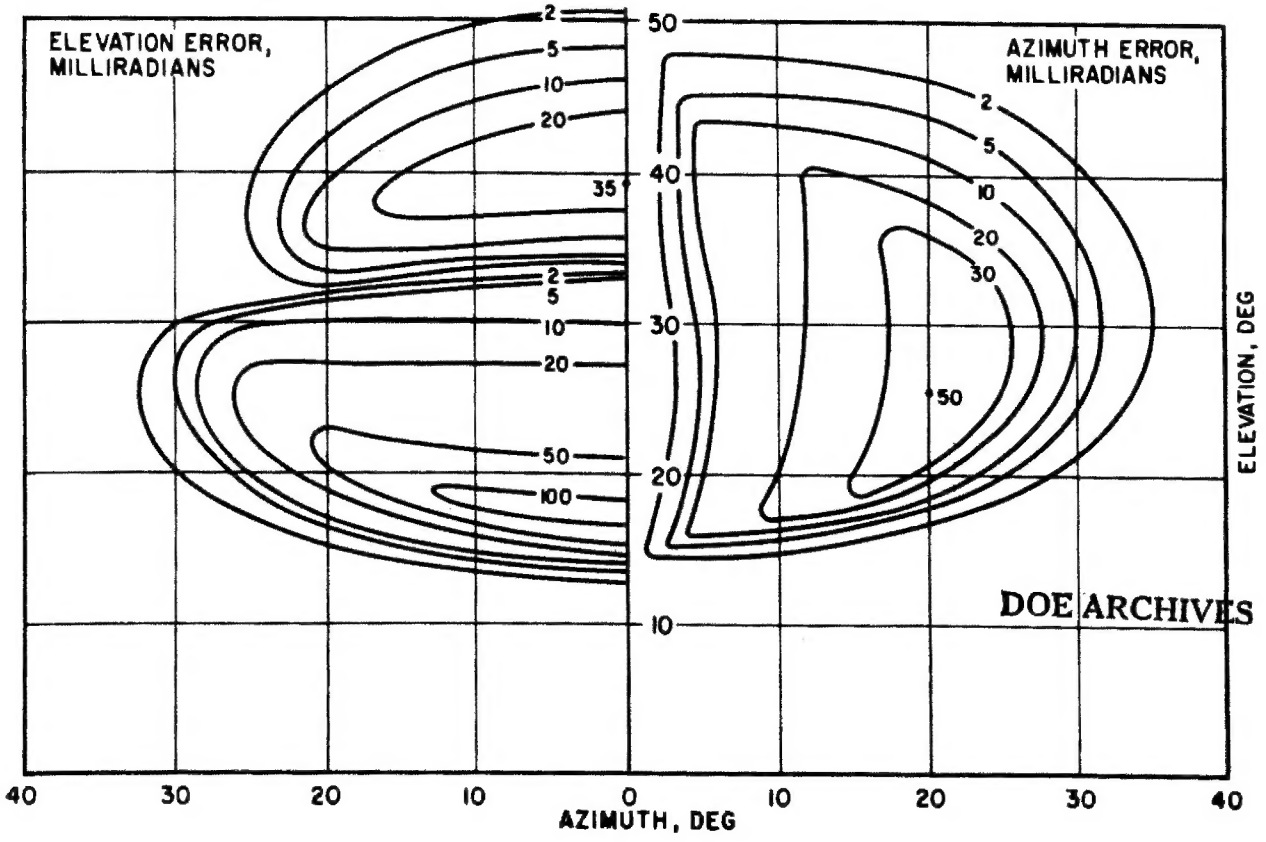

Figure 13-15. Elevation and Azimuth Errors

[redacted]

= .83 km. The absorption is 28 × $(1/2)^2$ × 50/150 = 2.3 db.

Reliability. The model used in obtaining refraction errors is hypothetical and is presented primarily to illustrate errors that may be experienced. By scaling the results with electron density, size, and temperature estimates of the uncertainty caused by these parameters may be obtained.

Related Material. See paragraph 13-13.

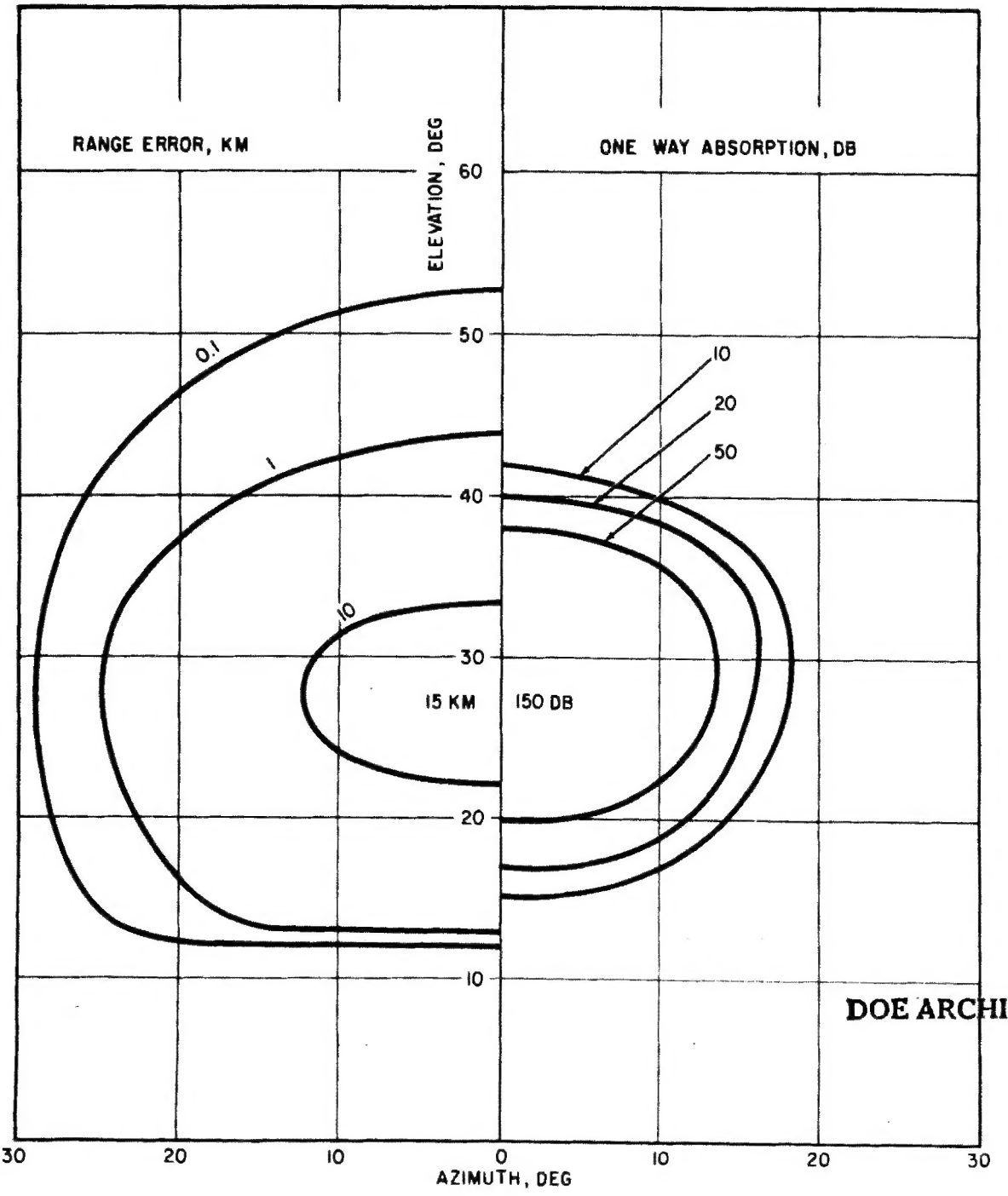

Figure 13-16. Absorption and Range Errors

PARTIAL DOCUMENT RECORD SHEET

Parts of this document were judged irrelevant to the CIC collection effort and were not copied:

Pages _____

Enclosures _____

Attachments _____

Other Appendix A-B-C-D AND index

Title page and table of contents have been copied for reference.

Dick Kogle
signature

9-15-87
date